

JYU DISSERTATIONS 696

Shuang Zhao

Kinematic and Kinetic Characteristics of Treadmill Roller Skiing and Validation of Force Measurement Roller Skis



UNIVERSITY OF JYVÄSKYLÄ
FACULTY OF SPORT AND
HEALTH SCIENCES

JYU DISSERTATIONS 696

Shuang Zhao

Kinematic and Kinetic Characteristics of Treadmill Roller Skiing and Validation of Force Measurement Roller Skis

Esitetään Jyväskylän yliopiston liikuntatieteellisen tiedekunnan suostumuksella
julkisesti tarkastettavaksi Sokos Hotel Vuokatin auditoriossa
lokakuun 6. päivänä 2023 kello 12.

Academic dissertation to be publicly discussed, by permission of
the Faculty of Sport and Health Sciences of the University of Jyväskylä,
at the auditorium of Sokos Hotel Vuokatti, on October 6, 2023, at 12 o'clock.



JYVÄSKYLÄN YLIOPISTO
UNIVERSITY OF JYVÄSKYLÄ

JYVÄSKYLÄ 2023

Editors

Simon Walker

Faculty of Sport and Health Sciences, University of Jyväskylä

Päivi Vuorio

Open Science Centre, University of Jyväskylä

Copyright © 2023, by the author and University of Jyväskylä

ISBN 978-951-39-9744-1 (PDF)

URN:ISBN:978-951-39-9744-1

ISSN 2489-9003

Permanent link to this publication: <http://urn.fi/URN:ISBN:978-951-39-9744-1>

ABSTRACT

Zhao, Shuang

Kinematic and kinetic characteristics of treadmill roller skiing and validation of force measurement roller skis

Jyväskylä: University of Jyväskylä, 2023, 85 p. + original articles

(JYU Dissertations

ISSN 2489-9003; 696)

ISBN 978-951-39-9744-1 (PDF)

Effective skiing biomechanics has been identified as one of the most important elements that could enhance performance in cross-country skiing. This study aimed to describe the biomechanical characteristics in treadmill roller skiing by simultaneously measuring the 2D forces from skis, the force from poles, and the kinematic data. The force acting on skiers' COM in the forward direction is the forward propulsion, and several approaches can be used to calculate it. These approaches were compared to discover the most suitable one (Article I). We mainly concentrated on the V2 skating technique, in which both skis and poles are used for forward propulsion. The biomechanical characteristics of this technique were investigated at different inclines (Article II) and speeds. The contributions from the skis and poles were also investigated while changing the treadmill speed using the point of view of external power (Article III). Finally, a new force measurement roller ski was validated for future studies (Article IV). Fourteen experienced skiers familiar with treadmill roller skiing participated in this study. Custom-made force measurement bindings, pole force sensors, and an eight-camera Vicon system were used to collect the force data and the trajectories of reflective markers (Article I-III). A pair of newly designed 2D force measurement roller ski, AMTI 3D force plates, and Vicon system were used as well (Article IV). The approach of calculating the forward component of GRF was found to be appropriate for quantifying the forward propulsion on a skier's COM (Article I). The cycle characteristics of the V2 skating technique were found to be affected by the treadmill incline (Article II) and the speed. From the propulsive force point of view, increasing both pole and ski force effectiveness was found to be needed at steeper grades, but the relative contribution of pole forces versus ski forces in overcoming the total resistance did not change with incline (Article II). While the treadmill speed was changed, the poles contributed more propulsive force and were more effective than skis in the skiing direction, and the contribution of legs slightly increased when the speed was increased. From the external power point of view, the relative contribution from the poles towards the total external power was smaller than when analyzed in the force domain (Article III) and was not affected by the increasing speed. Finally, the newly designed 2D force measurement roller ski was found to be valid for use in future research (Article IV).

Keywords: propulsive force, external power, contribution, effectiveness

TIIVISTELMÄ

Zhao, Shuang

Juoksumattorullahiihton kinemaattiset ja kineettiset ominaisuudet ja voimanmittausrullasuksien validointi

Jyväskylä: Jyväskylän yliopisto, 2023, 85 s. + alkuperäiset artikkelit

(JYU Dissertations

ISSN 2489-9003; 696)

ISBN 978-951-39-9744-1 (PDF)

Tehokas hiihdon biomekaniikka on tunnistettu yhdeksi tärkeimmistä tekijöistä, jotka voivat parantaa suorituskykyä murtomaahiihdossa. Tämän tutkimuksen tavoitteena oli kuvata juoksumattorullahiihdon biomekaanisia ominaisuuksia mittaamalla samanaikaisesti suksien 2D-voimat, sauvojen voimat ja kinemaattiset tiedot. Hiihtäjän massakeskipisteen eteenpäin vaikuttava voima on propulsio, ja sen laskemiseen voidaan käyttää useita lähestymistapoja. Näitä lähestymistapoja verrattiin sopivimman löytämiseksi (Artikkeli I). Tutkimuksessa keskityttiin pääasiassa V2-luistelutekniikkaan, jossa sekä suksia että sauvoja käytetään eteenpäin viemänä voimana. Tämän tekniikan biomekaanisia ominaisuuksia tutkittiin eri nousukulmilla (Artikkeli II) ja nopeuksilla. Myös suksien ja sauvojen suhteellista kontribuutiota tutkittiin muuttaessa juoksumaton nopeutta ulkoisen tehon näkökulmasta (Artikkeli III). Lopuksi uusi voimanmittausrullasuksi validoitiin tulevia tutkimuksia varten (Artikkeli IV). Tutkimukseen osallistui neljatoista kokenutta juoksumattorullahiihtoon perehtynyttä hiihtäjää. Räätelöityjä suksivoima- ja sauvavoima-antureita ja kahdeksan kameran Vicon-järjestelmää käytettiin voimatietojen ja heijastavien markkereiden liikeratojen keräämiseen (Artikkeli I-III). Lisäksi käytettiin äskettäin suunniteltuja 2D-voimanmittausrullasuksia, AMTI 3D -voimalevyjä ja Vicon-järjestelmää (Artikkeli IV). Eteenpäin suuntautuvan reaktiivoiman laskentatapa todettiin sopivaksi laskettaessa hiihtäjän massakeskipisteeseen vaikuttavaa eteenpäin vievää voimaa (Artikkeli I). V2-luistelutekniikan syklin ominaisuuksiin havaittiin vaikuttavan juoksumaton kaltevuus (Artikkeli II) ja nopeus. Propulsiovoiman näkökulmasta sekä sauvojen että hiihtovoiman tehokkuuden lisäämistä havaittiin jyrkemmällä nousukulmilla, mutta sauvavoimien suhteellinen osuus kokonaisvastuksen voittamiseksi ei muuttunut kaltevuuden myötä (Artikkeli II). Samalla kun juoksumaton nopeutta nostettiin, sauvat vaikuttivat enemmän propulsiovoimaan ja olivat tehokkaampia kuin sukset. Jalkojen suhteellinen osuus tosin kasvoi hieman, kun nopeutta nostettiin. Ulkoisen tehon näkökulmasta sauvojen suhteellinen panos ulkoiseen kokonaistehoon oli pienempi kuin pelkillä voima-arvoilla analysoituna (Artikkeli III), eikä lisääntyvä nopeus vaikuttanut siihen. Uusi 2D-voimanmittausrullasuksi havaittiin kelpaavan käytettäväksi tulevissa tutkimuksissa (Artikkeli IV).

Avainsanat: propulsiovoima, ulkoinen teho, tehokkuus

Author

Shuang Zhao
Faculty of Sport and Health Sciences
University of Jyväskylä, Finland
zhaosh@jyu.fi
0000-0002-7690-9582

Supervisors

Vesa Linnamo
Faculty of Sport and Health Sciences
University of Jyväskylä, Finland

Olli Ohtonen
Faculty of Sport and Health Sciences
University of Jyväskylä, Finland

Stefan Lindinger
Department of Food and Nutrition and Sport Science
University of Gothenburg, Sweden
LABIS-Laboratorio di Biomeccanica dello Sci
IIS Alberti Bormio, Italy

Reviewers

Barbara Pellegrini
Department of Engineering for Innovation Medicine
University of Verona, Italy

Erik Andersson
Swedish Winter Sports Research Centre
Mid Sweden University in Östersund, Sweden

Opponent

Walter Herzog
Faculty of Kinesiology
University of Calgary, Canada

ACKNOWLEDGEMENTS

This thesis was finished in 5 years from 2018 to 2023 and it was accomplished in the Sports Technology Unit, Vuokatti, Faculty of Sport and Health Sciences, University of Jyväskylä. I would like to express my deepest gratitude to all those people who have guided and supported me throughout my journey toward attaining this doctoral degree.

First of all, I would like to thank all of my supervisors. My main supervisor, Professor Vesa Linnamo, gave me the opportunity to study here. With the invitation letter he gave me, I could get the chance to apply for the scholarship to study abroad. I appreciate the guidance he gave me about my study and all his help in various aspects. My other supervisors, Professor Stefan Lindinger and Doctor Olli Ohtonen, I admire their experience and passion in the sport event cross-country skiing. I'm grateful for their advice and guidance on my articles and thesis.

I am also grateful to both of my reviewers for my thesis. Associate Professor Barbara Pellegrini from University of Verona and Associate Professor Erik Andersson from Mid Sweden University, thanks for their thorough review and the valuable comments which improved my final thesis. It is also my great honor to have Professor Walter Herzog from University of Calgary to be my opponent.

I want to express my gratitude to all the co-authors of my articles included in this study, Doctor Caroline Göpfert, Professor Lauri Kettunen, Mr. Timo Kananen, and Doctor Petri Koponen. Even though we haven't met each other face to face, I appreciate their contribution, help and patience while preparing and revising the articles.

I also want to thank all my colleagues in Vuokatti. Christina Mishica, Anni Hakkarainen, and Ritva Mikkonen who brought me a lot of company in my ordinary working life. I also want to thank Christina and Ritva for their help with the language revision of some of my articles. I appreciate that my colleague Oona Kettunen, Petra Torvinen, and Teemu Lemmettylä could be the participants in my study. I also want to thank Keijo Ruotsalainen, Teemu Heikkinen, Jarmo Piirainen, and Antti Leppävuori who helped me conduct the measurement, collecting the data, and find the subjects. In addition, I would like to express my gratitude to the athletes and coaches who participated in the study.

I would like to thank my friends Wen Luo, Lanju Zhao, Nijia Hu, Tiantian Yang, and Lili Tian who are in Finland, and my best friend Xiangnan Zhao as well as other friends who are in China. Thanks for their small talk from time to time and their emotional support during these years.

Finally, I want to express my gratitude to my mom Mrs. Junhua Zhang and my late father Mr. Yongcun Zhao. Thank them for their inclusiveness and understanding of all my decisions. Special thanks for the China Scholarship Council for their financial support for 48 months.

Sotkamo, 19.8.2023

Shuang Zhao

ORIGINAL PUBLICATIONS AND AUTHOR CONTRIBUTION

This thesis is based on the following original articles. The thesis also includes unpublished data.

- I. Zhao, S., Ohtonen, O., Ruotsalainen, K., Kettunen, L., Lindinger, S., Göpfert, C., & Linnamo, V. (2022). Propulsion calculated by force and displacement of center of mass in treadmill cross-country Skiing. *Sensors*, 22(7), 2777.
- II. Zhao, S., Lindinger, S., Ohtonen, O., & Linnamo, V. (2023). Contribution and effectiveness of ski and pole forces in selected roller skiing techniques on treadmill at moderate inclines. *Frontiers in Sports and Active Living*, 5.
- III. Zhao, S., Ohtonen, O., Linnamo, V., Ruotsalainen, K., Göpfert, C., Kettunen, L., Lindinger, S. The roles and contributions of skis and poles during treadmill V2 skiing technique at different speeds. (Submitted)
- IV. Zhao, S., Linnamo, V., Ruotsalainen, K., Lindinger, S., Kananen, T., Koponen, P., & Ohtonen, O. (2022). Validation of 2D force measurement roller ski and practical application. *Sensors*, 22(24), 9856.

All the original articles were written by the author considering the comments from the co-authors. The author, in collaboration with the co-authors, has designed the study questions and done the preparations and the data collections of the experiments. The author has had the main responsibility of the data preparation, data analysis, and the statistical analyses of all the articles.

ABBREVIATIONS

XC skiing	Cross-country skiing
DP	Double poling
V2 skating technique	Flat to moderate uphill terrain skating technique
COM	Center of mass
PFA	Point of force application
2D	2 dimensional
3D	3 dimensional
GRF	Ground reaction force
GCS	Global coordinate system
FCS	Force coordinate system
X, Y, Z	Axis of GCS
\vec{F}	Force calculated by multiplied the total mass of skier and the acceleration of COM
$\overrightarrow{F_{net}}$	Total GRFs
$\overrightarrow{F_{pro}}$	Total translational force
F, F_{net} , and F_{pro}	The Y component of \vec{F} , $\overrightarrow{F_{net}}$, and $\overrightarrow{F_{pro}}$ in GCS
CMC	Coefficient of multiple correlation
CR	Cycle rate
CL	Cycle length
PT	Poling time
RT	Recovery time for poles
KT	Kicking time
OLT	Overlap time
PGT	Pure gliding time
DCP	Duty cycle of pole
KT%	Kicking time of cycle
OLT%	Overlap time of cycle
PPF	Peak pole force
PKF	Peak kicking force
IMP	Resultant pole force impulse
IMPP	Propulsive pole force impulse
IMPV	Vertical pole force impulse
IML	Resultant leg force impulse
IMLP	Propulsive leg force impulse
IMLV	Vertical leg force impulse
IMT	Total force impulse
IMTP	Total propulsive force impulse
ACF	Average cycle force
APCF	Average propulsive cycle force
P_{tot}	Sum of ski and pole propulsive resultant power
P_{mean}	The sum of power against gravity and friction

FIGURES

FIGURE 1.	Equipment used in Experiment I.....	28
FIGURE 2.	2D force measurement roller ski.....	29
FIGURE 3.	Specialized equipment and an example of a static test.	31
FIGURE 4.	The definition of the push-off distance and the direction of the GCS in Experiment II.....	32
FIGURE 5.	The synchronization point and the push-off start point.	33
FIGURE 6.	The marker placement (without skis) and the geometric model for segments in the XC model.....	35
FIGURE 7.	Displacement of markers, PFA, and the definition of FCS.	37
FIGURE 8.	Diagram of force decomposition from skis.	38
FIGURE 9.	Illustrations of the GCS and the coordinate system moved with the treadmill.	39
FIGURE 10.	Definition of force producing phase of DP and V2 techniques....	41
FIGURE 11.	Time-force curves for skiers skating at 19km/h and the definition of action stages.....	42
FIGURE 12.	Definition of cycle and force variables and time-force curve of propulsive force with the V2 skating technique.....	44
FIGURE 13.	Cycle and kinetic characteristics of the V2 skating technique at 10km/h under different inclines.....	50
FIGURE 14.	Kinetic characteristics of the V2 skating technique at 10km/h under different inclines.	51
FIGURE 15.	Cycle characteristics at five different speeds under 2° incline.	52
FIGURE 16.	Kinetic characteristics in the V2 skating technique at different speeds under 2° incline.	54
FIGURE 17.	Linearity relation between mechanical power and skiing speed.	56
FIGURE 18.	Relative power contribution from the poles and the effectiveness of ski power.....	56
FIGURE 19.	The patterns of ski and pole forces, COM velocity, and ski and pole powers at 17km/h.....	58
FIGURE 20.	The mean positive and negative external power from skis while kicking and gliding at different speeds.	59
FIGURE 21.	The mean positive and negative external power from poles.....	60
FIGURE 22.	The relative difference in the resultant forces between the two force measurement systems.....	61
FIGURE 23.	Bland-Altman plot for the differences in the resultant force between two force measurement systems.....	62
FIGURE 24.	The coefficient of multiple correlation (CMC) for the time normalized force-time curve at different loads.	63

TABLES

TABLE 1.	Information of the subjects.	26
TABLE 2.	The calibration factors for each strain gauges mounted on the roller skis from the calibration done in December 2020.	30
TABLE 3.	The calibration factors for each strain gauges mounted on the roller skis from the calibration done in June 2022.	30
TABLE 4.	The vertical force combined expanded relative measurement uncertainty for different loadings.....	31
TABLE 5.	Values of the CMC for the DP technique (n = 9).	47
TABLE 6.	Values of the CMC for the V2 skating technique (n = 10).	47
TABLE 7.	Average absolute force difference between force curves with the DP technique (n = 9).	48
TABLE 8.	Average absolute force difference between force curves with the V2 skating technique (n = 10).	48
TABLE 9.	Cycle characteristics of the V2 skating technique at different speeds (N = 10).	53
TABLE 10.	Force characteristics of the V2 skating technique at different speeds (N = 10).	53
TABLE 11.	Comparison of Pmean and Ptot (n = 10).	55
TABLE 12.	The absolute difference (N) between force-time curves obtained by two force measurement systems in the X direction.	63
TABLE 13.	The absolute difference (N) between force-time curves obtained by two force measurement systems in the Z direction.	63

CONTENTS

ABSTRACT

TIIVISTELMÄ

ACKNOWLEDGEMENTS

ORIGINAL PUBLICATIONS AND AUTHOR CONTRIBUTION

ABBREVIATIONS

FIGURES AND TABLES

CONTENTS

1	INTRODUCTION	13
2	LITERATURE REVIEW	15
2.1	XC skiing techniques	15
2.2	Biomechanical characteristics of the DP and V2 skating techniques	16
2.2.1	Cycle characteristics	17
2.2.2	Kinetic characteristics	18
2.2.3	Center of mass and propulsion	20
2.3	Relative contributions of ski and pole forces	22
2.3.1	Relative contribution from the force domain	22
2.3.2	Relative contribution from the external power domain	23
3	PURPOSE OF THE THESIS	24
4	METHODS	26
4.1	Subjects	26
4.2	Experimental design	26
4.2.1	Experiment I	26
4.2.2	Experiment II	27
4.3	Data collection	27
4.3.1	Experiment I	27
4.3.2	Experiment II	29
4.4	Data processing	34
4.4.1	Labeling and filtering	34
4.4.2	Converting the measured forces from the force sensor into the GCS and the PFA	36
4.4.3	The translational force and the propulsive force	37
4.4.4	Propulsive force calculation when skiing at different inclines	38
4.4.5	Power calculation	39
4.4.6	Force calculation of the force measurement roller ski	40
4.4.7	Cycle definition and analyzed parameters	41
4.5	Statistical methods	45

5	RESULTS	46
5.1	The similarity (CMC) and the average absolute force differences between force-time curves (Article I)	46
5.2	Biomechanical characteristics of the V2 skating technique at different inclines (Article II)	49
5.3	Biomechanical characteristics of the V2 skating technique at different speeds	51
5.3.1	Cycle characteristics	51
5.3.2	Force characteristics	52
5.3.3	Contribution and effectiveness	55
5.4	The roles of skis and poles during the V2 skating technique at different speeds (Article III)	57
5.5	Validation of the 2D force measurement roller ski (Article IV)	61
6	DISCUSSION	64
6.1	Evaluation of different methods to calculate propulsion (Article I)	64
6.2	Biomechanical characteristics of the V2 skating technique at different inclines (Article II)	65
6.3	Biomechanical characteristics of the V2 skating technique at different speeds	67
6.3.1	Cycle characteristics	67
6.3.2	Force characteristics	68
6.3.3	Contribution and effectiveness	68
6.4	The roles of skis and poles during the V2 skating technique at different speeds (Article III)	71
6.5	Validation of a 2D force measurement roller ski (Article IV)	73
6.6	Limitations	74
7	MAIN FINDINGS AND CONCLUSIONS	75
	REFERENCES	77

ORIGINAL PUBLICATIONS

1 INTRODUCTION

In cross-country (XC) skiing, races and training are typically done at various speeds and on diverse track topographies. There are two fundamental skiing styles: classical and skating (often referred to as freestyle). The classical style has three main sub-techniques: double poling (DP), diagonal stride (DS), and kick double pole (KDP) (Smith, 2003, pp. 32-61); and the skating style has six sub-techniques: V1, V2, V2A, and so on (also referred to as Gear 2-7) (Andersson et al., 2010; Nilsson et al., 2004). Skiers modify these sub-techniques impulsively to sustain high speed and adapt to the changing terrains (Bilodeau et al., 1992; Ettema et al., 2017; Nilsson et al., 2004). Several studies have examined how speed and incline affect XC skiing athletes' metabolic efficiency (Løkkeborg & Ettema, 2020; Sandbakk et al., 2012; Sandbakk et al., 2013b), the shift in their skiing techniques (Ettema et al., 2017; Stöggl et al., 2018), and the changes in biomechanical characteristics (Lindinger & Holmberg, 2011; Lindinger et al., 2009; Millet et al., 1998c; Nilsson et al., 2013; Ohtonen et al., 2016; Stöggl & Holmberg, 2015). It has been identified that having effective skiing biomechanics is one of the most important elements that could enhance skiing performance (Hebert-Losier et al., 2017). Moreover, understanding how speed and incline influence skiing biomechanics may help skiers, coaches, and instructors improve the skiing techniques.

Propulsive force (Smith, 2003, pp. 32-61), typically defined as the forward direction component of the resultant reaction force from skis and poles acting on skiers (Stöggl & Holmberg, 2015), is the main mechanical factor affecting a skier's performance. Although Göpfert et al. (2017) demonstrated that the forward component of translational force is appropriate for determining the acceleration of XC skiers' center of mass (COM) during leg skating push-off, external forces will still cause a rigid body to accelerate in direct proportion to the magnitude of the force and in the same direction as the force (Caldwell et al., 2013, p. 80). The translational force was modeled as a part of the resultant reaction force from the skis and poles that acts in the direction from the point of force application (PFA) to the skier's COM (Göpfert et al., 2017), and it is calculated by projecting the resultant reaction force from the skis and poles to the line defined by the COM

and PFA. However, besides leg skating push-off, whether other skiing movements could use the forward component of translational force to estimate the acceleration of COM has not been investigated.

Early investigations (Komi, 1987; Leppävuori et al., 1993; Vahasoyrinki et al., 2008) directly measured the ski and pole forces using 2- or 3-dimensional (2D or 3D) force platforms buried in the snow. The forces from skis and poles were measured individually using instrumented roller skis (Hoset et al., 2014; Smith et al., 2006; Stöggl & Holmberg, 2015), skis (Göpfert et al., 2017; Ohtonen et al., 2018), pressure insoles (Andersson et al., 2014b; Stöggl & Holmberg, 2015), and instrumented poles (Göpfert et al., 2017; Ohtonen et al., 2018; Stöggl & Holmberg, 2015). As a result, many approaches have been used to address the issues relating to propulsive force in XC skiing, such as the relative contributions of the ski and pole forces to the total propulsion (Andersson et al., 2014b; Holmberg et al., 2006; Stöggl & Holmberg, 2015). Most of the studies on the relative contributions of ski and pole forces to overall propulsion were mainly focused on the forward direction by utilizing the propulsive force (Smith et al., 2006; Stöggl & Holmberg, 2015). Forces in the forward direction are crucial for sustaining a high speed in the intended direction during races. However, when the skate skiing technique is used, the sideward movement would somehow affect the forward velocity. Therefore, the sideward movement should also be considered (de Koning & van Ingen Schenau, 2008, pp. 232-245; Sandbakk et al., 2012; Sandbakk et al., 2013a).

The function of the extremities during locomotion involving lateral movement has been evaluated using external power analysis (Yamashita et al., 2017). The external power equals to the dot product of the force vector acting on the limb and the velocity vector of the COM. Consequently, the COM velocity and the force are related. Methodologically, whether the relative contribution from skis and poles is the same when analyzed in the energetic domain (power) and the kinetic domain (force) could be questioned. Furthermore, it is necessary to discuss how the contributions, propulsive force, and effectiveness of skis and poles alter with increasing speed and slope. Though force could be measured using a variety of systems, a valid, accurate, and lightweight system capable of synchronously measuring multiple force components is still required.

Therefore, this study will focus on the biomechanical characteristics of XC skiing on a treadmill. Since the DP and V2 skating (Gear 3) techniques have become the primary sub-techniques in XC skiing (Sandbakk & Holmberg, 2014; Stöggl & Holmberg, 2016; Stöggl et al., 2008), they will be used at varying speeds and inclines in this study. The method demonstrated by Göpfert et al. (2017) to compute forward propulsion will be re-evaluated in a controlled environment, and a new force measurement roller ski will be validated from a methodological and force-measuring equipment standpoint.

2 LITERATURE REVIEW

2.1 XC skiing techniques

XC skiing is a physically demanding activity that requires the cardiovascular system and a large number of muscles. There are two fundamental skiing techniques in XC skiing: classical style and skating style (also known as freestyle). Each fundamental skiing has several sub-techniques.

DP, DS, and KDP are sub-techniques of classical style XC skiing (Smith, 2003, pp. 32-61). The DP technique incorporates symmetrical arm movements and fewer leg movements. It consists of a poling phase and a recovery phase. Significant trunk and lower limb flexion are also required, and as previous studies have indicated, a more dynamic use of the legs may improve the utilization of body mass and gravitation (Holmberg et al., 2006; Holmberg et al., 2005). Typically, the DP technique is utilized in swift conditions or on flat or minor to moderately uphill terrains. The DS technique, which is used for the uphill parts during races, involves the poling and kicking phase. When one arm is poling, a brief opposite-leg kicking action is included. In this technique, both the pole and ski reaction forces contribute to propulsion. The KDP technique entails a brief ski kick before the poling action. A kicking motion is added to a DP technique to increase the total propulsive force. KDP is used in moderate uphill.

The skating style XC skiing has six distinct sub-techniques, or gears (Gear 2-7) (Andersson et al., 2010; Nilsson et al., 2004). The V1 skating technique (Gear 2), which is normally used under large resistive force conditions such as uphills, involves an asymmetric DP motion synchronized with a skating stroke on the strong side. When the opposite, or weaker, leg side is striking, the arms are in a phase of recovery. Several studies have investigated this technique using different perspectives (Bowen et al., 2009; Millet et al., 1998c; Myklebust et al., 2014; Stöggl et al., 2013b; Stöggl & Holmberg, 2015). The V2 skating technique

(also known as Gear 3) is primarily utilized on flat or moderately ascending terrains. Occasionally, it is employed even on steeper inclines (Ohtonen, 2019, p. 15). Every leg stroke in this technique entails symmetrical pole propulsion (Smith, 2003, pp. 32-61), and the propelling force is generated by both skis and poles (Ohtonen et al., 2019; Smith et al., 2010). The V2 alternate skating technique (Gear 4) involves a single poling motion for two leg strokes. It is utilized on flat terrains and mild downhill at high speed (Andersson et al., 2010; Göpfert et al., 2016). The skating without poles technique (Gear 5) only involves leg strokes. The Gear 6 and Gear 7 techniques were introduced by (Andersson et al., 2010) as curve technique and downhill tuck technique, respectively.

To sustain high speeds and adapt to changing terrains, skiers alter their sub-techniques spontaneously (Danielsen et al., 2019) in both classical and skating skiing (Bilodeau et al., 1992; Ettema et al., 2017; Nilsson et al., 2004). In recent years, in classical XC skiing races, the use and significance of the DP technique has increased, owing to enhanced upper body strength, more systematic strength training, and faster skiing speeds (Sandbakk & Holmberg, 2014; Stöggl & Holmberg, 2016). Similarly, in freestyle XC skiing races, the V2 skating technique has become the most common technique (Andersson et al., 2010; Stöggl et al., 2008). According to Andersson et al. (2010), skiers would have better races if they use the V2 skating technique more commonly. Thus, due to the increased use and significance of the DP and V2 skating techniques during the races in recent years (Sandbakk & Holmberg, 2014; Stöggl & Holmberg, 2016; Stöggl et al., 2008), this study primarily investigated the biomechanical characteristics of these two sub-techniques.

2.2 Biomechanical characteristics of the DP and V2 skating techniques

Skiers engaged in both classical and skating styles XC skiing change their sub-techniques spontaneously to sustain high speed and adapt to changing terrains (Bilodeau et al., 1992; Ettema et al., 2017; Nilsson et al., 2004). Some researchers have investigated the influence of speed and incline on metabolic efficiency (Løkkeborg & Ettema, 2020; Sandbakk et al., 2012; Sandbakk et al., 2013b), technique shift (Ettema et al., 2017; Stöggl et al., 2018), and changes in biomechanical characteristics (Lindinger & Holmberg, 2011; Lindinger et al., 2009; Millet et al., 1998c; Nilsson et al., 2013; Ohtonen et al., 2016; Stöggl & Holmberg, 2015) in XC skiing. Effective skiing biomechanics have been identified as one of the most important performance-enhancing factors (Hebert-Losier et al., 2017). Moreover, skiers and instructors may benefit from a greater understanding of the influence of speed and incline on skiing biomechanics when attempting to improve their skiing techniques.

2.2.1 Cycle characteristics

In XC skiing, it has been demonstrated that optimizing the cycle rate (CR) and the cycle length (CL) is associated with high skiing speeds in various skiing techniques (Andersson et al., 2014a; Sandbakk et al., 2010; Stöggl et al., 2011). As per the initial findings from field skiing (Nilsson et al., 2004; Ohtonen et al., 2016) and field roller skiing (Millet et al., 1998a; Millet et al., 1998c), when the speed was increased from submaximal to maximal, the CL reached a plateau, while the CR continued to grow. Compared to treadmill roller skiing—during which the friction coefficient has been proved to be constant (Sandbakk et al., 2012; Sandbakk et al., 2010)—field skiing may have a changeable friction coefficient, which may limit the usage of continuous increase in the CL (Ohtonen et al., 2016). Moreover, previous studies have indicated that, while using the V2 skating technique, increases in speed are associated with enhanced in CR and CL (Sandbakk et al., 2012), and that elite skiers can increase both of them continuously up to high speeds when roller skiing using the DP technique (Lindinger et al., 2009). This is also consistent with what has been observed in other human locomotion: that the CR and CL increased when the submaximal speed was increased (Hay, 2002). Regarding an increase in incline, when using the V2 (Bilodeau et al., 1992), V1, and DP technique, the CL was found to be shorter at steeper inclines (Millet et al., 1998b), while the CR was greater (Bilodeau et al., 1992; Millet et al., 1998b; Sandbakk et al., 2012; Stöggl et al., 2018).

The poling and swing action of arms in the DP and V2 skating techniques, as well as the kicking, gliding, and overlap actions of skis in the V2 skating technique, have also been investigated. The poling time (PT) during the techniques was found to decrease with increasing speed (Dahl et al., 2017; Danielsen et al., 2019, 2021; Lindinger et al., 2009; Millet et al., 1998c; Ohtonen et al., 2018; Ohtonen et al., 2016; Stöggl et al., 2013a; Stöggl & Muller, 2009; Stöggl et al., 2011). In the V2 skating technique, the ground contact time and the relative ground contact time of the legs remained constant for the submaximal speed and decreased toward the maximal speed (Ohtonen et al., 2016; Stöggl & Muller, 2009). The legs' overlap time increased by 33% when the speed increased from slowest to fastest (Ohtonen et al., 2016). Another study found that, in the DP technique, the PT at steeper inclines was longer than the PT at gentle inclines (Danielsen et al., 2019). In addition, in both techniques, the proportion of the cycle used to generate pole forces increased as the incline of the treadmill increased (Millet et al., 1998b).

After reviewing the literature, it appears that cycle characteristics have been investigated in most of the studies, and how they change to adapt to changes in speeds and inclines has been demonstrated. Most of the cycle characteristics analyzed are spatio-temporal parameters. This may be due to the relative ease of obtaining these parameters. Using a video-based system (e.g., a commonly used camera (Stöggl & Muller, 2009) or an infrared camera system (Göpfert et al., 2017), an accelerometer affixed to the skis or poles (Ohtonen et al., 2015), and force measurement systems (Ohtonen et al., 2013a; Stöggl & Holmberg, 2015; Stöggl & Martiner, 2017), the cycle characteristics could be obtained.

2.2.2 Kinetic characteristics

Early studies measured the ski and pole forces directly using 2D or 3D force platforms buried in snow (Komi, 1987; Leppävuori et al., 1993; Vahasoyrinki et al., 2008). Using instrumented roller skis (Hoset et al., 2014; Smith et al., 2006; Stöggl & Holmberg, 2015), skis (Göpfert et al., 2017; Ohtonen et al., 2018), and poles (Göpfert et al., 2017; Ohtonen et al., 2018; Stöggl & Holmberg, 2015), the forces generated from skis and poles can be measured separately. The researchers mainly investigated the kinetic parameters directly from the GRFs (peak force, average force, and so on), propulsive force, or associated impulse.

2.2.2.1 Force measurement in cross-country skiing

Researchers have access to numerous instruments for measuring ground reaction forces (GRFs). There are three primary methods for measuring the GRFs from skis in XC skiing: (1) using the external force plates buried in the snow, (2) using the pressure insoles or accelerometer sensor insoles inserted in footwear, and (3) using the instrumented skis or roller skis.

In early studies, force measurement systems buried in snow were used to measure the GRFs between skis and snow (Komi, 1985; Komi, 1987; Komi & Norman, 1987; Leppävuori et al., 1993; Vahasoyrinki et al., 2008). In XC skiing, the first under-snow force measurement system was a long force platform system (Komi, 1985; Komi, 1987), which had four rows of 6m-long force plates and could independently record the vertical and anterior-posterior forces of each ski and pole (Komi, 1985; Komi, 1987). Later, a similar system with four separate 20m-long rows of 1m-long force plates connected in series was devised (Vahasoyrinki et al., 2008). These systems enable skiers to freely ski on snow while simultaneously recording the force data. Due to the length and design of the force plate, only two or three ski contacts could be measured for one trial of classical XC skiing (Komi, 1987; Komi & Norman, 1987; Vahasoyrinki et al., 2008). Leppävuori's system (Leppävuori et al., 1993) could measure the GRFs using the skating technique. This system had 20 horizontal beams fitted with three strain gauge bridges for measuring the 3D forces operating on each beam. These beams were attached to a sturdy aluminum frame to form a 2.2m-long force platform. This system could measure 3D GRFs, but the skiers were required to position their skis directly over the force plate and avoid placing their poles on the plate. In addition, only one ski contact could be recorded per trial (Leppävuori et al., 1993). Although the force measurement systems which buried in the snow had no influence on the skiing technique, the movement was restricted to a small area. Consequently, a more adaptable ski force measurement apparatus was employed and developed.

In XC skiing research, pressure insoles have been utilized extensively to estimate the ski forces (Holmberg et al., 2005; Lindinger et al., 2009; Stöggl & Holmberg, 2015; Stöggl et al., 2010; Stöggl et al., 2011). Unlike force measurement systems submerged in snow, the insoles enabled researchers to measure multiple consecutive cycles and precisely determine the center of pressure. Moreover,

they were found to barely influence the skier's performance. Despite these benefits, the pressure measurement only provided forces in one unknown direction and could be unreliable, as the insoles may not detect all the forces transmitted between the foot and footwear (Hoset et al., 2014). Moreover, skiers must tote the data collection and/or data transfer equipment. Though one sensor insole containing a 3D accelerometer has been validated, it was only recommended for the detection of cycle characteristics and temporal parameters (Stöggl & Martiner, 2017).

Several studies have measured the forces between ski boots and skis (or roller skis) by attaching force transducers to the ski or roller ski bindings. To measure the forces in two (Ekström, 1987; Komi, 1987; Pierce et al., 1987; Street & Frederick, 1995) or three (Babiel, 2003; Ohtonen et al., 2013b) dimensions, small force measurement plates were attached to the skis. These plates were added to the bindings introduced by Komi (1987). The vertical and anterior-posterior forces were measured while skiing on snow, but the system was limited to one ski and could not be used with the skate skiing technique, which involves medio-lateral movements. The small force plates were implemented similar to roller ski bindings (Street & Frederick, 1995). The vertical and medio-lateral forces were then measured, but the equipped roller ski was approximately 50% heavier than the standard roller ski. In some experiments (Linnamo et al., 2012; Ohtonen et al., 2013a; Pierce et al., 1987), strain gauges were installed on the bindings to measure forces in multiple dimensions. Ohtonen et al.'s (2013a) force measurement bindings were used with the skis on snow (Göpfert et al., 2017; Ohtonen et al., 2018; Ohtonen et al., 2019; Ohtonen et al., 2016), and they are compatible with various skis and roller skis. However, their increased weight and height of these bindings may hinder the skier's performance (Ohtonen, 2019, p. 63).

Roller skiing is a primary training method for the majority of skiers during the dry land training season (Street & Frederick, 1995), and it is a ski-specific laboratory testing model that could examine skiing techniques in greater detail (Watts et al., 1993). Instrumented roller skis were thus devised (Bellizzi et al., 1998; Hladnik et al., 2018; Hoset et al., 2014). Strain gauges were mounted directly on the roller skis to measure the vertical (Bellizzi et al., 1998; Hoset et al., 2014) and anterior-posterior (Bellizzi et al., 1998) forces. Due to the predominant sagittal movement, these force measurement roller skis are ideal for analyzing classic techniques. However, skating techniques involve more 3D and medio-lateral movements. According to the findings of a previous study, as the friction coefficient increased in the skating technique, the lateral forces increased, but the vertical forces remained unaffected (Ohtonen et al., 2013b). This demonstrates the significance of measuring lateral forces. Using instrumented force measurement roller skis that can measure medio-lateral forces could be benefit research on skate skiing style. Though ski forces can be measured using multiple systems in XC skiing, there remains a need for a valid, and user-friendly system that can simultaneously measure multiple force components.

2.2.2.2 Forces and propulsive forces in the DP and V2 skating techniques

The common and basic force parameters analyzed in previous studies were peak, and the average forces measured using ski and pole force measurement systems (Millet et al., 1998b, 1998c; Ohtonen et al., 2016; Stöggl & Holmberg, 2015). A study accomplished on snow by Ohtonen et al. (2016) reported that higher forces from both arms and legs were generated at higher speeds with V2 skating technique. Millet et al. (1998b, 1998c) discovered that, when using the V2 skating technique, the increased speed and incline influenced the poling forces. For both the DP and V2 skating techniques, the peak pole force (PPF) increased with increasing submaximal speed (Danielsen et al., 2019; Ohtonen et al., 2016; Stöggl & Holmberg, 2016). However, for the DP technique, the PPF at the maximal speed has no difference when compared to the PPF force at submaximal speed (Stöggl et al., 2011). PPF, average pole force, and average cycle pole force were all greater in circumstances with a steeper incline for both DP and V1 skating technique (Millet et al., 1998b). Moreover, the PPF reported in the recent studies was about 150% greater than the PPF reported a decade ago (Stöggl & Holmberg, 2022).

In XC skiing, the term “propulsive force” refers to the forward component of the 3D resultant reaction force generated by skis and poles that acts on skiers (Stöggl & Holmberg, 2015). During classic skiing (e.g., DS), it is easier to calculate the propulsive (horizontal forward) force components of skis and poles, especially when the skis are kept in the prepared forward-directed double tracks. However, when it comes to the skating techniques, the ski orientation, ski-edging angle, and the track incline must be considered to specify the propulsive forces from skis (Smith, 1992; 2003, pp. 32-61; Stöggl & Holmberg, 2015).

2.2.3 Center of mass and propulsion

2.2.3.1 The center of mass

A rigid body's COM is the location where a body's mass is concentrated (Selbie et al., 2013, pp. 159-160). Though several approaches can be used to determine COM's position in sports, segmental method has been deemed the most suitable one (Mapelli et al., 2014). By assuming that all the segments behave as rigid bodies, the COM can be quantified using the segments' parameters (Selbie et al., 2013, pp. 159-160) derived from past anthropometric studies and the position of the anatomical land markers detected by motion capture system.

The model and marker set used for COM estimation should always be according to the purpose of the specific analysis (Rabuffetti & Baroni, 1999). For example, the position of one marker attached to the pelvis can be used to represent the vertical COM displacement in gait analysis (Kerrigan et al., 1995), but not the horizontal COM displacement in the standing activity (Eng & Winter, 1993). In XC skiing, a 14-marker 11-rigid-segment model has been used to estimate the position of the skier's COM (Pellegrini et al., 2014) while estimating the mechanical work. However, when estimating the position of COM while calculating the propulsion contributed to a skier's COM acceleration, a 51-marker 19-rigid-segment model, named as XC model, has been used, and the skis and

poles were added as additional segments included in these 19 segments (Göpfert et al., 2017). The XC model used for propulsion calculation has been validated and the accuracy of the COM in space has been tested (Göpfert et al., 2017).

2.2.3.2 Propulsion calculated by force and center of mass

Propulsive forces, which act on an XC skier's COM in a forward direction, are the main mechanical factors that determine their performance (Smith, 2003, pp. 32-61). A marker-based motion capture system with a segmental technique can be used to locate the COM (Mapelli et al., 2014). The forces exerted on a skier's COM can be thus calculated by multiplying the COM acceleration by the skier's total mass. This will reveal how skiers overcome resistive forces. Leg and pole thrusts could both contribute to the skiing movement, but their contribution cannot be determined separately using this calculation. Therefore, other approaches are needed to separately calculate the forces generated by the skis and poles that act on the COM.

Other methods have been developed, in addition to calculating the propulsive force using the forward acceleration of COM and the total mass. One method involves calculating the propulsive force as the horizontal component facing forward in the 3D GRFs from the skis and poles acting on the skier (F_{net}) (Stöggl & Holmberg, 2015). The forces produced by the skis and poles have been measured using roller skis (Hoset et al., 2014; Smith et al., 2006; Stöggl & Holmberg, 2015), skis (Göpfert et al., 2017; Ohtonen et al., 2018), and poles (Göpfert et al., 2017; Ohtonen et al., 2018; Stöggl & Holmberg, 2015) fitted with force sensors. The propulsive force from skis and poles can be calculated by combining the pole angle, ski angle, ski-edging angle, and treadmill or track inclination (Smith, 1992, 2003; Stöggl & Holmberg, 2015). Another method involves estimating the propulsive force using the forward component of translational force (F_{pro}), as shown by Göpfert et al. (2017). The translational force was estimated by projecting the GRFs to the line delineated by the COM and the PFA (Göpfert et al., 2017).

The propulsive forces computed using COM acceleration from a motion analysis system (F) in (Göpfert et al., 2017) were compared to the propulsive forces produced using the two aforementioned methodologies (F_{net} and F_{pro}). F was used as the reference value, as it has been demonstrated that the segmental technique is appropriate for determining the position of the COM in sports (Mapelli et al., 2014). The findings showed that, when compared to the force-time curves of F during the leg skating push-offs on snow, the force-time curves of F_{net} and F_{pro} all showed high similarity. F_{pro} was found to be a more suitable method for estimating F during leg skating push-offs (Göpfert et al., 2017). However, the accuracy of F_{net} and F_{pro} and whether they can be used to estimate F in other skiing styles remain unknown. Since XC skiing is a sport in which training and competition are typically conducted on tracks with varying topography and speed, further research is needed to determine whether F_{net} and F_{pro} could work steadily when estimating F at various terrains and speeds.

2.3 Relative contributions of ski and pole forces

2.3.1 Relative contribution from the force domain

Since knowing the role of pole and ski forces may offer possibilities for technique diagnosis, their relative contributions to the skate skiing movement have also been investigated. Their contributions are normally quantified using the propulsive force (Smith et al., 2006; Stöggl & Holmberg, 2015), which is often defined as the horizontal component of the resultant force from the skis (Smith, 1992; 2003, pp. 32-61; Stöggl & Holmberg, 2015) and poles (Smith, 2003, pp. 32-61; Stöggl & Holmberg, 2016). The contribution from poles and legs is normally calculated by expressing the propulsive impulse of poles and legs as a percentage of the total propulsive impulse (Göpfert et al., 2017). The effectiveness index is calculated for poles and legs separately by expressing the impulse of propulsive force as a percentage of the impulses of the pole and leg resultant force impulses, respectively (Stöggl & Holmberg, 2015). One study indicated that for the V2 skating technique, while the treadmill speed ranged from moderate ($2.5 \pm 0.2\text{m/s}$) to race speed ($3.4 \pm 0.3\text{m/s}$), about two-thirds of the propulsive force was from the force from poles and one-third from the skis (Smith et al., 2006). Another study indicated that, although more propulsive force was generated from skis in the V1 skating technique (Smith et al., 2006), 44% of the total propulsive force was still generated from poles and was shown to be more effective than the legs at any speed (Stöggl & Holmberg, 2015). Additionally, faster skiers were more effective when transforming the resultant force into propulsive force (Stöggl & Holmberg, 2015). Moreover, more well-synchronized poling and more symmetric forces from legs were demonstrated by faster skiers using the V1 skating technique (Stöggl & Holmberg, 2015). The symmetry of the force generated from both skis and poles may influence a skier's skiing performance. Because of the companion of a DP action for each skating stroke on each side, the V2 skating technique was treated as a symmetrical technique (Smith, 2003, pp. 32-61).

The DP and V2 skating techniques are typically utilized on flat grounds and mild uphill. Since the propulsive forces are only applied through poles, the DP technique has frequently been considered to involve upper body movements (Gaskill et al., 1999; Hoff et al., 1999; Mittelstadt et al., 1995). However, it is obvious that legs also contribute to the performance (Holmberg et al., 2006; Holmberg et al., 2013). In the V2 skating technique, both skis and the poles generate propulsive force (Ohtonen et al., 2019; Smith et al., 2010). Existing literature highlighted that the majority of the total propulsive force in skate skiing techniques is attributed to the forces exerted from the poles (Göpfert et al., 2017; Smith et al., 2006). However, there remains a need for further research to fully understand how ski and pole forces are used to maintain speed on different uphill inclines. The relative efficiency of the ski and pole forces in overcoming the total external resistance of both DP and V2 skating systems at various moderate uphill inclines should thus be investigated.

2.3.2 Relative contribution from the external power domain

The majority of the research on the comparative contribution of ski and pole forces to total propulsion is centered on forward motion. Typically, the contributions of these forces are measured using the propulsive force (Smith et al., 2006; Stöggl & Holmberg, 2015). As mentioned previously, approximately two-thirds of the forward propulsive force for the V2 skating technique is ascribed to the force from the poles, and one-third is attributed to the forces from the skis (Smith et al., 2006). To be competitive in contests, it is essential to maintain high speed in the desired direction, so forces in the forward direction are crucial. In contrast, in skate skiing, the combination of leg push-off and poling action propels the skier forward in a “zig-zag” motion (Sandbakk et al., 2013a). The leg push-off is executed perpendicular to the gliding ski (Sandbakk et al., 2012), which may result in a sideward velocity of COM that can be added to the gliding velocity in a more or less forward direction (de Koning & van Ingen Schenau, 2008, pp. 232-245). Therefore, the sideward movement in the V2 skating technique must also be considered.

External power analysis has been used to evaluate the role of limbs during the locomotion that contains sideward movements (Yamashita et al., 2017). The external power is the dot product of the force vector that acts on the limb and the COM velocity vector. The COM velocity and the force vectors are thus related. In forward and sideward walking, negative work is required by the leading leg when the heel makes contact with the ground to redirect the COM velocity (Donelan et al., 2002; Yamashita et al., 2017). Similar to walking, alternate supports on the left and right legs and a double support (overlap) phase have been found in the V2 technique. However, from the perspective of external power, how kicking and gliding ski would act to redirect the COM velocity in the V2 technique remains unclear.

In addition, mechanical power is often used in sport science for research and training purposes to estimate the muscular work (van der Kruk et al., 2018). Knowing how the external power is delivered and from what source (poles versus skis) at different speeds may benefit training and testing processes and help understand performance-related questions. However, it might be questioned from a methodological perspective whether the relative contribution from skis is the same when analyzed in the energetic domain (power) as when analyzed in the kinetic domain (force).

3 PURPOSE OF THE THESIS

Effective biomechanics involving propulsive forces are pivotal components influencing skiing performance. The calculation of propulsive forces in XC skiing and the joint involvement of ski and pole forces, can be approached in various methodologies. It is essential to determine the most appropriate approach, particularly within a controlled treadmill setting. Exploring how changes in treadmill speed and incline may impact the contribution and effectiveness of ski and pole forces within proper skiing technique is also an important focus. Therefore, the main purpose of this study was to describe the biomechanical characteristics in treadmill roller skiing, by measuring the 2D forces from skis and poles and the kinematic data simultaneously. Initially, three different methods for computing forward propulsion were compared to ascertain the optimal way for quantifying the propulsion. Subsequently, the study predominantly centered on analyzing the V2 skating technique as both ski and pole contribute to the whole V2 skating movement. Due to experiences in experiment, it was found that there is a need for a new sensor system which is lighter and more portable. Consequently, a newly designed 2D force measurement was validated at last.

The specific aims of the current thesis were:

1. Re-evaluate the approach developed by Göpfert et al. (2017) and find a proper way to quantify the propulsive force in future studies. Apply the method introduced by Göpfert et al. (2017) and calculate the propulsion for the DP and V2 techniques in a controlled environment (indoor treadmill roller skiing); evaluate and compare the two different mentioned methods (the forward component of the translational force and the forward component of the GRFs) to quantify forward acceleration while using the DP and V2 techniques; and investigate the stability of the methods to calculate the propulsive force by changing the treadmill speed and incline (Article I).
2. Provide the biomechanical characteristics of the V2 skating technique and compare the contribution and force effectiveness of skis and poles at different inclines (Article II).

3. Provide the biomechanical characteristics of the V2 skating technique and compare the contribution and force effectiveness of skis and poles regarding the force generated at a wide range of skiing speeds. Understanding how external power is delivered and from what source (poles versus skis) at different speeds may help training and testing processes and understand performance-related questions. This study will also compare the relative contributions and effectiveness of ski and pole power to the total external power at different speeds (Article III).
4. Validate a newly designed custom-made force measurement roller ski (Article IV).

Hypotheses:

1. The force-time curves of the forward propulsion obtained using the method of Göpfert et al. (2017) would offer a comparable shape with the reference force-time curves in both techniques; the force-time curves of the forward propulsion obtained using the method of Göpfert et al. (2017) would be more accurate than the curves obtained using another approach (Smith, 2003, pp. 32-61) when compared with the reference force-time curves (Göpfert et al., 2017)(Article I).
2. While using the V2 skating technique, pole forces would contribute more and would be more effective than ski forces in overcoming the total resistance (Smith et al., 2006; Stöggl & Holmberg, 2015). The relative contribution of ski forces would increase at steeper inclines (Article II).
3. From the kinetic domain (force), the relative contributions of the pole forces in overcoming external resistance would be greater than that of ski forces (Smith et al., 2006). In addition, the forces generated from poles would be more effective than the forces generated from skis in overcoming external resistance. From the energetic domain (power), over a cycle, the sum of pole and ski propulsive power would be equal to the sum of the power against gravity and friction (Danielsen et al., 2019). Since sideward and vertical movements were also involved in the power analysis (Dahl et al., 2017; Danielsen et al., 2019; van der Kruk et al., 2018; Yamashita et al., 2017), we hypothesized that the effectiveness and contribution of ski power to the total external power would be greater than what has been demonstrated from kinematic domain in a previous study (Smith et al., 2006) with the V2 skating technique (Article III).
4. The newly designed force measurement roller skis would be valid and appropriate for measuring forces while using skate skiing techniques. (Article IV).

4 METHODS

4.1 Subjects

Fourteen experienced skiers (TABLE 1) familiar with treadmill roller skiing participated in this study. Ten male subjects participated in the Experiment I, while two male and two female subjects participated in the Experiment II. The experimental protocol and the methods utilized in this Ph.D. study were approved by the Ethics Committee of the University of Jyväskylä. All the participants provided their written informed consent.

TABLE 1. Information of the subjects.

Experiment No.	Participants (n)	Age (years)	Height (cm)	Weight (kg)	Article
Exp I	10	29.4 ± 7.9	181.4 ± 5.7	77.9 ± 8.9	I, II, IV
Exp II	4	30.0 ± 8.8	173.4 ± 9.0	68.8 ± 15.6	III

4.2 Experimental design

4.2.1 Experiment I

This experiment aimed to re-evaluate the approach introduced by Göpfert et al. (2017) to calculate the forward propulsion (Article I) and investigate the biomechanical characteristics at different inclines (Article II) and different speeds (Article III). First, the anthropometric parameters required for motion analysis were measured, followed by the attachment of passive reflective markers to the participants and the skiing apparatus. After preparations, to warm up, the participants roller skied on a treadmill for 10min to 15min. Next, calibration was performed, with the skier standing and the incline of the treadmill set to 0°. On

an incline of 2°, the participants conducted the DP technique at five different speeds (13km/h, 15km/h, 17km/h, 19km/h, and 21km/h). The technique was then executed at 3°, 4°, and 5° inclines at a speed of 10km/h. Between each speed and incline, there was a 1min break. After the DP technique was completed, the participants' poles were adjusted to a comfortable length for the V2 skating technique. The pole length for the DP technique was $1.56 \pm 0.06\text{m}$ ($86\% \pm 2.5\%$ of body height), and the pole length for the V2 skating technique was $1.63 \pm 0.03\text{m}$ ($90\% \pm 1.3\%$ of body height). After this, the participants conducted the V2 skating technique on the treadmill. The speed and incline modification protocols were identical to that of the DP test.

4.2.2 Experiment II

This experiment was conducted to validate a newly designed roller ski that could measure the forces in 2D. The Technical Research Center of Finland (VTT MIKES, Kajaani, Finland) performed the initial calibration measurement. It was possible to measure the forces that perpendicularly affected the roller ski's body in the vertical and medio-lateral directions. The forces were converted into the global coordinate system (GCS) and compared to the force plate's force component measurements. To validate the system, a static and dynamic loading condition was applied to the measurement roller ski. To determine whether the force measurement roller ski would affect the efficacy of roller skiing on a treadmill, a maximum speed test with the V2 skating technique was conducted with both standard and force measurement roller skis.

4.3 Data collection

4.3.1 Experiment I

The 3D trajectories of the reflective markers were collected and recorded at a sampling rate of 150 Hz using an 8-video-camera motion capture system (Vicon, Oxford, UK) and the NEXUS 2.8.1 software. The GCS was determined when the incline of the treadmill was 0°. A total of 55 passive reflective markers were attached to the participants' bodies and skiing equipment, and three markers were attached to the treadmill. According to the XC model used in a previous study (Göpfert et al., 2017), anthropometric measurements and the positioning of markers on the participants' bodies were conducted. The measurements were taken on a motorized treadmill with a belt surface of 2.7m by 3.5m (Rodby Innovation AB, Vänge, Sweden). Both the techniques utilized the same pair of roller skis (Marwe SKATING 620 XC, wheel no. 0, Marwe Oy, Hyvinkää, Finland). The resistance friction coefficient (μ) on the treadmill surface was measured to be 0.025 using a custom-made friction measurement setup (University of Jyväskylä, Finland; FIGURE 1a).

The axial GRF from the poles was measured using two custom-made pole force sensors (VTT MIKES, Technical Research Center of Finland Ltd., Kajaani, Finland; FIGURE 1b). To measure the leg forces generated by roller skis, two custom-made 2D force measurement bindings (Neuromuscular Research Centre, University of Jyväskylä, Finland; FIGURE 1c) (Ohtonen et al., 2013a) were affixed on roller skis. The Coachtech online measurement and feedback system (Neuromuscular Research Center, University of Jyväskylä, Finland) (Ohtonen et al., 2015) was utilized to capture the pole and leg forces at a sample rate of 400Hz. The force measurement bindings were calibrated prior to the measurement (Ohtonen et al., 2013a) and measured the vertical (F_{skiz}) and medio-lateral (F_{skix}) forces. Coachtech (Ohtonen et al., 2015) sent a trigger signal to the Vicon system to designate the beginning of force capture. The nodes were used to supply power and transmit data to the pole force sensors and force measurement devices. The total weight of one prepared pole was 400g, and the entire weight of one prepared roller ski was 1650g.

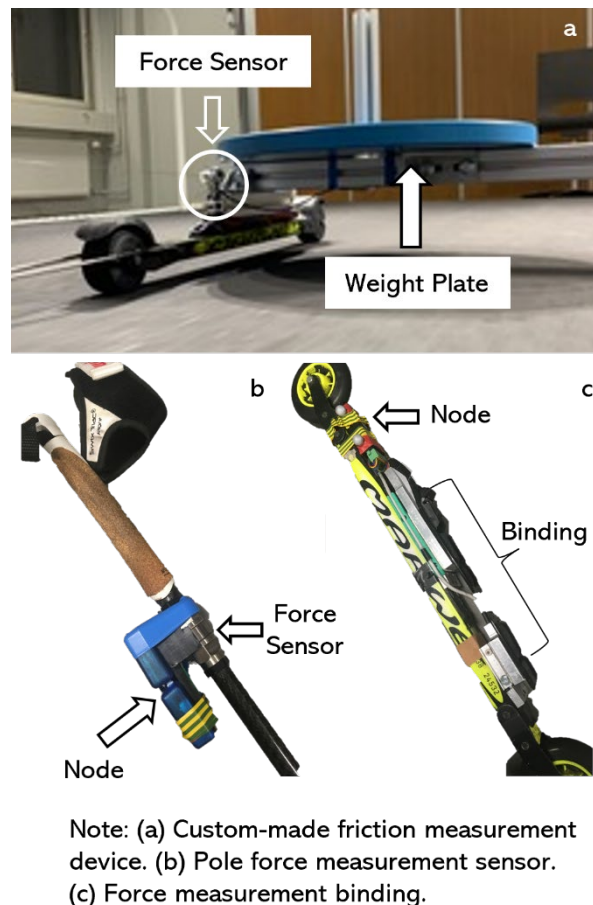
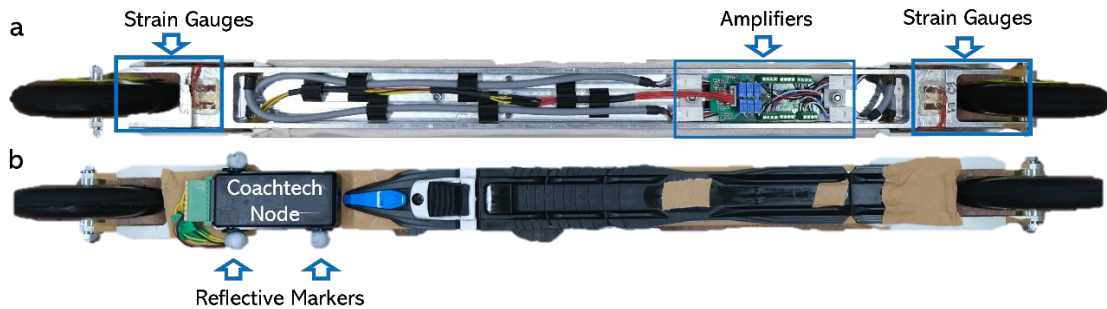


FIGURE 1. Equipment used in Experiment I.

4.3.2 Experiment II

4.3.2.1 2D force measurement roller ski and the calibration.

The roller skis capable of measuring 2D forces were conceived and manufactured by the Technical Research Center of Finland (VTT MIKES, Kajaani, Finland). Using the finite element method (FEM), a custom aluminum alloy frame for roller skis was designed. The dimensions of the structure and the location of strain gauges on the roller ski body were determined using the finite element analysis (FEA). Both the roller skis were equipped with four full-bridge strain gauge configurations (FIGURE 2). Four measurement channels were present on the rollerblades: two of them measured the vertical (front and rear) forces, while the other two measured the medio-lateral (front and rear) forces. The applied force changes the strain gauge resistance, which in turn changes the voltage that can be measured using a Wheatstone full-bridge configuration. The amplifiers (FIGURE 2a) were embedded into the roller skis' body, and the voltage-level signals were acquired by the nodes (FIGURE 2b; Sports Technology Unit Vuokatti, University of Jyväskylä, Finland) of the Coachtech online measurement and feedback system (Ohtonen et al., 2015). One roller ski for force measurement equipped with a Coachtech node weighed 1352g.



Note:(a) Bottom view of the force measurement roller ski. (b) Top view of the force measurement roller ski.

FIGURE 2. 2D force measurement roller ski.

Before this validation test, the Technical Research Center of Finland (VTT MIKES, Kajaani, Finland) calibrated the force measurement roller skis in December 2020 and June 2022. The strain gauges were set up to measure forces from 0N to 1000N in the vertical direction and from 0N to 400N in the medio-lateral direction. All the force measurement roller ski sensors were put through the load-up test, the signal-to-noise test, and the creep test. These tests were conducted in both the vertical and medio-lateral directions. When medio-lateral force was calibrated, it was loaded from both sides. In the load-up test, which is the same for both vertical and medio-lateral directions, there were three preloads followed by two heavier loads. The load then went up and down. Between each load, there was a 60s measurement period. In the signal-to-noise test, the voltage levels were recorded without putting a load on the circuit. The time it took to measure was 180s, and the sample rate was 0.5Hz. In the slide test, 1000N of force was put on

each roller ski thrice. The forces went straight from 0N to 1000N. The cycle time was 180s. The last load cycle was used to calculate the creep. The calibration factor was calculated from the calibration process, and the measuring uncertainty was thus estimated. For estimating uncertainty, the calibration force, repeatability, display device's resolution, instrument's creep, zero-point fluctuation, hysteresis, interpolation error, and crosstalk were used as uncertainty components. To calculate the correction factor (N/mV) for each sensor, a linear model was used. A second-order model and a third-order model were also tried, but the mistakes did not get much smaller. TABLE 2 and TABLE 3 show the correction factor (N/mV) from the tests conducted in December 2020 and June 2022, respectively. The forces were calculated using the factors in TABLE 3.

TABLE 4 shows the measurement error for the vertical direction that was set up during the calibration process.

TABLE 2. The calibration factors (N/mV) for each strain gauges mounted on the roller skis from the calibration done in December 2020.

Roller ski	Strain gauge	Calibration factor
Right roller ski	Front vertical	0.2428
	Front medio-lateral	0.1175
	Rear vertical	0.2431
	Rear medio-lateral	0.1148
Left roller ski	Front vertical	0.2442
	Front medio-lateral	0.1174
	Rear vertical	0.2459
	Rear medio-lateral	0.1161

TABLE 3. The calibration factors (N/mV) for each strain gauges mounted on the roller skis from the calibration done in June 2022.

Roller ski	Strain gauge	Calibration factor
Right roller ski	Front vertical	0.2444
	Front medio-lateral	0.1170
	Rear vertical	0.2418
	Rear medio-lateral	0.1154
Left roller ski	Front vertical	0.2452
	Front medio-lateral	0.1178
	Rear vertical	0.2489
	Rear medio-lateral	0.1157

TABLE 4. The vertical force combined expanded relative measurement uncertainty (%) for different loadings.

Force(kN)	Right Roller Ski W (k=2)	Left Roller Ski W (k=2)
0.2	3.5	4.5
0.4	3.4	3.6
0.6	2.7	2.9
0.7	2.5	2.7
0.8	2.3	2.2
0.9	1.0	1.4
1.0	0.4	0.8

4.3.2.2 Static test

Each roller ski (left and right) had its own set of static tests on two AMTI 3D force plates (AMTI, Watertown, USA). On June 7th, 2022, the AMTI's force plates were properly calibrated. Using specialized hardware (FIGURE 3a), one roller ski with a single wheel was positioned on each force plate at a time. Fifteen different loads, ranging from zero to 150kg, were placed on the roller ski. The weight of the roller ski and the specialized equipment was included in the forces measured by the force plates (FIGURE 3b), which measured the forces in three dimensions. Therefore, after deducting the weight of the roller ski and the equipment, the total force measured by the force measurement roller ski in this study should be the same as the total force measured by the force plate.

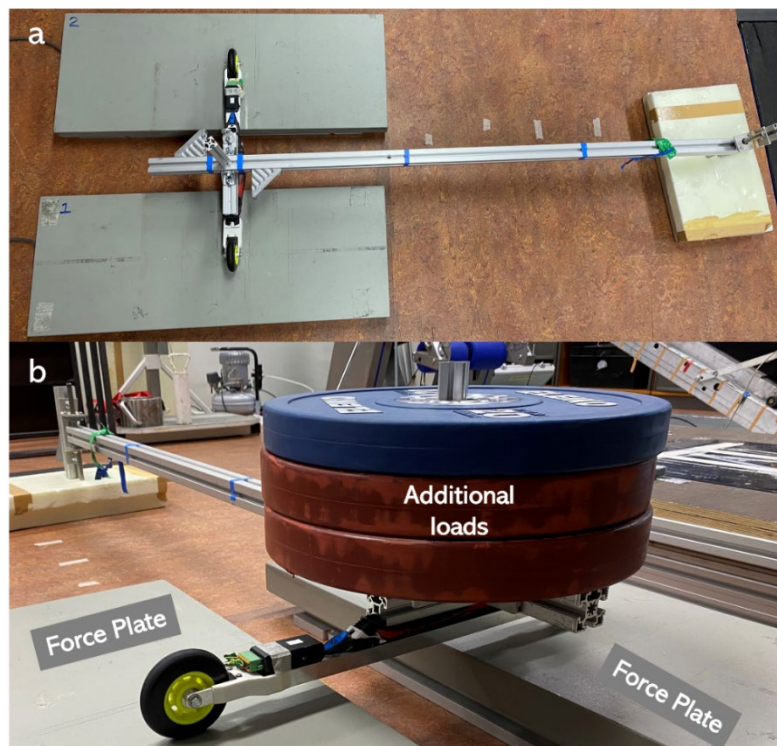


FIGURE 3. Specialized equipment and an example of a static test.

The roller ski's force data was sampled at 400Hz by the Coachtech online measurement and feedback system (Ohtonen et al., 2015). The AMTINetForce Version 3.5.2 (AMTI, Watertown, USA) was used to collect force data from AMTI force plates at a sampling rate of 1000Hz. Each load's force signal was recorded for at least 10s. The forces under each load were estimated by taking an average of over 3s of data. The force-measuring roller ski's precision was measured by comparing the resulting forces it generated to those generated by the AMTI force plates.

4.3.2.3 Simulated skating push-off jump test

One AMTI 3D force plate (AMTI, Watertown, USA) was used to replicate a skating push-off leap to evaluate the force-measuring roller ski in an applied dynamic environment. A male (aged 43) and female (aged 27) expert skier took part in the test. The longest possible push-off jumps were initially measured. The distance traveled by feet from the point of takeoff to the point of touchdown (FIGURE 4) is known as the push-off distance. The male subject was able to push off a maximum of 1.64m with his right foot and 1.70m with his left. For the female skier, the longest possible push-off distance was 1.49m with the right foot and 1.45m with the left. By varying the push-off distance and the person doing the pushing, the push-off load was altered. The goals were set at 65%, 75%, 85%, and 100% of the highest distance that could be jumped with a push-off. Ten attempts were recorded at each predetermined distance. The subjects wore their regular training shoes with the landing foot for safety reasons. The pushing foot employed the force measurement roller ski. Both left and right feet were used in the simulated skating push-off jump test separately.

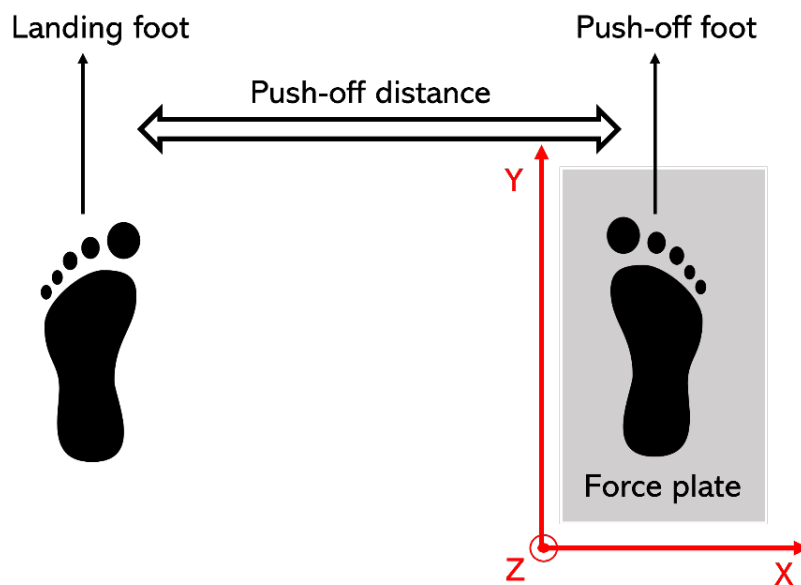


FIGURE 4. The definition of the push-off distance and the direction of the GCS in Experiment II.

The Coachtech system (Ohtonen et al., 2015) collected force data from the roller skis at a sample rate of 1000Hz. The AMTINetForce Version 3.5.2 (AMTI, Watertown, USA) was used to collect the force data from the AMTI force plates at a sampling rate of 1000Hz. To convert the forces sensed by the roller ski into the GCS, three passive reflective markers were affixed to the roller ski (FIGURE 2b). The Vicon (Oxford, UK) motion capture system sampled the movement of the markers at 250Hz. One roller ski equipped with a node and markers weighed 1358g.

Before each push-off jump, a manual synchronization hit was performed using the force measurement roller ski on the force plate (FIGURE 5). This brought the force signal and the marker displacement signal into sync. The force plate in the GCS was used to directly measure the forces (FIGURE 4). Since the Y-axis motion was negligible during the simulated skate push-offs, no Y-axis force comparisons were made between the force measurement roller ski and the force plate.

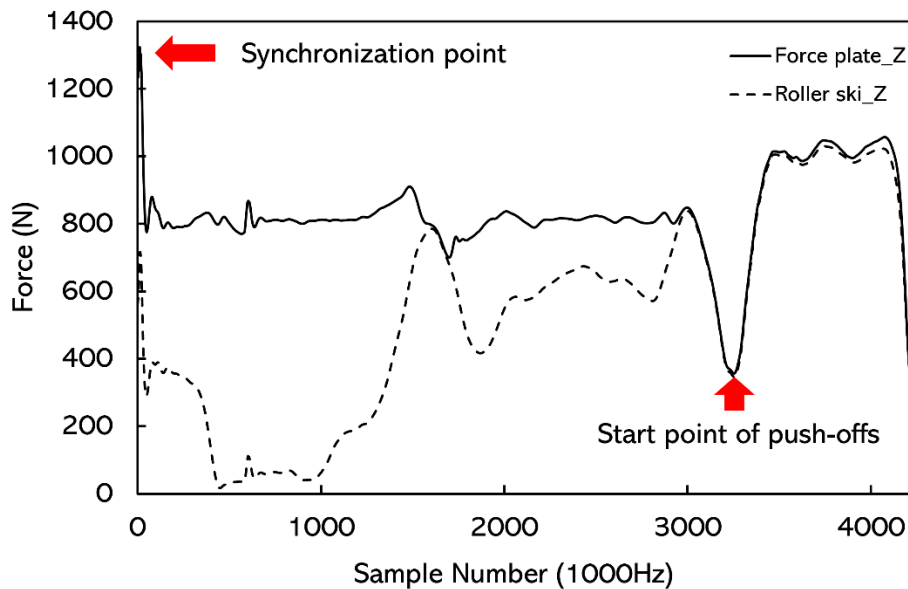


FIGURE 5. The synchronization point and the push-off start point.

4.3.2.4 Practical application

Two skiers, one male (Age: 24 years; Height: 1.79m; Weight: 81.5kg) and one female (Age: 26 years; Height: 1.67m; Weight: 55.5kg), roller skied on a treadmill, wearing the force measurement roller skis and the reference roller skis (Marwe, SKATING 620 XC, wheel no. 0) to show how the force measurement roller skis could be used in practice. The roller skis were used to measure force, and the reference roller skis were equipped with identical wheels. This experiment primarily aimed to determine whether the additional weight of the force measurement roller ski negatively affects skiing performance.

Each participant completed the following protocol twice, with a 5min warm up before the test and a 5min break in between each round. Both the female and male subjects skied on the treadmill with fixed degrees of incline (2° for the

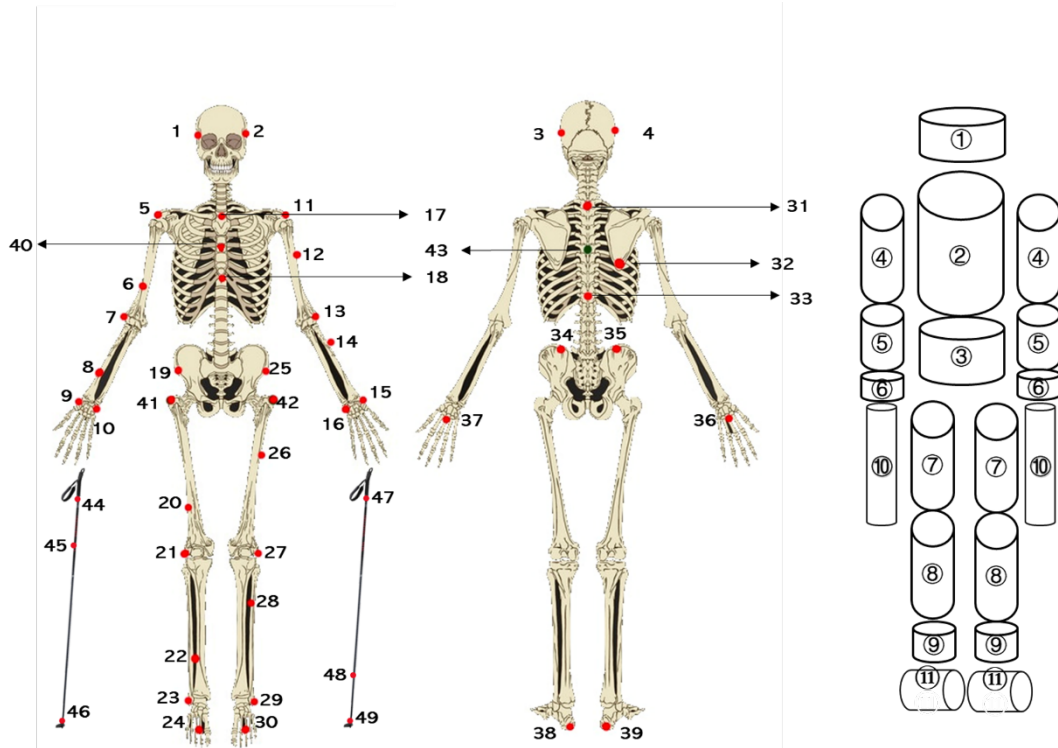
female and 3° for the male). The treadmill started at 18km/h and accelerated by 1km/h every 15s. When the skier could no longer keep up with the speed, the coach shut off the treadmill. Using the accelerometers on the skis and poles, the Coachtech system captured not only the total time and maximum speed but also the participants' cycle time, CR, CL, and ski contact time at each speed (Ohtonen et al., 2015). The longest duration and the highest final speed were used to present the performance. Each participant completed the program twice within a week on separate days, once with a standard pair of roller skis and once with the force-measuring roller skis.

A reference roller ski weighed 1025g, which is 333g less than the node-equipped force measurement roller ski. Due to the necessity of the Coachtech node for force signal collection, the balance point of a force measurement roller ski was measured using the Coachtech node affixed to the front of the roller ski. Compared to the reference roller ski, the balance point of the force measurement roller ski was shifted forward by 1.60cm. Using the gravitational force of the roller ski multiplied by the distance from the balancing point to the ski boot attach point, we determined the torque that exists around that part of the ski. The force measurement roller ski had a torque of 0.60Nm, while the reference roller ski had a torque of 0.61Nm.

4.4 Data processing

4.4.1 Labeling and filtering

The NEXUS 2.8.1 was used for marker labeling (for both Experiment I and II) and COM computations. For the Experiment I data, a low-pass (fourth-order, zero-lag, Butterworth filter) with a cutoff frequency of 11.3Hz (Yu et al., 1999) filter was applied at a cutoff frequency of 11.3Hz to the raw 3D trajectories of the reflecting markers and the COM acceleration. The COM of the entire body was computed using the XC model (Göpfert et al., 2017). FIGURE 6 depicts the subject marker placement and the geometric model used to create the XC model. Dempster's research described by Selbie et al. (2013, pp. 159-160) provided the segmental anthropometric data. An eighth-order, zero-lag, Butterworth filter was applied to the force data with a cutoff frequency of 15Hz (Danielsen et al., 2019). MATLAB R2018a (MathWorks, Natick, USA) was used to process the data and determine the parameters.



Note: 1–49 represent the placement of reflective markers on subjects and poles. 1–39 are the marker sets used in the plug-in-gait (PIG) model. 1–43 are the markers of the XC model on one subject. 44–49 are the markers on the poles. ①–⑪ represent the head, thorax, abdomen and pelvis, upper arm, forearm, hand, thigh, shank, foot, pole, and roller ski, respectively.

FIGURE 6. The marker placement (without skis) and the geometric model for segments in the XC model. The markers on the roller skis are shown in FIGURE 7.

The COM is a hypothetical location where the body’s mass is concentrated (Selbie et al., 2013, pp. 159-160). While several approaches can be employed to evaluate COM displacement, the segmental approach has been deemed appropriate for assessing the COM’s location in sports (Mapelli et al., 2014). By assuming that all the segments behave as rigid bodies, the COM of the human body can be quantified using the segments’ parameters (Selbie et al., 2013, pp. 159-160) derived from previous anthropometric studies in combination with the position of the anatomical land markers detected by motion capture systems. In this study, the COM displacement was estimated by the segmental method using the XC model, which was introduced by Göpfert et al. (2017). To compute the COM of the total body (including skis and poles), a weighted average of all the segments of the body was computed. The total body COM position is given by:

$$X = \sum_{s=1}^s P_s X_{cgs} \quad (1)$$

$$Y = \sum_{s=1}^s P_s Y_{cgs} \quad (2)$$

$$Z = \sum_{s=1}^s P_s Z_{cgs} \quad (3)$$

where (X, Y, Z) are the total body's COM coordinates, $(X_{cgs}, Y_{cgs}, Z_{cgs})$ is the segments' COM coordinates, and S is the number of body segments. Each segment is weighted based on its mass proportion, P_s , which is the segment's mass as a percentage of the total body mass. The contribution of each segment's COM to the total body's COM is proportional to its P_s value; the heavier the segment, the more it influences the location of the total body's COM.

The segments' COM coordinates $(X_{cgs}, Y_{cgs}, Z_{cgs})$ are given by:

$$X_{cgs} = X_{proximal} + R_{proximal}(X_{distal} - X_{proximal}) \quad (4)$$

$$Y_{cgs} = Y_{proximal} + R_{proximal}(Y_{distal} - Y_{proximal}) \quad (5)$$

$$Z_{cgs} = Z_{proximal} + R_{proximal}(Z_{distal} - Z_{proximal}) \quad (6)$$

where $(X_{proximal}, Y_{proximal}, Z_{proximal})$ and $(X_{distal}, Y_{distal}, Z_{distal})$ are the coordinates of the proximal and distal ends of each segment. $R_{proximal}$ is the distance from the segment's proximal end to its COM as a percentage of the length of the segment (Robertson, 2013a, pp. 63-78).

The COM acceleration (\vec{a}) was multiplied by the total mass of the subject and the equipment to get the reference force (\vec{F}). In the GCS, \vec{a} was the second derivative of the (X, Y, Z) COM coordinates. So, based on Newton's second law,

$$\vec{F} = (m_1 + m_2) * \vec{a} \quad (7)$$

where m_1 represents the body mass of each participant and m_2 represents the total mass of the equipment used by participants. \vec{F} indicates the total external forces acting on the COM in the GCS.

4.4.2 Converting the measured forces from the force sensor into the GCS and the PFA

The forces generated in the force coordinate system (FCS) of the roller skis were transferred into the GCS. The markers on the roller ski indicated the FCS ($\vec{i}, \vec{j}, \vec{k}$) unit vectors (FIGURE 7). The rotation matrix (Selbie et al., 2013, pp. 159-160) from the GCS to FCS of the roller ski was

$$R = \begin{bmatrix} i_x & i_y & i_z \\ j_x & j_y & j_z \\ k_x & k_y & k_z \end{bmatrix} \quad (8)$$

Thus, the transformation from the roller ski system to the GCS is given by:

$$\begin{bmatrix} F_x \\ F_y \\ F_z \end{bmatrix} = R' \begin{bmatrix} F_{skix} \\ 0 \\ F_{skiz} \end{bmatrix} \quad (9)$$

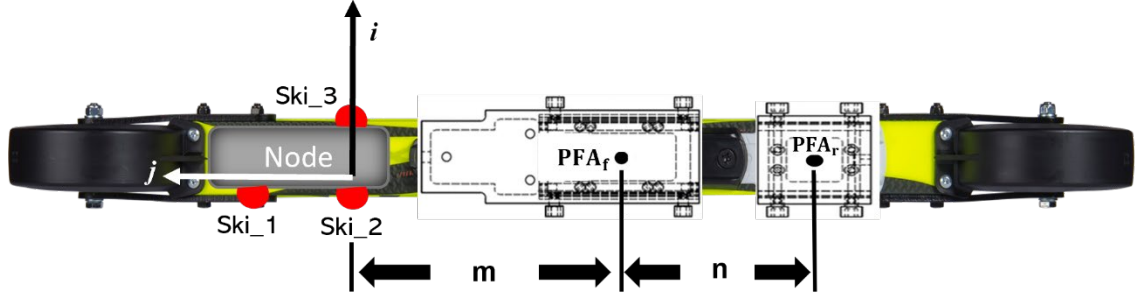
where F_x , F_y , and F_z are the components of forces generated from the legs in the GCS.

The magnitude of the resultant force from legs (\vec{F}_r) was calculated as follows:

$$|\vec{F}_r| = \sqrt{F_x^2 + F_y^2 + F_z^2} \quad (10)$$

Göpfert et al. (2017) established a translational force that can be calculated using PFA. Over time, the force distribution between the binding's front and back sensors (Winter, 1995) was used to determine the PFA's (PFA_{ski}) translation along

the binding. Each sensor's geographic center was used to determine the PFA for the corresponding binding segment (PFA_f and PFA_r). Before the measurement, the distances between the marker Ski_2 and PFA_f (m) and between PFA_f and PFA_r (n) were measured. By shifting the midpoint of Ski_2 and Ski_3 in the opposite direction of \vec{j} , we calculated the displacements of PFA_f and PFA_r in GCS. The moving distances were m and m + n, respectively. The PFA_{ski} shuttled back and forth between the PFA_f and PFA_r (FIGURE 7).



NOTE: Three markers (Ski_1, Ski_2, and Ski_3) were attached to the side of the node. The node for power supply and data transmission was attached to the front part of the roller ski. The surface defined by the markers was parallel to the roller ski surface. \vec{i} was defined by Ski_3 and Ski_2. Another unit vector (\vec{j}) located on the surface of the roller ski was defined by Ski_1 and Ski_2. The surface norm, which was the \vec{k} of FCS, was the cross product of \vec{i} and \vec{j} . The last unit vector \vec{j} was computed by using the right-hand rule with \vec{k} and \vec{i} . The PFA_f and PFA_r were the points of force application of the front and rear sensors, respectively. The distance between Ski_2 and PFA_f was m, and the distance between PFA_f and PFA_r was n.

FIGURE 7. Displacement of markers, PFA, and the definition of FCS (\vec{i} , \vec{j} , \vec{k}).

4.4.3 The translational force and the propulsive force

The forward component of the translational force has been shown to be appropriate for estimating forward acceleration in the push-off phase of skating without poles (Göpfert et al., 2017). The translational force is the portion of the resulting GRF acting in the direction from the PFA to COM. The skier's translational force from skis (\vec{F}_{ts} , FIGURE 8) is the fraction of the ski GRF (\vec{F}_r) acting in the direction determined by the PFA_{ski} and COM,

$$\vec{F}_{ts} = (\vec{F}_r \cdot \vec{u})\vec{u} \quad (11)$$

where the PFA_{ski} to COM unit vector was denoted by \vec{u} . The translational force from poles (\vec{F}_{tp}) is calculated by using the following formula:

$$\vec{F}_{tp} = (\vec{F}_p \cdot \vec{v})\vec{v} \quad (12)$$

where the PFA_p to COM unit vector was denoted by \vec{v} . The total translational force (\vec{F}_{pro}) is the sum of the translational force from the legs, poles, and the resistance. As part of the resistance force, the frictional force ($\vec{F}_{friction}$) between the roller ski and the treadmill is directed along the path of the ski motion, and the magnitude is computed as follows:

$$|\vec{F}_{friction}| = \mu F_{skiz} \quad (13)$$

The magnitude of gravitational force (\vec{G}) is calculated from

$$|\vec{G}| = (m_1 + m_2) * g \quad (14)$$

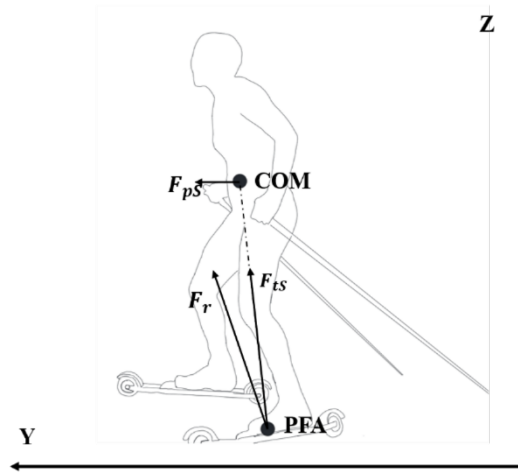
where m_1 and m_2 represent the body mass and the whole mass of the equipment used by the participants, and g is the gravitational acceleration.

Thus, \vec{F}_{pro} can be computed as follows:

$$\vec{F}_{pro} = \vec{F}_{ts} + \vec{F}_{tp} + \vec{F}_{friction} + \vec{G} \quad (15)$$

The way to quantify the propulsive forces (\vec{F}_{net}) is to compute the component of GRFs in the desired skiing direction independently from considering the position of the COM (Smith, 2003, pp. 32-61). The total (\vec{F}_{net}) is presented as

$$\vec{F}_{net} = \vec{F}_r + \vec{F}_p + \vec{F}_{friction} + \vec{G} \quad (16)$$



NOTE: F_r is the resultant force generated from legs. F_{ts} is the translational component, which went through COM. F_{ps} represents the propulsion generated from legs in the forward direction.

FIGURE 8. Diagram of force decomposition from skis.

4.4.4 Propulsive force calculation when skiing at different inclines

First, the forces measured in the FCS were transformed into the GCS. The measured axial pole forces were interpreted as the GRFs operating along the pole from its base to its apex. In GCS, the pole forces vector (\vec{F}_p) were calculated as follows:

$$\vec{F}_p = F * \vec{n} \quad (17)$$

where F is the magnitude of the measured axial pole force, and \vec{n} is the direction vector from the pole's tip to its top. Using the reflective markers affixed to the pole, the direction vector was defined. As the measurements were conducted at various inclines, the ski (F_{p_ski}) and pole (F_{p_pole}) propulsive force components were calculated as follows:

$$F_{p_ski} = F_y * \cos \alpha + F_z * \sin \alpha \quad (18)$$

$$F_{p_pole} = F_{pole_y} * \cos \alpha + F_{pole_z} * \sin \alpha \quad (19)$$

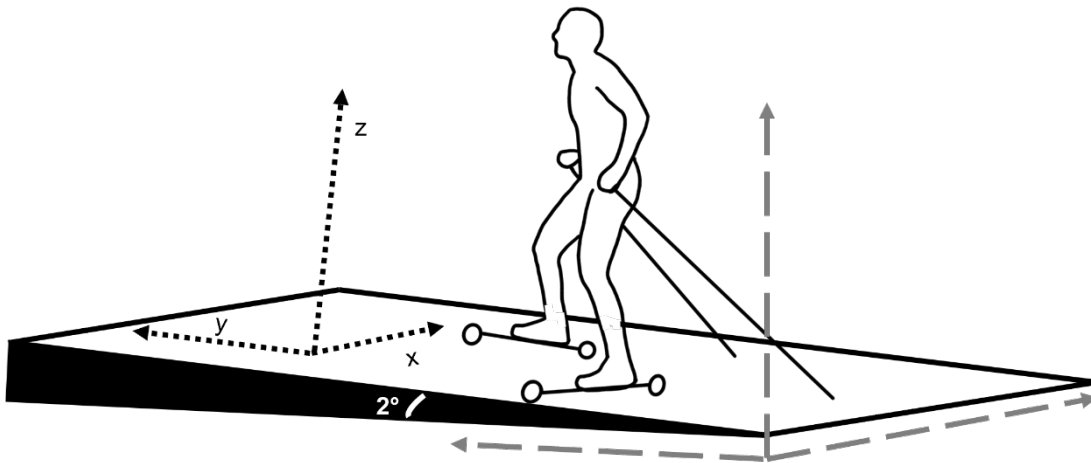
where α was the incline of the treadmill (2° , 3° , 4° , or 5°); F_{pole_y} and F_{pole_z} were the corresponding pole force components in GCS; F_y and F_z were the components of the GRF vector derived from legs in GCS.

4.4.5 Power calculation

The mean external power (P_{mean}) was calculated in accordance with previous studies (Dahl et al., 2017; Danielsen et al., 2019; Sandbakk et al., 2012). P_{mean} is the sum of power against gravity and friction, which could be calculated as follows:

$$P_{\text{mean}} = mgv_{\text{Belt}} \sin \alpha + (mg \cos \alpha - F_p^\perp) \mu v_{\text{Ski}} \quad (20)$$

where m is the mass of the skier and the skiing equipment, g is the gravitational constant, v_{Belt} is the treadmill belt speed, α is the incline of the treadmill, and μ is the friction coefficient. The v_{Ski} is the speed of the roller ski. The skis were angled with respect to the forward direction while using the skating technique, with the roller ski moving faster than the treadmill belt. The value of the v_{Ski} was calculated by $v_{\text{Belt}} / \cos(\text{ski orientation angle})$. The F_p^\perp is the mean pole force component in the vertical direction (FIGURE 9), which is perpendicular to the treadmill surface. The incline of the treadmill was 2° . The external power analysis was conducted for the V2 skating technique when the treadmill speed was changed.



NOTE: The long dash arrows represent the axis of global coordinate system which was defined by using the right-hand rule when the incline of the treadmill was 0° . x , y , and z (round dot arrow) represent the axis when the incline of the treadmill was 2° . Note that the x , y , and z components are orthogonal to each other.

FIGURE 9. Illustrations of the GCS and the coordinate system moved with the treadmill.

To understand the role of each limb and how each limb contributes to the overall power generation and absorption, the individual limbs method (Donelan et al., 2002) was used to calculate the external mechanical power of the COM. Poling (P_p) and ski (P_s) powers were calculated as the dot product of force vectors and the COM's velocity vector ($\overrightarrow{v_{\text{com}}}$):

$$P_p = \overrightarrow{F_{POLE}} \cdot \overrightarrow{v_{com}} \quad (21)$$

$$P_s = \overrightarrow{F_{SKI}} \cdot \overrightarrow{v_{com}} \quad (22)$$

$\overrightarrow{F_{POLE}}$, $\overrightarrow{F_{SKI}}$ and $\overrightarrow{v_{com}}$ are the pole force, ski force, and COM velocity vectors in the coordinate system moving with the treadmill. The $\overrightarrow{v_{com}}$ is the first derivative of the COM position relative to the treadmill speed. The P_s for the left and right skis were calculated in the same way.

To evaluate the medio-lateral, fore-aft, and vertical contribution of skis and poles, the P_p and P_s were decomposed to their x, y, and z components.

$$P_{p,x} = F_{p,x} \cdot v_{com,x} \quad (23)$$

$$P_{p,y} = F_{p,y} \cdot v_{com,y} \quad (24)$$

$$P_{p,z} = F_{p,z} \cdot v_{com,z} \quad (25)$$

$$P_{s,x} = F_{s,x} \cdot v_{com,x} \quad (26)$$

$$P_{s,y} = F_{s,y} \cdot v_{com,y} \quad (27)$$

$$P_{s,z} = F_{s,z} \cdot v_{com,z} \quad (28)$$

The subscripts x, y, and z stand for the medio-lateral, fore-aft, and vertical directions, respectively. Both the left and right ski power were computed in the same way. The time rate of change in medio-lateral and fore-aft kinetic energy was used to characterize the external power in the medio-lateral and fore-aft directions, respectively. The rate of change of gravitational potential energy and vertical kinetic energy is the definition of vertical external power (Yamashita et al., 2017).

The average positive and negative external power was determined by adding the positive or negative values and dividing them by the CT.

$$P_p^+ = \frac{\int_+ P_p}{CT} \quad (29)$$

$$P_p^- = \frac{\int_- P_p}{CT} \quad (30)$$

$$P_s^+ = \frac{\int_+ P_s}{CT} \quad (31)$$

$$P_s^- = \frac{\int_- P_s}{CT} \quad (32)$$

The average medio-lateral (x), fore-aft (y), and vertical (z) power for the kicking and gliding leg were calculated in the same way. The positive power was defined as the propulsive power, and the negative power was defined as the braking power (Yamashita et al., 2017).

4.4.6 Force calculation of the force measurement roller ski

The force from each signal channel (F_i) was calculated with the following equation:

$$F_i = a_i * U_i \quad (33)$$

where U_i is the voltage of the signal channel i (mV), and a_i is the calibration factor (N/mV).

The total force of each direction (vertical or medio-lateral) can be derived with the following equation:

$$F_{\text{sum}} = F_{\text{front}} + F_{\text{rear}} \quad (34)$$

where F_{sum} represents the total force in one direction, F_{front} and F_{rear} are the forces in this direction from the front suspension and the rear suspension respectively. In this study, only the sum forces were used.

4.4.7 Cycle definition and analyzed parameters.

4.4.7.1 Cycle definition

Article I analyzed ten consecutive poling phases for each DP technique trial and ten consecutive kicking phases (5 left ski kicking and 5 right ski kicking) for each V2 technique trial. This was determined as the force-producing phase. The time from the beginning of pole ground contact to the end of ground contact (FIGURE 10a) is known as the poling phase. Kicking was defined as the period from the ski force minimum (Ohtonen et al., 2018) (FIGURE 10b) until the end of ground contact. When determining the total propulsion for both methods, the forces exerted by the skis and poles from both the left and right sides were considered.

In Article II and Article III, five cycles from each V2 skating technique trail were assessed. The V2 skating technique includes kicking, overlapping, pure gliding action from both the left and right skis, and two DP action (FIGURE 11). One cycle is defined as the period between successive same-side ski force minima following ski plant.

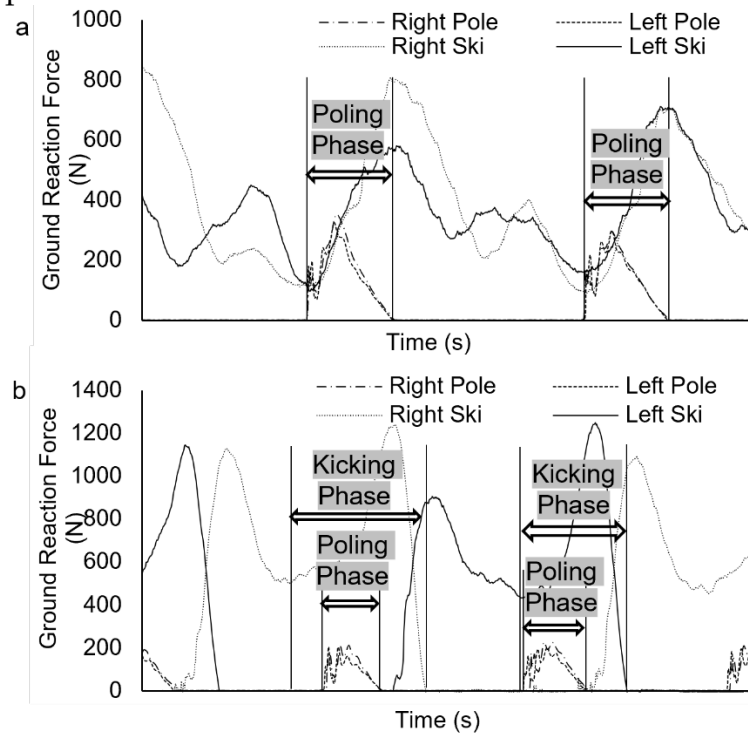


FIGURE 10. Definition of the force producing phase of DP and V2 techniques. (a) DP technique. (b) V2 skating technique.

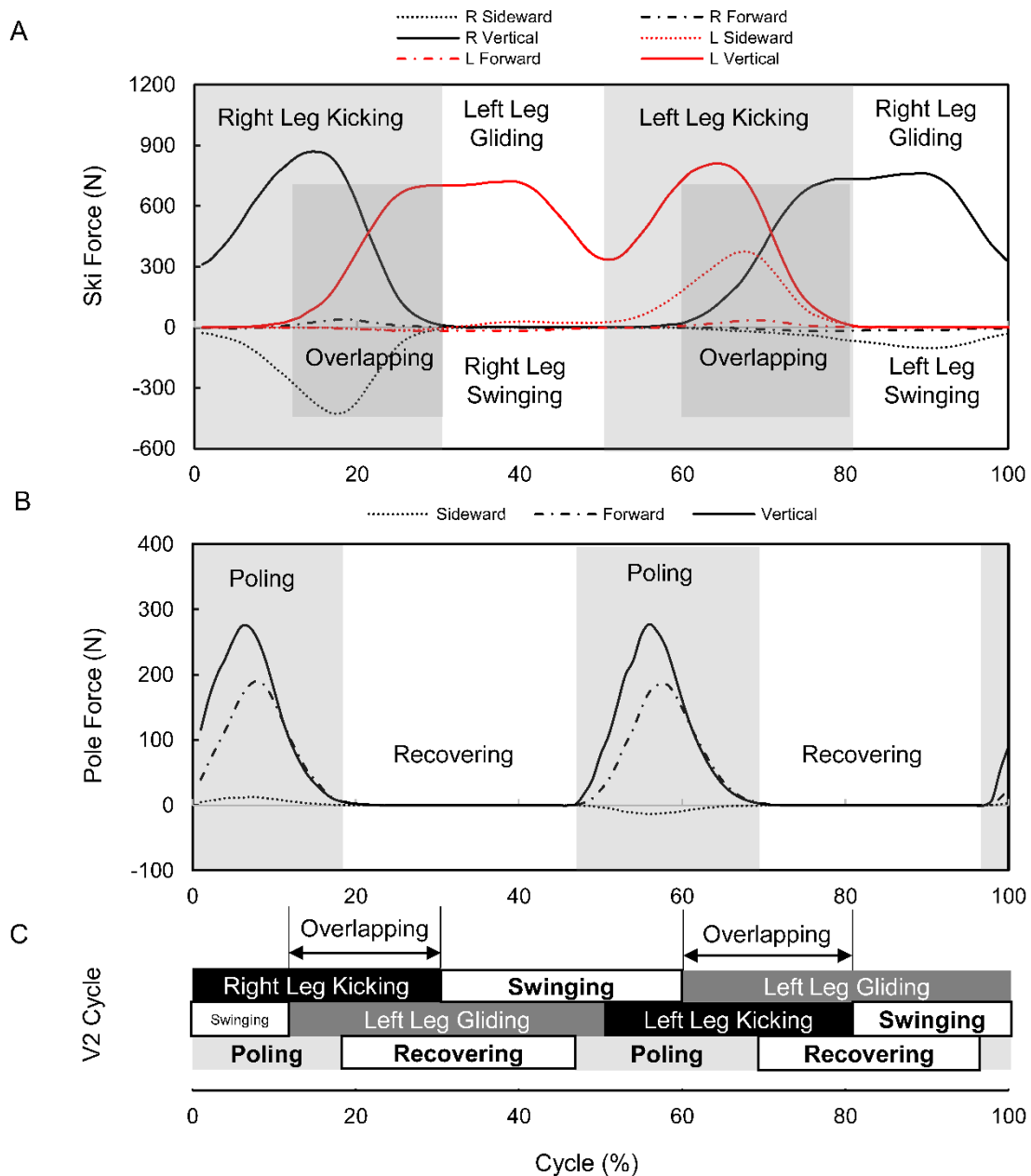


FIGURE 11. Time-force curves for skiers ($n = 10$) skating at 19km/h and the definition of action stages. (A) Time-force curve of ski forces. The gray areas represent the kicking phase of the right and left skis; the dark gray areas represent the ski overlapping phase. (B) Time-force curve of the pole forces. The gray areas represent the poling phase, and the rest are recovering phases. (C) The action stages of the V2 skating technique. Periods of kicking (black solid bar), periods of gliding (dark gray solid bar), periods of poling (gray solid bar), and periods of ski swinging and pole recovering (white solid bar). Note: The horizontal time scale for each figure is normalized to the V2 skating cycle.

The forces beneath each load in Experiment II's static test were calculated as an average across 3s of data. The vertical force minima during the unweighting phase (FIGURE 5) marked the beginning of the push-off in the simulated skate

push-off jump test. When the vertical force measured by the force plate dropped below 5N, the push-off was considered to be over.

4.4.7.2 Analyzed parameters

In Article I, the Y component (FIGURE 8) of \vec{F} , \vec{F}_{net} , and \vec{F}_{pro} (F , F_{net} , and F_{pro}) was compared and examined. To compare the force-time curves, the positive square root of the adjusted coefficient of multiple correlation (CMC, $0 < \text{CMC} < 1$) (Kadaba et al., 1989; Yu et al., 1997) was computed. One comparison was between the F_{net} and F force-time curves. CMC_{net} was used to illustrate the similarities between F_{net} and F . The average force difference between F_{net} and F was $M_{F_{\text{net}}-F}$, and the average absolute force difference was $M_{|F_{\text{net}}-F|}$. Another comparison was between the F_{pro} and F force-time curves. The CMC_{pro} was used to illustrate the similarities between F_{pro} and F . The average force difference ($M_{F_{\text{pro}}-F}$) and the average absolute force difference ($M_{|F_{\text{pro}}-F|}$) were also calculated, respectively. Similar curves will have a CMC close to one. The mean force differences and mean absolute force differences were calculated based on the force curves averaging over 10 force-producing phases. The mean force differences ($M_{F_{\text{net}}-F}$ and $M_{F_{\text{pro}}-F}$) were computed only for descriptive purposes. The forces were reported in terms of the percentage of body weight (%BW) in Article I.

In Articles II and III, the CR was calculated by dividing the CT by one to get the rate in hertz. CL was calculated as the multiplication of CT by treadmill velocity. The PT was the ground contact time of the right poles. The recovery time for poles (RT) was defined as the difference between CT and PT. For the V2 skating technique (FIGURE 12A), from the point of unweighting minima to the point of ski release is the kicking time (KT) of one leg. The overlap time (OLT) between the two legs was measured from the moment one ski was planted to the moment the next ski was released in proximity. The pure gliding time (PGT) of one ski was defined as the time in seconds between the end of the ground contact of this ski and the following ski force minima after the ski contact of the other ski. The relative poling, kicking, and overlap times were calculated for the analysis. The duty cycle of pole (DCP), kicking time of cycle (KT%), and the overlap time of cycle (OLT%) were the PT, KT, and OT as the percentage of the CT, respectively.

The peak pole force (PPF) and peak kicking force (PKF) were determined by the resultant force from pole and leg, respectively (FIGURE 12A). The resultant pole force impulse (IMP), propulsive pole force impulse (IMPP), vertical pole force impulse (IMPV), resultant leg force impulse (IML), propulsive leg force impulse (IMLP), and vertical leg force impulse (IMLV) were calculated. The total force impulse (IMT) was calculated by summing the IMP and the IML. Similarly, the total propulsive force impulse (IMTP) was calculated by summing the IMPP and the IMLP. The effectiveness index was calculated for poles and legs separately by expressing the IMPP and the IMLP as a percentage of IMP and IML, respectively (Stöggl & Holmberg, 2015). The contribution from poles and legs was calculated by expressing the IMPP and IMLP as a percentage of IMTP

(Göpfert et al., 2017). The average cycle force (ACF) and average propulsive cycle force (APCF) were determined by dividing the IMT and the IMTP by CT, respectively (Stöggl & Holmberg, 2015). The power output in the skiing direction was calculated by multiplying the APCF and the treadmill speed (m/s) (Stöggl & Holmberg, 2015).

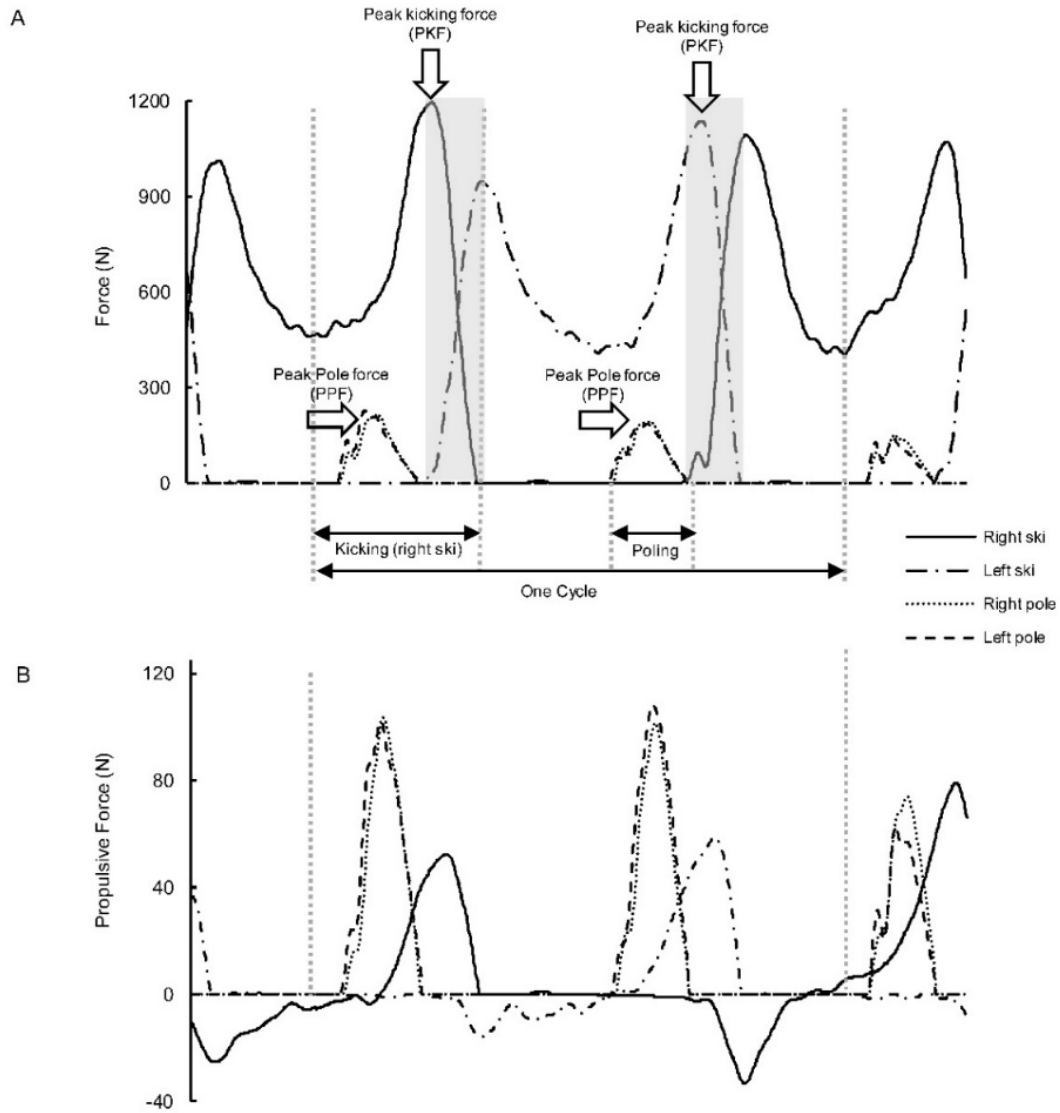


FIGURE 12. Definition of cycle and force variables (A) and time-force curve of propulsive force (B) with the V2 skating technique.

External power was also analyzed with the V2 skating technique while changing the treadmill speed. The COM is propelled by both pole and ski forces. Therefore, averaged over a cycle, the sum of ski and pole propulsive resultant power (P_{tot}) should be equal to the sum of power against gravity and friction (P_{mean}). The relative power contribution from the poles toward the total external power was determined by expressing the propulsive pole resultant power P_p^+ as a percentage of P_{tot} . The relative power contribution from the skis towards the total

external power was determined by expressing the propulsive ski resultant power P_s^+ as a percentage of P_{tot} . The effectiveness index of pole power was calculated by expressing the propulsive pole power P_p^+ as a percentage of $(P_p^+ + |P_p^-|)$. The effectiveness index of ski power was calculated by expressing the propulsive ski power P_s^+ as a percentage of $(P_s^+ + |P_s^-|)$.

In Article IV, the time-normalized curves between the force-measuring roller ski and the force plate were used to determine the coefficient of multiple correlation (CMC, $0 < CMC < 1$) (Kadaba et al., 1989; Yu, 2003; Yu et al., 1997) in MATLAB R2018a (MathWorks, Natick, MA, USA). The absolute force differential between the force measurement roller ski and the force plates in the X and Z directions was used to quantify the precision of the force measurement roller ski.

4.5 Statistical methods

For Article I, a two-way mixed factorial ANOVA was conducted. In the analyses, the dependent variables were (1) CMCs and (2) the mean absolute force differences. The independent variables were the treadmill's speed (or the incline) and the comparisons (i.e., the comparison between F_{net} and F and the comparison between F_{pro} and F). The treadmill's speed (or the incline) was considered as the within-subject factor, while the comparison pair was considered as the between-subject factor. In SPSS, pairwise comparisons of the dependent variable were performed using the EMMEANS subcommand with the Bonferroni adjustment when interactions were detected (Malek et al., 2018, pp. 32-47).

For Article II, one-way ANOVA with repeated-measures and Bonferroni post hoc analysis were performed to determine the influence of incline on each characteristic.

For Article III, the difference between P_{mean} and P_{tot} at varied speeds was tested by two-way ANOVA with repeated measures (2 ways to calculate the power *5 speeds). When significant differences were found between P_{mean} and P_{tot} , linear regression was used to determine the relation between the calculated external powers (P_{mean} and P_{tot}) and the treadmill speeds. For other parameters, one-way ANOVA with repeated measures and Bonferroni post hoc analysis were conducted. No statistical methods were used in Article IV.

The descriptive statistics are presented as mean \pm SD. The normal distribution of the data was confirmed by the Shapiro-Wilk normality test. The effect size (Partial Eta Squared) and statistical power were also provided for further evaluation. The level of statistical significance was set at 0.05. All statistical analyses were conducted using the SPSS 22.0 Software (SPSS Inc., Chicago, U.S.A.).

5 RESULTS

Only the main results of the thesis are presented below, and the full results being presented in the original articles (Article I-IV).

5.1 The similarity (CMC) and the average absolute force differences between force-time curves (Article I)

With the DP technique, no difference was found between CMC_{pro} and CMC_{net} at any speed ($p \geq 0.106$, TABLE 5). Moreover, no difference was found between CMC_{pro} and CMC_{net} when the incline was changed ($p = 0.218$, TABLE 5). With the DP technique, the CMC_{pro} was not affected by the speed ($p = 0.371$, TABLE 5). However, the CMC_{net} decreased at 21km/h when compared to CMC_{net} at 13km/h, 15km/h, and 17km/h ($p \leq 0.046$). From 3° to 5°, the overall CMC increased by approximately 2% ($p = 0.001$, TABLE 5).

Changing the pace of the treadmill with the V2 skating technique resulted in a CMC_{pro} that was around 5% lower than the CMC_{net} ($p = 0.011$, TABLE 6). When the treadmill incline was set to 3° ($p = 0.042$, TABLE 6), the CMC_{net} was greater than the CMC_{pro} . From 13km/h to 21km/h, the CMC dropped by around 2%. The incline of the treadmill had no effect on CMC_{net} ($p = 0.479$, TABLE 6). CMC_{pro} increased from 3° to 5° ($p = 0.007$, TABLE 6).

TABLE 5. Values of the CMC for the DP technique (n = 9).

		DP Technique			
		CMC _{net}	CMC _{pro}	P-value	P η^2
Speeds (km/h)	13	0.935 \pm 0.022	0.910 \pm 0.038	0.106 ^b	0.155
	15	0.933 \pm 0.023	0.916 \pm 0.034	0.230 ^b	0.089
	17	0.920 \pm 0.030	0.919 \pm 0.030	0.951 ^b	0.001
	19	0.901 \pm 0.045	0.908 \pm 0.046	0.778 ^b	0.005
	21	0.883 \pm 0.058 ^{1,2,3}	0.907 \pm 0.042	0.330 ^b	0.059
		P-value	0.043 ^d	0.371 ^d	
	P η^2	0.509	0.264		
Inclines (°)	3°	0.933 \pm 0.024	0.914 \pm 0.046	0.218 ^a	0.093
	4°	0.946 \pm 0.016	0.932 \pm 0.033		
	5°	0.955 \pm 0.015	0.936 \pm 0.037		
		P-value	0.001 ^e		
		P η^2	0.464		

TABLE 6. Values of the CMC for the V2 skating technique (n = 10).

		V2 Technique			
		CMC _{net}	CMC _{pro}	P-value	P η^2
Speeds (km/h)	13	0.901 \pm 0.048	0.853 \pm 0.043	0.011 ^a	0.309
	15	0.908 \pm 0.047	0.862 \pm 0.050		
	17	0.905 \pm 0.040	0.861 \pm 0.035		
	19	0.885 \pm 0.045	0.837 \pm 0.047		
	21	0.879 \pm 0.044	0.832 \pm 0.041		
		P-value	0.008 ^c		
	P η^2	0.216			
Inclines (°)	3	0.911 \pm 0.032	0.856 \pm 0.073	0.042 ^b	0.210
	4	0.922 \pm 0.041	0.896 \pm 0.044 [*]	0.179 ^b	0.098
	5	0.912 \pm 0.047	0.900 \pm 0.055 [*]	0.617 ^b	0.014
		P-value	0.479 ^f	0.007 ^f	
		P η^2	0.083	0.446	

Note: For TABLE 5 and TABLE 6, the CMC_{net} represents the similarity between F and F_{net}. CMC_{pro} represents the similarity between F and F_{pro}. ^a P-value for the main effect of comparison in a two-way mixed factorial ANOVA. ^b P-value for pairwise comparisons when interactions were detected. ^c P-value for the main effect of speed in a two-way mixed factorial ANOVA. ^d P-value for the simple effect of speed when interactions were detected. ^e P-value for the main effect of incline in a two-way mixed factorial ANOVA. ^f P-value for the simple effect of incline when interactions were detected.^{1,2,3} Significantly different from 13km/h, 15km/h, and 17km/h. * Significantly different from 3°.

When using the DP technique, the difference between M_{|F_{net}-F|} and M_{|F_{pro}-F|} at 15km/h was 24% (p = 0.028, TABLE 7). When compared to M_{|F_{pro}-F|}, M_{|F_{net}-F|} was around 39% lower. Increase in treadmill speed was associated with increases in both M_{|F_{net}-F|} and M_{|F_{pro}-F|} (p < 0.001, p < 0.001, TABLE 7). The overall absolute mean difference increased by 23% from 3° to 5°. The overall M_{|F_{pro}-F|}

with V2 skating technique was around 37% higher than $M_{|F_{net}-F|}$. At 3° and 4°, $M_{|F_{net}-F|}$ was considerably less than $M_{|F_{pro}-F|}$ ($p \leq 0.013$, TABLE 8). The overall absolute difference from 13km/h to 21km/h increased by 33%. $M_{|F_{net}-F|}$ was dependent on the incline of the treadmill ($p = 0.014$, TABLE 8), whereas $M_{|F_{pro}-F|}$ was not affected by the incline of the treadmill ($p = 0.577$, TABLE 8).

TABLE 7. Average absolute force difference between force curves with the DP technique (n = 9).

		DP Technique			
		$M_{ F_{net}-F }$	$M_{ F_{pro}-F }$	P-value	$P\eta^2$
Speed (km/h)	13	6.1 ± 1.1	8.1 ± 2.9	0.058 ^b	0.207
	15	6.9 ± 1.1	9.1 ± 2.6 ⁴	0.028 ^b	0.268
	17	8.5 ± 1.5 ^{1,2,5}	10.2 ± 3.3 ^{1,4}	0.166 ^b	0.116
	19	9.0 ± 1.3 ^{1,2}	11.6 ± 3.6 ^{1,2,3}	0.057 ^b	0.209
	21	10.8 ± 2.2 ^{1,2,3}	10.9 ± 2.4 ¹	0.992 ^b	0.001
	P-value	0.001 ^d	0.001 ^d		
	$P\eta^2$	0.856	0.857		
Incline (°)	3	6.2 ± 0.9	8.7 ± 3.0		
	4	7.1 ± 1.1	9.6 ± 2.7	0.015 ^a	0.315
	5	7.6 ± 1.3	10.7 ± 2.9		
	P-value		0.001 ^e		
	$P\eta^2$		0.615		

TABLE 8. Average absolute force difference between force curves with the V2 skating technique (n = 10).

		V2 Technique			
		$M_{ F_{net}-F }$	$M_{ F_{pro}-F }$	P-value	$P\eta^2$
Speed (km/h)	13	2.9 ± 0.4	4.4 ± 0.8		
	15	3.1 ± 0.5	4.7 ± 0.4		
	17	3.6 ± 0.6	4.8 ± 0.5	0.001 ^a	0.633
	19	4.0 ± 0.9	5.4 ± 0.8		
	21	4.4 ± 0.9	5.3 ± 0.5		
	P-value		0.001 ^c		
	$P\eta^2$		0.588		
Incline (°)	3	2.9 ± 0.5	4.5 ± 0.8	0.001 ^b	0.617
	4	3.4 ± 1.1	4.5 ± 0.6	0.013 ^b	0.295
	5	3.7 ± 0.7 [*]	4.3 ± 0.9	0.115 ^b	0.132
	P-value	0.014 ^f	0.577 ^f		
	$P\eta^2$	0.394	0.063		

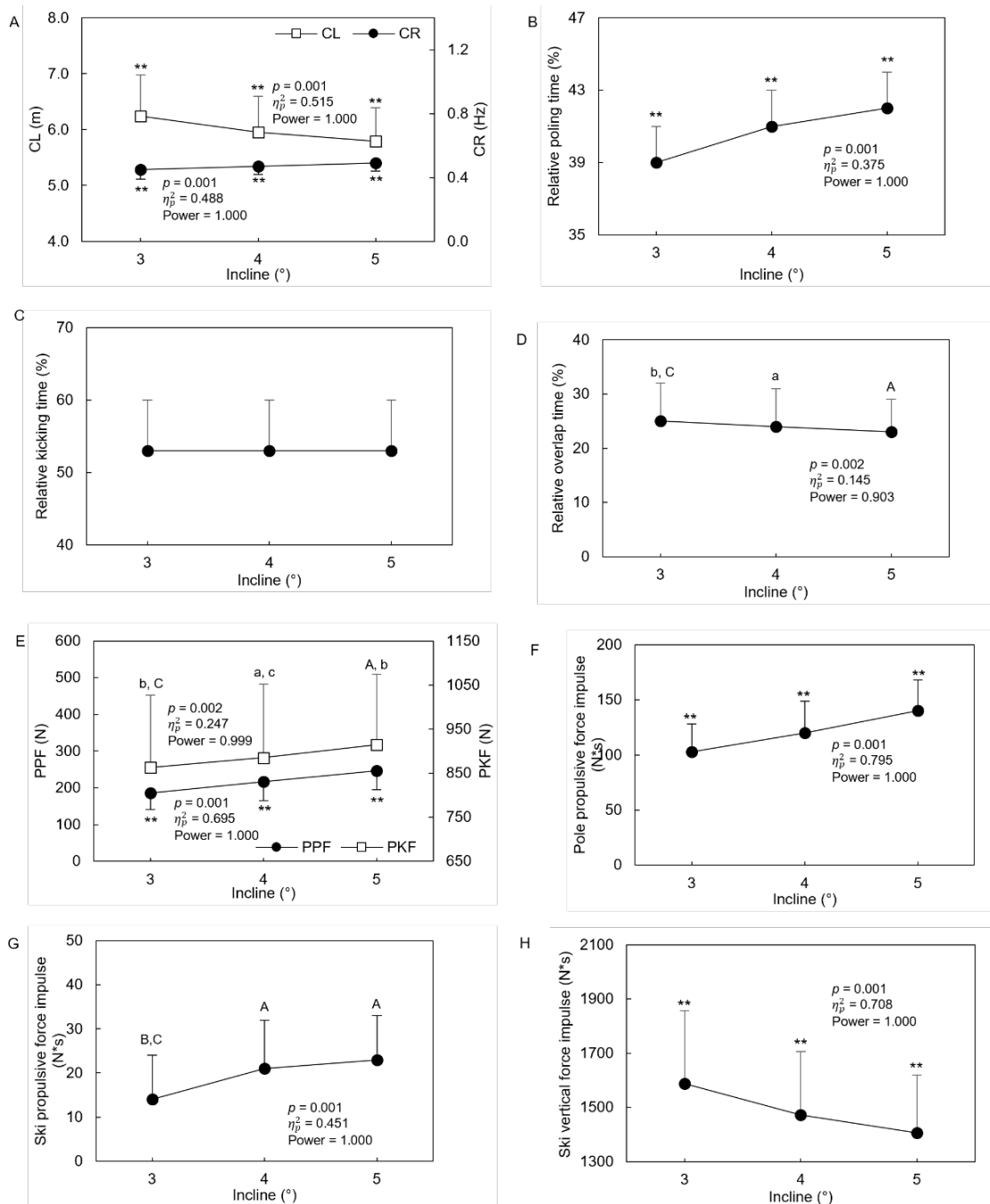
Note: For TABLE 7 and TABLE 8, $M_{|F_{net}-F|}$ represents the absolute difference between F and F_{net} and is calculated by $|F - F_{net}|$. $M_{|F_{pro}-F|}$ represents the absolute difference between F and F_{pro} and is calculated by $|F - F_{pro}|$. ^a P-value for the main effect of comparison in a two-way mixed factorial ANOVA. ^b P-value for pairwise comparisons when interactions were detected. ^c P-value for the main effect of speed in a two-way mixed factorial ANOVA. ^d P-value for the simple effect of speed when interactions were detected. ^e P-value for the main effect of incline in a two-way mixed factorial ANOVA. ^f P-value for the simple effect of incline when interactions were detected. ^{1,2,3,4,5} Significantly different from 13km/h, 15km/h, 17km/h, 19km/h, and 21km/h. ^{*} Significantly different from 3°.

5.2 Biomechanical characteristics of the V2 skating technique at different inclines (Article II).

Changing the treadmill's incline from 3° to 5° resulted in a 7% decrease in CL (FIGURE 13A, $p \leq 0.001$). From 3° to 5°, there was a 9% ($p < 0.001$) and 8% ($p \leq 0.008$) increase in CR (FIGURE 13A) and the relative poling time (FIGURE 13B), respectively. The relative kicking time (FIGURE 13C) did not differ significantly between the inclines ($p = 0.794$). When the incline of the treadmill was at 3°, the relative overlap time (FIGURE 13D) was greater than it was at 4° and 5° ($p = 0.101$).

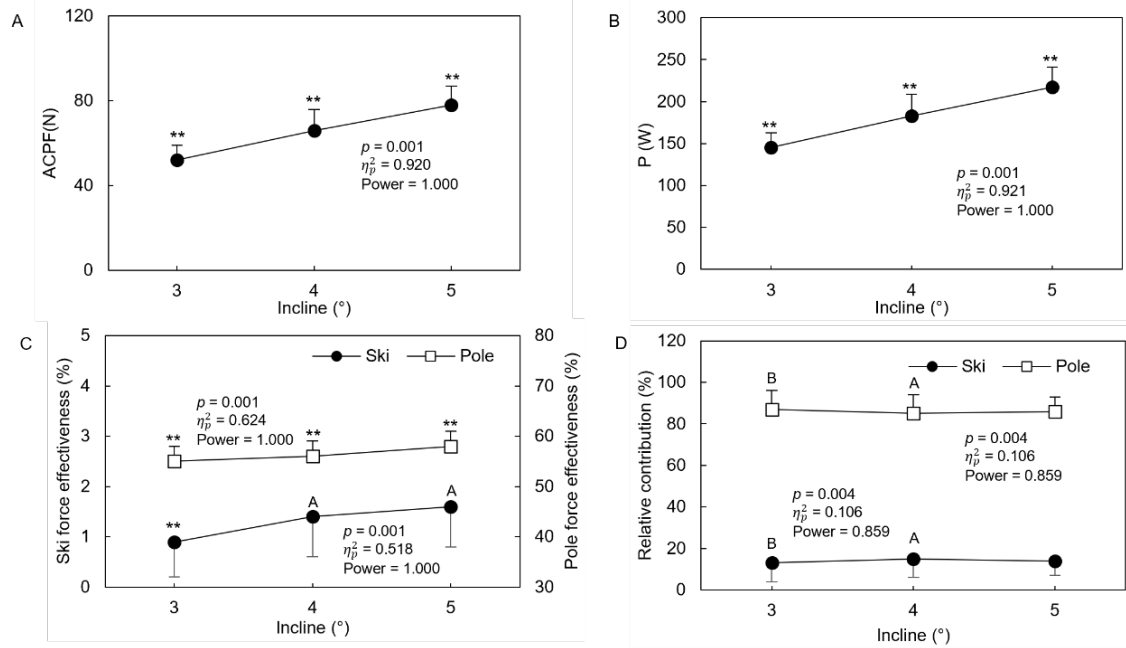
The PPF and PKF both increased from 3° to 5°; the PPF increased by 32% ($p < 0.001$, FIGURE 13E), and the PKF increased by 6% ($p \leq 0.037$, FIGURE 13E). There was a 36% increase in the pole propulsive force impulse from 3° to 5° ($p < 0.001$, FIGURE 13F). The ski propulsive force impulse (FIGURE 13G) at 4° did not differ from that at 5° ($p = 0.338$), but both impulses were greater than the impulse at 3° ($p < 0.001$). From 3° to 5°, the ski vertical force impulse decreased by 11% ($p < 0.001$, FIGURE 13H).

The ACPF was improved by 50% ($p < 0.001$, FIGURE 14A). The power output required to overcome the total resistance increased by 50% ($p < 0.001$, FIGURE 14B). The pole force effectiveness increased by 5% ($p < 0.001$, FIGURE 14C). The pole force effectiveness at 3° was significantly lower than it was at 4° to 5° ($p < 0.001$, $p < 0.001$, FIGURE 14C). Approximately 85% of the total propulsive force was contributed by the pole forces (FIGURE 14D). The incline of the treadmill affected the relative contributions of ski and pole forces to total resistance (FIGURE 14D), but the only significant difference was between 3° and 4° ($p = 0.003$).



Note: A: Cycle length (CL, left axis) and Cycle rate (CR, right axis); B: Relative poling time (%); C: Relative kicking time (%); D: Relative overlap time (%); E: Peak Pole force (PPF, left axis), Peak kicking force (PKF, right axis); F: Pole propulsive force impulse; G: Ski propulsive force impulse; H: Ski vertical force impulse. The data are presented as mean \pm SD. The p value, η_p^2 , and power presented in the figure are from the One-Way ANOVA with repeated measurement test. $**p < 0.01$, compared with all other inclines. a, A; b, B; c, C, represent different to 3°, 4°, 5°, respectively. a, b, c = $p < 0.05$; A, B, C = $p < 0.01$.

FIGURE 13. Cycle and kinetic characteristics of the V2 skating technique at 10km/h under different inclines.



Note: A: Average cycle propulsive force (ACPF); B: Power output in overcoming the total resistance (Power); C: Ski force effectiveness (left axis) and Pole force effectiveness (right axis); D: Relative contribution of ski and pole forces in overcoming the total resistance. The data are presented as mean \pm SD. The p value, η_p^2 , and power presented in the figure are from the One-Way ANOVA with repeated measurement test. $**p < 0.01$, compared with all other inclines. a, A; b, B; c, C, represent different to 3°, 4°, 5°, respectively. a, b, c = $p < 0.05$; A, B, C = $p < 0.01$.

FIGURE 14. Kinetic characteristics of the V2 skating technique at 10km/h under different inclines.

5.3 Biomechanical characteristics of the V2 skating technique at different speeds

5.3.1 Cycle characteristics

The cycle characteristics of the V2 skating technique at different speeds are presented in TABLE 9 and FIGURE 15. The CR was greater at 17km/h, 19km/h, and 21km/h than at 13km/h and 15km/h ($p \leq 0.005$). The CR increased by 6% as the speed of the treadmill elevated from 17km/h to 21km/h ($p \leq 0.005$, FIGURE 15A). The CL increased by 31% with the increasing speed of the treadmill ($p < 0.001$, FIGURE 15A). The CT (TABLE 9) decreased by 6% from 17km/h to 21km/h and was significantly greater than the CT at 13km/h and 15km/h ($p \leq 0.005$). The PT (TABLE 9) decreased by 28% ($p < 0.001$), and the DCP decreased by 20% ($p < 0.001$, FIGURE 15B) with the increasing treadmill speed, whereas the RT was independent of the treadmill speed ($p = 0.055$, TABLE 9). The KT (TABLE 9) decreased significantly from 13km/h to 17km/h ($p \leq 0.001$), with no difference between at 17km/h and at 19km/h ($p = 0.085$). The KT (TABLE 9) at 21km/h was significantly lower than KT at any other speeds ($p \leq 0.044$). The KT% was greater at 13km/h than at other speeds ($p < 0.001$, FIGURE 15B); however, no difference of KT% was found from 15km/h to 21km/h ($p \geq 0.450$, FIGURE 15B). The PGT

(TABLE 9) increased as the speed was elevated from 13km/h to 17km/h ($p \leq 0.046$) and decreased to the same level as PGT at 13km/h when the treadmill speed was 21km/h. The OLT decreased as speed of the treadmill increased ($p \leq 0.001$, TABLE 9). The OLT (TABLE 9) at 19km/h and 21km/h decreased about 12% when compared to the OLT at 13km/h to 17km/h ($p \leq 0.033$). The OLT% decreased when the speed increased as well ($p = 0.001$, FIGURE 15C). No significant difference in the OLT% was found when the speed increased from 13km/h to 17km/h ($p > 0.05$). The OLT% at 21km/h decreased by about 7% when compared to the OLT% at 13km/h and 15km/h ($p \leq 0.027$).

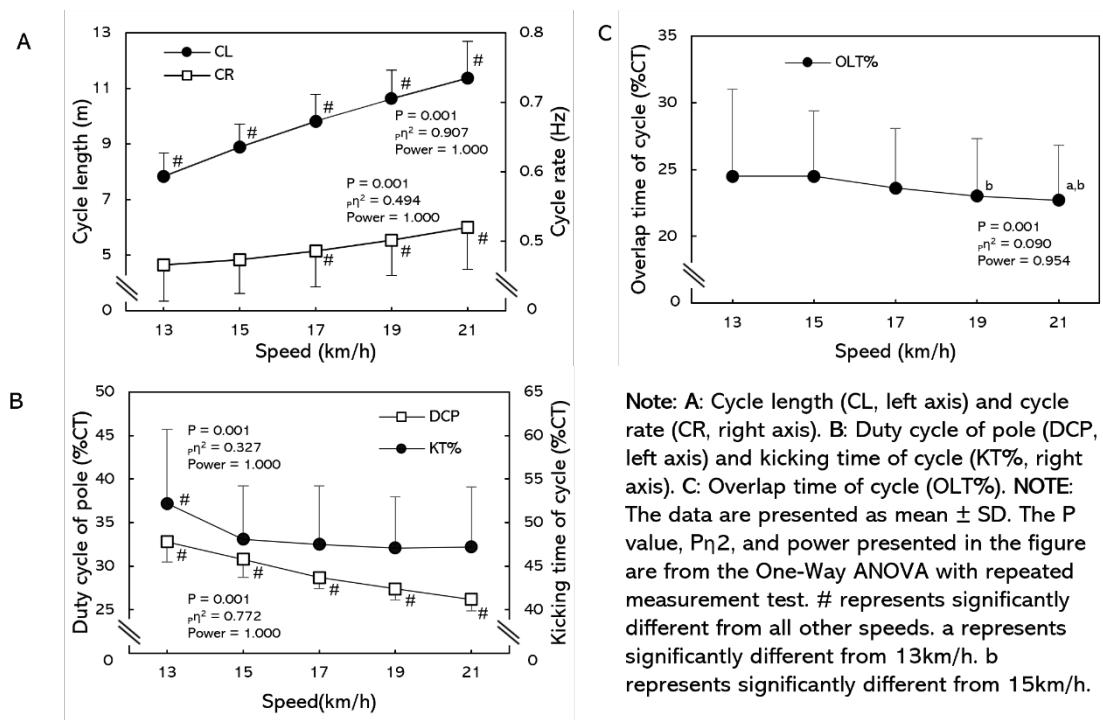


FIGURE 15. Cycle characteristics at five different speeds under 2° incline.

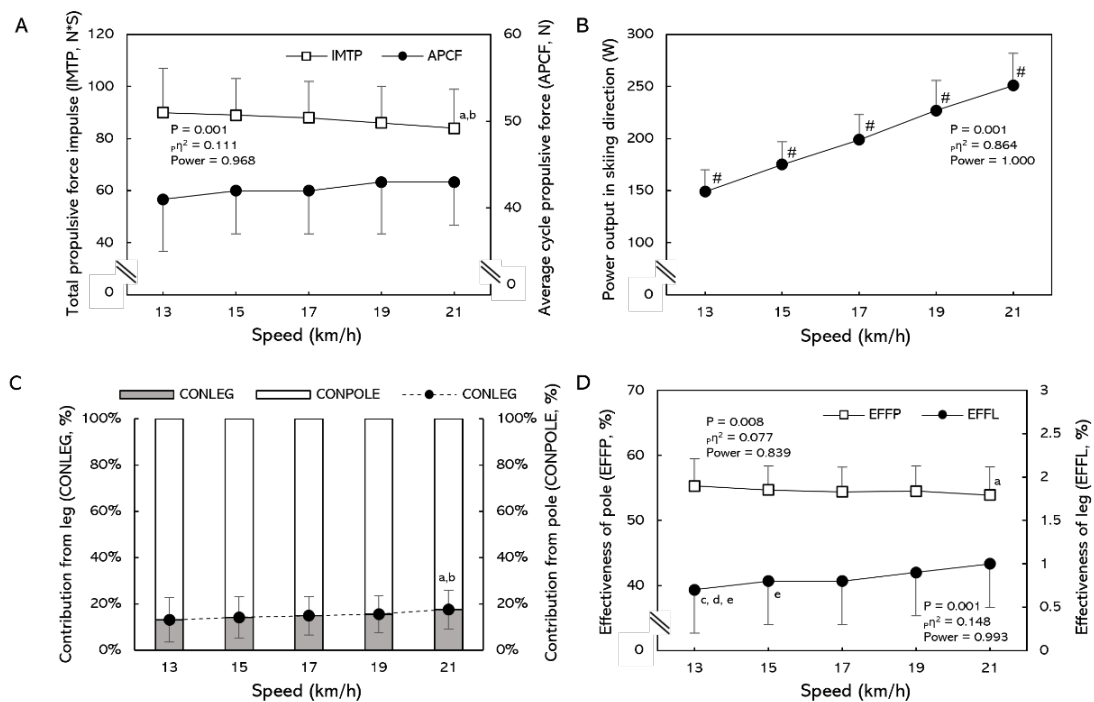
TABLE 9. Cycle characteristics of the V2 skating technique at different speeds (N = 10).

	Speeds (km/h)					F	P	$p\eta^2$	Power
	13	15	17	19	21				
Cycle time (CT, s)	2.17 ± 0.23	2.13 ± 0.20	2.08 ± 0.20 ^{ss}	2.01 ± 0.20 ^{ss}	1.95 ± 0.22 ^{ss}	F (3,170) =51	0.001	0.511	1.000
Poling time (PT, s)	0.71 ± 0.09 ^{ss}	0.65 ± 0.07 ^{ss}	0.60 ± 0.05 ^{ss}	0.55 ± 0.05 ^{ss}	0.51 ± 0.05 ^{ss}	F (3,127) =291	0.001	0.856	1.000
Recovery time of pole (RT, s)	1.46 ± 0.17	1.48 ± 0.15	1.48 ± 0.16	1.46 ± 0.16	1.44 ± 0.18	F (3,168) =2.5	NS		
Kicking time (KT, s)	1.12 ± 0.17 ^{ss}	1.02 ± 0.14 ^{ss}	0.98 ± 0.13	0.94 ± 0.13	0.91 ± 0.12 ^{ss}	F (3,145) =64	0.001	0.567	1.000
Pure gliding time (PGT, s)	1.05 ± 0.25 ^{‡§}	1.11 ± 0.18 ^{†¶††}	1.10 ± 0.21 ^{†††}	1.07 ± 0.18 [†]	1.04 ± 0.22 ^{‡§}	F (3,164) =6.9	0.001	0.123	0.984
Overlap time (OLT, s)	0.53 ± 0.15	0.52 ± 0.12	0.49 ± 0.10 ^{ss}	0.46 ± 0.09 ^{†‡§}	0.44 ± 0.09 ^{†‡§}	F (3,140) =26	0.001	0.344	1.000

TABLE 10. Force characteristics of the V2 skating technique at different speeds (N = 10).

	Speeds (km/h)					F	P	$p\eta^2$	Power
	13	15	17	19	21				
Pole force									
Peak force (PPF, N)	175 ± 50 ^{ss}	191 ± 51 ^{ss}	207 ± 50 ^{ss}	223 ± 51 ^{ss}	239 ± 68 ^{ss}	F (3,346) =127	0.001	0.562	1.000
Resultant force impulse (IMP, N*S)	142 ± 35	141 ± 30	138 ± 26	134 ± 26 [†]	129 ± 27 ^{†‡§}	F (3,139) =10	0.001	0.164	0.996
Propulsive force impulse (IMPP, N*S)	79 ± 19	77 ± 16	75 ± 15	73 ± 15 [†]	70 ± 16 ^{ss}	F (3,142) =13	0.001	0.206	1.000
Vertical force impulse (IMPV, N*S)	117 ± 30	117 ± 26	114 ± 22	111 ± 22 [†]	107 ± 23 ^{†‡§}	F (3,143) =9.3	0.001	0.160	0.996
Leg force									
Peak kicking force (PKF, N)	914 ± 165 ^{ss}	950 ± 176 ^{ss}	1003 ± 182 ^{ss}	1061 ± 185 ^{ss}	1139 ± 182 ^{ss}	F (3,151) =188	0.001	0.793	1.000
Resultant force impulse (IML, N*S)	1611 ± 252	1581 ± 233	1543 ± 236 ^{ss}	1493 ± 234 ^{ss}	1449 ± 225 ^{ss}	F (3,162) = 54	0.001	0.523	1.000
Propulsive force impulse (IMLP, N*S)	11 ± 8	12 ± 8	13 ± 7	13 ± 7	14 ± 7 [†]	F (3,151) =4	0.009	0.075	0.832
Vertical force impulse (IMLV, N*S)	1573 ± 247	1542 ± 230	1501 ± 232 ^{ss}	1449 ± 230 ^{ss}	1400 ± 223 ^{ss}	F (3,162) =60	0.001	0.551	1.000
Total force									
Total force impulse (IMT, N*S)	1753 ± 278	1722 ± 254	1680 ± 255 ^{ss}	1628 ± 255 ^{ss}	1578 ± 246 ^{ss}	F (3,162) =53	0.001	0.519	1.000
Average cycle force (ACF, N)	807 ± 93	807 ± 91	808 ± 93	808 ± 92	809 ± 91	F (3,166) =0.6	NS		

Note: For TABLE 9 and TABLE 10, the values presented are means ± SD. F and P values were obtained from one-way ANOVA with repeated measures. NS, not statistically significant. †Significantly difference from 13 km/h. ‡Significantly difference from 15 km/h. §Significantly difference from 17 km/h. ¶Significantly difference from 19 km/h. ††Significantly difference from 21 km/h. †††Significantly difference from all other speeds



Note: Total propulsive force impulse (A, left axis), average cycle propulsive force (A, right axis), power output in skiing direction (B), contribution from leg (C, left axis), contribution from pole (C, right axis), effectiveness of pole (D, left axis) and effectiveness of leg (D, right axis) at different speeds. The data are presented as mean \pm SD. The P value, $P\eta^2$, and power presented in the figure are form the One-Way ANOVA with repeated measurement test. # represents significantly different from all other speeds. a represents significantly different from 13km/h. b represents significantly different from 15km/h. c represents significantly different from 17km/h. d represents significantly different from 19km/h. e represents significantly different from 21km/h.

FIGURE 16. Kinetic characteristics in the V2 skating technique at different speeds under 2° incline.

5.3.2 Force characteristics

The force characteristics of the V2 skating technique at different speeds are documented in TABLE 10. The PPF increased by 37%, whereas the PKF increased by 25% from 13km/h to 21km/h. The IMP and the IMPV were lower at 21km/h than at 13km/h, 15km/h, and 17km/h ($p \leq 0.001$, $p \leq 0.001$). The IMP and IMPV at 19km/h were lower than that at 15km/h ($p = 0.042$, $p = 0.031$), with no difference between any other two speeds ($p \geq 0.467$, $p \geq 0.108$). The IMPP at 21km/h was lower than that at other speeds ($p \leq 0.010$). The IML and IMLV decreased by 6% and 7%, respectively, as the speed of the treadmill increased from 17km/h to 21km/h ($p \leq 0.005$, $p \leq 0.001$), with no significant difference between 13km/h and 15km/h ($p = 0.284$, $p = 0.277$). However, the difference in IMLP was only found between 21km/h and 13km/h. The IMLP was greater at 21km/h than at 13km/h ($p = 0.031$). The IMT at 13km/h did not differ from that at 15km/h ($p = 0.428$); however, both were greater than the IMT at 17km/h, 19km/h, and 21km/h ($p \leq 0.003$). Moreover, the ACF was independent of the treadmill speed ($p = 0.662$). The IMTP (FIGURE 16A) at 21km/h was significantly lower than the IMTP at 13km/h and 15km/h ($p \leq 0.008$). However, the APCF (FIGURE 16A) was also independent of the treadmill speeds ($p = 0.076$). The

power output in the skiing direction increased by 68% with increasing treadmill speed ($p < 0.001$, FIGURE 16B).

5.3.3 Contribution and effectiveness

5.3.3.1 Force domain.

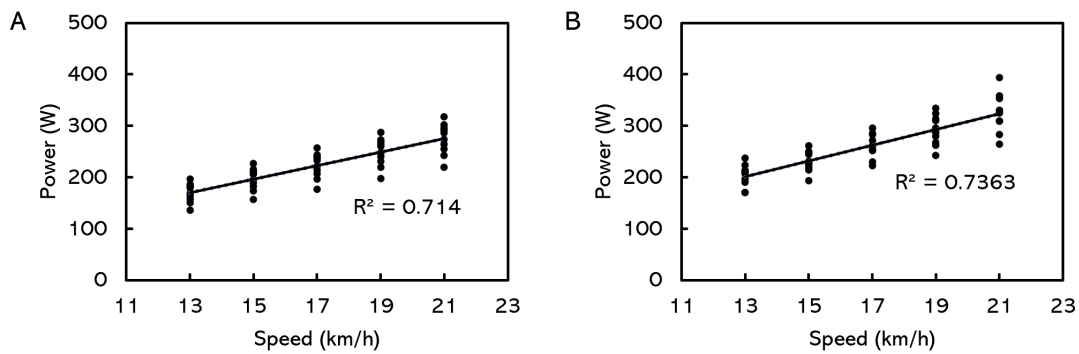
The contribution and effectiveness of legs and poles are shown in FIGURE 16. The contribution of the pole was about 4 to 6 times the amount of the contribution of the leg (FIGURE 16C). Although the contribution of the pole decreased and the contribution of leg increased with changing speeds, the only difference was found between 21km/h and 13km/h as well as at 15km/h (FIGURE 16C). The contribution of the leg was greater at 21km/h than at 13km/h and 15km/h ($p \leq 0.008$). The effectiveness of the pole force had a descending trend when the treadmill speed was increased ($p = 0.008$), and the effectiveness of pole force was lower at 21km/h than at 13km/h ($p = 0.004$). The forces generated from legs were more effective at 21km/h than at 13km/h and 15km/h ($p \leq 0.009$, FIGURE 16D). Thus, the forces generated from poles were more effective than forces generated from legs in the skiing direction at any speed ($p < 0.001$).

5.3.3.2 External power domain (Article III)

The interaction between speed * power calculation method was significant with the estimated total external power ($p < 0.001$, $P\eta^2 = 0.421$, observed power = 0.982). P_{mean} and P_{tot} increased by 61.6% and 60.3%, respectively, from 13 km/h to 21 km/h ($p < 0.001$, $p < 0.001$, TABLE 11). At any speed, P_{tot} was found about 17.7% to 19.5% greater than P_{mean} ($p < 0.001$, TABLE 11). However, both P_{mean} and P_{tot} show high linearity with skiing speed ($r^2 = 0.714$, $r^2 = 0.736$, FIGURE 17).

TABLE 11. Comparison of P_{mean} and P_{tot} (n = 10).

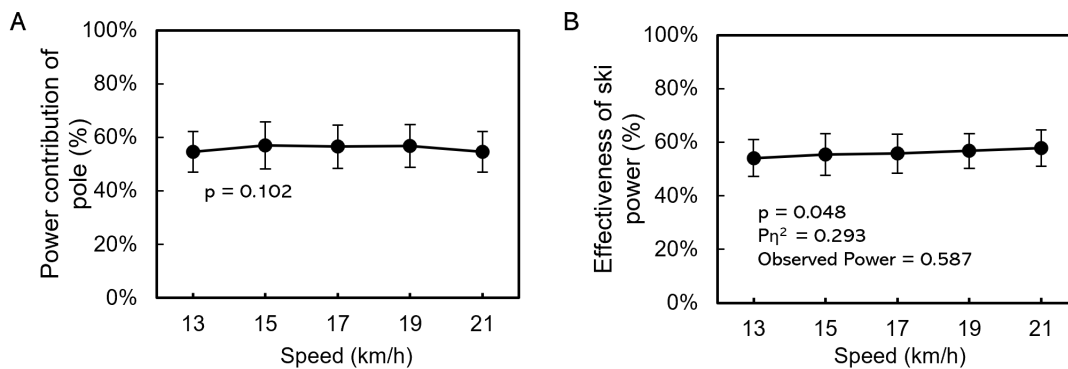
	Speed (km/h)	$P_{mean}(W)$	$P_{tot}(W)$	Effect of power calculation method			
				p	$P\eta^2$	Observed Power	Relative difference (%)
	13	170.1 ± 18.6	203.0 ± 21.6	<0.001	0.934	1.000	19.5 ± 5.9
	15	196.3 ± 21.5	231.2 ± 20.2	<0.001	0.831	1.000	18.4 ± 10.4
	17	222.5 ± 24.4	261.5 ± 23.6	<0.001	0.837	1.000	18.1 ± 9.3
	19	248.6 ± 27.2	291.6 ± 29.3	<0.001	0.869	1.000	17.7 ± 8.3
	21	274.8 ± 30.1	325.5 ± 37.5	<0.001	0.866	1.000	18.6 ± 7.3
	p	<0.001	<0.001				
Effect of	$P\eta^2$	0.990	0.988				
speed	Observed Power	1.000	1.000				



Note: (A) Linearity relation between P_{mean} and skiing speed. (B) Linearity relation between P_{tot} and skiing speed.

FIGURE 17. Linearity relation between mechanical power and skiing speed.

The relative contribution from the poles toward the total external power ranged between 55% and 57% and was independent from the skiing speed ($p = 0.102$, FIGURE 18A). The relative contribution from poles was expressed by expressing the P_p^+ as the sum of P_p^+ and P_s^+ , and the relative contribution from skis ranged between 43% and 45%. The relative pole power contribution was about 0.2 to 0.3 times greater than the ski power contribution to the total external power. The skiing speed affected the effectiveness of the ski power ($p = 0.048$, FIGURE 18B); however, no significant difference was found when the effectiveness of the ski power was compared between any two speeds ($p \geq 0.283$).



Note: (A) Relative power contribution from the poles towards the total external power. (B) The effectiveness of ski power. The data are presented as mean \pm SD. The p value, $P\eta^2$, and observed power presented in the figures are from the One-way ANOVA with repeated measurement test.

FIGURE 18. Relative power contribution from the poles and the effectiveness of ski power.

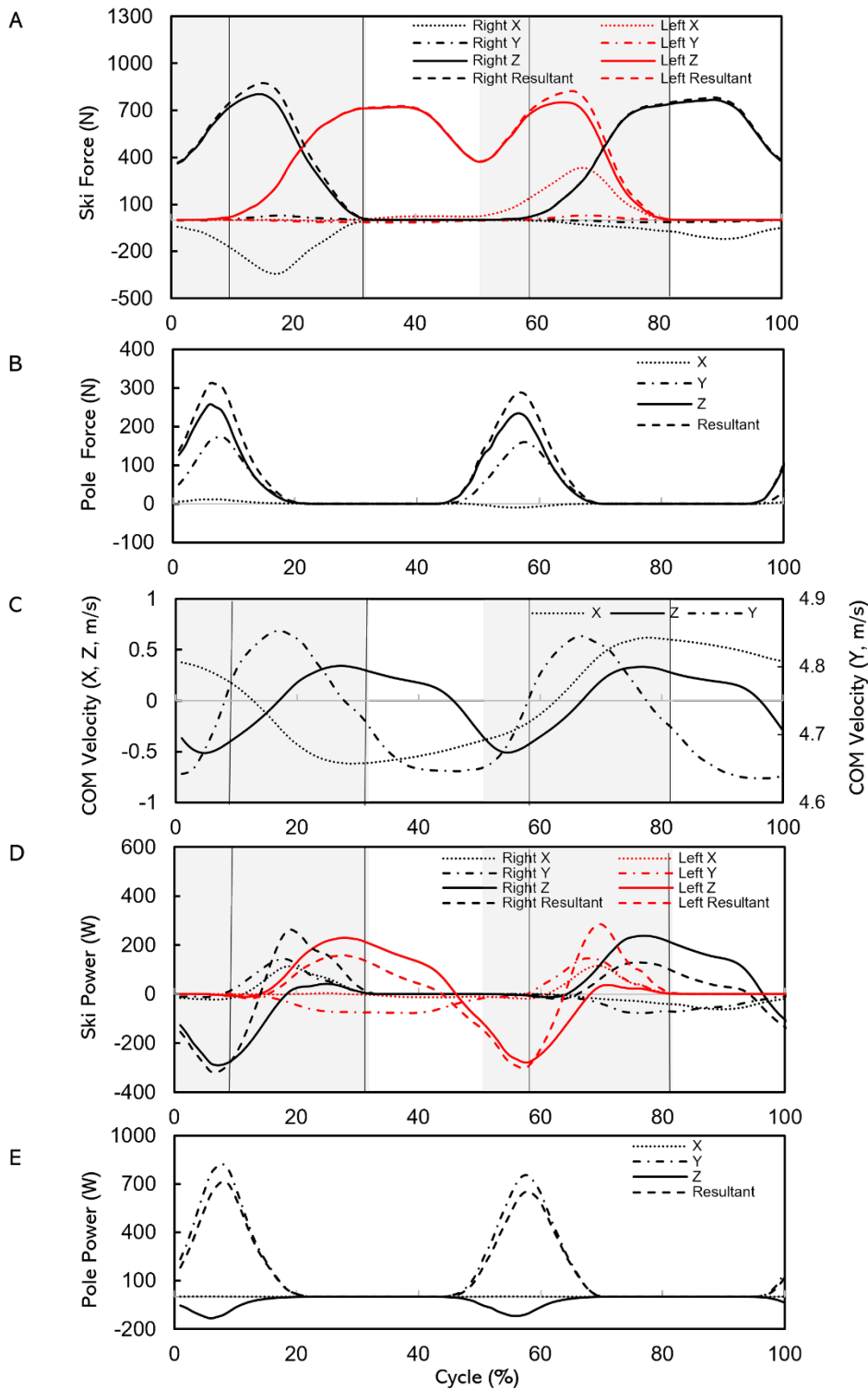
5.4 The roles of skis and poles during the V2 skating technique at different speeds (Article III)

The patterns of ski and pole forces, COM velocity, and external powers are shown in FIGURE 19. During the kicking phase, the GRFs produced by the push-off ski accelerate the medio-lateral velocity in the opposite direction (i.e., when the right ski acts as the kicking ski, the COM velocity accelerates to the left). The direction change of the medio-lateral, and vertical COM velocity was observed during the overlap phase (FIGURE 19). During the kicking phase, the kicking ski offered both negative and positive resultant external power. The power changed to mostly positive during the overlap phase. During the overlap phase, the gliding ski mainly produced positive resultant external power. Moreover, the poles produced positive resultant external power while poling.

When acting as kicking ski, both P_s^+ and P_s^- were dependent on the treadmill speed ($p < 0.001$, $p < 0.001$, FIGURE 20A), and the magnitude increased with the increasing speed. In the X (medio-lateral) component, the $P_{s,x}^+$ was independent of the treadmill speed ($p = 0.279$, FIGURE 20B). However, the magnitude of $P_{s,x}^-$ increased with the increasing speed ($p < 0.001$, FIGURE 20B). In the Y (fore-aft) component, the $P_{s,y}^+$ increased with the increasing speed ($p < 0.001$, FIGURE 20C). The $P_{s,y}^-$ was independent of the treadmill speed ($p = 0.518$, FIGURE 20C). In the Z (vertical) component, both $P_{s,z}^+$ and $P_{s,z}^-$ were dependent on the treadmill speed ($p < 0.001$, $p < 0.001$, FIGURE 20D).

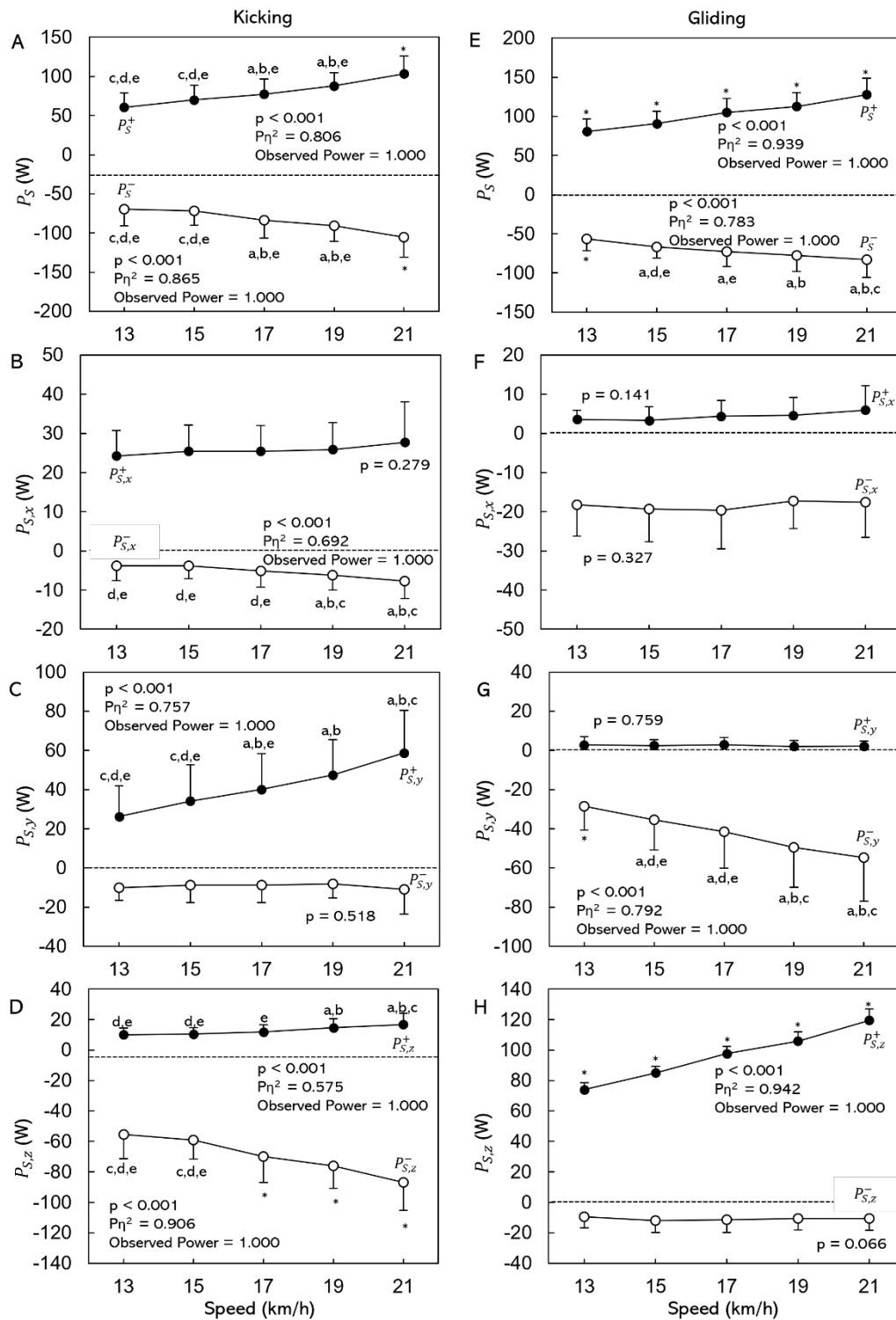
When acting as gliding ski, both P_s^+ and P_s^- were dependent on the treadmill speed ($p < 0.001$, $p < 0.001$, FIGURE 20E). The P_s^+ increased by 58.6% from 13 km/h to 21 km/h ($p \leq 0.010$). In the X component, the $P_{s,x}^+$ and $P_{s,x}^-$ were all independent of the treadmill speed ($p = 0.141$, $p = 0.327$, FIGURE 20F). In the Y component, the $P_{s,y}^+$ was small and unaffected by the treadmill speed ($p = 0.759$, FIGURE 20G). The magnitude of $P_{s,y}^-$ increased with the increasing speed ($p \leq 0.001$, FIGURE 20G). In the Z component, the $P_{s,z}^+$ increased by 61.6% from 13km/h to 21km/h ($p \leq 0.001$). No effect of speed was found on the $P_{s,z}^-$ ($p = 0.066$, FIGURE 20H).

Both P_p^+ and P_p^- were affected by the treadmill speed ($p < 0.001$, $p < 0.001$, FIGURE 21A). The P_p^+ increased by 60.8% from 13km/h to 21km/h ($p < 0.001$). The magnitude of P_p^- increased by 83.6% from 13km/h to 19km/h ($p \leq 0.002$), but no difference was found between 19km/h and 21km/h ($p = 0.056$). In the X component, the $P_{p,x}^+$ was dependent on the treadmill speed ($p = 0.040$, FIGURE 21B), whereas the $P_{p,x}^-$ was independent of the treadmill speed ($p = 0.362$, FIGURE 21B). In the Y component, no negative external power was found (FIGURE 21C), and the $P_{p,y}^+$ increased by 61.2% from 13km/h to 21km/h ($p < 0.001$, FIGURE 21C). In the Z component, no $P_{p,z}^+$ was found at any speed (FIGURE 21D). The magnitude of $P_{p,z}^-$ increased by 59.4% from 13km/h to 19km/h ($p \leq 0.001$), but no significant difference was found between 19km/h and 21km/h ($p = 0.059$).



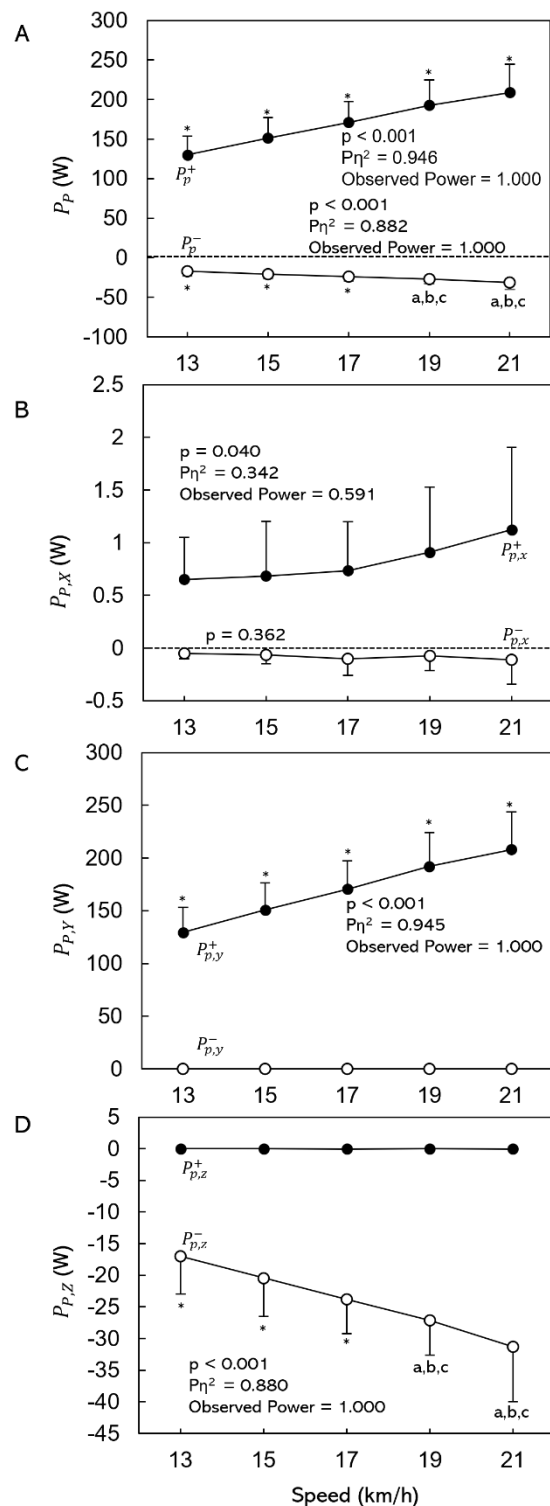
Note: (A) Forces from right and left skis. (B) Forces from poles. Pole forces were the sum of left and right. (C) COM velocity. X, and Z components, left axis; Y component, right axis. (D) Power from right and left skis. (E) Power from poles. Note: Dotted, dot-dash, solid, and dash curves represent the X, Y, Z, and resultant component, respectively. Black and red curves represent the right and left ski, respectively. The light gray areas represent the kicking phase of right and left skis. The areas between the vertical solid lines represent the ski overlapping phase. The horizontal time scale for each figure is normalized to the V2 skating cycle.

FIGURE 19. The patterns of ski and pole forces, COM velocity, and ski and pole powers at 17km/h.



Note: (A) Mean external power (P_S) while kicking. (B) Mean medio-lateral external power ($P_{S,x}$) while kicking. (C) Mean fore-aft external power ($P_{S,y}$) while kicking. (D) Mean vertical external power ($P_{S,z}$) while kicking. (E) Mean external power (P_S) while gliding. (F) Mean medio-lateral external power ($P_{S,x}$) while gliding. (G) Mean fore-aft external power ($P_{S,y}$) while gliding. (H) Mean vertical external power ($P_{S,z}$) while gliding. The data are presented as mean \pm SD. The p value, $P\eta^2$, and observed power presented in the figures are from the One-way ANOVA with repeated measurement test. * represents significantly different from all other speeds. a, b, c, d, e represent significantly different from 13, 15, 17, 19, 21 km/h, respectively.

FIGURE 20. The mean positive and negative external power from skis while kicking and gliding at different speeds.



Note: (A) Mean external pole power (P_p). (B) Mean medio-lateral external pole power ($P_{p,x}$). (C) Mean medio-lateral external pole power ($P_{p,y}$). (D) Mean vertical external pole power ($P_{p,z}$). The data are presented as mean \pm SD. The p value, $P\eta^2$, and observed power presented in the figures are from the One-way ANOVA with repeated measurement test. * represents significantly different from all other speeds. a, b, c represent significantly different from 13, 15, 17km/h, respectively.

FIGURE 21. The mean positive and negative external power from poles.

5.5 Validation of the 2D force measurement roller ski (Article IV)

The relative difference in the resultant forces between the force measurement roller ski and the AMTI force plate was less than 2.0% (from 0.11% to 1.92%) in the static test, as shown in FIGURE 22. The difference in the resultant forces between the force measurement roller ski and the AMTI force plate was shown in FIGURE 23. During the simulated skating push-off test, the CMC values for the force-time curves derived from the force measurement roller ski and the force plate were typically greater than 0.940 (FIGURE 24). The average absolute differences in forces in the X direction during one push-off cycle for various push-off loads ranged between 8.5 N and 33.3 N (TABLE 12). The average absolute differences in the Z direction forces for various push-off loads were between 3.9N and 23.4 N (TABLE 13). When using the force measurement roller skis to ski on the treadmill, the durations for the tests did not differ significantly from when using the reference roller skis. Using the force measurement roller ski, the male skier even achieved a longer duration and better performance with the force measurement roller ski than with the reference roller ski (143 s with force measurement roller ski, 134 s with reference roller ski).

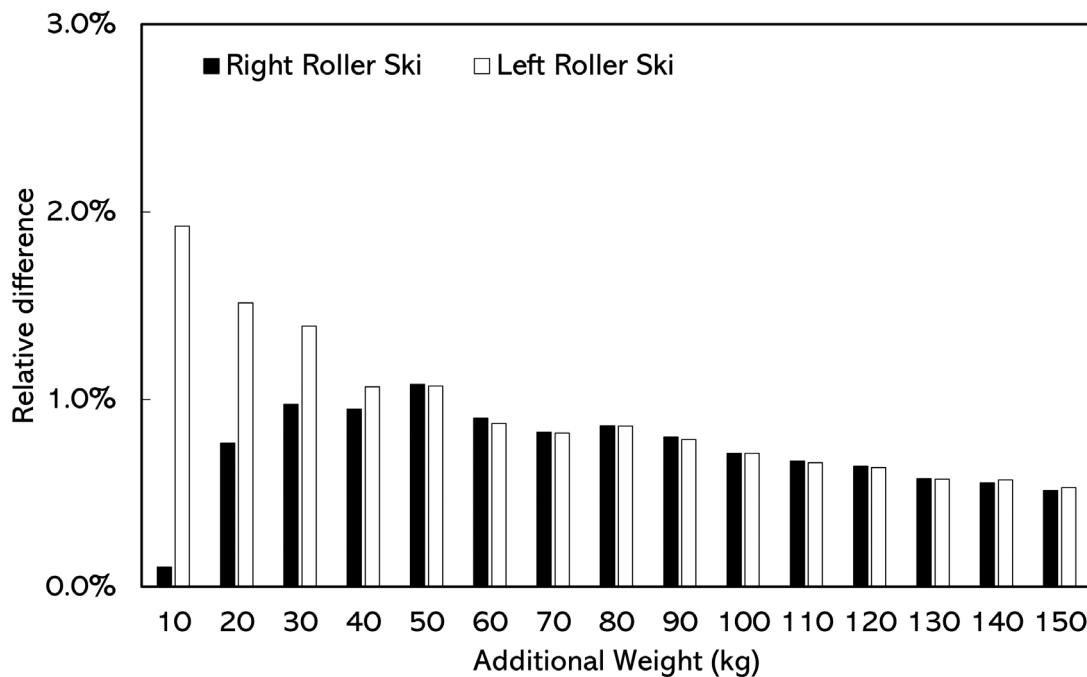
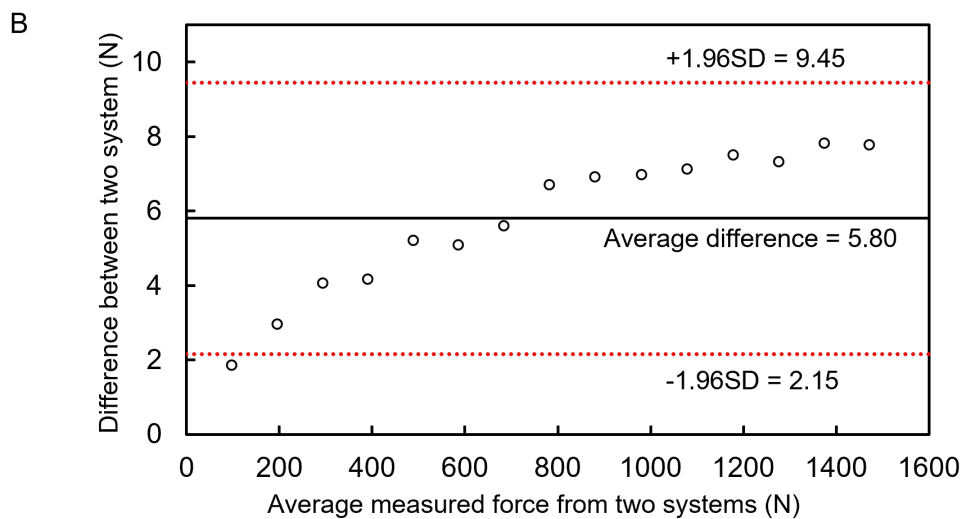
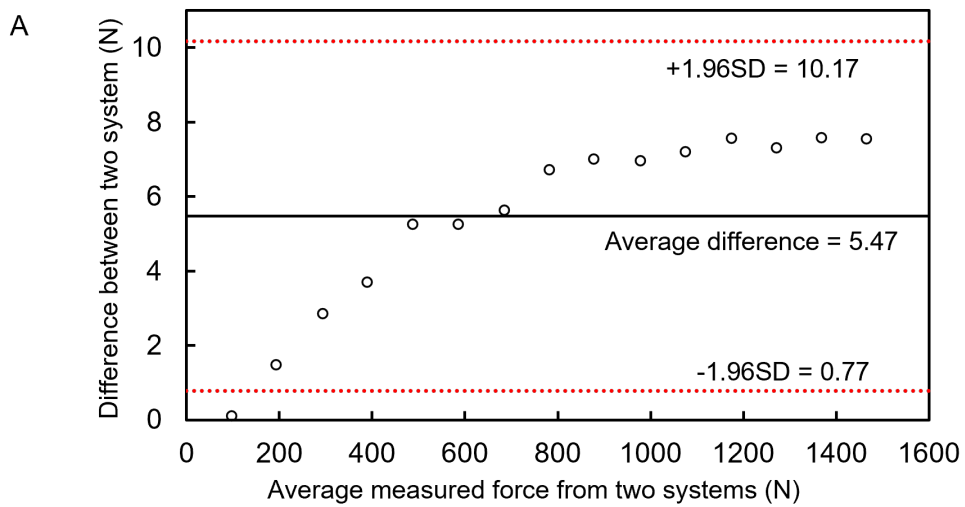


FIGURE 22. The relative difference in the resultant forces between the two force measurement systems.



Note: A. For right roller ski; B. For left roller ski. Lines are plotted indicating the limits of agreement (average \pm 1.96SD), and the average force difference.

FIGURE 23. Bland-Altman plot for the differences in the resultant force between two force measurement systems.

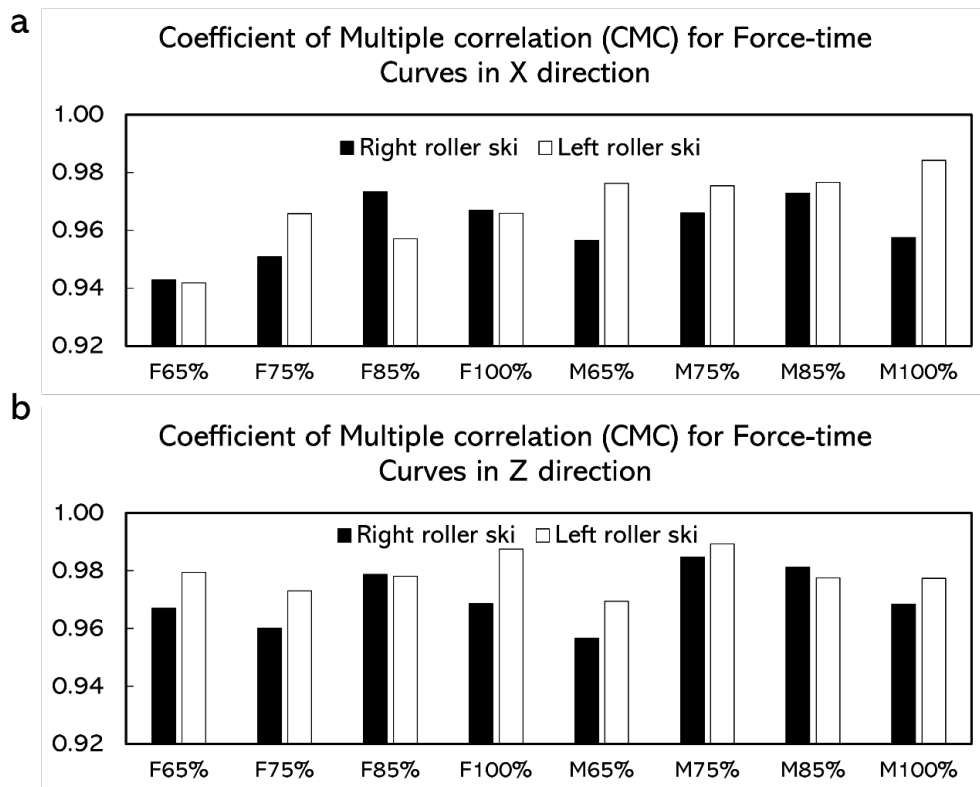


FIGURE 24. The coefficient of multiple correlation (CMC) for the time normalized force-time curve at different loads.

TABLE 12. The absolute difference (N) between force-time curves obtained by two force measurement systems in the X direction.

Loads	Right roller ski	Left roller ski
F65%	8.5 ± 5.6	18.8 ± 14.2
F75%	15.4 ± 12.3	26.1 ± 20.9
F75%	22.1 ± 17.0	28.2 ± 21.3
F100%	23.4 ± 26.5	32.5 ± 25.4
M65%	22.2 ± 10.2	18.8 ± 9.2
M75%	24.4 ± 12.6	19.4 ± 9.1
M85%	30.6 ± 19.0	21.1 ± 15.9
M100%	33.3 ± 25.0	24.4 ± 17.4

TABLE 13. The absolute difference (N) between force-time curves obtained by two force measurement systems in the Z direction.

Loads	Right roller ski	Left roller ski
F65%	15.8 ± 2.2	9.9 ± 3.3
F75%	18.3 ± 5.0	13.5 ± 7.1
F75%	20.7 ± 8.1	14.7 ± 8.5
F100%	23.4 ± 14.9	18.8 ± 13.4
M65%	11.7 ± 5.1	3.9 ± 3.4
M75%	11.7 ± 3.2	4.1 ± 4.0
M85%	13.8 ± 6.6	5.7 ± 7.2
M100%	15.2 ± 9.7	7.3 ± 9.8

6 DISCUSSION

6.1 Evaluation of different methods to calculate propulsion (Article I)

In this study, F , F_{net} , and F_{pro} represent the forward propulsion calculated by using different methods. F was calculated using the acceleration of the COM and the body mass. The F_{net} was the forward component of the 3D GRFs, and the F_{pro} was the forward component of translational force.

CMC_{pro} ranged from 0.907 to 0.936 for the DP technique, while CMC_{net} ranged from 0.883 to 0.955 and did not differ from CMC_{pro} (TABLE 5). CMC_{pro} ranged from 0.832 to 0.900 for the V2 skating technique, while CMC_{net} ranged from 0.879 to 0.922 (TABLE 6). The CMC close to one indicated that the curves involved were similar (Kadaba et al., 1989; Yu et al., 1997). Consequently, the force-time curves of F_{net} and F_{pro} were comparable to F during the force-generating phase for both the DP technique and V2 skating techniques. As the CMC_{net} was 5% higher than CMC_{pro} while altering the speed in the V2 skating technique (TABLE 6), the force-time curves of F_{net} were more similar to the force-time curves of F than those of F_{pro} .

F_{net} was directly calculated from the GRF. F_{net} did not consider the costs associated with the energy transformation (Robertson, 2013b, p. 132) between each segment and the elastic potential energy of the muscle. F_{pro} was determined by integrating the position of GRF and COM. The resultant GRF was separated into a translational component that acted via the COM and a rotational component that was always perpendicular to the translational component (Göpfert et al., 2017; Schwameder, 2008). Since the rotational component had no effect on the COM's translation, it was not included in the calculation of F_{pro} . Consequently, the forward component of the translational component in both the DP and V2 techniques may underestimate forward acceleration. The absolute mean force differences (TABLE 7 and TABLE 8) were determined to establish

which force-time curve was closest to the standard. When comparing the force-time curves, a higher degree of precision is indicated by a smaller absolute mean force difference, which indicates a force-time curve closer to the reference force curve. The absolute mean force difference between F_{pro} and F with the DP and V2 techniques was either greater than or equal to the absolute mean force difference between F_{net} and F , suggesting that the force-time curves of F_{net} were closer to the force-time curves of F when compared to F_{pro} .

All the methods used to determine forward propulsion were affected by the treadmill's speed or incline. While it is impossible to achieve a perfect replication of the reference value F , we expected the CMC_{net} , CMC_{pro} , and absolute mean force difference over the force-generating cycle to be stable across both methods of calculation for F_{net} and F_{pro} . In this study, the CMCs were somehow affected by the speed and incline of the treadmill in both the DP and V2 techniques. In addition, it was found that the absolute mean force differences between F_{net} and F ($M_{|F_{\text{net}}-F|}$) and between F_{pro} and F ($M_{|F_{\text{pro}}-F|}$) were all affected by the treadmill speed regardless of the technique performed. Although F_{pro} and F_{net} can be used to estimate the force-time curve of F , they were not stable when the speed changed (TABLE 7 and TABLE 8), as the absolute mean force differences increased with increasing speed.

In this study, both F_{net} and F_{pro} were utilized to assess the trend of the force-time curve of forward propulsion. F_{net} , the forward-directed horizontal component of 3D GRF, was found to be more appropriate due to its greater similarity with the reference force curve and a higher degree of precision. Therefore, subsequent investigations utilized the same method to determine the propulsive force.

6.2 Biomechanical characteristics of the V2 skating technique at different inclines (Article II)

In response to increases in incline, the CR increased significantly at steeper inclines with the V2 skating technique (FIGURE 13A). At steeper inclines, one cycle was completed in less time. This result is consistent with previous research, indicating that the CR is greater on steeper inclines when using the V2 skating technique (Bilodeau et al., 1992). As the pace of the treadmill remained constant regardless of the incline, the CL decreased with increasing incline. A similar finding was found in a previous study that the CL decreased with both the V1 skating technique and DP techniques in response to a steeper incline (Millet et al., 1998b). Similar phenomena have been observed in uphill running, in which the increased incline of a treadmill decreased the step length and increased the step frequency (Gottschall & Kram, 2005; Padulo et al., 2013). The adjustment of CL and CR during uphill running was influenced by the incline gradient and the available metabolic power (Padulo et al., 2013).

In this study, the relative PT (FIGURE 13B) was greater at steeper inclines when using the V2 skating technique. The time required to prepare for the next pole plant was reduced at a steeper incline, and the proportion of cycles devoted to generating pole forces increased as the incline was increased (Millet et al., 1998b). The relative kicking time (FIGURE 13C) was independent of the incline. With increased inclines, the proportion of the cycle for generating ski propulsive forces did not change.

The relative overlap time (FIGURE 13D) was shorter at 4° and 5° than at 3°. The shorter relative overlap time indicates that the skier may begin “seeking ground contact” with the swinging leg later at steeper inclines (Ohtonen et al., 2016). The magnitude of the relative overlap time in this study (23%–25%) was higher than that reported by Ohtonen et al. (2016) (around 10%). This distinction may be attributable to environmental factors (snow versus treadmill) and athlete ability (elite skiers versus skiers of varying ability). Elite skiers who are faster than average-level skiers may have greater balance control (Ohtonen et al., 2016).

The PPF (FIGURE 13E) and the pole propulsive force impulse (FIGURE 13F) increased continuously up to the steepest incline. In light of these findings and the cycle characteristics, it should be possible to achieve larger pole force and pole propulsive force at steeper inclines, despite the fact that less time was spent preparing for pole planting. These results supported the conclusion from the previous study that, in both DP and V1 skating techniques, the force variables from poles were all greater on steeper grades (Millet et al., 1998b).

With the V2 skating technique, greater ski force and ski propulsive force must be generated to overcome the increased total resistance at steeper inclines. In this study, both the PKF and ski propulsive force impulse increased at steeper inclines. Nevertheless, despite the fact that the study participants had identical bodyweights to those in other previous studies (Ohtonen et al., 2016; Stöggl et al., 2010), the magnitude of PKF in this study was smaller. The additional weight and height of the roller skis equipped with force measurement bindings might have reduced leg utilization, preventing the attainment of greater ski forces. In addition, the difference in PKF may also account for the difference in the levels of the skiers. The skiers who participated in this study were also amateurs, which might have resulted in lower PKF values.

The gravity component parallel to the treadmill surface increased with incline (Danielsen et al., 2019), so a steeper grade necessitates greater forces and power output. Consequently, the ACPF increased continuously as the incline was increased while using the V2 skating technique (FIGURE 14A). In response to the increased incline, the power output required to overcome the total resistance increased by 50% in this study (FIGURE 14B). With the V2 skating technique, both poles and skis must generate more propulsive force. It is also important to note that, on a treadmill, skiers do not have to contend with wind resistance as they do when they ski outdoors. Especially with higher speeds, wind resistance would significantly impact propulsive forces (Ainegren et al., 2022). Therefore, the results of this study regarding the magnitude of forces may differ from those of studies that focused on snow skiing (Ohtonen et al., 2016).

6.3 Biomechanical characteristics of the V2 skating technique at different speeds

6.3.1 Cycle characteristics

In this study, the CL ranged from 7.84 m to 11.37 m and the CR ranged from 0.47 to 0.52 Hz were both affected by the treadmill speed. The CL increased constantly from 13km/h to 21km/h, but the CR only increased continuously from 17km/h. The observations from different terrestrial movements indicated that the primary factor that contributes to speed increases at low speeds was CL, whereas the factor that contributes to speed increases at high speed was CR (Hay, 2002). This may help explain why CR did not increase significantly when the treadmill speed increased from 13km/h to 15km/h. However, wind resistance in treadmill skiing was not found to be a factor, thus the speeds may not be directly comparable to outdoor skiing. The study results are also in line with the findings from field skiing (Nilsson et al., 2004; Ohtonen et al., 2016), field roller skiing (Millet et al., 1998c), and treadmill roller skiing (Sandbakk et al., 2012), indicating that both CL and CR increase when speed increases across submaximal speeds.

The DCP in this study decreased with increasing treadmill speed from 13km/h to 21km/h. Previous studies have indicated that DCP consistently decreased during submaximal speeds (Millet et al., 1998c; Ohtonen et al., 2016), in which the range of submaximal speeds approximately matched the range of speed in this study. The DCP' magnitude was lower than the DCP in previous studies (Millet et al., 1998c; Ohtonen et al., 2016), which might be due to the difference in incline of the terrain (Ohtonen et al., 2016), the friction coefficient of the field measurement (Millet et al., 1998c; Ohtonen et al., 2016), and the evolution of skiing during the last two decades. Though the KT% at 15km/h to 21km/h were all significantly shorter than the KT% at 13km/h, the KT% did not change significantly after 15km/h. Combined the results associated with both DCP and KT%, the increase of CR might be a more pronounced contribution to the decrease in DCP at relatively high speeds (from 17km/h to 21km/h). Ranging from 24.5% to 22.7%, the OLT% decreased with increasing treadmill speed. The magnitude of the OLT% presented in this study was about twice as much as that presented in a previous study (Ohtonen et al., 2016). This is because the variables analyzed in the previous study were only from the right side of the body. During the overlap phase, both the left and right skis were on the treadmill. This result is similar to what has been found in gait analysis in walking: that the double support time decreases with increasing walking speed (Hebenstreit et al., 2015; Schwartz et al., 2008). However, this is contrary to the results observed in the V2 skating technique on snow where the OLT% increased at the maximum speed (6.6 m/s) (Ohtonen et al., 2016). The OLT% is related to the time when the kicking leg stops kicking and the start time when the contralateral leg starts gliding. At higher speeds while skiing on snow, skiers may start the gliding phase earlier, as body weight is transferred crossways from one side to the other (Ohtonen et al.,

2016). The force measurement binding made the roller skis used in the present study heavier and higher than the normal ones. This increased height and more unstable roller skis led to the contralateral leg to set into the ground earlier, which might have further caused the decrease in the OLT%.

6.3.2 Force characteristics

The PPF in this study was affected by treadmill speed. Ranging from 175 N to 239 N, the PPF increased by 37% with the increasing treadmill speed. This result is consistent with what was reported in a recent study, where the maximum pole forces increased about 44% from the lowest speed up to the maximum speed (Ohtonen et al., 2016). Similar results were also demonstrated by Millet et al. (1998c): the PKF constantly increased by 25% with increasing treadmill speed; however, the enhancement in PPF was greater. In this study, although both PPF and PKF were increasing, as a consequence of the decreasing DCP and DCL, both IMP and IML decreased while the treadmill speed increased. These results also indicate that greater forces should be reached in a shorter time to adapt to the increasing treadmill speeds. Considering the balance of forces under a laboratory condition, where there is no air resistance, constant friction coefficient, and constant gravitational force while just changing the speed, the average propulsive force should stay constant. Thus, in this study, ACF and APCF were all independent of the treadmill speed.

6.3.3 Contribution and effectiveness

6.3.3.1 Force domain

The relative contribution from the leg kicking to the total propulsive force had an increasing trend, especially increasing at the highest speed; at the same time, the relative contribution from the poling decreased. The relative contribution from poling was about 4 to 6 times the amount of from the leg kicking. Findings reported in a previous study showed that for the V2 skating technique, about two-thirds of the propulsive force is due to the force from poles and one-third is due to the force from skis (Smith et al., 2006). The difference between this previous study and our study may be attributed to the slower treadmill speed and higher treadmill incline in the previous study. In addition, roller skiing with the roller skis equipped with force measurement bindings on the treadmill may cause instability. The skiers who participated in this study were not at a high level. Such reasons might have decreased the use of legs and produced a more pronounced relative contribution from poling. Moreover, the decrease in the relative contribution from poling when the speed was increased was mainly caused by the decrease in the IMPP. With the same applied force, the more the poles inclined away from the vertical direction, the more the propulsive force increased (Smith, 2003, pp. 32-61). IMPP is also related to the duration of the force applied. Despite the poles being inclined farther away from the vertical direction and the increase in the change of pole angle with increasing speed, the

continuously decreasing PT and DCP might be possible for the decrease in IMPP, thus affecting the relative contribution from poling.

In a previous study, the effectiveness index was implemented as a useful tool to evaluate an athlete's overall economy on force production (Stöggl & Holmberg, 2015). As it is calculated by expressing the propulsive force impulse as the percentage of the resultant force impulse, the effectiveness index could also represent the effectiveness of forces in the skiing direction. Ranging from 0.7% to 1.0%, the effectiveness of legs increased with elevated treadmill speeds, indicating that, although it was quite small, more resultant force generated from the legs were transformed into propulsive force with increasing speeds. This is possible because of the slight increase in IMLP and the increase of edging angle at the end of kicking with increasing speed. About 50% of the resultant force generated from the poles could be transformed into propulsive force, which was more effective than the legs. A sinusoidal motion was made after both the legs had experienced both kicking and gliding movements (de Koning & van Ingen Schenau, 2008, pp. 232-245). Thus, to have a forward skiing velocity, the forces generated from both legs also provided lateral movement and supported the body against gravity (Stöggl & Holmberg, 2015).

6.3.3.2 External power domain (Article III)

Knowing how external power is delivered and from what source (poles versus skis) at varying speeds may enhance not only training and testing procedures but also the understanding of performance-related queries. Since the COM is propelled by both pole and ski forces in the skating technique, the total of pole and ski propulsive power should equal the sum of the forces against gravity and friction over the course of a cycle. Therefore, before calculating the relative contributions, we first examined whether the total pole and ski propulsive power could be used to represent the total power against gravity and friction. The sum of propulsive ski and pole power (P_{tot}) was found to be 17.7% to 19.5% greater than the sum of the power against gravity and friction (P_{mean}). The delivered ski and pole power is used for power against gravitational losses, against roller friction, and driving changes of kinetic energy (Dahl et al., 2017; De Koning et al., 2005). As the skier was roller skiing at a constant treadmill speed, we assumed that the changes in the kinetic energy of the COM over one cycle could be neglected. Therefore, the delivered propulsive power from skis and poles should be equal to the power against gravitational losses and roller friction. However, the V2 skating technique also involves sideward movements. If a skier adapted to the treadmill and did not drop out from it, the average forward speed should be equal to the treadmill speed. However, the average speed in the sideward (medio-lateral) direction over one cycle does not have to be zero, and medio-lateral kinetic energy may exist. This kinetic energy change rate in the V2 skating technique might be one reason that the P_{mean} is unequal to P_{tot} . Results from a previous study related to the DP technique demonstrated that the propulsive power was approximately equal to the P_{mean} (Danielsen et al., 2019). Compared with the DP technique, the V2 technique involves more angular displacements of

the limbs (e.g., leg swinging). This might be another reason that the P_{mean} may be unequal to P_{tot} . Both P_{mean} and P_{tot} are external power and are calculated to estimate the total energy use. It has been demonstrated that, with the V2 skating technique, the oxygen uptake as a measure of energy use increased in an approximately linear manner with skiing speed (Kvamme et al., 2005). Both P_{mean} ($r^2 = 0.714$) and P_{tot} ($r^2 = 0.736$) in this study showed high linearity (FIGURE 17) with the skiing speed, and their increase with speed were found to be similar (P_{mean} increased by 61.6% and P_{tot} increased by 60.3%). This indicated that P_{mean} and P_{tot} can be used for energy use estimation and further analysis.

The relative power contribution from the poles toward the total external power was determined by expressing the averaged propulsive resultant pole power (P_p^+) as a percentage of P_{tot} . The P_{tot} in this study was not exactly same with the P_{mean} . As they all have a stable relation with the speed, the P_{tot} was used to represent the total external power. About 55% to 57% of the external propulsive power was generated from poles; therefore, about 43% to 45% was generated from skis (FIGURE 18A). The relative contribution to the total external power from poles was 22% to 32% greater than from skis, which is different from the result obtained by calculating the propulsive force (Smith, 2003, pp. 32-61). Previous findings showed that, for the V2 skating technique, about two-thirds of the propulsive force is attributed to the force from poles, while one-third is attributed to the force from skis (Smith et al., 2006). The relative contribution from skis to maintain the speed calculated in this study was found to be greater than what has been reported, which supports our last hypothesis. Skiers who use the V2 technique do not move forward directly; they move forward in a “zig-zag” movement (Sandbakk et al., 2013a). The leg push-off is performed perpendicular to gliding ski (Sandbakk et al., 2012), which may lead to the sideward velocity of COM. As the sideward velocity can be added to the gliding velocity in a more or less forward direction (de Koning & van Ingen Schenau, 2008, pp. 232-245), the forces and sideward COM velocity also must be considered when calculating the relative contributions from skis. The external power is the dot product of the force vector that acts on the limb and the COM velocity vector. Therefore, the power analysis involved the movements in all directions. By calculating the propulsive force, the contribution of the ski forces to the sideward velocity was not included. Thus, it would underestimate the relative contribution of the ski force. Although the relative contribution from poles increased from 55% to 57%, the enhancement was not statistically significant (FIGURE 18A). Changing the relative contribution from the skis and poles might not be a strategy to cope with the increase in speed.

The effectiveness index has been used as a helpful tool to evaluate an athlete’s overall economy in terms of force production and was calculated by expressing the propulsive force impulse as a percentage of the resultant force impulse (Stöggl & Holmberg, 2015). In the present study, the effectiveness index of ski power was calculated by expressing the mean propulsive resultant ski external power P_s^+ as a percentage of ($P_s^+ + |P_s^-|$) over a cycle. The positive power indicated that the generated forces vectors acted in the same direction as the

COM velocity vector, which is the “propulsive power”. About 54% to 58% of the ski power acted as the “propulsive power” (FIGURE 18B). The effectiveness index was dependent on speed, but no significant difference was found when it was compared between any two speeds. This may be because the p-value for the effect of speed was close to 0.05. The effectiveness index of pole power was not analyzed, as almost all the pole power was positive (propulsive) power. It should be noted that the force measurement bindings used in this study were higher and heavier than the normal ones, which may have caused instability that decreased the use of legs and, therefore, resulted in a more pronounced amount of pole contribution and affected the effectiveness of the ski power.

6.4 The roles of skis and poles during the V2 skating technique at different speeds (Article III)

The patterns of the ski and pole forces, the COM velocity, and the external powers are shown in FIGURE 19. It was observed that the X (medio-lateral) and Z (vertical) velocity of the COM started to accelerate in the opposite direction at the beginning of the kicking phase (FIGURE 19), and the velocities' directions changed after the other ski touched the treadmill during the overlap phase. At the beginning of the kicking phase, one ski was lifted off the treadmill. The angular moment induced by the horizontal distance between the COM and the ski force application point may produce a sideward velocity (Hof, 2007; Yamashita et al., 2017). Therefore, at the beginning of the kicking phase, the sideward velocity of the COM started to accelerate in the opposite direction. Both negative and subsequent positive resultant ski external power was observed in the kicking phase for the kicking ski (FIGURE 20). The values of the mean positive and negative power while kicking were similar and increased with treadmill speed (FIGURE 20A). For the resultant external power, the positive power was the propulsive power, and the negative power was the braking power (Yamashita et al., 2017). This power-producing pattern is similar to what has been found in running (Arampatzis et al., 2000). Mechanical energy is temporally stored and recovered before the end of kicking in the overlap phase, and the magnitude of the mechanical power increases with increasing speed. When observing the ski mechanical power from different components separately (FIGURE 20), while acting as the kicking ski, the negative vertical ski power was produced at the beginning of the kicking phase, and the positive medio-lateral and forward ski power were then generated in the overlap phase (FIGURE 20D). This indicates that, when the kicking action began, the potential and vertical kinetic energy started getting transformed into kinetic energy in the forward and medio-lateral directions. During the kicking phase, the knee flexion of the kicking leg increased first and then decreased (Ohtonen et al., 2016), which might have decreased and then increased the potential energy. This could help explain the positive vertical ski power of kicking ski at the end of the kicking phase. In

addition, the higher the speed that needs to be maintained, the more potential and vertical kinetic energy are converted into medio-lateral and forward kinetic energy (FIGURE 20C and FIGURE 20D).

During the overlap phase, positive external ski power was generated by the gliding ski after ski contact (FIGURE 19D). The gliding ski generated more vertical power (FIGURE 19D), which increased with the increasing speed (FIGURE 20H). The kicking leg leaned sideways, which might have prevented the COM from moving upwards, but more upward COM velocity should be gained by the extension of the kicking leg (Yamashita et al., 2017). Therefore, the positive vertical power from the gliding ski filled up the deficiency of the vertical power by the kicking leg, and this effect became more pronounced as the speed to be maintained increased.

While gliding, the ski power decreased (FIGURE 19D), which may be due to the decrease in positive vertical ski power and the negative forward power (FIGURE 19D, FIGURE 20G, and FIGURE 20H). The negative forward power stemmed from the resistance. The decrease in vertical ski power was mainly due to the decrease in vertical kinetic energy. After the ski touched the ground, the extension of the knee joint of the gliding ski increased (Ohtonen et al., 2016), which may have increased the potential energy. However, the vertical speed decreased (FIGURE 19C) while gliding. Due to the conservation of energy, the vertical kinetic energy decreased. Therefore, when the leg acted as the kicking leg, the required negative external power was produced as the leading leg did in walking to redirect the COM velocity (Donelan et al., 2002; Yamashita et al., 2017). At the beginning of the kicking action, the body weight is “dropped” from a high body position over the poles and skis to achieve high force, which can be seen in the external power perspective as negative external power to redirect the COM velocity, especially in the medio-lateral and vertical directions. This is inconsistent with our hypothesis that, in the V2 technique, the kicking and gliding skis play similar roles as the trailing and leading legs in walking. The role played by the kicking ski is more like the role of the leading leg in walking. When the leg acts as the gliding leg, its main role is to gain more vertical power and then prepare for the next kick.

Poles predominately produced positive resultant external power while poling (FIGURE 19E, FIGURE 21A). This positive pole power is mainly due to the positive pole forward power (FIGURE 19E and FIGURE 21C). While poling, the negative vertical pole external power was found (FIGURE 19E and FIGURE 21D), and the magnitude increased with the increasing speeds (FIGURE 21D), indicating that the potential and vertical kinetic energy were transformed mainly into forward kinetic energy. Moreover, more energy or faster transformation is needed while increasing the speed. Therefore, in the V2 technique, the main role of pole power is to propel the body to catch up with the treadmill speed.

6.5 Validation of a 2D force measurement roller ski (Article IV)

The inspiration for the force measurement roller ski validated in this study came from Ohtonen et al.'s (Ohtonen et al., 2013a) force measurement bindings. These bindings were used in our initial treadmill experiment, and one equipped roller ski weighed 1650g, which is 27.6% heavier than the force measurement roller ski. The Coachtech nodes allow the force measurement roller ski data to be wirelessly transmitted via the Coachtech system. Therefore, from a construction standpoint, this force measurement roller ski has the advantage of being lightweight and able to wirelessly measure forces in multiple dimensions without the need for transport cables and transmitters. This study's calibration factors were obtained from the calibration test conducted in June 2022. Another calibration test was conducted in December 2020. During these 18 months, skiers utilized the force measurement roller skis extensively to test signal collection via the Coachtech system. The calibration factors used in this study were comparable to those obtained in the earlier calibration test, indicating that the measurements could continue to be reliable and stable for several months. However, periodic calibration is advised.

A static test was conducted to determine the precision of the force measurement roller ski's output forces. The results of the test fall within the measurement uncertainty for the vertical direction established during the calibration procedure. In this study, the relative difference in the resultant forces varied between 0.11% and 1.92%. In a previous investigation, the difference between the vertical resultant forces measured by the force plate and the instrumented one-dimensional roller ski ranged from 5.40% to 10.59% (Hoset et al., 2014), which is greater than what we observed. The different construction of the force measurement roller skis may be responsible for the enhanced precision.

The simulated skating push-off jump test was conducted to validate the force measurement roller ski in a dynamic application. In this study, the CMC values were typically greater than 0.940, indicating that, at each push-off load, the force-time curves obtained by the force plate and the force measurement roller ski after being transformed into the GCS were comparable in each direction. The average absolute discrepancies in the Z direction forces for various push-off loads ranged from 3.9 N to 23.4 N. According to the findings of a previous study, the change in the leg vertical force change during a single skate skiing cycle from submaximal speed to the maximum speed was approximately 60 N to 1415 N (Ohtonen et al., 2016). Since the differences between the forces measured by the force measurement roller ski and the reference force plate in this study are smaller than those observed during skiing at varying intensities, the accuracy of the forces measured by the force measurement roller ski is sufficient for use in practice, such as for making skiing technique observations.

The additional weight of the force measurement roller ski had no effect on athletes' performance. The duration roller skiers spent on the treadmill and the maximum speed they could attain were not significantly affected by the roller

skis used. Though there was a 333g difference between the roller skis, the balance point of the roller ski also shifted. This caused the torque difference around the ski boot attachment location on the roller ski to be 0.01 Nm, which is negligible. Therefore, the additional weight of the force measurement roller ski appears to be acceptable to the athletes.

6.6 Limitations

The study has some limitations. The primary disadvantage of the publications based on the Experiment I data is that the skiers' ability levels varied, and female participants were not included. As a result, the findings could only imply a general pattern of the V2 skating technique while roller skiing on the treadmill among males. To determine whether a homogeneous group of elite skiers would exhibit the same pattern, additional research is required. The highest speed attained in this study was not the maximal speed that the skiers were capable of attaining, so it does not represent their top performance. The force measurement bindings and the pole force sensors used are all heavier than normal ones, which is one of the reasons the skiers were unable to attain higher speeds. Moreover, it might have influenced their skiing technique, including pole and leg movements. This is also one of the reasons we improved and validated the force measurement roller ski in Experiment II. The absence of wind resistance (Ainegren et al., 2022) and the treadmill's motor and belt (Van Hooren et al., 2020) may prevent the applicability of the findings of this study to snow skiing.

The validity of the force in the Y direction was not investigated for the article that was published using the data from Experiment II. The movement in the Y direction during the simulated push-off jump test was quite minimal. In addition, the skiers who participated in the practical application test were all adult skiers. Further research is required to determine whether the force measurement roller ski would influence the roller skiing performance of junior and adolescent skiers.

7 MAIN FINDINGS AND CONCLUSIONS

This study's main aim was to describe the biomechanical characteristics of treadmill roller skiing. Since several approaches can be used to calculate forward propulsion, the approaches were first compared to discover the most suitable method. Due to the interests in the contribution from skis and poles, this study mainly concentrated on the V2 skating technique. The technique's biomechanical characteristics were investigated at different inclines and speeds. It was found that the leg push-off in V2 skating technique may lead to sideward velocity, and from the point of view of external power, the COM velocity and the external force were in a relation. The contribution of skis and poles was thus investigated from the external power point of view. Finally, a new force measurement roller ski was validated for future studies. The main findings of this study are as follows:

- 1) In Article I, two approaches for estimating the total propulsion on the skier's COM were evaluated. Both approaches can estimate the trend (force-time curve) of the total forward propulsion, but the approach that calculated the forward-directed horizontal component of 3D GRF is more appropriate.
- 2) When using the V2 skating technique, in response to incline changes (Article II), the CL decreased by 7% and the CR increased by 9%. To overcome the external resistance, 55% to 58% of the resultant pole force was generated, and about 85% of the total propulsive force was contributed by poles.
- 3) In response to speed changes, with the V2 skating technique, the CR increased by 6% from 17km/h to 21km/h, and the CL increased by 31%. From the force domain, the contribution of poling was about four to six times of the contribution of leg kicking. In addition, the pole forces were more effective than the leg forces in the skiing direction. The contribution of leg kicking slightly increased with increasing speeds. From the external power domain (Article III), the relative contribution from poling towards the total external power ranged between 55% to 57% and was independent of the skiing speed. In addition, the direction change of the medio-lateral and vertical COM velocity was observed during the overlap phase. The kicking and gliding skis all delivered both positive (propulsive) and

negative (braking) resultant external power. At the beginning of kicking phase, the negative external power was delivered by the kicking ski, and poles were always found to deliver positive external power while poling. Moreover, the magnitude of positive and negative resultant external power was found to increase when the speed was increased.

- 4) In Article IV, the force-time curves obtained by the force measurement roller ski and the 3D force plates were found to be highly similar. The absolute force difference in the X and Z directions over one push-off cycle was smaller than the observed force difference during different-intensity skiing.

In conclusion, the method of calculating the forward component of GRF is more appropriate to quantify the forward propulsion on a skier's COM when skiing on a treadmill. The cycle characteristics of the V2 skating technique (e.g., CL, CR, and so on) were affected by the treadmill incline and speed. From the propulsive force point of view, the relative contribution of pole forces versus ski forces in overcoming the total resistance did not change at different inclines. Pole forces contributed more propulsive force and were found to be more effective in skiing direction than ski forces. The contribution of legs slightly increased with increasing speeds. From the external power point of view, the relative contribution from the poles toward the total external power was smaller than when analyzed in the force domain. Changing the relative contribution from skis and poles may not be a strategy to cope with the increasing speeds. From the external power domain, the main role for the gliding leg is to gain more vertical power and prepare the next push off. The main role for poles is to propel the body to catch up with the increasing speeds. Finally, the newly designed 2D force measurement roller ski was found to be valid for use in future research for skate skiing techniques during daily training.

REFERENCES

- Ainegren, M., Linnamo, V., & Lindinger, S. (2022). Effects of aerodynamic drag and drafting on propulsive force and oxygen consumption in double poling cross-country skiing. *Medicine & Science in Sports & Exercise*, 54(7), 1058. <https://doi.org/10.1249/MSS.0000000000002885>
- Andersson, E., Pellegrini, B., Sandbakk, O., Stuggl, T., & Holmberg, H. C. (2014a). The effects of skiing velocity on mechanical aspects of diagonal cross-country skiing. *Sports Biomechanics*, 13(3), 267-284. <https://doi.org/10.1080/14763141.2014.921236>
- Andersson, E., Stoggl, T., Pellegrini, B., Sandbakk, O., Ettema, G., & Holmberg, H. C. (2014b). Biomechanical analysis of the herringbone technique as employed by elite cross-country skiers. *Scandinavian Journal of Medicine & Science in Sports*, 24(3), 542-552. <https://doi.org/10.1111/sms.12026>
- Andersson, E., Supej, M., Sandbakk, Ø., Sperlich, B., Stöggel, T., & Holmberg, H. C. (2010). Analysis of sprint cross-country skiing using a differential global navigation satellite system. *European Journal of Applied Physiology*, 110(3), 585-595. <https://doi.org/10.1007/s00421-010-1535-2>
- Arampatzis, A., Knicker, A., Metzler, V., & Brüggemann, G.-P. (2000). Mechanical power in running: a comparison of different approaches. *Journal of Biomechanics*, 33(4), 457-463. [https://doi.org/10.1016/S0021-9290\(99\)00187-6](https://doi.org/10.1016/S0021-9290(99)00187-6)
- Babel, S. (2003). Studies on intra-individual variability of selected cross-country skiing techniques. *European Journal of Sport Science*, 3(3), 1-10. <https://doi.org/10.1080/17461390300073305>
- Bellizzi, M. J., King, K. A., Cushman, S. K., & Weyand, P. G. (1998). Does the application of ground force set the energetic cost of cross-country skiing? *Journal of Applied Physiology*, 85(5), 1736-1743. <https://doi.org/10.1152/jappl.1998.85.5.1736>
- Bilodeau, B., Boulay, M. R., & Roy, B. (1992). Propulsive and gliding phases in four cross-country skiing techniques. *Medicine and Science in Sports and Exercise*, 24(8), 917-925. <https://doi.org/10.1249/00005768-199208000-00014>
- Bowen, R. S., Jensen, R. L., Ryan, J. M., & Watts, P. B. (2009). Modeling oxygen uptake during V1 treadmill roller skiing. *International Journal of Exercise Science*, 2(1), 48-59. <http://www.ncbi.nlm.nih.gov/pubmed/27182311>
- Caldwell, G. E., Robertson, G. E., & Whittlesey, S. (2013). Forces and Their Measurement. In G. E. Robertson, G. E. Caldwell, J. Hamill, G. Kamen, & S. Whittlesey (Eds.), *Research methods in biomechanics* (2 ed., pp. 80). Human kinetics.
- Dahl, C., Sandbakk, O., Danielsen, J., & Ettema, G. (2017). The role of power fluctuations in the preference of diagonal vs. double poling sub-technique at different incline-speed combinations in elite cross-country skiers. *Frontiers in Physiology*, 8, 94. <https://doi.org/10.3389/fphys.2017.00094>

- Danielsen, J., Sandbakk, Ø., McGhie, D., & Ettema, G. (2019). Mechanical energetics and dynamics of uphill double-poling on roller-skis at different incline-speed combinations. *PloS One*, 14(2), e0212500. <https://doi.org/10.1371/journal.pone.0212500>
- Danielsen, J., Sandbakk, Ø., McGhie, D., & Ettema, G. (2021). Mechanical energy and propulsion mechanics in roller-skiing double-poling at increasing speeds. *PloS One*, 16(7), e0255202. <https://doi.org/10.1371/journal.pone.0255202>
- De Koning, J. J., Foster, C., Lampen, J., Hettinga, F., & Bobbert, M. F. (2005). Experimental evaluation of the power balance model of speed skating. *Journal of Applied Physiology*, 98(1), 227-233. <https://doi.org/10.1152/jappphysiol.01095.2003>
- de Koning, J. J., & van Ingen Schenau, G. J. (2008). Performance-Determining Factors in Speed Skating. In V. M. Zatsiorsky (Ed.), *Biomechanics in sport: performance enhancement and injury prevention* (pp. 232-245). John Wiley & Sons. <https://doi.org/https://doi.org/10.1002/9780470693797.ch11>
- Donelan, J. M., Kram, R., & Kuo, A. D. (2002). Simultaneous positive and negative external mechanical work in human walking. *Journal of Biomechanics*, 35(1), 117-124. [https://doi.org/10.1016/S0021-9290\(01\)00169-5](https://doi.org/10.1016/S0021-9290(01)00169-5)
- Ekström, H. (1987). The force interplay between the foot, binding, and ski in cross-country skiing. *Skiing Trauma and Safety: Sixth International Symposium*, Japan.
- Eng, J., & Winter, D. (1993). Estimations of the horizontal displacement of the total body centre of mass: considerations during standing activities. *Gait & Posture*, 1(3), 141-144. [https://doi.org/10.1016/0966-6362\(93\)90055-6](https://doi.org/10.1016/0966-6362(93)90055-6)
- Ettema, G., Kveli, E., Øksnes, M., & Sandbakk, Ø. (2017). The role of speed and incline in the spontaneous choice of technique in classical roller-skiing. *Human Movement Science*, 55, 100-107. <https://doi.org/10.1016/j.humov.2017.08.004>
- Gaskell, S. E., Serfass, R. C., & Rundell, K. W. (1999). Upper body power comparison between groups of cross-country skiers and runners. *International Journal of Sports Medicine*, 20(5), 290-294. <https://doi.org/10.1055/s-2007-971133>
- Göpfert, C., Lindinger, S. J., Ohtonen, O., Rapp, W., Muller, E., & Linnamo, V. (2016). The effect of swinging the arms on muscle activation and production of leg force during ski skating at different skiing speeds. *Human Movement Science*, 47, 209-219. <https://doi.org/10.1016/j.humov.2016.03.009>
- Göpfert, C., Pohjola, M. V., Linnamo, V., Ohtonen, O., Rapp, W., & Lindinger, S. J. (2017). Forward acceleration of the centre of mass during ski skating calculated from force and motion capture data. *Sports Engineering*, 20(2), 141-153. <https://doi.org/10.1007/s12283-016-0223-9>

- Gottschall, J. S., & Kram, R. (2005). Ground reaction forces during downhill and uphill running. *Journal of Biomechanics*, 38(3), 445-452.
<https://doi.org/10.1016/j.jbiomech.2004.04.023>
- Hay, J. G. (2002). Cycle rate, length, and speed of progression in human locomotion. *Journal of Applied Biomechanics*, 18(3), 257-270.
<https://doi.org/10.1123/jab.18.3.257>
- Hebenstreit, F., Leibold, A., Krinner, S., Welsch, G., Lochmann, M., & Eskofier, B. M. (2015). Effect of walking speed on gait sub phase durations. *Human Movement Science*, 43, 118-124.
<https://doi.org/10.1016/j.humov.2015.07.009>
- Hebert-Losier, K., Zinner, C., Platt, S., Stoggl, T., & Holmberg, H. C. (2017). Factors that Influence the performance of elite sprint cross-country skiers. *Sports Medicine*, 47(2), 319-342. <https://doi.org/10.1007/s40279-016-0573-2>
- Hladnik, J., Supej, M., & Jerman, B. (2018). Force measurement system for roller-ski skating. *Tehnički Vjesnik*, 25(5), 1291-1297.
<https://doi.org/10.17559/TV-20161219111250>
- Hof, A. L. (2007). The equations of motion for a standing human reveal three mechanisms for balance. *Journal of Biomechanics*, 40(2), 451-457.
<https://doi.org/10.1016/j.jbiomech.2005.12.016>
- Hoff, J., Helgerud, J., & Wisløff, U. (1999). Maximal strength training improves work economy in trained female cross-country skiers. *Medicine & Science in Sports & Exercise*, 31(6), 870-877. <https://doi.org/10.1097/00005768-199906000-00016>
- Holmberg, H. C., Lindinger, S., Stöggl, T., Björklund, G., & Müller, E. (2006). Contribution of the legs to double-poling performance in elite cross-country skiers. *Medicine & Science in Sports & Exercise*, 38(10), 1853-1860.
<https://doi.org/10.1249/01.mss.0000230121.83641.d1>
- Holmberg, H. C., Lindinger, S., Stöggl, T., Eitzlmair, E., & Müller, E. (2005). Biomechanical analysis of double poling in elite cross-country skiers. *Medicine & Science in Sports & Exercise*, 37(5), 807.
<https://doi.org/10.1249/01.mss.0000162615.47763.c8>
- Holmberg, L. J., Lund Ohlsson, M., Supej, M., & Holmberg, H.-C. (2013). Skiing efficiency versus performance in double-poling ergometry. *Computer Methods in Biomechanics & Biomedical Engineering*, 16(9), 987-992.
<https://doi.org/10.1080/10255842.2011.648376>
- Hoset, M., Rognstad, A., Rølvåg, T., Ettema, G., & Sandbakk, Ø. (2014). Construction of an instrumented roller ski and validation of three-dimensional forces in the skating technique. *Sports Engineering*, 17(1), 23-32. <https://doi.org/10.1007/s12283-013-0130-2>
- Kadaba, M., Ramakrishnan, H., Wootten, M., Gainey, J., Gorton, G., & Cochran, G. (1989). Repeatability of kinematic, kinetic, and electromyographic data in normal adult gait. *Journal of Orthopaedic Research*, 7(6), 849-860.
<https://doi.org/10.1002/jor.1100070611>
- Kerrigan, D. C., Viramontes, B. E., Corcoran, P. J., & LaRaia, P. J. (1995). Measured versus predicted vertical displacement of the sacrum during

- gait as a tool to measure biomechanical gait performance. *American Journal of Physical Medicine & Rehabilitation*, 74(1), 3-8.
<https://doi.org/10.1097/00002060-199501000-00002>
- Komi, P. V. (1985). Ground reaction forces in cross-country skiing. *Biomechanics IX-B*, Champaign.
- Komi, P. V. (1987). Force measurements during cross-country skiing. *Journal of Applied Biomechanics*, 3(4), 370-381. <https://doi.org/10.1123/ijsb.3.4.370>
- Komi, P. V., & Norman, R. W. (1987). Preloading of the thrust phase in cross-country skiing. *International Journal of Sports Medicine*, 08(S 1), 48-54.
<https://doi.org/10.1055/s-2008-1025703>
- Kvamme, B., Jakobsen, V., Hetland, S., & Smith, G. (2005). Ski skating technique and physiological responses across slopes and speeds. *European Journal of Applied Physiology*, 95(2), 205-212. <https://doi.org/10.1007/s00421-005-1332-5>
- Leppävuori, A. P., Karras, M., Rusko, H., & Viitasaio, J. T. (1993). A new method of measuring 3-D ground reaction forces under the ski during skiing on snow. *Journal of Applied Biomechanics*, 9(4), 315-328.
<https://doi.org/10.1123/jab.9.4.315>
- Lindinger, S. J., & Holmberg, H. C. (2011). How do elite cross-country skiers adapt to different double poling frequencies at low to high speeds? *European Journal of Applied Physiology*, 111(6), 1103-1119.
<https://doi.org/10.1007/s00421-010-1736-8>
- Lindinger, S. J., Stöggl, T., Müller, E., & Holmberg, H. C. (2009). Control of speed during the double poling technique performed by elite cross-country skiers. *Medicine & Science in Sports & Exercise*, 41(41), 210-220.
<https://doi.org/10.1249/mss.0b013e318184f436>
- Linnamo, V., Ohtonen, O., Stöggl, T., Komi, P., Müller, E., & Lindinger, S. (2012). Multi-dimensional force measurement binding used during skating in cross-country skiing. *Science & Skiing V*, 540-548.
- Løkkeborg, J., & Ettema, G. (2020). The role of incline, speed and work rate on the choice of technique in classical roller skiing. *PLoS One*, 15(7), e0236102.
<https://doi.org/10.1371/journal.pone.0236102>
- Malek, M. H., Coburn, J. W., & Marelich, W. D. (2018). *Advanced statistics for kinesiology and exercise science: a practical guide to ANOVA and regression analyses*. Routledge.
- Mapelli, A., Zago, M., Fusini, L., Galante, D., Colombo, A., & Sforza, C. (2014). Validation of a protocol for the estimation of three-dimensional body center of mass kinematics in sport. *Gait & Posture*, 39(1), 460-465.
<https://doi.org/10.1016/j.gaitpost.2013.08.025>
- Millet, G. Y., Hoffman, M. D., Candau, R. B., Buckwalter, J. B., & Clifford, P. S. (1998a). Effect of rolling resistance on poling forces and metabolic demands of roller skiing. *Medicine & Science in Sports & Exercise*, 30(5), 755-762. <https://doi.org/10.1097/00005768-199805000-00018>
- Millet, G. Y., Hoffman, M. D., Candau, R. B., & Clifford, P. S. (1998b). Poling forces during roller skiing: effects of grade. *Medicine & Science in Sports &*

- Exercise*, 30(11), 1637-1644. <https://doi.org/10.1097/00005768-199811000-00013>
- Millet, G. Y., Hoffman, M. D., Candau, R. B., & Clifford, P. S. (1998c). Poling forces during roller skiing: effects of technique and speed. *Medicine & Science in Sports & Exercise*, 30(11), 1645-1653. <https://doi.org/10.1097/00005768-199811000-00014>
- Mittelstadt, S. W., Hoffman, M. D., Watts, P. B., O'Hagan, K. P., Sulentic, J. E., Drobish, K. M., . . . Clifford, P. S. (1995). Lactate response to uphill roller skiing: diagonal stride versus double pole techniques. *Medicine & Science in Sports & Exercise*, 27(11), 1563-1568. <https://doi.org/10.1249/00005768-199205001-00631>
- Myklebust, H., Losnegard, T., & Hallen, J. (2014). Differences in V1 and V2 ski skating techniques described by accelerometers. *Scandinavian Journal of Medicine & Science in Sports*, 24(6), 882-893. <https://doi.org/10.1111/sms.12106>
- Nilsson, J., Tinmark, F., Halvorsen, K., & Arndt, A. (2013). Kinematic, kinetic and electromyographic adaptation to speed and resistance in double poling cross country skiing. *European Journal of Applied Physiology*, 113(6), 1385-1394. <https://doi.org/10.1007/s00421-012-2568-5>
- Nilsson, J., Tveit, P., & Eikrehagen, O. (2004). Effects of speed on temporal patterns in classical style and freestyle cross - country skiing. *Sports Biomechanics*, 3(1), 85-108. <https://doi.org/10.1080/14763140408522832>
- Ohtonen, O. (2019). *Biomechanics in cross-country skiing skating technique and measurement techniques of force production*. Doctoral dissertation, University of Jyväskylä. Jyväskylä.
- Ohtonen, O., Lindinger, S., Lemmettylä, T., Seppälä, S., & Linnamo, V. (2013a). Validation of portable 2D force binding systems for cross-country skiing. *Sports Engineering*, 16(4), 281-296. <https://doi.org/10.1007/s12283-013-0136-9>
- Ohtonen, O., Lindinger, S., & Linnamo, V. (2013b). Effects of gliding properties of cross-country skis on the force production during skating technique in elite cross-country skiers. *International Journal of Sports Science & Coaching*, 8(2), 407-416. <https://doi.org/10.1260/1747-9541.8.2.407>
- Ohtonen, O., Lindinger, S. J., Gopfert, C., Rapp, W., & Linnamo, V. (2018). Changes in biomechanics of skiing at maximal velocity caused by simulated 20-km skiing race using V2 skating technique. *Scandinavian Journal of Medicine & Science in Sports*, 28(2), 479-486. <https://doi.org/10.1111/sms.12913>
- Ohtonen, O., Linnamo, V., Göpfert, C., & Lindinger, S. (2019). *Effect of 20km simulated race load on propulsive forces during ski skating*. Science and skiing VIII, Finland.
- Ohtonen, O., Linnamo, V., & Lindinger, S. J. (2016). Speed control of the V2 skating technique in elite cross-country skiers. *International Journal of Sports Science & Coaching*, 11(2), 219-230. <https://doi.org/10.1177/1747954116637156>

- Ohtonen, O., Ruotsalainen, K., Mikkonen, P., Heikkinen, T., Hakkarainen, A., Leppävuori, A., & Linnamo, V. (2015). *Online feedback system for athletes and coaches* 3rd International Congress on Science and Nordic Skiing, Finland.
- Padulo, J., Powell, D., Milia, R., & Ardigò, L. P. (2013). A paradigm of uphill running. *PloS One*, 8(7), e69006.
<https://doi.org/10.1371/journal.pone.0069006>
- Pellegrini, B., Zoppiroli, C., Bortolan, L., Zamparo, P., & Schena, F. (2014). Gait models and mechanical energy in three cross-country skiing techniques. *Journal of Experimental Biology*, 217(Pt 21), 3910-3918.
<https://doi.org/10.1242/jeb.106740>
- Pierce, J. C., Pope, M. H., Renstrom, P., Johnson, R. J., Dufek, J., & Dillman, C. (1987). Force measurement in cross-country skiing. *Journal of Applied Biomechanics*, 3(4), 382-391. <https://doi.org/10.1123/ijsb.3.4.382>
- Rabuffetti, M., & Baroni, G. (1999). Validation protocol of models for centre of mass estimation. *Journal of Biomechanics*, 32(6), 609-613.
[https://doi.org/10.1016/S0021-9290\(99\)00040-8](https://doi.org/10.1016/S0021-9290(99)00040-8)
- Robertson, G. E. (2013a). Body Segment Parameters. In G. E. Robertson, G. E. Caldwell, J. Hamill, G. Kamen, & S. Whittlesey (Eds.), *Research methods in biomechanics* (2 ed., pp. 63-78). Human kinetics.
- Robertson, G. E. (2013b). Energy, Work, and Power. In G. E. Robertson, G. E. Caldwell, J. Hamill, G. Kamen, & S. Whittlesey (Eds.), *Research methods in biomechanics* (2 ed., pp. 132). Human kinetics.
- Sandbakk, Ø., Ettema, G., & Holmberg, H.-C. (2012). The influence of incline and speed on work rate, gross efficiency and kinematics of roller ski skating. *European Journal of Applied Physiology*, 112(8), 2829-2838.
<https://doi.org/10.1007/s00421-011-2261-0>
- Sandbakk, Ø., Ettema, G., & Holmberg, H. C. (2013a). The physiological and biomechanical contributions of poling to roller ski skating. *European Journal of Applied Physiology*, 113(8), 1979-1987.
<https://doi.org/10.1007/s00421-013-2629-4>
- Sandbakk, Ø., Hegge, A. M., & Ettema, G. (2013b). The role of incline, performance level, and gender on the gross mechanical efficiency of roller ski skating. *Frontiers in Physiology*, 4, 293.
<https://doi.org/10.3389/fphys.2013.00293>
- Sandbakk, Ø., & Holmberg, H. C. (2014). A reappraisal of success factors for Olympic cross-country skiing. *International Journal of Sports Physiology and Performance*, 9(1), 117-121. <https://doi.org/10.1123/ijsp.2013-0373>
- Sandbakk, Ø., Holmberg, H. C., Leirdal, S., & Ettema, G. (2010). Metabolic rate and gross efficiency at high work rates in world class and national level sprint skiers. *European Journal of Applied Physiology*, 109(3), 473-481.
<https://doi.org/10.1007/s00421-010-1372-3>
- Schwameder, H. (2008). Biomechanics research in ski jumping, 1991–2006. *Sports Biomechanics*, 7(1), 114-136.
<https://doi.org/10.1080/14763140701687560>

- Schwartz, M. H., Rozumalski, A., & Trost, J. P. (2008). The effect of walking speed on the gait of typically developing children. *Journal of Biomechanics*, 41(8), 1639-1650. <https://doi.org/10.1016/j.jbiomech.2008.03.015>
- Selbie, S., Hamill, J., & Kepple, T. (2013). Three-Dimensional Kinetics. In G. E. Robertson, G. E. Caldwell, J. Hamill, G. Kamen, & S. Whittlesey (Eds.), *Research methods in biomechanics* (2 ed., pp. 159-160). Human kinetics.
- Smith, G., Kvamme, B., & Jakobsen, V. (2006). *Ski skating technique choice: mechanical and physiological factors affecting performance* 24 International Symposium on Biomechanics in Sports Austria.
- Smith, G. A. (1992). Biomechanical analysis of cross-country skiing techniques. *Medicine & Science in Sports & Exercise*, 24(9), 1015-1022. <http://www.ncbi.nlm.nih.gov/pubmed/1406185>
- Smith, G. A. (2003). Biomechanics of cross country skiing. In H. Rusko (Ed.), *Cross Country Skiing. Handbook of Sports Medicine* (pp. 32-61). Wiley.
- Smith, G. A., McNitt-Gray, J., & Nelson, R. C. F. (2010). Kinematic analysis of alternate stride skating in cross country skiing. *International Journal of Sport Biomechanics*, 4(1), 49-58. <https://doi.org/10.1123/ijsb.4.1.49>
- Stöggl, T., Bjorklund, G., & Holmberg, H. C. (2013a). Biomechanical determinants of oxygen extraction during cross-country skiing. *Scandinavian Journal of Medicine & Science in Sports*, 23(1), e9-20. <https://doi.org/10.1111/sms.12004>
- Stöggl, T., Hebert-Losier, K., & Holmberg, H. C. (2013b). Do anthropometrics, biomechanics, and laterality explain V1 side preference in skiers? *Medicine & Science in Sports & Exercise*, 45(8), 1569-1576. <https://doi.org/10.1249/MSS.0b013e31828b815a>
- Stöggl, T., & Holmberg, H.-C. (2022). A systematic review of the effects of strength and power training on performance in cross-country skiers. *Journal of Sports Science & Medicine*, 21(4), 555-579. <https://doi.org/10.52082%2Fjssm.2022.555>
- Stöggl, T., & Holmberg, H. C. (2015). Three-dimensional force and kinematic interactions in V1 skating at high speeds. *Medicine & Science in Sports & Exercise*, 47(6), 1232-1242. <https://doi.org/10.1249/MSS.0000000000000510>
- Stöggl, T., & Holmberg, H. C. (2016). Double-poling biomechanics of elite cross-country skiers: flat versus uphill terrain. *Medicine & Science in Sports & Exercise*, 48(8), 1580-1589. <https://doi.org/10.1249/MSS.0000000000000943>
- Stöggl, T., Kämpel, W., Müller, E., & Lindinger, S. (2010). Double-push skating versus V2 and V1 skating on uphill terrain in cross-country skiing. *Medicine & Science in Sports & Exercise*, 42(1), 187-196. <https://doi.org/10.1249/MSS.0b013e3181ac9748>
- Stöggl, T., & Martinier, A. (2017). Validation of Moticon's OpenGo sensor insoles during gait, jumps, balance and cross-country skiing specific imitation movements. *Journal of Sports Sciences*, 35(2), 196-206. <https://doi.org/10.1080/02640414.2016.1161205>
- Stöggl, T., & Müller, E. (2009). Kinematic determinants and physiological response of cross-country skiing at maximal speed. *Medicine & Science in*

- Sports & Exercise*, 41(7), 1476-1487.
<https://doi.org/10.1249/MSS.0b013e31819b0516>
- Stöggl, T., Müller, E., Ainegren, M., & Holmberg, H. C. (2011). General strength and kinetics: fundamental to sprinting faster in cross country skiing? *Scandinavian Journal of Medicine & Science in Sports*, 21(6), 791.
<https://doi.org/10.1111/j.1600-0838.2009.01078.x>
- Stöggl, T., Stöggl, J., & Müller, E. (2008). *Competition analysis of the last decade (1996–2008) in crosscountry skiing* Science and Skiing IV, UK.
- Stöggl, T., Welde, B., Supej, M., Zoppirolli, C., Rolland, C. G., Holmberg, H. C., & Pellegrini, B. (2018). Impact of Incline, sex and level of performance on kinematics during a distance race in classical cross-country skiing. *Journal of Sports Science & Medicine*, 17(1), 124-133.
<http://www.ncbi.nlm.nih.gov/pubmed/29535586>
- Street, G. M., & Frederick, E. C. (1995). Measurement of skier-generated forces during roller-ski skating. *Journal of Applied Biomechanics*, 11(3), 245-256.
<https://doi.org/10.1123/jab.11.3.245>
- Vahasoyrinki, P., Komi, P. V., Seppala, S., Ishikawa, M., Kolehmainen, V., Salmi, J. A., & Linnamo, V. (2008). Effect of skiing speed on ski and pole forces in cross-country skiing. *Medicine & Science in Sports & Exercise*, 40(6), 1111-1116. <https://doi.org/10.1249/MSS.0b013e3181666a88>
- van der Kruk, E., Van Der Helm, F., Veeger, H., & Schwab, A. L. (2018). Power in sports: a literature review on the application, assumptions, and terminology of mechanical power in sport research. *Journal of Biomechanics*, 79, 1-14. <https://doi.org/10.1016/j.jbiomech.2018.08.031>
- Van Hooren, B., Fuller, J. T., Buckley, J. D., Miller, J. R., Sewell, K., Rao, G., . . . Willy, R. W. (2020). Is motorized treadmill running biomechanically comparable to overground running? A systematic review and meta-analysis of cross-over studies. *Sports Medicine*, 50(4), 785-813.
<https://doi.org/10.1007/s40279-019-01237-z>
- Watts, P. B., Sulentic, J. E., Drobish, K. M., Gibbons, T. P., Newbury, V. S., Hoffman, M. D., . . . Clifford, P. S. (1993). Physiological responses to specific maximal exercise tests for cross-country skiing. *Canadian Journal of Applied Physiology*, 18(4), 359-365. <https://doi.org/10.1139/h93-030>
- Winter, D. A. (1995). Human balance and posture control during standing and walking. *Gait & Posture*, 3(4), 193-214. [https://doi.org/10.1016/0966-6362\(96\)82849-9](https://doi.org/10.1016/0966-6362(96)82849-9)
- Yamashita, D., Fujii, K., Yoshioka, S., Isaka, T., & Kouzaki, M. (2017). Asymmetric interlimb role-sharing in mechanical power during human sideways locomotion. *Journal of Biomechanics*, 57, 79-86.
<https://doi.org/10.1016/j.jbiomech.2017.03.027>
- Yu, B. (2003). Effect of external marker sets on between-day reproducibility of knee kinematics and kinetics in stair climbing and level walking. *Research in Sports Medicine*, 11(4), 209-218. <https://doi.org/10.1080/714041037>

- Yu, B., Gabriel, D., Noble, L., & An, K.-N. (1999). Estimate of the optimum cutoff frequency for the Butterworth low-pass digital filter. *Journal of Applied Biomechanics*, 15(3), 318-329. <https://doi.org/10.1123/jab.15.3.318>
- Yu, B., Kienbacher, T., Growney, E. S., Johnson, M. E., & An, K. N. (1997). Reproducibility of the kinematics and kinetics of the lower extremity during normal stair - climbing. *Journal of Orthopaedic Research*, 15(3), 348-352. <https://doi.org/10.1002/jor.1100150306>



ORIGINAL PAPERS

I

PROPULSION CALCULATED BY FORCE AND DISPLACEMENT OF CENTER OF MASS IN TREADMILL CROSS-COUNTRY SKIING

by

Zhao, S., Ohtonen, O., Ruotsalainen, K., Kettunen, L., Lindinger, S.,
Göpfert, C., Linnamo, V. 2022



Sensors, 22, 2777

doi:10.3390/s22072777

© 2022 by the authors. Licensee MDPI, Basel, Switzerland. This article is an open access article distributed under the terms and conditions of [the Creative Commons Attribution \(CC BY\) license](#).

Article

Propulsion Calculated by Force and Displacement of Center of Mass in Treadmill Cross-Country Skiing

Shuang Zhao ¹, Olli Ohtonen ¹, Keijo Ruotsalainen ¹, Lauri Kettunen ², Stefan Lindinger ³, Caroline Göpfert ⁴ and Vesa Linnamo ^{1,*}

- ¹ Faculty of Sport and Health Sciences, University of Jyväskylä, 40014 Jyväskylä, Finland; zhaoshuangzs@hotmail.com (S.Z.); olli.ohtonen@jyu.fi (O.O.); keijo.s.ruotsalainen@gmail.com (K.R.)
- ² Faculty of Information Technology, University of Jyväskylä, 40014 Jyväskylä, Finland; lauri.y.o.kettunen@jyu.fi
- ³ Center of Health and Performance (CHP), Department of Food and Nutrition and Sport Science, University of Gothenburg, 40530 Göteborg, Sweden; stefan.lindinger@gu.se
- ⁴ Department of Sport Science and Kinesiology, University of Salzburg, 5400 Salzburg, Austria; caro.goepfert@gmx.de
- * Correspondence: vesa.linnamo@jyu.fi

Abstract: This study evaluated two approaches for estimating the total propulsive force on a skier's center of mass (COM) with double-poling (DP) and V2-skating (V2) skiing techniques. We also assessed the accuracy and the stability of each approach by changing the speed and the incline of the treadmill. A total of 10 cross-country skiers participated in this study. Force measurement bindings, pole force sensors, and an eight-camera Vicon system were used for data collection. The coefficient of multiple correlation (CMC) was calculated to evaluate the similarity between the force curves. Mean absolute force differences between the estimated values and the reference value were computed to evaluate the accuracy of each approach. In both DP and V2 techniques, the force–time curves of the forward component of the translational force were similar to the reference value (CMC: 0.832–0.936). The similarity between the force and time curves of the forward component of the ground reaction force (GRF) and the reference value was, however, greater (CMC: 0.879–0.955). Both approaches can estimate the trend of the force–time curve of the propulsive force properly. An approach by calculating the forward component of GRF is a more appropriate method due to a better accuracy.

Keywords: propulsive force; V2-skating skiing technique; double-poling skiing technique



Citation: Zhao, S.; Ohtonen, O.; Ruotsalainen, K.; Kettunen, L.; Lindinger, S.; Göpfert, C.; Linnamo, V. Propulsion Calculated by Force and Displacement of Center of Mass in Treadmill Cross-Country Skiing. *Sensors* **2022**, *22*, 2777. <https://doi.org/10.3390/s22072777>

Academic Editor: Christian Peham

Received: 17 January 2022

Accepted: 2 April 2022

Published: 5 April 2022

Publisher's Note: MDPI stays neutral with regard to jurisdictional claims in published maps and institutional affiliations.



Copyright: © 2022 by the authors. Licensee MDPI, Basel, Switzerland. This article is an open access article distributed under the terms and conditions of the Creative Commons Attribution (CC BY) license (<https://creativecommons.org/licenses/by/4.0/>).

1. Introduction

Forces acting on a skier's center of mass (COM) in a forward direction are propulsive forces, which are the primary mechanical determinants of an cross-country (XC) skier's performance [1]. The position of skier's COM can be obtained by using the marker-based motion capture system with a segmental method [2]. Thus, forces acting on a skier's COM can be obtained by multiplying COM acceleration with the total mass of the skier, and this will indicate how athletes overcome resistive forces. However, the contribution of single pole and leg thrusts could not be revealed. Therefore, it is essential to compute forces acting on the COM from the ground reaction forces (GRFs) generated from skis and poles, separately.

Except for estimating the propulsive force with the forward acceleration of COM and the total mass, other approaches have been developed. One approach is to estimate the propulsive force as the forward-directed horizontal component of the three-dimensional (3D) GRFs from both skis and poles that act on a skier (F_{net}) [3]. The roller skis [3–5], skis [6,7], and poles [3,6,7] equipped with force sensors have been used to measure the forces generated from skis and poles. Combined with the pole angle, ski angle, ski-edging angle, and the incline of the track or the treadmill, the propulsive force from skis and poles

can be specified [1,3,8]. Therefore, questions related to the propulsive force, including the contribution of skis and poles in different techniques [3,9,10], and the comparison of different techniques [11,12] have been addressed. Another approach, demonstrated by Göpfert et al. [6], is to estimate the propulsive force with the forward component of translational force (F_{pro}). The translational force was modeled as the component of the 3D resultant GRFs that acts in the direction from the point of force application (PFA) to a skier's COM [6], and calculated by projecting the GRFs to the line defined by the COM and PFA.

The propulsive forces obtained with the two mentioned approaches (F_{net} and F_{pro}) have been compared to the propulsive force calculated with COM acceleration from a motion analysis system (F) in [6]. As using the segmental method has been shown to be suitable for estimating the position of the COM in sports [2], F was considered as the reference value. The results indicated that the force–time curves of F_{net} and F_{pro} all showed high similarity when compared to the force–time curves of F during the leg skating push-offs on snow. F_{net} overestimated F , and F_{pro} was found to be a more appropriate approach to estimate F during leg skating push-offs [6]. However, whether F_{net} and F_{pro} could be used to estimate F , and which one is more accurate in other techniques, are still unknown. As XC skiing is a sport whose competition and training are normally performed on varying track topography and speed, whether F_{net} and F_{pro} could work steadily when estimating F at different terrain with different speeds need further investigation.

Therefore, the first aim of the present study was to obtain the force–time curves of F_{net} and F_{pro} with different skiing techniques and evaluate which can estimate the force–time curves of F better. As the use and importance of double poling (DP) and V2 skating (V2) as main techniques in XC skiing have increased for the past few years [12–14], DP and V2 skating techniques will be performed in this study. The second aim is to investigate which approach is more accurate when estimating F . Another aim is to explore the stability of the approaches to calculate F_{net} and F_{pro} by changing the speed and incline of the treadmill. We hypothesized that the force–time curves of F_{net} and F_{pro} all give comparable shape with F in both techniques [6]. We also hypothesized that F_{net} would give a considerable overestimation, and F_{pro} would be more accurate than F_{net} , when estimating F in both DP and V2 techniques [6]. We further hypothesized that the approaches to calculate the F_{net} and F_{pro} would not be affected by the speed and incline of the treadmill in both techniques.

2. Materials and Methods

2.1. Participants

A total of 10 experienced male skiers (age: 29.4 ± 7.9 years; height: 181.4 ± 5.7 cm; weight: 77.9 ± 8.9 kg) who were familiar with treadmill roller skiing volunteered to participate in this study. The experimental protocol and all methods used in this study were approved by the Ethics Committee of the University of Jyväskylä. All participants provided written informed consent before the measurement and were free to withdraw from the experiments at any point.

2.2. Protocol

The anthropometric parameters needed for motion analysis (e.g., bilateral leg length, knee width, ankle width, shoulder offset, elbow width, and hand thickness) were measured first, and passive reflective markers were attached to the participants and equipment. Once the preparations were made, participants completed a 10–15 min warm-up roller skiing on the treadmill. Next, calibration was performed with the skier in a standing position and the treadmill at a 0° incline. Participants then performed the DP technique at five speeds (13, 15, 17, 19, and 21 km/h) on a 2° incline. The comfortable pole length for the DP technique was 1.56 ± 0.06 m. After the trials with varying speeds at a 2° incline, the DP technique was performed at three inclines (3° , 4° , and 5°) with a speed of 10 km/h. There was a 1 min rest between each speed and incline. When participants finished performing the DP technique, the pole length was adjusted to a comfortable length for the V2 skating

technique (which was 1.63 ± 0.03 m in this study). The participants were given a short rest period while adjusting the pole length. The participants then performed the V2 technique on the treadmill. The protocol for speed and incline change was the same as during the DP test.

2.3. Data Collection

An eight-video-camera motion capture system (Vicon, Oxford, UK) and NEXUS 2.8.1 software were used to collect and record the 3D trajectories of reflective markers at a sampling rate of 150 Hz. The global coordinate system (GCS) was defined using the right-hand rule when the incline of the treadmill was 0° . The X-axis of the GCS was defined as the direction from side to side across the treadmill. The Y-axis of the GCS was the longitudinal axis of the treadmill. The Z-axis of the GCS was perpendicular to the ground, pointing upward. The GCS was calibrated according to Vicon's specifications. A total of 58 passive reflective markers were used in this current study: 43 passive reflective markers were attached to the participants' bodies, and 15 markers were attached to the equipment, including both skis (3 each), both poles (3 each), and the treadmill (3). Anthropometric measurements and the placement of markers on the participants' bodies were conducted according to the XC model [6] used in previous studies. Measurements were performed on a motorized treadmill with a belt surface of 2.7 m wide and 3.5 m long (Rodby Innovation AB, Vänge, Sweden). The same pair of roller skis were used for both techniques (Marwe, SKATING 620 XC, wheel no. 0), with a resistance friction coefficient of $\mu = 0.025$ measured before the measurement (Appendix A).

Two custom-made pole force sensors (VTT MIKES, Technical Research Centre of Finland Ltd., Kajaani, Finland, Figure 1a) were used to measure the axial GRF from the poles. Two custom-made two-dimensional (2D) force measurement bindings (Neuromuscular Research Centre, University of Jyväskylä, Jyväskylä, Finland, Figure 1b) [15] were mounted on roller skis to measure the leg forces generated from roller skis. Both pole and leg forces were collected synchronously with the Coachtech online measurement and feedback system (Neuromuscular Research Centre, University of Jyväskylä, Jyväskylä, Finland) at a sample rate of 400 Hz. The force measurement bindings measured the vertical (F_{skiz}) and mediolateral (F_{skix}) forces and were calibrated before the measurement [15]. A trigger signal was sent from the Coachtech [16] to the motion capture system to mark the start of the force capture. The nodes for the pole force sensors and force measurement bindings were used to supply power and transmit data.

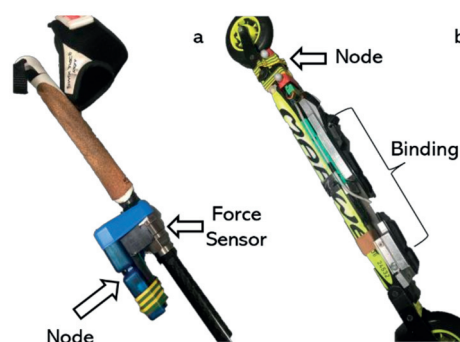


Figure 1. Equipment used in this study: (a) Pole force measurement sensor. (b) Force measurement binding.

2.4. Data Reduction

Marker labeling and COM calculations were performed using NEXUS 2.8.1 software. The raw 3D trajectories of all reflective markers and the acceleration of COM were low-pass filtered (fourth-order, zero-lag, and Butterworth filter) with a cutoff frequency of 11.3 Hz [17]. The XC model [6], which contained the head, thorax, abdomen and pelvis, upper arms, hands, thighs, shanks, feet, skis, and poles, was used to calculate the whole-

body COM. The marker placement on the subject and geometric model for the XC model is shown in Figure 2. The segmental anthropometric data were taken from Dempster’s study as described in Selbie et al. [18]. Force data were low-pass filtered (eighth-order, zero-lag, and Butterworth filter) with a cutoff frequency of 15 Hz [19]. Data filtering and parameter calculations were performed using MATLAB R2018a (MathWorks, Natick, MA, USA).

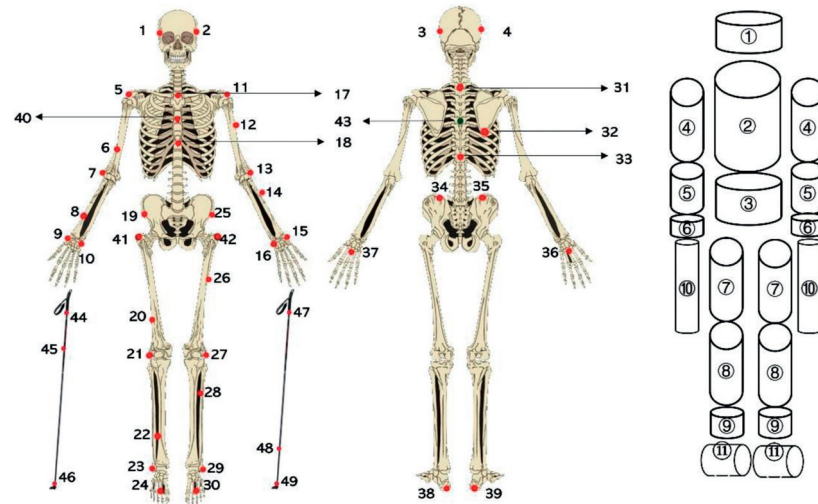


Figure 2. Marker placement on the subject and geometric model for segments in the XC model. The numbers 1–49 represent the placement of reflective markers on subjects and poles. The displacement of reflective markers on roller skis is shown in Figure 3. The numbers 1–39 are the markers used in the plug-in-gait (PIG) model. 1–43 are the markers used in the XC model [6] on one subject. The numbers 44–49 are the markers on the poles. ①–⑪ represent the head, thorax, abdomen and pelvis, upper arm, forearm, hand, thigh, shank, foot, pole, and roller ski, respectively.

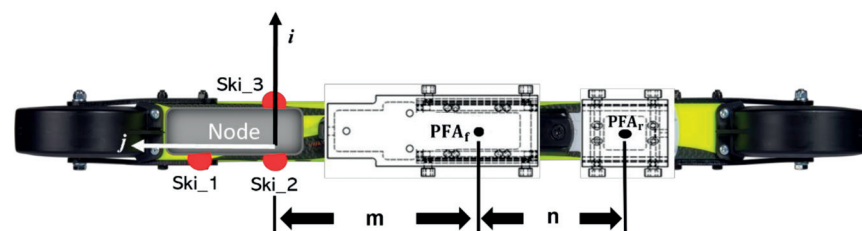


Figure 3. Displacement of markers, PFAs, and the definition of FCS (\vec{i} , \vec{j} , \vec{k}). Three markers (Ski_1, Ski_2, and Ski_3) were attached to the side of the node. The node for power supply and data transmission was attached to the front part of the roller ski. The surface defined by the markers was parallel to the roller ski surface. \vec{i} was defined by Ski_3 and Ski_2. Another unit vector (\vec{r}) located on the surface of the roller ski was defined by Ski_1 and Ski_2. The surface norm, which was the \vec{k} of FCS, was the cross product of \vec{i} and \vec{r} . The last unit vector \vec{j} was computed by using the right-hand rule with \vec{k} and \vec{i} . The PFA_f and PFA_r were the points of force application of the front and rear sensors, respectively. The distance between Ski_2 and PFA_f was m , and the distance between PFA_f and PFA_r was n .

2.4.1. Transforming the Forces Measured from the Force Sensor into the GCS and the PFA

The forces generated from the roller ski force coordinate system (FCS) were transformed into the GCS. The unit vector of each axis of FCS (\vec{i} , \vec{j} , \vec{k}) was identified by

markers on the roller ski (Figure 3). The transformation from the roller ski system to the GCS is given by

$$\begin{bmatrix} F_x \\ F_y \\ F_z \end{bmatrix} = R' \begin{bmatrix} F_{skix} \\ 0 \\ F_{skiz} \end{bmatrix} \quad (1)$$

where F_x , F_y , and F_z are the components of forces generated from legs (\vec{F}_r) in the GCS. R' [18] is the rotation matrix from FCS to GCS.

The PFA is needed for calculating the translational force introduced by Göpfert et al. [6]. The displacement of the PFA along the binding (PFA_{ski}) was calculated from the force distribution between the front and rear sensors of the binding [20] over time. The PFA for each part of the binding (PFA_f and PFA_r) was defined as the center of each sensor. The distance between the marker Ski_2 and PFA_f (m), and the distance between PFA_f and PFA_r (n) were measured before the measurement. The displacements of PFA_f and PFA_r in GCS were obtained by moving the midpoint of Ski_2 and Ski_3 along the opposite direction of \vec{j} . The moving distances were m and $m + n$, respectively. The mediolateral sway of PFA_{ski} on ski binding was not considered in this study. Thus, the PFA_{ski} moved between the PFA_f and PFA_r (Figure 3).

The measured axial pole forces (\vec{F}_p) were considered the GRFs acting along the pole from the tip to the top of the pole and expressed that way in the GCS. The magnitude of \vec{F}_p was collected using a pole force sensor. The direction of \vec{F}_p was defined using the reflective markers that were attached to the pole. The PFA of poles (PFA_p) was defined as the intersection of the plane of the treadmill and the long axis of the pole. The plane of the treadmill was defined using the three markers attached to the treadmill.

2.4.2. The Reference Force, the Total Resultant Force, and the Translational Force

As using the segmental method has been shown to be suitable for estimating the position of the COM in sports [2], forces calculated by COM acceleration (\vec{a}) multiplied the total mass of the subject, and the equipment was the reference force (\vec{F}) in this study.

One approach to estimate forces acting on skier's COM is to calculate the total resultant force (\vec{F}_{net}) without considering the position of COM. \vec{F}_{net} is calculated as

$$\vec{F}_{net} = \vec{F}_r + \vec{F}_p + \vec{F}_{friction} + \vec{G} \quad (2)$$

where \vec{G} is the gravitational force of each participant and all the equipment. $\vec{F}_{friction}$ is the frictional force between the roller ski and the treadmill, which was directed along the path of the ski motion, and the magnitude was computed by multiplying μ with F_{skiz} .

Another approach to estimate forces acting on skier's COM is to calculate the total translational force (the mechanical principle of translational force, see Appendix B). The translational force is the share of the resultant GRF acting in the direction from PFA to COM. The translational force from skis (\vec{F}_{IS} , Figure 4) is the share of ski GRF (\vec{F}_r) acting in the direction defined from PFA_{ski} to COM and is calculated from

$$\vec{F}_{IS} = (\vec{F}_r \bullet \vec{u}) \vec{u} \quad (3)$$

where \vec{u} is the unit vector determined from PFA_{ski} to COM. The translational force from poles (\vec{F}_{IP}) is calculated from

$$\vec{F}_{IP} = (\vec{F}_p \bullet \vec{v}) \vec{v} \quad (4)$$

where \vec{v} is the unit vector determined from PFA_p to COM. The total translational force (\vec{F}_{pro}) is the sum of the translational force from the legs, poles, and the resistance. Thus, \vec{F}_{pro} can be computed as

$$\vec{F}_{\text{pro}} = \vec{F}_{\text{IS}} + \vec{F}_{\text{TP}} + \vec{F}_{\text{friction}} + \vec{G} \quad (5)$$

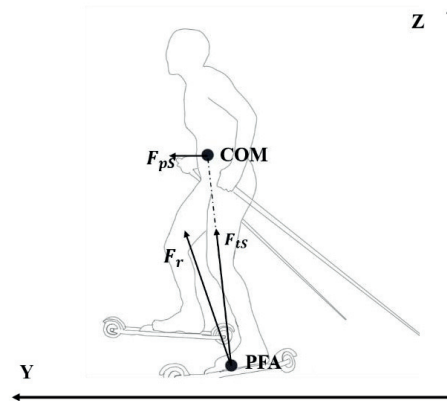


Figure 4. Diagram of force decomposition from skis. F_r is the resultant force generated from legs. F_{IS} is the translational component, which went through the COM. F_{pS} represents the propulsion generated from legs in the forward direction.

As forces acting on skier's center of mass (COM) in forward direction are the propulsive forces, the Y component of \vec{F} , \vec{F}_{net} , and \vec{F}_{pro} (F , F_{net} , and F_{pro}) was compared and analyzed in the present study.

2.4.3. Cycle Definition and Analyzed Parameters

A total of 10 consecutive poling phases for each DP technique trial and 10 consecutive kicking phases (5 left ski kicking and 5 right ski kicking) for each V2 technique trial were analyzed. The poling phase was defined as the period from the start of the pole ground contact to the end of the pole ground contact (Figure 5a). The kicking phase was defined as the ski force minima until the end of ground contact [7] (Figure 5b). The forces of skis and poles from both the left and right sides were included while calculating the total propulsion in both techniques.

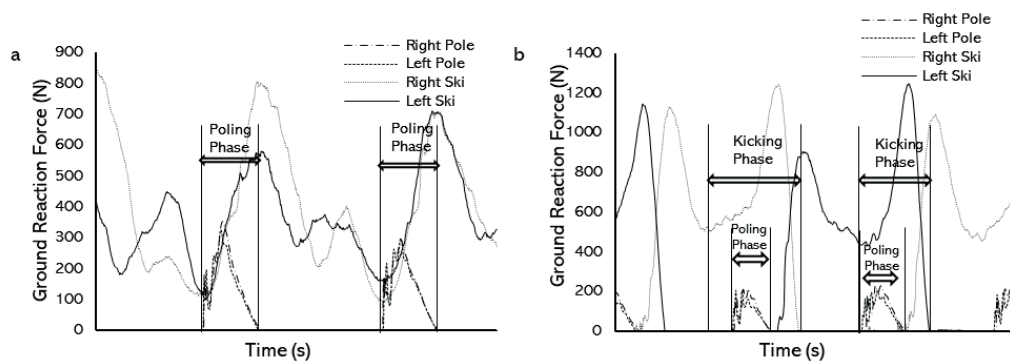


Figure 5. Definition of the force producing phase of DP and V2 techniques: (a) GRFs from skis and poles in the DP technique and the definition of the poling phase. (b) GRFs from skis and poles in the V2 technique and the definition of the kicking phase.

The positive square root of the adjusted coefficient of multiple determination, which is the adjusted coefficient of multiple correlation (CMC, $0 < \text{CMC} < 1$) [21,22], was calculated for evaluating the similarity of force–time curves. One comparison was between F_{net} and F force–time curves. The similarity between F_{net} and F was represented by CMC_{net} . The mean force difference and mean absolute force difference between F_{net} and F were $M_{F_{\text{net}}-F}$ and $M_{|F_{\text{net}}-F|}$. Another comparison was between F_{pro} and F force–time curves. The similarity between F_{pro} and F was represented by CMC_{pro} . The mean force difference and mean absolute force difference between F_{pro} and F were $M_{F_{\text{pro}}-F}$ and $M_{|F_{\text{pro}}-F|}$. The mean force differences and mean absolute force differences were computed over force curves averaged over 10 force-producing phases. The mean force differences, which are $M_{F_{\text{net}}-F}$ and $M_{F_{\text{pro}}-F}$, were calculated to provide descriptive statistics only. The forces in this study were presented as values relative to body weight (%BW).

2.5. Statistical Analyses

A two-way mixed factorial ANOVA was performed. The dependent variables of the analyses were (1) CMCs and (2) mean absolute force differences. The independent variables were the speed (or the incline) of the treadmill and the comparisons (i.e., comparison between F_{net} and F and comparison between F_{pro} and F). The speed (or the incline) of the treadmill was treated as the within-subject factor, and the comparison pair was treated as the between-subject factor. The EMMEANS subcommand with the Bonferroni adjustment in SPSS was used to perform the pairwise comparisons of the dependent variable when interactions were detected [23], and the effect size ($p\eta^2$) was calculated for further evaluation. The level of statistical significance was set at $\alpha = 0.05$. All data are presented as mean \pm standard deviation (SD). Data analyses were conducted using version 23.0 of the SPSS program package for statistical analysis (SPSS Inc., Chicago, IL, USA).

3. Results

The force–time curves of F , F_{net} , and F_{pro} for the DP and the V2 techniques are shown in Figure 6. The interaction effect (comparison * speed) was significant on CMC with the DP technique ($p = 0.038$), but not with the V2 technique ($p = 0.988$). CMC_{pro} did not differ from CMC_{net} at any speed in the DP technique ($p \geq 0.106$, Table 1). With the V2 technique, the overall CMC_{pro} was about 5% lower than CMC_{net} ($p = 0.011$, Table 1). The interaction effect (comparison * incline) was not significant on CMC in the DP technique ($p = 0.620$) but was significant in the V2 technique ($p = 0.042$). In the DP technique, the main effect of comparison on CMC was not significant ($p = 0.218$, Table 1). In the V2 technique, CMC_{net} was significantly greater than CMC_{pro} at 3° ($p = 0.042$, Table 1).

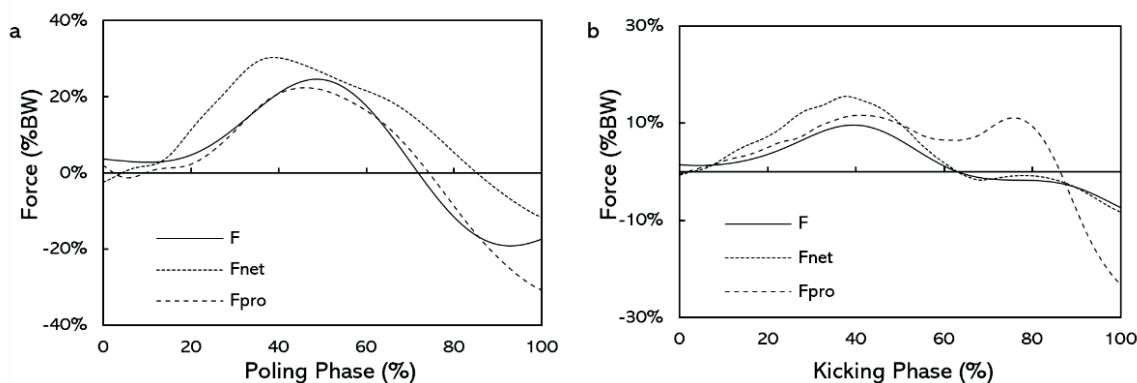


Figure 6. Force-time curves of F , F_{net} , and F_{pro} : (a) DP technique, (b) V2 technique. Values are averaged over 10 force-producing phases of one subject from each technique (speed of the treadmill was 19 km/h; incline of the treadmill was 2°).

Table 1. Mean and standard deviation of the CMC for the DP technique ($n = 9$) and the V2 technique ($n = 10$).

	DP Technique				V2 Technique				
	CMC _{net}	CMC _{pro}	<i>p</i> -Value	$P\eta^2$	CMC _{net}	CMC _{pro}	<i>p</i> -Value	$P\eta^2$	
Speeds	13 km/h	0.935 ± 0.022	0.910 ± 0.038	0.106 ^b	0.155	0.901 ± 0.048	0.853 ± 0.043		
	15 km/h	0.933 ± 0.023	0.916 ± 0.034	0.230 ^b	0.089	0.908 ± 0.047	0.862 ± 0.050		
	17 km/h	0.920 ± 0.030	0.919 ± 0.030	0.951 ^b	0.001	0.905 ± 0.040	0.861 ± 0.035	0.011 ^a	0.309
	19 km/h	0.901 ± 0.045	0.908 ± 0.046	0.778 ^b	0.005	0.885 ± 0.045	0.837 ± 0.047		
	21 km/h	0.883 ± 0.058 ^{1,2,3}	0.907 ± 0.042	0.330 ^b	0.059	0.879 ± 0.044	0.832 ± 0.041		
	<i>p</i> -value	0.043 ^d	0.371 ^d			0.008 ^c			
	$P\eta^2$	0.509	0.264			0.216			
Inclines	3°	0.933 ± 0.024	0.914 ± 0.046		0.093	0.911 ± 0.032	0.856 ± 0.073	0.042 ^b	0.210
	4°	0.946 ± 0.016	0.932 ± 0.033	0.218 ^a		0.922 ± 0.041	0.896 ± 0.044 [*]	0.179 ^b	0.098
	5°	0.955 ± 0.015	0.936 ± 0.037			0.912 ± 0.047	0.900 ± 0.055 [*]	0.617 ^b	0.014
	<i>p</i> -value		0.001 ^e			0.479 ^f	0.007 ^f		
	$P\eta^2$		0.464			0.083	0.446		

Note: CMC_{net} represents the similarity between F and F_{net}. CMC_{pro} represents the similarity between F and F_{pro}. ^a *p*-value for the main effect of comparison in a two-way mixed factorial ANOVA. ^b *p*-value for pairwise comparisons when interactions were detected. ^c *p*-value for the main effect of speed in a two-way mixed factorial ANOVA. ^d *p*-value for the simple effect of speed when interactions were detected. ^e *p*-value for the main effect of incline in a two-way mixed factorial ANOVA. ^f *p*-value for the simple effect of incline when interactions were detected. ¹ Significantly different from 13 km/h. ² Significantly different from 15 km/h. ³ Significantly different from 17 km/h. ^{*} Significantly different from 3°.

On average, the $M_{F_{net}-F}$ was lower than zero and the $M_{F_{pro}-F}$ was greater than zero (Figure 7) for both the DP and V2 techniques at any speeds and any inclines. The interaction effect (comparison * speed) was significant on the absolute mean force difference with the DP technique ($p = 0.025$) but not with the V2 technique ($p = 0.165$). In the DP technique, $M_{|F_{net}-F|}$ was 24% lower than $M_{|F_{pro}-F|}$ at 15 km/h ($p = 0.028$, Table 2). For the V2 technique, the overall $M_{|F_{pro}-F|}$ was about 37% greater than $M_{|F_{net}-F|}$. The interaction effect (comparison * incline) was not significant on absolute mean force difference in the DP technique ($p = 0.393$) but was significant in the V2 technique ($p = 0.016$). In the DP technique, the overall $M_{|F_{net}-F|}$ was about 39% lower than $M_{|F_{pro}-F|}$. With the V2 technique, $M_{|F_{net}-F|}$ was significantly lower than $M_{|F_{pro}-F|}$ at 3° and 4° ($p \leq 0.013$, Table 2).

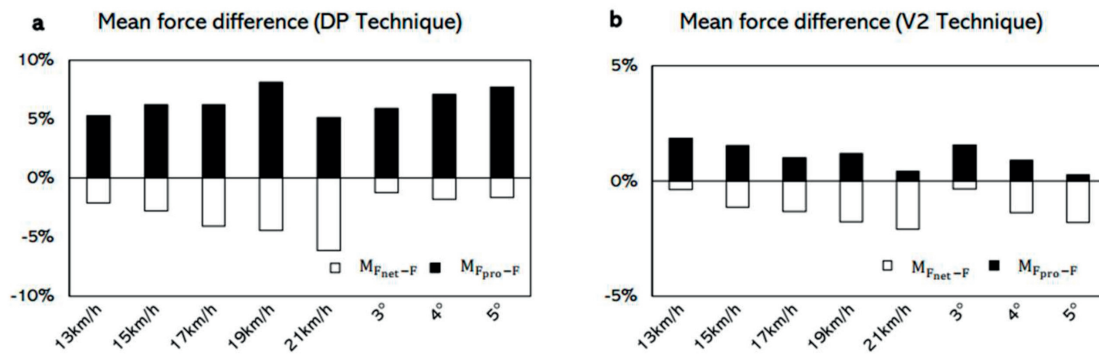


Figure 7. Mean force difference over force producing phases in DP and V2 techniques (%BW). $M_{F_{net}-F}$ represents the difference between F and F_{net} and is calculated by $F - F_{net}$. $M_{F_{net}-F}$ lower than zero indicates that F_{net} is greater than F. $M_{F_{pro}-F}$ represents the difference between F and F_{pro} and is calculated by $F - F_{pro}$. $M_{F_{pro}-F}$ greater than zero indicates that F_{pro} is lower than F.

Table 2. Mean and standard deviation of the mean absolute difference for the DP technique ($n = 9$) and V2 technique ($n = 10$) (BW%).

	DP Technique				V2 Technique				
	$M_{ F_{net}-F }$	$M_{ F_{pro}-F }$	p -Value	$P\eta^2$	$M_{ F_{net}-F }$	$M_{ F_{pro}-F }$	p -Value	$P\eta^2$	
Speed	13 km/h	6.1 ± 1.1	8.1 ± 2.9	0.058 ^b	0.207	2.9 ± 0.4	4.4 ± 0.8	0.001 ^a	0.633
	15 km/h	6.9 ± 1.1	9.1 ± 2.6 ⁴	0.028 ^b	0.268	3.1 ± 0.5	4.7 ± 0.4		
	17 km/h	8.5 ± 1.5 ^{1,2,5}	10.2 ± 3.3 ^{1,4}	0.166 ^b	0.116	3.6 ± 0.6	4.8 ± 0.5		
	19 km/h	9.0 ± 1.3 ^{1,2}	11.6 ± 3.6 ^{1,2,3}	0.057 ^b	0.209	4.0 ± 0.9	5.4 ± 0.8		
	21 km/h	10.8 ± 2.2 ^{1,2,3}	10.9 ± 2.4 ¹	0.992 ^b	0.001	4.4 ± 0.9	5.3 ± 0.5		
	p -value	0.001 ^d	0.001 ^d			0.001 ^c			
$P\eta^2$	0.856	0.857			0.588				
Inclines	3°	6.2 ± 0.9	8.7 ± 3.0	0.015 ^a	0.315	2.9 ± 0.5	4.5 ± 0.8	0.001 ^b	0.617
	4°	7.1 ± 1.1	9.6 ± 2.7			3.4 ± 1.1	4.5 ± 0.6	0.013 ^b	0.295
	5°	7.6 ± 1.3	10.7 ± 2.9			3.7 ± 0.7 [*]	4.3 ± 0.9	0.115 ^b	0.132
	p -value	0.001 ^e				0.014 ^f	0.577 ^f		
	$P\eta^2$	0.615				0.394	0.063		

Note: $M_{|F_{net}-F|}$ represents the absolute difference between F and F_{net} and is calculated by $|F - F_{net}|$. $M_{|F_{pro}-F|}$ represents the absolute difference between F and F_{pro} and is calculated by $|F - F_{pro}|$. ^a p -value for the main effect of comparison in a two-way mixed factorial ANOVA. ^b p -value for pairwise comparisons when interactions were detected. ^c p -value for the main effect of speed in a two-way mixed factorial ANOVA. ^d p -value for the simple effect of speed when interactions were detected. ^e p -value for the main effect of incline in a two-way mixed factorial ANOVA. ^f p -value for the simple effect of incline when interactions were detected. ¹ Significantly different from 13 km/h. ² Significantly different from 15 km/h. ³ Significantly different from 17 km/h. ⁴ Significantly different from 19 km/h. ⁵ Significantly different from 21 km/h. * Significantly different from 3°.

With the DP technique, CMC_{pro} was independent from the speed ($p = 0.371$, Table 1). However, CMC_{net} decreased significantly at 21 km/h when compared to CMC_{net} at 13, 15, and 17 km/h ($p \leq 0.046$). The overall CMC increased by about 2% from 3 to 5°. Both $M_{|F_{net}-F|}$ and $M_{|F_{pro}-F|}$ increased with the increasing speed of the treadmill ($p < 0.001$, $p < 0.001$, Table 2). The overall absolute mean difference increased by 23% from 3 to 5°. With the V2 technique, the overall CMC decreased by about 2% from 13 to 21 km/h. CMC_{net} was independent of the incline of the treadmill ($p = 0.042$, Table 1). CMC_{pro} increased from 3 to 5° ($p = 0.007$, Table 1). The overall absolute difference increased by 33% from 13 to 21 km/h. $M_{|F_{net}-F|}$ was dependent on the incline of the treadmill ($p = 0.014$, Table 2), and $M_{|F_{pro}-F|}$ was independent of the incline of the treadmill ($p = 0.577$, Table 2).

4. Discussion

The results of this study support our first hypothesis that the force-time curves of F_{net} and F_{pro} all give comparable shape with F in both techniques. In the DP technique, CMC_{pro} ranged from 0.907 to 0.936, CMC_{net} ranged from 0.883 to 0.955 and did not differ from CMC_{pro} (Table 1). In the V2 technique, CMC_{pro} ranged from 0.832 to 0.900, and CMC_{net} ranged from 0.879 to 0.922 (Table 1). The CMC depicting the similarity between waveforms and CMC close to 1 indicated that the curves involved were similar [21,22]. Therefore, the shapes of force-time curves of F_{pro} and F_{net} all showed similar to force-time curves of F, and both could be used to describe the shape of F during the poling phase of the DP technique and the kicking phase of the V2 technique. In addition, in the V2 technique, CMC_{net} was 5% higher than CMC_{pro} while changing the speed (Table 1), indicating that the force-time curves of F_{net} was more comparable to the force-time curves of F than F_{pro} while using the V2 technique. Consequently, F_{net} appears to be more appropriate for determining the trend of the forward acceleration in the V2 technique.

The results of this study partly support our second hypothesis that F_{net} would give a considerable overestimation and F_{pro} would be more accurate than F_{net} when estimating F in both the DP and V2 techniques. In this present study, the F_{net} had a considerable overestimation when estimating F in both the DP and V2 techniques, but F_{pro} was not more accurate than F_{net} in both techniques. The mean force differences over force curves between F_{pro} and F ($M_{|F_{pro}-F|}$), as well as F_{net} and F ($M_{|F_{net}-F|}$), were computed (Figure 7).

The mean force differences in this study indicated that, on average, F_{net} would overestimate ($M_{F_{\text{net}}-F} < 0$, Figure 7) the F in both the DP and V2 techniques. F_{net} was calculated from the GRF directly. The costs associated with the transformations of energy [24] between each segment and the elastic potential energy of the muscle were not taken out from F_{net} . Thus, a considerable difference in F_{net} and F may exist. The F_{pro} underestimate ($M_{F_{\text{pro}}-F} > 0$, Figure 7) the F , but it was not more accurate than F_{net} in both techniques. F_{pro} was calculated by combining the GRF and the position of COM. The resultant GRF was subdivided into a translational component, which acted through the COM, and a rotational component, which was always perpendicular to the translational component [6,25]. Because the rotational component will not have a translational effect on the COM, when F_{pro} was calculated, the rotational component was not involved. Therefore, the forward component of the translational component might underestimate the forward acceleration in both the DP and V2 techniques. The absolute mean force differences (Table 2) were computed to evaluate which force-time curve was closer to the reference one. A smaller absolute mean force difference indicates a force-time curve closer to the reference curve and further shows a relatively higher accuracy. The results of this study showed that with both the DP and V2 techniques, the absolute mean force difference between F_{pro} and F were greater than or have no difference with the absolute mean force difference between F_{net} and F . This indicates that the force-time curves of F_{net} were closer to or have no difference with the force-time curves of F . Thus, F_{pro} was not more accurate than F_{net} .

The results of this study do not support our third hypothesis that the approaches to calculate the F_{net} and F_{pro} would not be affected by the speed and incline of the treadmill in both techniques. The approaches to calculate the F_{net} and F_{pro} were all influenced by the speed or the incline of the treadmill. As there was a balance of forces under laboratory conditions with no air resistance, constant friction coefficient, and constant gravitational force, the total external force remained constant when the speed was changed. The gravity component parallel to the treadmill surface increased with the incline [19]; thus, more forces were needed at a steeper incline. It is impossible to have an exact reproduction of the reference value F ; however, if the methods for calculating F_{net} and F_{pro} were independent from the speed and the incline of the treadmill, the CMC_{net} , CMC_{pro} , and the absolute mean force difference over the force-generating cycle should remain constant in both techniques. The CMCs in this study were somehow affected by the speed and incline of the treadmill in both the DP and V2 techniques. In addition, the results of this study showed that the absolute mean force differences between F_{net} and F ($M_{|F_{\text{net}}-F|}$) and between F_{pro} and F ($M_{|F_{\text{pro}}-F|}$) were all affected by the speed of the treadmill regardless of whether the DP or V2 technique was performed (Table 2). The absolute mean force differences increased with increasing speed (Table 2), which means that although F_{pro} and F_{net} can be used to estimate the force-time curve of F , they do not remain stable when the speed changes. Thus, when investigating how F adapts to increasing speed by using F_{net} or F_{pro} , the increasing mean force differences should be considered. Both $M_{|F_{\text{net}}-F|}$ and $M_{|F_{\text{pro}}-F|}$ increased when the DP technique was used while increasing the incline of the treadmill (Table 2). However, when the V2 technique was used, $M_{|F_{\text{net}}-F|}$ was affected by the increasing incline, and the significant increase was only found at the steepest incline (Table 2), but $M_{|F_{\text{pro}}-F|}$ was not influenced by the incline of the treadmill. Thus, compared to F_{net} , F_{pro} was more stable when estimating F while changing the incline of the treadmill.

Therefore, when considering the whole poling phase in the DP technique, both F_{pro} and F_{net} are appropriate for estimating the trend of F . The similarity between the F_{pro} and F is stable while changing the speed in the DP technique. However, F_{net} has better accuracy than F_{pro} when the speed and the incline is changed. When considering the whole kicking phase in the V2 technique, the trend of F_{net} fits F better. However, the similarity between the F_{pro} and F is stable in the V2 technique when the incline is changed. As the result in the DP technique, F_{net} also has better accuracy than F_{pro} in the V2 technique. There are some limitations of this study. The calculation of the COM is dependent on the assumed mass distributions. Although this has been proved to be suitable for estimating the position of

COM in sports, it can still cause the golden standard of the reference to be inaccurate. In addition, the PFAs of the leg force and pole force were estimated points, and this may also have some effects on the accuracy of F_{pro} . Furthermore, the added measurement equipment could have affected skiing performance.

5. Conclusions

The present study evaluated two approaches for estimating the total propulsive force on skier's COM. Both approaches can estimate the trend of the force-time curve of the propulsive force properly. Although both had a considerable overestimation; an approach by calculating the forward-directed horizontal component of 3D GRF is a more appropriate method due to a better accuracy. Future studies could investigate the contribution of skis and poles to forward COM acceleration by calculating the propulsive force from skis and poles separately. Moreover, as for the gliding phase that exists in XC skiing, the velocity at the end of the force generating phase is important. Future studies could also investigate the contributions of skis and poles to velocity change separately.

Author Contributions: Conceptualization, S.Z., O.O., K.R., L.K., S.L., C.G. and V.L.; Data curation, S.Z.; Formal analysis, S.Z.; Funding acquisition, S.Z. and V.L.; Investigation, S.Z., O.O., K.R., L.K., S.L., C.G. and V.L.; Methodology, S.Z., O.O., K.R., L.K., S.L., C.G. and V.L.; Project administration, S.Z.; Resources, S.Z., O.O. and K.R.; Supervision, S.Z., O.O., S.L. and V.L.; Validation, S.Z.; Visualization, S.Z.; Writing—original draft, S.Z.; Writing—review and editing, S.Z., O.O., K.R., L.K., S.L., C.G. and V.L. All authors have read and agreed to the published version of the manuscript.

Funding: This research was funded by the China Scholarship Council, grant number 201806520003.

Institutional Review Board Statement: The study was conducted according to the guidelines of the Declaration of Helsinki and approved by the Ethics Committee of the University of Jyväskylä.

Informed Consent Statement: Informed consent was obtained from all subjects involved in the study. Written informed consent was obtained from the patient(s) to publish this paper.

Data Availability Statement: The data presented in this study are available on request from the corresponding author. The data are not publicly available because the data also form part of ongoing studies.

Acknowledgments: The author Shuang Zhao wants to thank Christina Mishica and Ritva Mikkonen for language optimization. The authors would like to express their appreciation and thanks to the staff, athletes, and coaches for their participation, enthusiasm, and cooperation in this study.

Conflicts of Interest: The authors declare no conflict of interest.

Appendix A. Measurement and Calculation of Resistance Friction Coefficient of Roller Ski

The resistance friction coefficient of roller ski was measured on the treadmill surface using a custom-made friction measurement device (University of Jyväskylä, Jyväskylä, Finland, Figure A1) and calculated with the LabVIEW software package (National Instruments, Austin, TX, USA) before the measurement. A commercial force sensor (Raute precision TB5, Nastola, Finland) that measures the anterior–posterior force along the roller ski (F_Y) was contained in the friction measurement device. The friction coefficient between the treadmill surface and the roller ski was obtained by $\mu = \frac{F_Y}{F_Z}$, where F_Z is the vertical force that equals the weight of the weight plate placed on the roller ski.

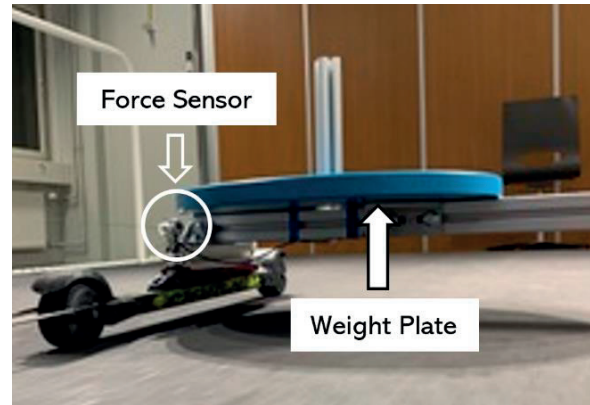


Figure A1. Custom-made friction measurement device.

Appendix B. Mechanical Principle of Translational Force

The motion of a rigid body under external forces can be reduced to (i) the acceleration of the COM and to (ii) the angular acceleration of the object around its COM. These change the rate of momentum and angular momentum, respectively. Correspondingly, in a 3D space, the motion problem involves six degrees of freedom (DoF). These DoFs can be expressed with three components of a translational force and another three components of a moment. The forces and torques make a rigid body translate and rotate. It is worth noting that it is a modeler's decision to express the six DoFs with translational forces and torques with respect to the COM. Accordingly, this is not the only, but rather a practical, option to model motion. The decomposition of an external force into translational force and torque components acting on a rigid object is illustrated in Figure B1. An external force $\vec{F}_{\text{resultant}}$ acts on point a of a rigid sphere. $\vec{F}_{\text{resultant}}$ is decomposed to the translational component $\vec{F}_{\text{translational}}$ that acts in the direction of the line joining the COM and point a. The (displacement) vector from COM to point a is denoted by \vec{l} . The rotational component $\vec{F}_{\text{rotational}}$ of the force is perpendicular to vector \vec{l} such that condition $\vec{F}_{\text{resultant}} = \vec{F}_{\text{rotational}} + \vec{F}_{\text{translational}}$ holds (Figure B1a). Precisely, the same situation is expressed in terms of a translational force $\vec{F}_{\text{translational}}$ and torque τ , which is the product of \vec{l} and $\vec{F}_{\text{rotational}}$ (Figure B1b).

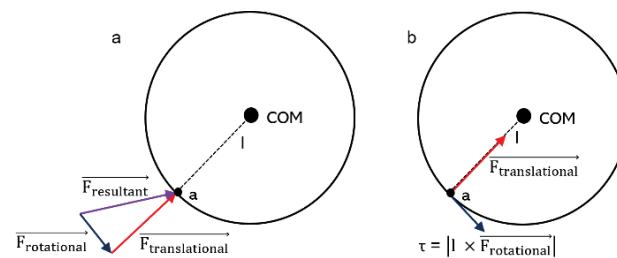


Figure B1. Diagram of the mechanical principle of translational force.

As the principles of mechanics do not depend on the object—that is, Newton's laws apply to all objects—the basic setting does not change from that of a single rigid object. However, in the case of joined bodies, the COM cannot be specified a priori, as it depends on the position of the parts in relation to each other (see Figure B2). When external forces

$\vec{F}_{\text{resultant}}$ act on the object (Figure B2a), the whole object translates, and each part moves with respect to each other. Because of this, the COM moves with respect to the parts. However, the motion of the object still fulfils Newton's laws (Figure B2b). Consequently, nothing prevents one from decomposing the external forces into components of translational forces and torques with respect to the COM.

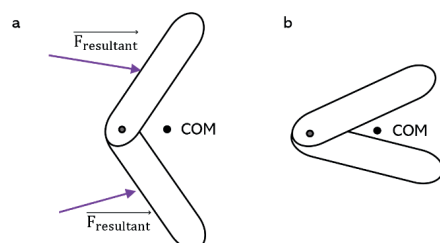


Figure B2. Diagram of forces acting on connected rigid bodies.

References

- Smith, G.A. Biomechanics of cross country skiing. In *Cross Country Skiing. Handbook of Sports Medicine*; Rusko, H., Ed.; Wiley: New York, NY, USA, 2003; pp. 32–61.
- Mapelli, A.; Zago, M.; Fusini, L.; Galante, D.; Colombo, A.; Sforza, C. Validation of a protocol for the estimation of three-dimensional body center of mass kinematics in sport. *Gait Posture* **2014**, *39*, 460–465. [[CrossRef](#)] [[PubMed](#)]
- Stoggl, T.; Holmberg, H.C. Three-dimensional Force and Kinematic Interactions in V1 Skating at High Speeds. *Med. Sci. Sports Exerc.* **2015**, *47*, 1232–1242. [[CrossRef](#)] [[PubMed](#)]
- Smith, G.; Kvamme, B.; Jakobsen, V. Ski skating technique choice: Mechanical and physiological factors affecting performance. In *Proceedings of the ISBS-Conference Proceedings Archive, Ouro Preto, Brazil, 23–27 August 2007*.
- Hoset, M.; Rognstad, A.; Rølvåg, T.; Ettema, G.; Sandbakk, Ø. Construction of an instrumented roller ski and validation of three-dimensional forces in the skating technique. *Sports Eng.* **2014**, *17*, 23–32. [[CrossRef](#)]
- Göpfert, C.; Pohjola, M.V.; Linnamo, V.; Ohtonen, O.; Rapp, W.; Lindinger, S.J. Forward acceleration of the centre of mass during ski skating calculated from force and motion capture data. *Sports Eng.* **2017**, *20*, 141–153. [[CrossRef](#)]
- Ohtonen, O.; Lindinger, S.J.; Gopfert, C.; Rapp, W.; Linnamo, V. Changes in biomechanics of skiing at maximal velocity caused by simulated 20-km skiing race using V2 skating technique. *Scand. J. Med. Sci. Sports* **2018**, *28*, 479–486. [[CrossRef](#)] [[PubMed](#)]
- Smith, G.A. Biomechanical analysis of cross-country skiing techniques. *Med. Sci. Sports Exerc.* **1992**, *24*, 1015–1022. [[CrossRef](#)] [[PubMed](#)]
- Holmberg, H.C.; Lindinger, S.; Stöggel, T.; Björklund, G.; Müller, E. Contribution of the legs to double-poling performance in elite cross-country skiers. *Med. Sci. Sports Exerc.* **2006**, *38*, 1853–1860. [[CrossRef](#)] [[PubMed](#)]
- Andersson, E.; Stoggl, T.; Pellegrini, B.; Sandbakk, O.; Ettema, G.; Holmberg, H.C. Biomechanical analysis of the herringbone technique as employed by elite cross-country skiers. *Scand. J. Med. Sci. Sports* **2014**, *24*, 542–552. [[CrossRef](#)] [[PubMed](#)]
- Stoggl, T.; Muller, E.; Lindinger, S. Biomechanical comparison of the double-push technique and the conventional skate skiing technique in cross-country sprint skiing. *J. Sports Sci.* **2008**, *26*, 1225–1233. [[CrossRef](#)] [[PubMed](#)]
- Stoggl, T.L.; Holmberg, H.C. Double-Poling Biomechanics of Elite Cross-country Skiers: Flat versus Uphill Terrain. *Med. Sci. Sports Exerc.* **2016**, *48*, 1580–1589. [[CrossRef](#)] [[PubMed](#)]
- Sandbakk, O.; Holmberg, H.C. A reappraisal of success factors for Olympic cross-country skiing. *Int. J. Sports Physiol. Perform.* **2014**, *9*, 117–121. [[CrossRef](#)] [[PubMed](#)]
- Stöggel, T.; Stöggel, J.; Müller, E. Competition analysis of the last decade (1996–2008) in crosscountry skiing. In *Science and Skiing IV*; Erich Müller, S.L., Thomas, S., Eds.; Meyer & Meyer Sport: Berkshire, UK, 2008; pp. 657–677.
- Ohtonen, O.; Lindinger, S.; Lemmettylä, T.; Seppälä, S.; Linnamo, V. Validation of portable 2D force binding systems for cross-country skiing. *Sports Eng.* **2013**, *16*, 281–296. [[CrossRef](#)]
- Ohtonen, O.; Ruotsalainen, K.; Mikkonen, P.; Heikkinen, T.; Hakkarainen, A.; Leppävuori, A.; Linnamo, V. Online feedback system for athletes and coaches. In *Proceedings of the 3rd International Congress on Science and Nordic Skiing, Vuokatti, Finland, 5–8 June 2015*; p. 35.
- Yu, B.; Gabriel, D.; Noble, L.; An, K.-N. Estimate of the optimum cutoff frequency for the Butterworth low-pass digital filter. *J. Appl. Biomech.* **1999**, *15*, 318–329. [[CrossRef](#)]
- Selbie, W.S.; Hamill, J.; Kepple, M.T. Three-Dimensional Kinetics. In *Research Methods in Biomechanics*, 2nd ed.; Robertson, G.E., Caldwell, G.E., Hamill, J., Kamen, G., Whittlesey, S., Eds.; Human Kinetics: Champaign, IL, USA, 2013; pp. 159–160.
- Danielsen, J.; Sandbakk, Ø.; McGhie, D.; Ettema, G. Mechanical energetics and dynamics of uphill double-poling on roller-skis at different incline-speed combinations. *PLoS ONE* **2019**, *14*, e0212500. [[CrossRef](#)] [[PubMed](#)]
- Winter, D.A. Human balance and posture control during standing and walking. *Gait Posture* **1995**, *3*, 193–214. [[CrossRef](#)]

21. Kadaba, M.; Ramakrishnan, H.; Wootten, M.; Gainey, J.; Gorton, G.; Cochran, G. Repeatability of kinematic, kinetic, and electromyographic data in normal adult gait. *J. Orthop. Res.* **1989**, *7*, 849–860. [[CrossRef](#)] [[PubMed](#)]
22. Yu, B.; Kienbacher, T.; Growney, E.S.; Johnson, M.E.; An, K.N. Reproducibility of the kinematics and kinetics of the lower extremity during normal stair-climbing. *J. Orthop. Res.* **1997**, *15*, 348–352. [[CrossRef](#)] [[PubMed](#)]
23. Malek, M.H.; Coburn, J.W.; Marelich, W.D. *Advanced Statistics for Kinesiology and Exercise Science: A Practical Guide to ANOVA and Regression Analyses*; Routledge: Oxfordshire, UK, 2018.
24. Robertson, G.E. Energy, Work, and Power. In *Research Methods in Biomechanics*, 2nd ed.; Robertson, G.E., Caldwell, G.E., Hamill, J., Kamen, G., Whittlesey, S., Eds.; Human Kinetics: Champaign, IL, USA, 2013; p. 132.
25. Schwameder, H. Biomechanics research in ski jumping, 1991–2006. *Sports Biomech.* **2008**, *7*, 114–136. [[CrossRef](#)] [[PubMed](#)]



II

CONTRIBUTION AND EFFECTIVENESS OF SKI AND POLE FORCES IN SELECTED ROLLER SKIING TECHNIQUES ON TREADMILL AT MODERATE INCLINES

by

Zhao, S., Lindinger, S., Ohtonen, O., Linnamo, V. 2023

Frontiers in Sports and Active Living, 5

doi:10.3389/fspor.2023.948919

© 2023 Zhao, Lindinger, Ohtonen, and Linnamo. This is an open-access article distributed under the terms of [the Creative Commons Attribution License \(CC BY\)](#). The use, distribution or reproduction in other forums is permitted, provided the original author(s) and the copyright owner(s) are credited and that the original publication in this journal is cited, in accordance with accepted academic practice. No use, distribution or reproduction is permitted, which does not comply with these terms.



OPEN ACCESS

EDITED BY
Thomas Leonhard Stöggel,
University of Salzburg, Austria

REVIEWED BY
Shih-Wun Hong,
Tzu Chi University, Taiwan
Zihan Yang,
Capital Medical University, China

*CORRESPONDENCE
Shuang Zhao
✉ zhaoshuangzs@hotmail.com

SPECIALTY SECTION
This article was submitted to Sports Science,
Technology and Engineering, a section of the
journal Frontiers in Sports and Active Living

RECEIVED 20 May 2022
ACCEPTED 06 February 2023
PUBLISHED 22 February 2023

CITATION
Zhao S, Lindinger S, Ohtonen O and Linnamo V
(2023) Contribution and effectiveness of ski and
pole forces in selected roller skiing techniques
on treadmill at moderate inclines.
Front. Sports Act. Living 5:948919.
doi: 10.3389/fspor.2023.948919

COPYRIGHT
© 2023 Zhao, Lindinger, Ohtonen and
Linnamo. This is an open-access article
distributed under the terms of the Creative
Commons Attribution License (CC BY). The use,
distribution or reproduction in other forums is
permitted, provided the original author(s) and
the copyright owner(s) are credited and that the
original publication in this journal is cited, in
accordance with accepted academic practice.
No use, distribution or reproduction is
permitted which does not comply with these
terms.

Contribution and effectiveness of ski and pole forces in selected roller skiing techniques on treadmill at moderate inclines

Shuang Zhao^{1*}, Stefan Lindinger², Olli Ohtonen¹
and Vesa Linnamo¹

¹Faculty of Sport and Health Sciences, University of Jyväskylä, Jyväskylä, Finland, ²Center of Health and Performance (CHP), Department of Food and Nutrition and Sport Science, University of Gothenburg, Gothenburg, Sweden

Background: Most of the studies about the effects of incline on cross-country skiing are related to the metabolic efficiency. The effective skiing biomechanics has also been indicated to be among the key factors that may promote good performance. The aims of this study were to provide biomechanical characteristics and investigate the relative contribution and effectiveness of ski and pole forces in overcoming the total external resistance with double poling (DP) and Gear 3 (G3) techniques at varying moderate uphill inclines.

Methods: 10 male cross-country skiers participated in this study. Custom-made force measurement bindings, pole force sensors, and an 8-camera Vicon system were used to collect force data and ski and pole kinematics at 3°, 4° and 5° with 10 km/h skiing speed.

Results: The cycle length (CL) decreased by 10% and 7% with DP and G3 technique from 3° to 5° ($p < 0.001$, $p < 0.001$). The cycle rate (CR) increased by 13% and 9% from 3° to 5° with DP and G3 technique respectively. From 3° to 5°, the peak pole force increased by 25% ($p < 0.001$) and 32% ($p < 0.001$) with DP and G3 technique. With DP technique, the average cycle propulsive force (ACPF) increased by 46% ($p < 0.001$) from 3° to 5° and with G3 technique, the enhancement for ACPF was 50% ($p < 0.001$). In G3 technique, around 85% was contributed by poles in each incline.

Conclusion: The higher power output in overcoming the total resistance was required to ski at a greater incline. With DP technique, the upper body demands, and technical effectiveness were increasing with incline. With G3 technique, the role of external pole work for propulsion is crucial over different terrains while role of legs may stay more in supporting the body against gravity and repositioning body segments.

KEYWORDS

double poling technique, gear 3 technique, speed maintain, crosscountry skiing, effectiveness

1. Introduction

Cross-country (XC) skiing is a sport in which competition and training are normally performed on varying track topography. The classical and skating style (also known as freestyle) are the two basic skiing techniques. Techniques such as double poling, diagonal stride, and kick double pole, are sub-techniques of classical skiing technique (1). In skating technique, there are six different sub-techniques, so called gears (Gear 2–Gear 7) (2, 3). In both classical and skate skiing, skiers change the sub-techniques spontaneously to maintain high speed and adapt to the change of the terrain (4–6). Several researchers

have studied the effect of incline and speed on metabolic efficiency (7–9), technique shift (5, 10), as well as kinematics and kinetics change (11–16). The effects of incline on metabolic efficiency have been studied a lot (7–9), as it is a key factor for endurance sports (17). The effective skiing biomechanics has also been indicated to be among the key factors that may promote good performance (18). Therefore, having more knowledge about the effects of incline on skiing biomechanics may be beneficial for skiers and coaches with skiing technique improvements for maintaining the skiing speed at varying uphill inclines.

Several studies have investigated the effects of incline on cycle and force characteristics of different skiing techniques. The cycle rate (CR) has been proved to be higher at steeper inclines (4, 19). In both DP and Gear 2 (G2) technique, the peak pole force (PPF), average pole force and average cycle pole force were all greater at the higher incline situations (19). The primary mechanical determinant of skier's performance is the propulsive force (1), which has been defined as the forward directed component of the 3D resultant reaction force from skis and poles acting on skiers (1, 16, 20–22). The total external resistance should be overcome by the total propulsive force in XC skiing. However, less works (16, 22) have examined the effects of incline on the forces and propulsive forces generated from skis.

As one of the main techniques in classic XC skiing, the usage and the importance of DP technique have been increased during the past years due to increased upper body power, more systematic strength training and higher skiing speeds (20, 23). The Gear 3 (G3) technique has also become the most commonly used technique in the freestyle XC skiing competition (24). DP and G3 technique are normally used in level terrain up to moderate uphill inclines. The DP technique, which involves both arms acting in unison and leg involvement, has often been considered as an upper-body movement (25–27) as the propulsive forces are exerted only through the poles even though it is clear that also legs contribute to the performance (28, 29). The G3 contains symmetrical pole thrust on every leg stroke (1). The propulsive force in G3 are generated from both skis and poles (30, 31). Although most of the total propulsive force has been proved to be attributed to the forces from poles in skate skiing techniques (32, 33), how the ski and pole forces are performed to maintain the speed with varying uphill inclines need further investigation.

Therefore, the current study was conducted to (1) provide biomechanical characteristics and (2) investigate the relative contribution and effectiveness of ski and pole forces in overcoming the total external resistance of both DP and G3 techniques at varying moderate uphill inclines. We hypothesized that with DP technique, we could measure some propulsive forces from skis, but it would be quite small, and pole forces would be more effective at steeper inclines than at relative lower inclines. We also hypothesized that pole forces contribute more and would be more effective than the ski forces with G3 technique (32, 33) in overcoming the total resistance at any incline, but the relative contribution of ski forces to overcome the total resistance would increase at steeper grade.

2. Materials and methods

2.1. Participants

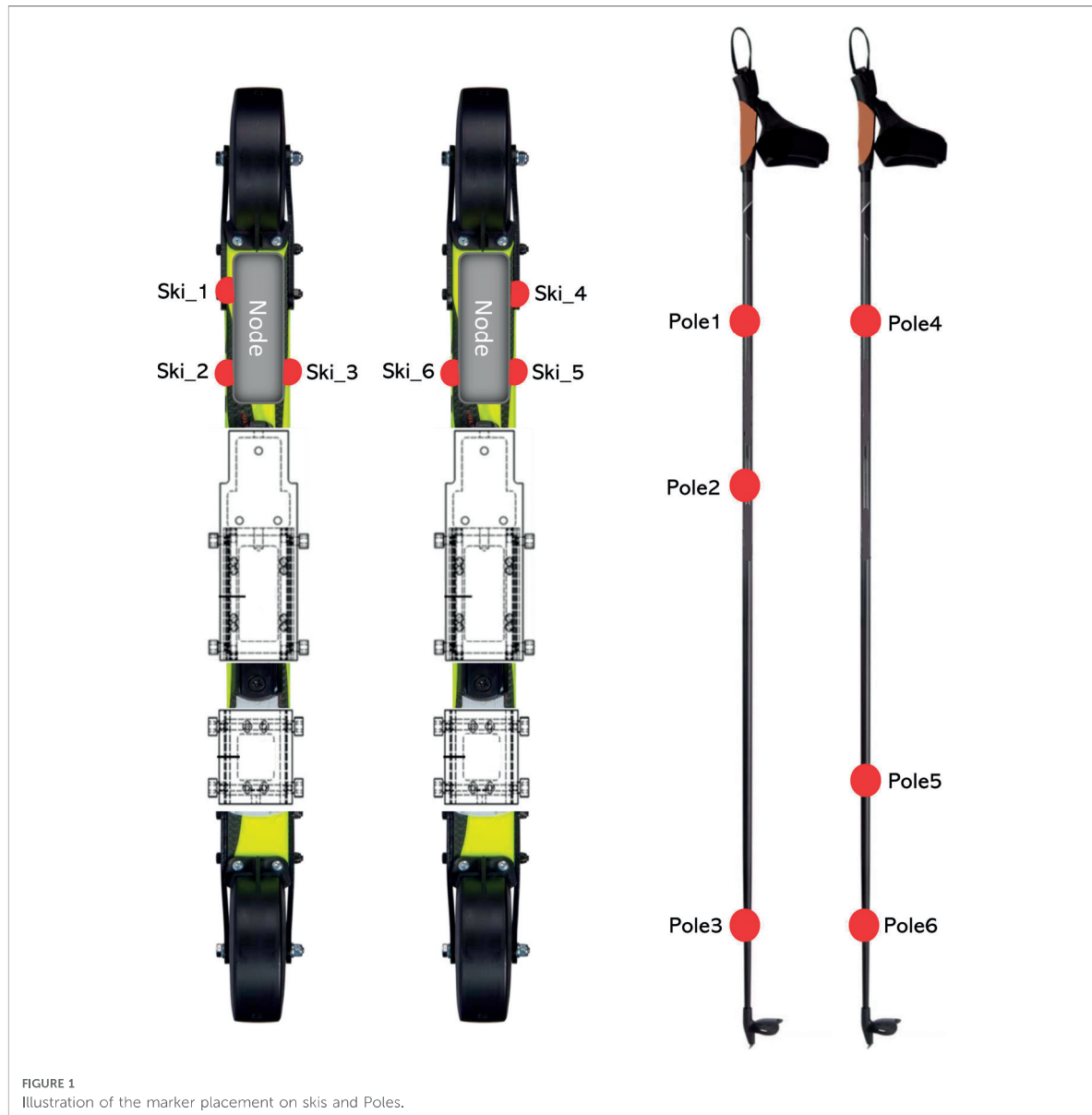
10 male participants (age: 29.4 ± 7.9 years; height: 181.4 ± 5.7 cm; weight: 77.9 ± 8.9 kg) who were familiar with treadmill roller-skiing volunteered to participate in this study. The participants' group included experienced skiers, such as high-level junior athletes, recently retired athletes from the national team, local skiing club members and national team coaches, both latter ones are with high roller skiing skill and fitness levels. All protocol used in this study were approved by the Ethics Committee of the University of Jyväskylä. All participants were provided written informed consent before the measurement and were free to withdraw from the experiments.

2.2. Protocol

Passive reflective markers were attached onto skiing equipment before the measurement. First, participants completed a 10–15 min warm-up roller skiing on the treadmill. After the warm-up activity, the DP technique was performed at 3°, 4° and 5° at a speed of 10 km/h. This speed is commonly used in aerobic capacity tests where the speed is kept constant. There was a 1-min rest between each incline. When the DP technique was done, pole length was adjusted to a comfortable length for G3 technique (1). The comfortable pole length for DP technique were $85.9\% \pm 2.5\%$, and for G3 were $90.0\% \pm 1.3\%$ of skiers' body height in this study. The participants were given a 5-min rest period while adjusting the pole length. The G3 technique was then performed on the treadmill. The protocol for changing the incline was the same as during the DP test.

2.3. Data collection

An 8-video-camera motion capture system and NEXUS 2.8.1 software (Vicon, Oxford, United Kingdom) were used to collect and record the three-dimensional (3D) trajectories of reflective markers at a sampling rate of 150 Hz. The global coordinate system (GCS) was defined by using the right-hand rule when the incline of the treadmill was 0° and was calibrated according to Vicon's specifications. The Y-axis of GCS was defined as the longitudinal axis of the treadmill. The Z-axis of GCS was perpendicular to the ground pointing upward. 15 reflective markers were used in this study. 6 markers were attached onto the roller skis (3 markers each, **Figure 1**) and 6 markers were attached onto the poles (3 markers each, **Figure 1**). Another 3 markers were attached onto the treadmill. Two markers were attached to the front and rear right corners of the treadmill. Another one was attached to the rear left corner of the treadmill. All markers in this study were used to provide the position of roller skis, poles, and the treadmill in the GCS.



Measurements were performed on a motorized treadmill with a belt surface 2.7 m wide and 3.5 m long (Rodby Innovation AB, Vänge, Sweden). A same pair of roller-skis (Marwe SKATING 620 XC, wheel no. 0, Marwe Oy, Hyvinkää, Finland) were used for both techniques and all participants. Two custom-made pole force sensors (VTT MIKES, Technical Research Centre of Finland Ltd., Kajaani, Finland) were used to measure axial ground reaction force (GRF) from poles at a sample rate of 400 Hz. The pole force sensors were mounted below the pole grip and were calibrated in a certified laboratory for force and mass measurements (VTT MIKES, Technical Research Centre of Finland Ltd., Kajaani, Finland). Two custom-made 2D (vertical and medio-lateral) force

measurement bindings (Neuromuscular Research Centre, University of Jyväskylä, Finland) (34) were mounted on the roller-skis to measure the leg forces generated from roller-skis at a sampling rate of 400 Hz. Both pole force sensor and ski measurement bindings have been used in our previous study (35). The total mass of one equipped pole and one equipped roller ski were 202 g and 664 g greater than the normal ones. A trigger signal was sent from the Coachtech online measurement and feedback system (36) (Neuromuscular Research Centre, University of Jyväskylä, Finland) to the motion capture system to mark the start of the force capture. Data from each subject at each incline were collected for at least 30 s when the treadmill speed was constant at 10 km/h.

2.4. Data processing

The marker labeling was performed by using NEXUS 2.8.1 software. The raw 3D trajectories of all reflective markers were low-pass filtered (fourth-order, zero-lag, Butterworth filter) with a cut-off frequency of 11.3 Hz (37). Force data were low-pass filtered (eighth-order, zero-lag, Butterworth filter) with a cutoff frequency of 15 Hz (38). Filtering and parameter calculation were performed in MATLAB R2018a (MathWorks, Natick, United States). 10 cycles from each DP technique trail and 5 cycles from each G3 technique trail were analyzed in this current study. For DP technique trails, one cycle was defined as the period between two consecutive right pole plant. For G3 technique, one cycle was defined as the time between consecutive same side ski force minima after ski plant and contained the kicking, overlapping,

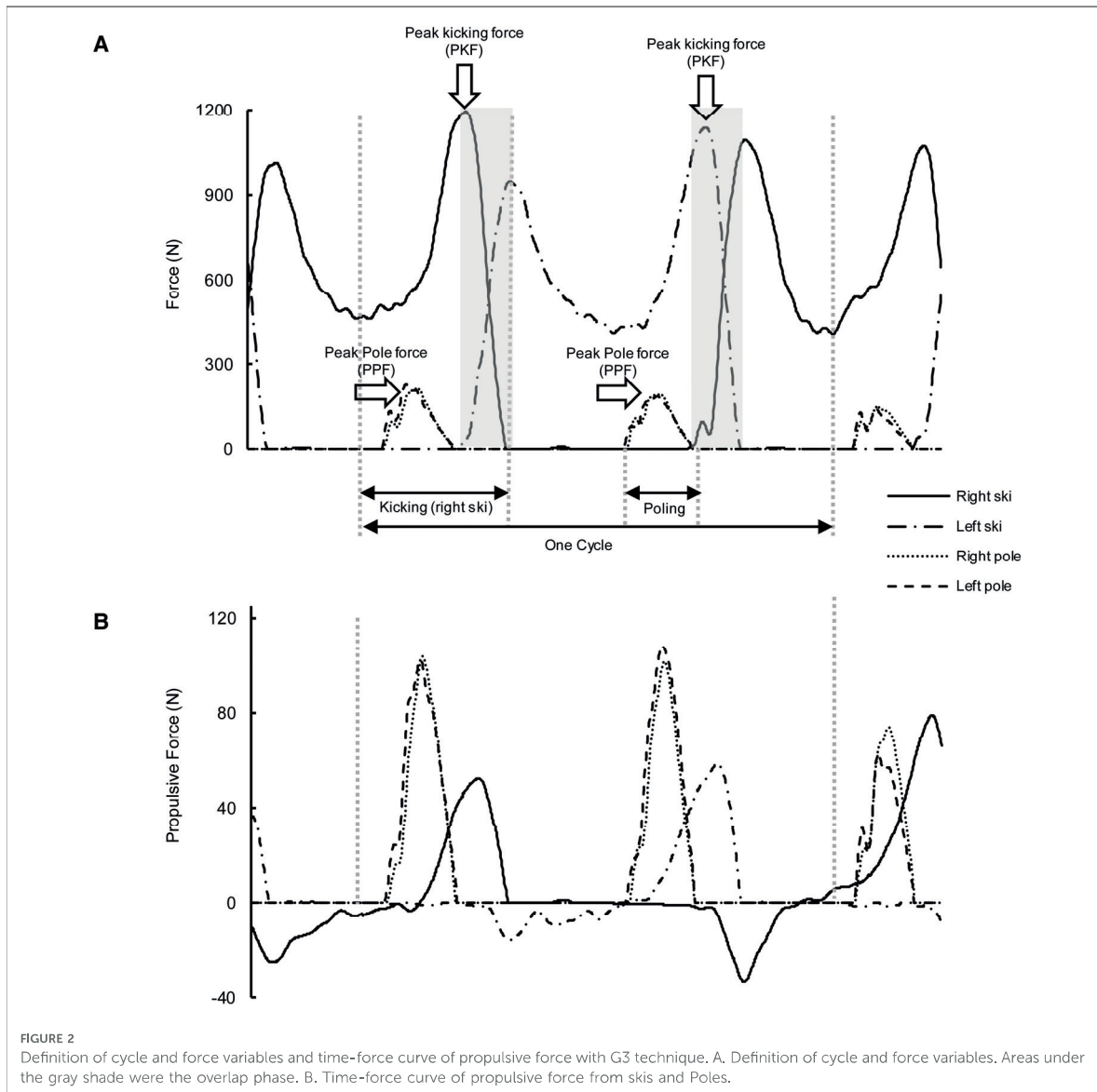
pure gliding action of both left and right ski and two double poling action from both poles (Figure 2A).

2.4.1. Propulsive force calculation

Forces measured in the force coordinate system were first transformed into the GCS (35). The measured axial pole forces were considered as the ground reaction forces acting along the pole from the tip to the top. The pole forces vector (\vec{F}_{pole}) in GCS were calculated as:

$$\vec{F}_{pole} = F * \vec{u}$$

where F was the magnitude of the measured axial pole force and \vec{u} was the direction vector from the tip to the top of the pole.



The direction vector was defined by using the reflective markers that were attached to the pole. As the measurements were performed at different inclines, the propulsive force component from ski (F_{p_ski}) and from pole (F_{p_pole}) were calculated by:

$$F_{p_ski} = F_{skiy} * \cos \alpha + F_{skiz} * \sin \alpha$$

$$F_{p_pole} = F_{pole_y} * \cos \alpha + F_{pole_z} * \sin \alpha$$

where α was the incline of the treadmill (3°, 4°, or 5°); F_{pole_y} and F_{pole_z} were the corresponding pole force components in GCS; F_{skiy} and F_{skiz} were the components of GRFs' vector generated from legs in GCS.

2.4.2. Cycle characteristics

The cycle rate (CR) for each technique was the cycles per second ($CR = 1/\text{Cycle time}$, Hz). The cycle length (CL) was defined as the product of cycle time and the speed of the treadmill. In both techniques, the poling time was the ground contact time of the right poles. For G3 technique (Figure 2A), the kicking time of one leg was the time from unweighting minima to the ski release. The overlap time of the legs were defined as the time from one ski plant to the adjacent ski release of the other ski. The relative poling, kicking, and overlap times were calculated for the analysis.

2.4.3. Impulses, effectiveness and contributions of ski and pole forces

The kinetic variables analyzed in this study were similar to those in another study which we concentrated on the effect of changing the treadmill speed. The peak pole force (PPF) for both techniques, and peak kicking force (PKF) for G3 technique were determined by the resultant force from pole and ski respectively (Figure 2A). For both techniques, pole and ski propulsive force impulses as well as ski vertical impulse were calculated. The propulsive force impulse was equal to the cumulative time integral of the propulsive force, restricting the integral to the intervals over which the integrand was positive. The effectiveness index of pole and ski forces was calculated by expressing the pole propulsive impulse and the ski propulsive impulse as a percentage of pole and ski resultant force impulse, respectively (16). The contribution of pole and ski forces in overcoming the total resistance were calculated by expressing the pole and ski propulsive impulse as a percentage of total propulsive impulse (32), respectively. The average cycle propulsive force (ACPF) were determined by dividing the total propulsive impulse by cycle time (16). The power output in overcoming the total resistance in skiing direction was calculated by multiplying the ACPF and the speed of the treadmill (m/s) (16).

2.5. Statistical analyses

All the data in this current study were shown as means \pm SD. One-way ANOVA with repeated-measures and *Bonferroni post hoc* analysis were conducted to reveal the effect of incline on each characteristic. The effect size (η_p^2) and statistical power were also

provided for further evaluation. The level of statistical significance was set at 0.05. All statistical analyses were carried out by using SPSS 22.0 Software (SPSS Inc., Chicago, United States.).

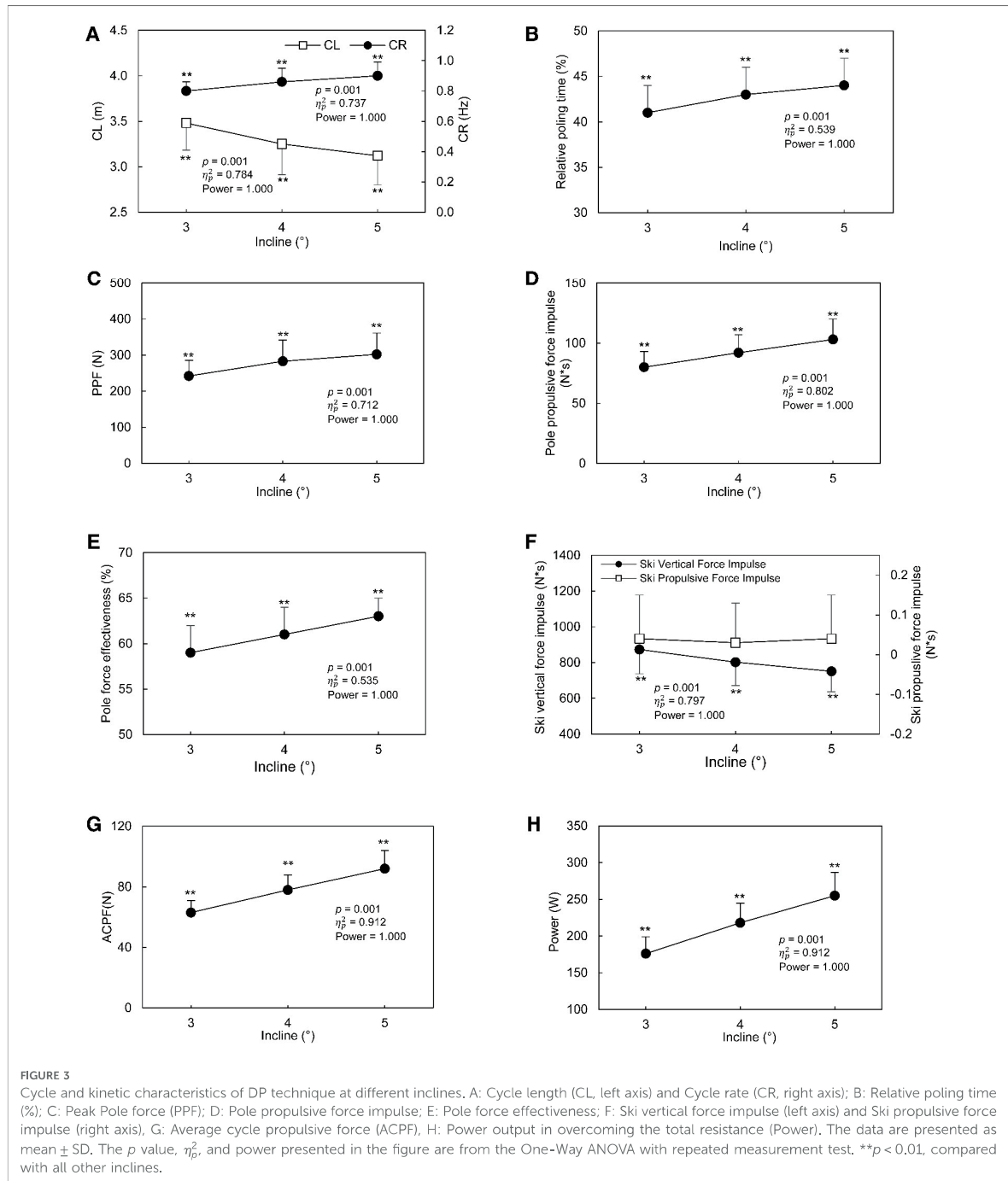
3. Results

In DP technique, the CL (Figure 3A) decreased by 10% as the incline of the treadmill elevated from 3° to 5° ($p < 0.001$). The CR (Figure 3A) and relative poling time (Figure 3B) increased by 13% ($p < 0.001$) and 7% ($p < 0.001$) from 3° to 5°, respectively. From 3° to 5°, PPF increased by 25% ($p < 0.001$, Figure 3C) and the pole propulsive force impulse increased by 29% ($p < 0.001$, Figure 3D). The pole force effectiveness increased by 7% from 3° to 5° ($p < 0.001$, Figure 3E). With DP technique, the ski vertical force impulse decreased with the increasing incline ($p < 0.001$, Figure 3F). The ski propulsive force impulse was small and independent from the incline of the treadmill ($p = 0.284$, Figure 3F). The ACPF and the power output in overcoming the total resistance increased by 46% ($p < 0.001$, Figure 3G) and 45% ($p < 0.001$, Figure 3H) with DP technique, respectively.

With G3 technique, the CL (Figure 4A) decreased by 7% as the incline of the treadmill elevated from 3° to 5° ($p \leq 0.001$). The CR (Figure 4A) and the relative poling time (Figure 4B) with G3 technique increased by 9% ($p < 0.001$) and 8% ($p \leq 0.008$) from 3° to 5°, respectively. With G3 technique, the relative kicking time (Figure 4C) was independent from the incline ($p = 0.794$). The relative overlap time (Figure 4D) at 3° was greater than relative overlap time at 4° and 5° ($p = 0.101$). From 3° to 5°, the PPF and the PKF increased by 32% ($p < 0.001$, Figure 4E) and 6% with G3 ($p \leq 0.037$, Figure 4E) technique, respectively. From 3° to 5°, the pole propulsive force impulse increased by 36% ($p < 0.001$) with G3 technique (Figure 4F). The ski propulsive force impulse (Figure 4G) at 4° was not different from that at 5° ($p = 0.338$), but both were greater than the ski propulsive force impulse at 3° ($p < 0.001$). The ski vertical force impulse decreased by 11% from 3° to 5° ($p < 0.001$, Figure 4H). With G3 technique, the enhancements for ACPF were 50% ($p < 0.001$, Figure 5A). The power output in overcoming the total resistance increased by 50% ($p < 0.001$, Figure 5B). The pole force effectiveness (Figure 5C) increased by 5% ($p < 0.001$). The ski force effectiveness (Figure 5C) at 3° was significantly lower than at 4° to 5° ($p < 0.001$, $p < 0.001$). No significant difference on ski force effectiveness between 4° and 5° was found ($p = 0.101$). In G3 technique, around 85% of the total propulsive force was contributed by poles (Figure 5D). The relative contributions of ski and pole forces to overcome the total resistance were affected by the treadmill incline (Figure 5D), but the only difference was between 3° and 4° ($p = 0.003$).

4. Discussion

This study provided the biomechanical characteristics and investigated the relative contribution and effectiveness of ski and pole forces in overcoming the total external resistance



of both DP and G3 techniques at varying moderate uphill inclines. 0.03–0.04 N*s ski propulsive force impulse was found, and the pole force effectiveness increased by 7% from 3° to 5° with DP technique, which support our hypothesis that some propulsive forces from skis could be measured but it would be quite small and pole forces

would be more effective at steeper inclines. With G3 technique, 55%–58% of the resultant pole forces was generated to overcome the external resistance and about 85% of the total propulsive force was contributed by poles. Thus, the hypothesis of more contribution from poles and greater pole effectiveness was satisfied.

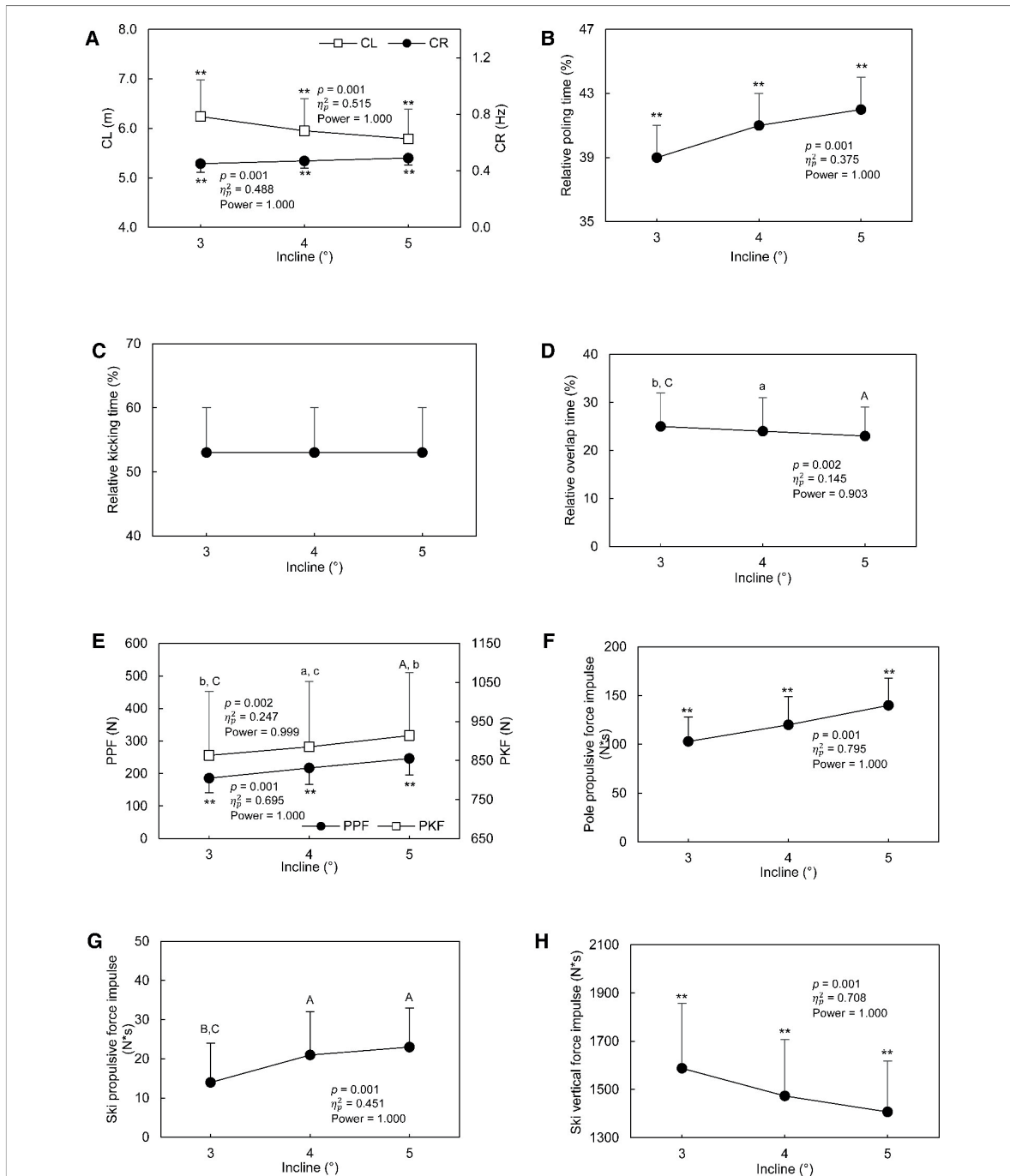
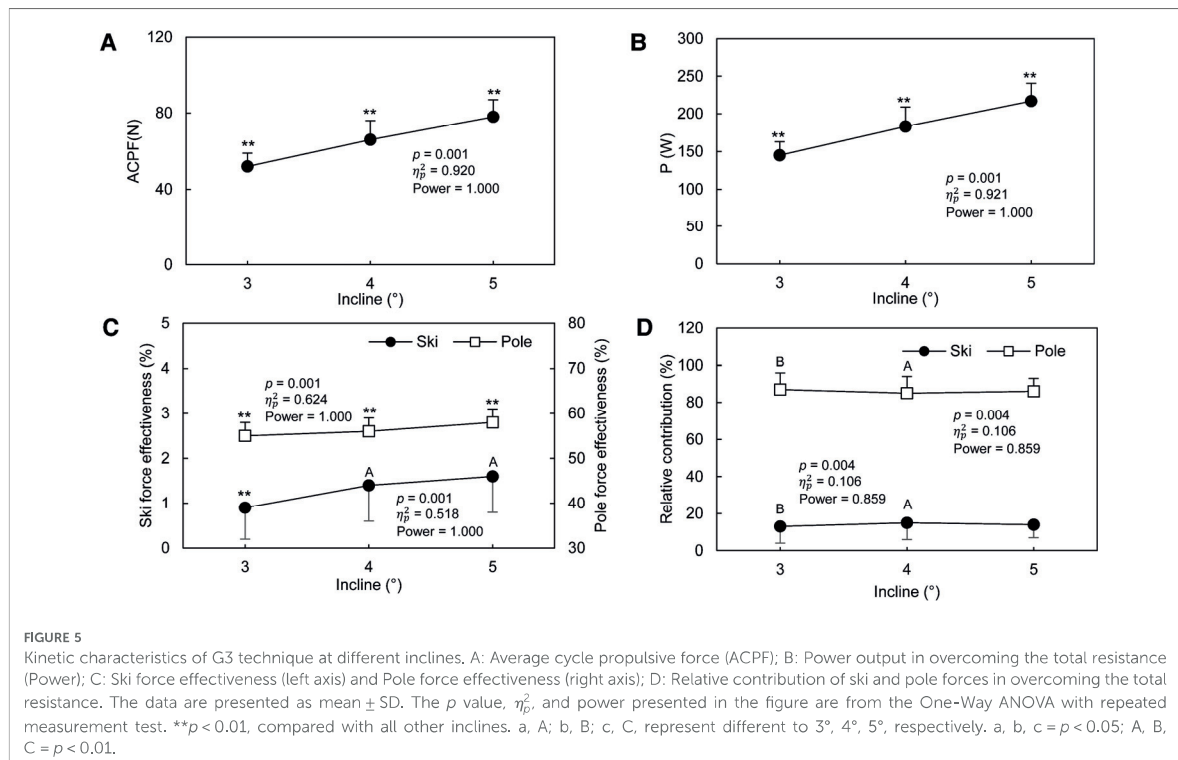


FIGURE 4 Cycle and kinetic characteristics of G3 technique at different inclines. A: Cycle length (CL, left axis) and Cycle rate (CR, right axis); B: Relative poling time (%); C: Relative kicking time (%); D: Relative overlap time (%); E: Peak Pole force (PPF, left axis), Peak kicking force (PKF, right axis); F: Pole propulsive force impulse; G: Ski propulsive force impulse; H: Ski vertical force impulse. The data are presented as mean \pm SD. The p value, η_p^2 , and power presented in the figure are from the One-Way ANOVA with repeated measurement test. $**p < 0.01$, compared with all other inclines. a, A; b, B; c, C, represent different to 3°, 4°, 5°, respectively. a, b, c = $p < 0.05$; A, B, C = $p < 0.01$.



4.1. Cycle characteristics

In response to increases in incline, the CR increased significantly at steeper inclines with both techniques (Figures 3A, 4A). This indicated that shorter time was used by subjects to finish one cycle at steeper inclines. This finding is consistent with previous studies that the CR was higher at steeper inclines with G3 technique (4), and DP technique (19). Since the treadmill speed remained the same at different incline, the CL decreased at steeper inclines with both techniques. Similar finding was found in a previous study that the CL was decreased with both G2 and DP techniques in response to a steeper incline (19). Comparable phenomenon has been demonstrated in uphill running where step length (CL) was decreased and step frequency (CR) was increased with the elevated treadmill incline (39, 40). The adjustment of CL and CR in uphill running was coped with the uphill progression and the available metabolic power (40).

The relative poling time (Figures 3B, 4B) are greater at steeper incline with both technique in this study. Specifically, the time for getting ready for the next pole plant was shorter at steeper incline, and the proportion of cycle for generating pole forces increased with the elevated treadmill incline in both techniques (19). As the G3 technique contains both pole and ski thrusts, the ski movements were analyzed as well. The relative kicking time (Figure 4C) was independent from the incline of the treadmill. This indicated that in response to the increased treadmill incline, the proportion of cycle for generating ski forces would not change.

The relative overlap time (Figure 4D) at 4° and 5° were shorter when compared to that at 3°. The less relative overlap time indicated that the skier may start “seeking ground contact” with the new glide ski later at steeper grade (15). The magnitude of the relative overlap time in this study (23%–25%) was higher than that reported by Ohtonen et al. (15) (around 10%). This difference might be attributed to environmental difference (on snow vs. on treadmill) and athletes’ level (a group of elite skiers vs. a group of diverse level skiers). Faster elite skiers may control balance more securely than averaged level skiers (15).

4.2. Forces and impulses

With both techniques, the PPF (Figure 3C and Figure 4E), and pole propulsive force impulse (Figure 3D and Figure 4F) increased continuously up to the steepest incline in this present study. Combined these results with results from cycle characteristics, although less time was used for getting ready for pole plant, greater pole force and pole propulsive force should be reached at steeper incline. These results were consistent with the previous study that in both DP and G2 technique, the force variables from poles were all greater at the steeper grade than the lower grade (19). 0.03–0.04 N*s ski propulsive force impulse was found (Figure 3F) for DP technique in this study. This result supports our hypothesis that with DP technique, we could measure some propulsive force from skis, but it would be quite small. The magnitude of the ski propulsive force impulse was very small and

seems to be negligible. Therefore, from overcoming the total resistance point of view, DP technique could be considered as an upper-body movement as indicated by other previous studies (25–27).

Greater ski force and ski propulsive force should also be generated to overcome the increased total resistance at steeper incline with G3 technique, as the PKF and ski propulsive force impulse all increased at steeper incline in this study. However, although participants in this study had similar bodyweight with participants in other previous studies (15, 41), the magnitude of PKF in this study was lower than those in previous studies. The additional weight and height of the roller ski equipped with the force measurement bindings may decrease the usage of legs, thereby greater ski forces could not be reached. In addition, the difference in skiers' level and the skiing intensity level may also be attributed to the difference in PKF.

The gravity component parallel to the treadmill surface increased with the incline (38), thus more forces and greater power output are needed at a steeper grade. Therefore, the ACPF increased continuously with the elevated treadmill incline with both techniques (Figure 3G and Figure 5A). In response to the elevated treadmill incline, the power output in overcoming the total resistance increased by 45% and 50% with the DP and G3 technique respectively in this study (Figure 3H and Figure 5B). For DP technique, the propulsive impulse was mainly generated by poles and more pole propulsive force impulse are needed if skier intend to maintain the speed with increasing incline. But with G3 technique, increase the propulsive force generated from both poles and skis are needed. It is also worth remembering that in treadmill conditions skiers do not have to work against wind resistance as is the situation when skiing outside. Especially with higher speed, the wind resistance would have a great influence on propulsive forces (42). Therefore, the results about the magnitude of forces in this study may be different from studies which concentrated on snow skiing (15).

4.3. Effectiveness and contributions of ski and pole forces at different inclines

Effectiveness index has been used as a useful tool to evaluate athlete's overall economy on force production (16). The results of this study support our hypothesis that with DP technique, the effectiveness of pole force in overcoming the total resistance would be greater at steeper inclines than at relative lower inclines. The pole force effectiveness increased by 7% from 3° to 5° with DP technique, indicating that a greater proportion of the resultant force is generated to overcome the total resistance and a higher overall economy on force production. For DP technique, the increase in power output in overcoming the resistance was mainly due to the increase in pole force effectiveness because none of the propulsive force could be obtained by skis.

The results of our study support our hypothesis that pole forces would contribute more to overcome the total resistance and more effective than ski forces at any incline. Our results indicated that the relative contributions of pole forces were 5–6 times greater

than the relative contributions of ski forces (Figure 5D), and 55%–58% of the resultant pole forces is generated to overcome the external resistance which is greater than the effectiveness of ski force (0.9%–1.6%, Figure 5C). A previous study demonstrated that for G3 skating technique, about two thirds of propulsive is due to the pole forces and one-third due to the ski forces (33). The difference between our current study and the previous study (33) may be attributed to the difference in treadmill incline and speed. In addition, the extra weight and height of roller-skis caused by the force measurement bindings may decrease the usage of legs. Therefore, more pole force than ski forces were used in overcoming the total resistance. However, the results of our study do not support our hypothesis that the relative contribution of ski forces to overcome the total resistance would increase at steeper grade. Although the relative contribution from ski and pole forces were affected by the incline of the treadmill, the effects were medium ($\eta_p^2 = 0.106$), and the magnitude of the change did not vary so much. Specifically, increasing the propulsive force generated from both poles and skis are needed at steeper grade but the contribution ratio will not change.

However, what should be noted was that the contribution mentioned in this study were the relative amount of force to overcome the external resistance. The internal work, which is used to move the internal structures and not used to perform work on external objects (43), was not included. A previous study reported that about 37%–46% of the external power was contributed by the trunk and legs in DP technique (38). During the recovery phase of the DP technique or the pure gliding phase in the V2 skating technique, the lower extremity also contributes to repositioning the body, which may help skiers enhance the use of body weight (29, 44) and may increase the forces generated from skis and poles. However, this kind of contribution of lower extremity could not be revealed by the propulsive force. Therefore, only 0.9%–1.6% of the ski forces were generated to overcome the resistance. Results from this study suggests that the role of legs is quite small, but this might be affected by the height and weight of the roller ski and the level of study group. This result needs to be confirmed with higher level athletes and more advanced measurement equipment.

Our study has several limitations. The first limitation is that subjects in this study had varying skiing levels, and we recruited make subjects only. Therefore, future studies with a group of more skilled skiers of both genders will enhance the generality of our conclusion. The measurements of this study were performed in an indoor laboratory and on the treadmill. The lack of wind resistance (42) and the motor and belt of the treadmill (45) may prevent the results of this study from being directly applicable to snow skiing. In addition, the roller skiing equipment used in this study contained force measurement sensors, which are heavier and add extra height compared to the normal ones, may affect the skiing techniques. Future study could reduce the impact of measurement equipment by using portable force measurement roller skis (46) and lighter force measurement poles to help the results more easily transferable to daily roller ski training.

5. Conclusions

The present study provides detailed biomechanical information of DP and G3 techniques at three different uphill inclines. The higher power output in overcoming the total resistance was required to manage skiing at a greater incline. With DP technique this was supplied by greater pole forces and pole force effectiveness, which means that the upper body demands, and technical effectiveness were increasing with incline. This fact plays a role when skiers using DP also to a greater extent in moderate uphill sections like e.g., in “Visma Ski Classic” race events or when skiers are forced to use DP in uphill sections due to worse grip wax conditions for diagonal skiing. With G3 technique, increasing both pole and ski force effectiveness were needed at steeper grade, but the much larger relative contribution of pole forces vs. ski forces in overcoming the total resistance did not change over incline. This underlines the crucial role of external pole work for propulsion during G3 over different terrains while the role of legs may stay more in supporting the body against gravity and repositioning body segments.

Data availability statement

The original contributions presented in the study are included in the article/Supplementary materials, further inquiries can be directed to the corresponding author.

Ethics statement

The studies involving human participants were reviewed and approved by Ethics Committee of the University of Jyväskylä. The patients/participants provided their written informed consent to participate in this study.

References

- Smith GA. Biomechanics of cross country skiing. In: H Rusko, editors. *Cross country skiing handbook of sports medicine*. New York: Wiley (2003). p. 32–61.
- Andersson E, Supej M, Sandbakk Ø, Sperlich B, Stöggl T, Holmberg HC. Analysis of sprint cross-country skiing using a differential global navigation satellite system. *Eur J Appl Physiol*. (2010) 110(3):585–95. doi: 10.1007/s00421-010-1535-2
- Nilsson J, Tveit P, Eikrehagen O. Effects of speed on temporal patterns in classical style and freestyle cross-country skiing. *Sports Biomechanics*. (2004) 3(1):85–107. doi: 10.1080/14763140408522832
- Bilodeau B, Boulay MR, Roy B. Propulsive and gliding phases in four cross-country skiing techniques. *Med Sci Sports Exerc*. (1992) 24(8):917–25. doi: 10.1249/00005768-199208000-00014
- Ettema G, Kvæli E, Øksnes M, Sandbakk Ø. The role of speed and incline in the spontaneous choice of technique in classical roller-skiing. *Hum Mov Sci*. (2017) 55:100–7. doi: 10.1016/j.humov.2017.08.004
- Nilsson J, Tveit P, Eikrehagen O. Cross-country skiing: effects of speed on temporal patterns in classical style and freestyle cross-country skiing. *Sports Biomechanics*. (2004) 3(1):85–108. doi: 10.1080/14763140408522832

Author contributions

Conceptualization, SZ, OO, SL, and VL; Data curation, SZ; Formal analysis, SZ; Funding acquisition, SZ and VL; Investigation, SZ, OO, SL, and VL; Methodology, SZ, OO, SL, and VL; Project administration, SZ; Resources, SZ, and OO; Supervision, SZ, OO, SL and VL; Validation, SZ; Visualization, SZ; Writing – original draft, SZ; Writing – review & editing, SZ, OO, SL, and VL. All authors contributed to the article and approved the submitted version.

Funding

The author Shuang Zhao was funded by the China Scholarship Council, grant number 201806520003.

Acknowledgments

The author SZ would like to express her appreciation and thanks to the staff, athletes, and coaches for their participation, enthusiasm, and cooperation in this study.

Conflict of interest

The authors declare that the research was conducted in the absence of any commercial or financial relationships that could be construed as a potential conflict of interest.

Publisher's note

All claims expressed in this article are solely those of the authors and do not necessarily represent those of their affiliated organizations, or those of the publisher, the editors and the reviewers. Any product that may be evaluated in this article, or claim that may be made by its manufacturer, is not guaranteed or endorsed by the publisher.

- Løkkeborg J, Ettema G. The role of incline, speed and work rate on the choice of technique in classical roller skiing. *PLoS one*. (2020) 15(7):e0236102. doi: 10.1371/journal.pone.0236102

- Sandbakk Ø, Ettema G, Holmberg H-C. The influence of incline and speed on work rate, gross efficiency and kinematics of roller ski skating. *Eur J Appl Physiol*. (2012) 112(8):2829–38. doi: 10.1007/s00421-011-2261-0

- Sandbakk Ø, Hegge AM, Ettema G. The role of incline, performance level, and gender on the gross mechanical efficiency of roller ski skating. *Front Physiol*. (2013) 4:293. doi: 10.3389/fphys.2013.00293

- Stöggl T, Welde B, Supej M, Zoppirolli C, Rolland CG, Holmberg H-C, et al. Impact of incline, sex and level of performance on kinematics during a distance race in classical cross-country skiing. *J Sports Sci Med*. (2018) 17(1):124.

- Lindinger SJ, Holmberg HC. How do elite cross-country skiers adapt to different double poling frequencies at low to high speeds? *Eur J Appl Physiol*. (2011) 111(6):1103–19. doi: 10.1007/s00421-010-1736-8

- Lindinger SJ, Stöggl T, Müller E, Holmberg HC. Control of speed during the double poling technique performed by elite cross-country skiers. *Med Sci Sports Exerc*. (2009) 41(41):210–20. doi: 10.1249/MSS.0b013e318184f436

13. Millet GY, Hoffman MD, Candau RB, Clifford PS. Poling forces during roller skiing: effects of technique and speed. *Med Sci Sports Exerc.* (1998) 30(11):1645–53. doi: 10.1097/00005768-199811000-00014
14. Nilsson J, Tinmark F, Halvorsen K, Kinematic AA. Kinetic and electromyographic adaptation to speed and resistance in double poling cross country skiing. *Eur J Appl Physiol.* (2013) 113(6):1385–94. doi: 10.1007/s00421-012-2568-5
15. Ohtonen O, Linnamo V, Lindinger SJ. Speed control of the V2 skating technique in elite cross-country skiers. *Int J Sports Sci Coach.* (2016) 11(2):219–30. doi: 10.1177/1747954116637156
16. Stoggl T, Holmberg HC. Three-Dimensional force and kinematic interactions in V1 skating at high speeds. *Med Sci Sports Exerc.* (2015) 47(6):1232–42. doi: 10.1249/MSS.0000000000000510
17. Bassett DR, Howley ET. Limiting factors for Maximum oxygen uptake and determinants of endurance performance. *Med Sci Sports Exerc.* (2000) 32(1):70–84. doi: 10.1097/00005768-200001000-00012
18. Hebert-Losier K, Zinner C, Platt S, Stoggl T, Holmberg HC. Factors that influence the performance of elite sprint cross-country skiers. *Sports Medicine.* (2017) 47(2):319–42. doi: 10.1007/s40279-016-0573-2
19. Millet GY, Hoffman MD, Candau RB, Clifford PS. Poling forces during roller skiing: effects of grade. *Med Sci Sports Exerc.* (1998) 30(11):1637–44. doi: 10.1097/00005768-199811000-00013
20. Stoggl TL, Holmberg HC. Double-Poling biomechanics of elite cross-country skiers: flat versus uphill terrain. *Med Sci Sports Exerc.* (2016) 48(8):1580–9. doi: 10.1249/MSS.0000000000000943
21. Pellegrini B, Bortolan L, Schena F. Poling force analysis in diagonal stride at different grades in cross country skiers. *Scand J Med Sci Sports.* (2011) 21(4):589–97. doi: 10.1111/j.1600-0838.2009.01071.x
22. Andersson E, Stoggl T, Pellegrini B, Sandbakk O, Ettema G, Holmberg HC. Biomechanical analysis of the herringbone technique as employed by elite cross-country skiers. *Scand J Med Sci Sports.* (2014) 24(3):542–52. doi: 10.1111/sms.12026
23. Sandbakk O, Holmberg HC. A reappraisal of success factors for Olympic cross-country skiing. *Int J Sports Physiol Perform.* (2014) 9(1):117–21. doi: 10.1123/ijssp.2013-0373
24. Stöggel T, Stöggel J, Müller E. Competition Analysis of the Last Decade (1996–2008) in Cross-Country Skiing. In: Erich Müller SL, Thomas Stöggel, editor. *Science and Skiing IV*; UK: Meyer & Meyer Sport (2008). p. 657–77.
25. Gaskill SE, Serfass RC, Rundell KW. Upper body power comparison between groups of cross-country skiers and runners. *Int J Sports Med.* (1999) 20(5):290–4. doi: 10.1055/s-2007-971133
26. Hoff J, Helgerud J, Wisloff U. Maximal strength training improves work economy in trained female cross-country skiers. *Med Sci Sports Exerc.* (1999) 31(6):870–7. doi: 10.1097/00005768-199906000-00016
27. Mittelstadt SW, Hoffman MD, Watts PB, O'Hagan KP, Sulentic JE, Drobish KM, et al. Lactate response to uphill roller skiing: diagonal stride versus double pole techniques. *Med Sci Sports Exerc.* (1995) 27(11):1563–8. doi: 10.1249/00005768-199205001-00631
28. Holmberg LJ, Lund Ohlsson M, Supej M, Holmberg H-C. Skiing efficiency versus performance in double-poling ergometry. *Comput Methods Biomech Biomed Engin.* (2013) 16(9):987–92. doi: 10.1080/10255842.2011.648376
29. Holmberg H-C, Lindinger S, Stoggl T, Bjorklund G, Muller E. Contribution of the legs to double-poling performance in elite cross-country skiers. *Med Sci Sports Exerc.* (2006) 38(10):1853. doi: 10.1249/01.mss.0000230121.83641.d1
30. Ohtonen O, LV, Göpfert C, Lindinger S. Effect of 20km Simulated Race Load on Propulsive Forces During Ski Skating. In: Karczewska-Lindinger M, HA, Linnamo V., Lindinger S., editor. *Science and skiing VIII*; Finland: University of Jyväskylä (2019). p. 130–7.
31. Smith GA, Mcnitt-Gray J, Nelson RCF. Kinematic analysis of alternate stride skating in cross country skiing. *Int J Sport Biomech.* (2010) 4(1):49–58. doi: 10.1123/ijsb.4.1.49
32. Göpfert C, Pohjola MV, Linnamo V, Ohtonen O, Rapp W, Lindinger SJ. Forward acceleration of the centre of mass during ski skating calculated from force and motion capture data. *Sports Engineering.* (2017) 20(2):141–53. doi: 10.1007/s12283-016-0223-9
33. Smith G, Kvamme B, Jakobsen V. Ski Skating Technique Choice: Mechanical and Physiological Factors Affecting Performance. In: Schwameder H SG, Fastenbauer V, Lindinger S, Müller E, editor. *24 International Symposium on Biomechanics in Sports*; Austria: University of Salzburg (2006). p. 397–400.
34. Ohtonen O, Lindinger S, Lemmettylä T, Seppälä S, Linnamo V. Validation of portable 2d force binding systems for cross-country skiing. *Sports Engineering.* (2013) 16(4):281–96. doi: 10.1007/s12283-013-0136-9
35. Zhao S, Ohtonen O, Ruotsalainen K, Kettunen L, Lindinger S, Göpfert C, et al. Propulsion calculated by force and displacement of center of mass in treadmill cross-country skiing. *Sensors.* (2022) 22(7):2777. doi: 10.3390/s22072777
36. Ohtonen O, Ruotsalainen K, Mikkonen P, Heikkinen T, Hakkarainen A, Leppävuori A, et al. Online Feedback System for Athletes and Coaches. In: Hakkarainen A, Lindinger S, Linnamo V, editors. *3rd International Congress on Science and Nordic Skiing*; Finland: University of Jyväskylä (2015). p. 35
37. Yu B, Gabriel D, Noble L, An K-N. Estimate of the Optimum cutoff frequency for the butterworth low-pass digital filter. *J Appl Biomech.* (1999) 15(3):318–29. doi: 10.1123/jab.15.3.318
38. Danielsen J, Sandbakk Ø, McGhie D, Ettema G. Mechanical energetics and dynamics of uphill double-poling on roller-skis at different incline-speed combinations. *PloS one.* (2019) 14(2):e0212500. doi: 10.1371/journal.pone.0212500
39. Gottschall JS, Kram R. Ground reaction forces during downhill and uphill running. *J Biomech.* (2005) 38(3):445–52. doi: 10.1016/j.jbiomech.2004.04.023
40. Padulo J, Powell D, Milia R, Ardigo LP. A paradigm of uphill running. *PloS one.* (2013) 8(7):e69006. doi: 10.1371/journal.pone.0069006
41. Stoggl T, Kappel W, Muller E, Lindinger S. Double-Push skating versus V2 and V1 skating on uphill terrain in cross-country skiing. *Med Sci Sports Exerc.* (2010) 42(1):187–96. doi: 10.1249/MSS.0b013e3181ac9748
42. Ainegren M, Linnamo V, Lindinger S. Effects of aerodynamic drag and drafting on propulsive force and oxygen consumption in double poling cross-country skiing. *Med Sci Sports Exerc.* (2022) 54(7):1058. doi: 10.1249/MSS.0000000000002885
43. Robertson GE. Energy, work, and power. In: GE Robertson, GE Caldwell, J Hamill, G Kamen, S Whittlesey, editors. *Research methods in biomechanics. 2 ed.* USA: Human kinetics (2013). p. 132.
44. Holmberg HC, Lindinger S, Stöggel T, Eitzlmaier E, Müller E. Biomechanical analysis of double poling in elite cross-country skiers. *Med Sci Sports Exerc.* (2005) 37(5):807. doi: 10.1249/01.MSS.0000162615.47763.C8
45. Van Hooren B, Fuller JT, Buckley JD, Miller JR, Sewell K, Rao G, et al. Is motorized treadmill running biomechanically comparable to overground running? A systematic review and meta-analysis of cross-over studies. *Sports Med.* (2020) 50(4):785–813. doi: 10.1007/s40279-019-01237-z
46. Zhao S, Linnamo V, Ruotsalainen K, Lindinger S, Kananen T, Kojonen P, et al. Validation of 2d force measurement roller ski and practical application. *Sensors.* (2022) 22(24):9856. doi: 10.3390/s22249856



III

THE ROLES AND CONTRIBUTIONS OF SKIS AND POLES DURING TREADMILL V2 SKIING TECHNIQUE AT DIFFERENT SPEEDS

by

Zhao, S., Ohtonen, O., Linnamo, V., Ruotsalainen, K., Göpfert, C.,
Kettunen, L., Lindinger, S.

Submitted (Under review).

The roles and contributions of skis and poles during treadmill V2 skiing technique at different speeds

Shuang Zhao ^{1*}, Olli Ohtonen ^{1&}, Vesa Linnamo ^{1&}, Keijo Ruotsalainen ^{1&}, Caroline Göpfert ^{2&},
Lauri Kettunen ^{3&}, and Stefan Lindinger ^{4&}

¹ Faculty of Sport and Health Sciences, University of Jyväskylä, Jyväskylä, Finland

² Department of Sport Science and Kinesiology, University of Salzburg, Salzburg, Austria

³ Faculty of Information Technology, University of Jyväskylä, Jyväskylä, Finland

⁴ Center of Health and Performance (CHP), Department of Food and Nutrition and Sport Science, University of Gothenburg, Gothenburg, Sweden

* Correspondence:

Shuang Zhao, zhaoshuangzs@hotmail.com

& These authors contributed equally to this work.

Abstract

The V2 skating technique in cross-country skiing contains both forward, sideward, and vertical movement. Knowing how the external power is generated and by what source (poles versus skis) at different speeds may help training and testing processes and understand performance related questions. The aims of this study were to characterize the role of skis and poles during treadmill roller skiing with V2 skating technique and compare the relative contributions and effectiveness of ski and pole power to the total external power at a variety of speeds. Ten cross-country skiers participated in this study. Custom-made force measurement bindings, pole force sensors, and an eight-camera Vicon system were used to collect force data and the trajectories of reflective markers at five different treadmill speeds (13, 15, 17, 19, and 21 km/h). The external power was the dot product of force and COM velocity vectors. The direction change of medio-lateral, and vertical COM velocity was observed during the overlap phase. The kicking and gliding skis all produced both positive (propulsive) and negative (braking) resultant external power. At the beginning of the kicking phase, the negative external power was produced by the kicking ski. Poles always produced positive external power while poling. The magnitude of positive and negative resultant external power all increased with the increasing speed ($p < 0.001$). The relative contribution from the poles toward the total external power ranged from 55%-57% which was 22%-32% greater than from skis and was independent from the skiing speed ($p = 0.102$). The kicking leg generated negative external power to redirect the COM velocity. The main role for the gliding leg is to gain more vertical power and prepare the next push off. The main role for poles is to propel the body to catch up with the increasing speed. Changing the relative contribution from skis and poles may not be a strategy to cope with the increasing speed.

Key words: external power, V2 skating skiing technique, contribution, effectiveness.

1 **1 Introduction**

2 The V2 skating (V2, also gear 3) technique has become the most commonly used technique during
3 competitions throughout the last decade [1]. Several studies [2-6] have investigated the biomechanical
4 characteristics of the V2 technique, as they have been indicated as key factors that promote good
5 performance [7]. Studies have shown that the cycle length (CL) and cycle rate (CR) were all depended
6 on the skiing speed [3, 5, 6, 8]. Greater maximum pole and ski forces were found at higher speeds
7 when compared to the lower speeds [3, 5]. Because of knowing the role of pole and ski forces may
8 offer possibilities for technique diagnosis, the relative contributions of ski and pole forces to the V2
9 skate skiing movement were also investigated.

10 The research on relative contribution of ski and pole forces to total propulsion mainly focused on
11 forward direction. The contributions of ski and pole forces are normally quantified by using the
12 propulsive force [9, 10], which are often defined as the horizontal component of the resultant force
13 from skis [10-12] and poles [11, 13]. For the V2 skating technique, about two thirds of the forward
14 propulsive force is attributed to the forces from poles, and one third is attributed to the forces from
15 skis [9]. Forces in the forward direction are important as maintaining high speed in desired direction
16 in races is a necessity to become competitive. But in skate skiing technique, the combination of leg
17 push-off and the poling action propel the skier forward in a “zig-zag” movement [14]. The leg push-
18 off is performed perpendicular to gliding ski [6] which may lead to sideward velocity of COM that
19 can be added to the gliding velocity in a more or less forward direction [15]. Therefore, the sideward
20 movement in V2 skating technique should also be taken into account.

21 External power analysis has been used to evaluate the role of the limbs during the locomotion which
22 contains sideward movement [16]. The external power is the dot product of the force vector which
23 acts on the limb and the COM velocity vector. Thus, the COM velocity and the force are in a relation.
24 In forward and sideward walking, negative work was required by the leading leg at the beginning of
25 the heel contact to redirect the COM velocity [16, 17]. Similar to walking, alternate supports on the
26 left and right legs and a double support (overlap) phase could be found in V2 technique. But from the
27 aspect of external power, how the kicking ski and gliding ski would act to redirect the COM velocity
28 in V2 technique remains unclear.

29 In addition, mechanical power is often used in sport science for researching and training purpose to
30 estimate the muscular work [18]. Knowing how the external power is generated and by what source
31 (poles versus skis) at different speed may help training and testing processes and understand
32 performance related questions. However, it might be questioned from a methodological aspect if the
33 relative contribution from skis is the same when analyzed in the energetic domain (power) as when
34 analyzed in the kinetic domain (force).

35 Consequently, the current study was conducted to (1) characterize the role of skis and poles during
36 treadmill roller skiing with V2 skating technique, and (2) compare the relative contributions and
37 effectiveness of ski and pole power to the total external power at a variety of speeds. We hypothesized
38 that in V2 technique the kicking and gliding skis play similar roles as trailing and leading legs in
39 walking to redirect the COM velocity. As the COM is propelled by both pole and ski forces in skating
40 technique, we hypothesize that over a cycle, the sum of pole and ski propulsive power would be equal
41 to the sum of the power against gravity and friction. We also hypothesized that in V2 technique the
42 contribution of ski propulsive power to the total external power would be greater than the contribution
43 of ski propulsive force to the forward propulsion.

44 **2 Materials and Methods**

45 **2.1 Participants**

46 Ten male XC skiers (age: 29.4 ± 7.9 years; height: 181.4 ± 5.7 cm; weight: 77.9 ± 8.9 kg [means \pm
47 SD]) who are familiar with treadmill roller skiing volunteered to participate in this study. Participants
48 cover athletes of different levels, but all of them are with high roller skiing skill and fitness. The
49 experimental protocol and all methods used in this study were approved by the Ethics Committee of
50 the University of Jyväskylä. All participants provided written informed consent before the
51 measurement and were free to withdraw from the experiments at any time.

52 **2.2 Overall design**

53 Participants completed a 10-15 min warm-up roller skiing on the treadmill after the passive reflective
54 markers were attached to the participants and equipment. Then they engaged in roller skiing with
55 increasing speeds on a treadmill using the V2 skating technique. The forces generated from the poles
56 and skis, and trajectories of the reflective markers were collected at five submaximal speeds (13, 15,

57 17, 19, and 21 km/h) on a 2° incline. The 2° incline was chosen to simulate the relative flat terrain and
58 to compensate for the lack of air drag while roller skiing on an indoor treadmill [6]. Between each
59 speed, a short break of about 1 min was provided. During this rest period, markers on the subjects'
60 bodies and analog signals from the force sensors were checked.

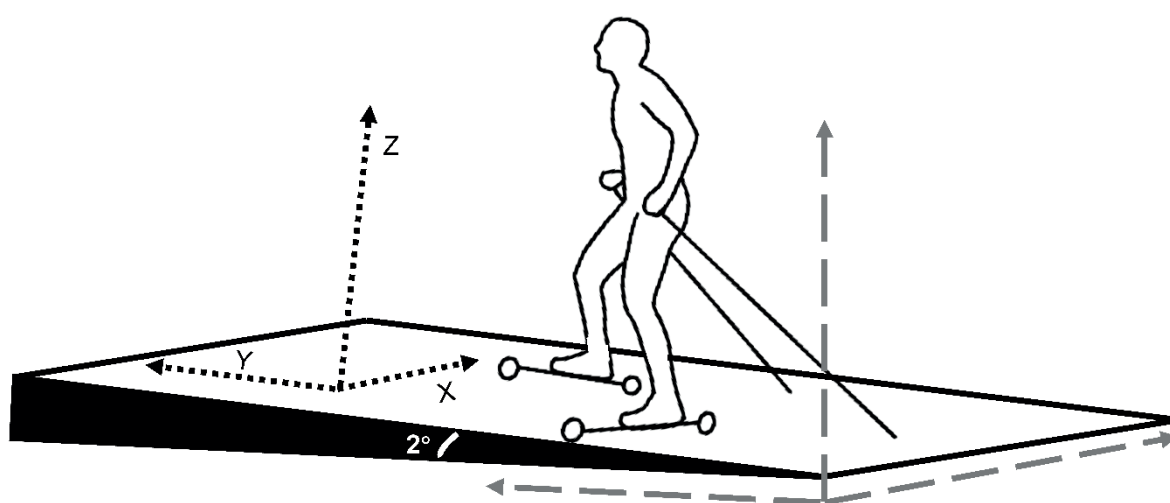
61 **2.3 Measurement devices**

62 All participants used the same pair of roller skis (Marwe, SKATING 620 XC, wheel no. 0) with a
63 resistance friction coefficient of $\mu=0.025$ measured before the measurement [19]. The measurements
64 were performed on a motorized treadmill with a belt surface 2.7 m wide and 3.5 m long (Rodby
65 Innovation AB, Vänge, Sweden). During all measurements, the participants were secured with a
66 safety harness connected with the ceiling above the treadmill.

67 The force measurement equipment have been used in our another study [19]. Custom-made pole force
68 sensors for XC skiing (VTT MIKES, Technical Research Centre of Finland Ltd., Kajaani, Finland)
69 were mounted below the pole grip [19]. The total mass of one equipped pole was 202 g greater than
70 the mass of a normal pole. The pole length in this study was 1.63 ± 0.03 m, which was comfortable
71 length for the subjects involved with V2 skating technique. Pole spikes (Biomekanikk AS, Oslo,
72 Norge) specifically made for treadmill skiing were used to get the grip on the treadmill. The forces
73 from the roller skis were measured using two custom-made 2D force measurement bindings mounted
74 on the roller skis for XC skiing (Neuromuscular Research Centre, University of Jyväskylä, Finland)
75 [20]. The bindings measured vertical and medio-lateral forces that were perpendicular to the roller ski
76 body. The total mass of one equipped roller ski was 664 g greater than the total mass of a roller ski
77 with a normally used binding.

78 The 3D trajectories of all passive reflective markers were captured using an eight-camera motion
79 capture system (Vicon, Oxford, UK) at a sampling rate of 150 Hz. The space of measurement was
80 calibrated according to Vicon's specifications. The global coordinate system was defined using the
81 right-hand rule when the incline of the treadmill was 0° (Fig.1). 55 markers were used and the
82 placement of markers on the participants were conducted according to the XC model [21] used in a
83 previous study. The XC model contained 19 segments [19]. Each ski (attached with 3 markers) and

84 each pole (attached with 3 markers) were treated as one segment, respectively. COM was determined
 85 from the marker position and the segments masses (masses of skis and poles were included). The
 86 segmental anthropometric data were taken from Dempster's study as described in Selbie et al. [22].
 87 Two markers were attached to the front and rear right corners of the treadmill. The vector defined by
 88 these two markers on the treadmill was parallel to the longitudinal axis of the treadmill and was used
 89 to provide the incline of the treadmill. XYZ is the coordinate system when the incline of the treadmill
 90 was 2°. X is medio-lateral direction. Y is fore-aft direction. Z is vertical direction. The positive X
 91 direction is right, the positive Y direction is forward, and the positive Z direction is up.



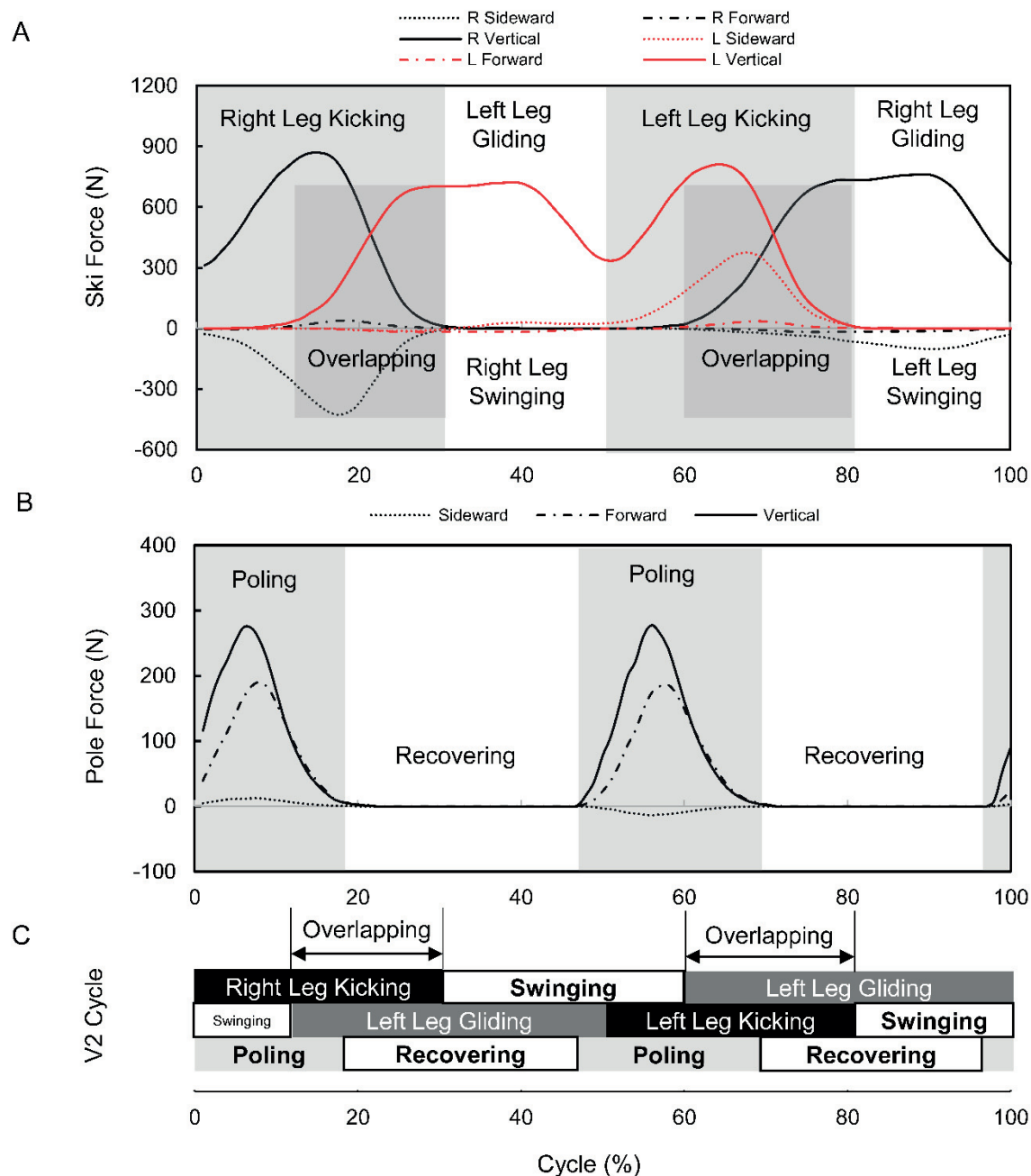
92

93 **Fig 1. Illustrations of global coordinate system and the coordinate system moved with the treadmill.** The
 94 long dash arrows represent the axis of global coordinate system which was defined by using the right-hand rule
 95 when the incline of the treadmill was 0°. X, Y, and Z (round dot arrow) represent the axis of the coordinate
 96 system when the incline of the treadmill was 2°. Note that the X, Y, and Z components are orthogonal to each
 97 other. X, medio-lateral direction; Y, fore-aft direction; Z, vertical direction.
 98

99 2.4 Data collection and data processing

100 The Coachtech online measurement and feedback system [23] (Neuromuscular Research Centre,
 101 University of Jyväskylä, Finland) was used to collect force data. Both pole and roller ski forces were
 102 collected at a sampling rate of 400 Hz. A trigger signal sent by the Coachtech system to the Vicon
 103 system was used to synchronize the forces and marker trajectory data. NEXUS 2.8.1 (Vicon, Oxford,
 104 UK) software was used to record the 3D trajectories of the reflective markers. Marker labeling and the
 105 COM position calculation was performed using NEXUS 2.8.1 software. The raw 3D trajectories of all

106 reflective markers and the COM were low-pass filtered (fourth-order, zero-lag, Butterworth filter)
 107 with a cut-off frequency of 11.3 Hz [24]. Force data were low-pass filtered (eighth-order, zero-lag,
 108 Butterworth filter) with a cutoff frequency of 15 Hz [25]. Filtering and parameter calculations were
 109 performed in MATLAB R2018a (MathWorks, Natick, USA). For each parameter, the means of 5
 110 successive cycles at each speed from each subject were analyzed. The kicking, overlap, and pure
 111 gliding actions of both the left and right skis, as well as two double poling actions from both poles,
 112 were included in one cycle (Fig. 2).



114 **Fig 2. Time-force curves for skiers (n = 10) skating at 19km/h and definition of action stages.** (A) Time-
 115 force curve of ski forces. The gray areas represent the kicking phase of right and left skis, The dark gray areas
 116 represent the ski overlapping phase. (B) Time-force curve of the pole forces. The gray areas represent the poling
 117 phase, and the rest are recovering phase. (C) Action stages of V2 skating technique. Periods of kicking (black
 118 solid bar), periods of gliding (dark gray solid bar), periods of poling (gray solid bar), and periods of ski
 119 swinging and pole recovering (white solid bar). Note: The horizontal time scale for each figure is normalized to
 120 the V2 skating cycle.
 121

122 2.5 Calculation of power

123 The mean external power (P_{mean}) was calculated in accordance with previous studies [6, 25, 26].

124 P_{mean} is the sum of power against gravity and friction, which could be calculated as:

$$125 \quad P_{mean} = mgv_{Belt} \sin 2^\circ + (mg \cos 2^\circ - F_p^\perp) \mu v_{Ski}$$

126 where m is the mass of the skier and the skiing equipment, g is the gravitational constant, v_{Belt} is the

127 treadmill belt speed, and μ is the friction coefficient. The v_{Ski} is the speed of the roller ski. Skis

128 were angled with respect to the forward direction while using the skating technique, the roller ski

129 moves faster than the treadmill belt. The value of the v_{Ski} is calculated by

130 $v_{Belt}/\cos(\text{ski orientation angle})$. The F_p^\perp is the mean pole force component in vertical direction

131 (Fig.1) which is perpendicular to the treadmill surface. The 2° is the incline of the treadmill in this

132 study.

133 To understand the role of each limb and how each limb contributes to the overall power generation

134 and absorption, the individual limbs method [17] was used to calculate the external mechanical power

135 of the COM. Poling (P_p) and ski (P_s) powers were calculated as the dot product of force vectors and

136 the COM's velocity vector ($\overrightarrow{v_{com}}$):

$$137 \quad P_p = \overrightarrow{F_p} \cdot \overrightarrow{v_{com}}$$

$$138 \quad P_s = \overrightarrow{F_s} \cdot \overrightarrow{v_{com}}$$

139 $\overrightarrow{F_p}$, $\overrightarrow{F_s}$ and $\overrightarrow{v_{com}}$ are the force and velocity vectors in the coordinate system moving with the

140 treadmill. The $\overrightarrow{v_{com}}$ is the first derivative of the COM position relative to the treadmill speed. The P_s

141 for left and right ski were calculated in the same way.

142 To evaluate the medio-lateral, fore-aft, and vertical contribution of skis and poles, the P_p and P_s

143 were decomposed to their X, Y and Z components.

$$144 \quad P_{p,x} = F_{p,x} \cdot v_{com,x}$$

$$145 \quad P_{p,y} = F_{p,y} \cdot v_{com,y}$$

$$146 \quad P_{p,z} = F_{p,z} \cdot v_{com,z}$$

$$147 \quad P_{s,x} = F_{s,x} \cdot v_{com,x}$$

$$148 \quad P_{s,y} = F_{s,y} \cdot v_{com,y}$$

$$149 \quad P_{s,z} = F_{s,z} \cdot v_{com,z}$$

150 The subscripts x, y, and z represent the medio-lateral, fore-aft, and vertical directions. The power from
 151 skis were calculated in the same way for left and right ski. The medio-lateral and fore-aft external
 152 power were defined as the time rate of change in medio-lateral and fore-aft kinetic energy. The
 153 vertical external power was defined as the time rate of change in gravitational potential energy and
 154 vertical kinetic energy [16].

155 Mean positive and negative resultant external power were calculated by the sum of positive or
 156 negative values and divided by the cycle time (CT), respectively.

$$157 \quad P_p^+ = \int_+ P_p / CT$$

$$158 \quad P_p^- = \int_- P_p / CT$$

$$159 \quad P_s^+ = \int_+ P_s / CT$$

$$160 \quad P_s^- = \int_- P_s / CT$$

161 The mean medio-lateral, fore-aft, and vertical power for the kicking and gliding leg were calculated in
 162 the same way. The positive power was defined as the propulsive power and the negative power was
 163 defined as the braking power [16].

164 In V2 skating technique, the COM is propelled by both pole and ski forces. Therefore, averaged over
 165 a cycle, the sum of ski and pole propulsive resultant power (P_{tot}) should be equal to the sum of power
 166 against gravity and friction (P_{mean}). The relative power contribution from the poles towards the total
 167 external power was determined by expressing the propulsive pole resultant power P_p^+ as a percentage
 168 of P_{tot} . The effectiveness index of ski power was calculated by expressing the propulsive ski power

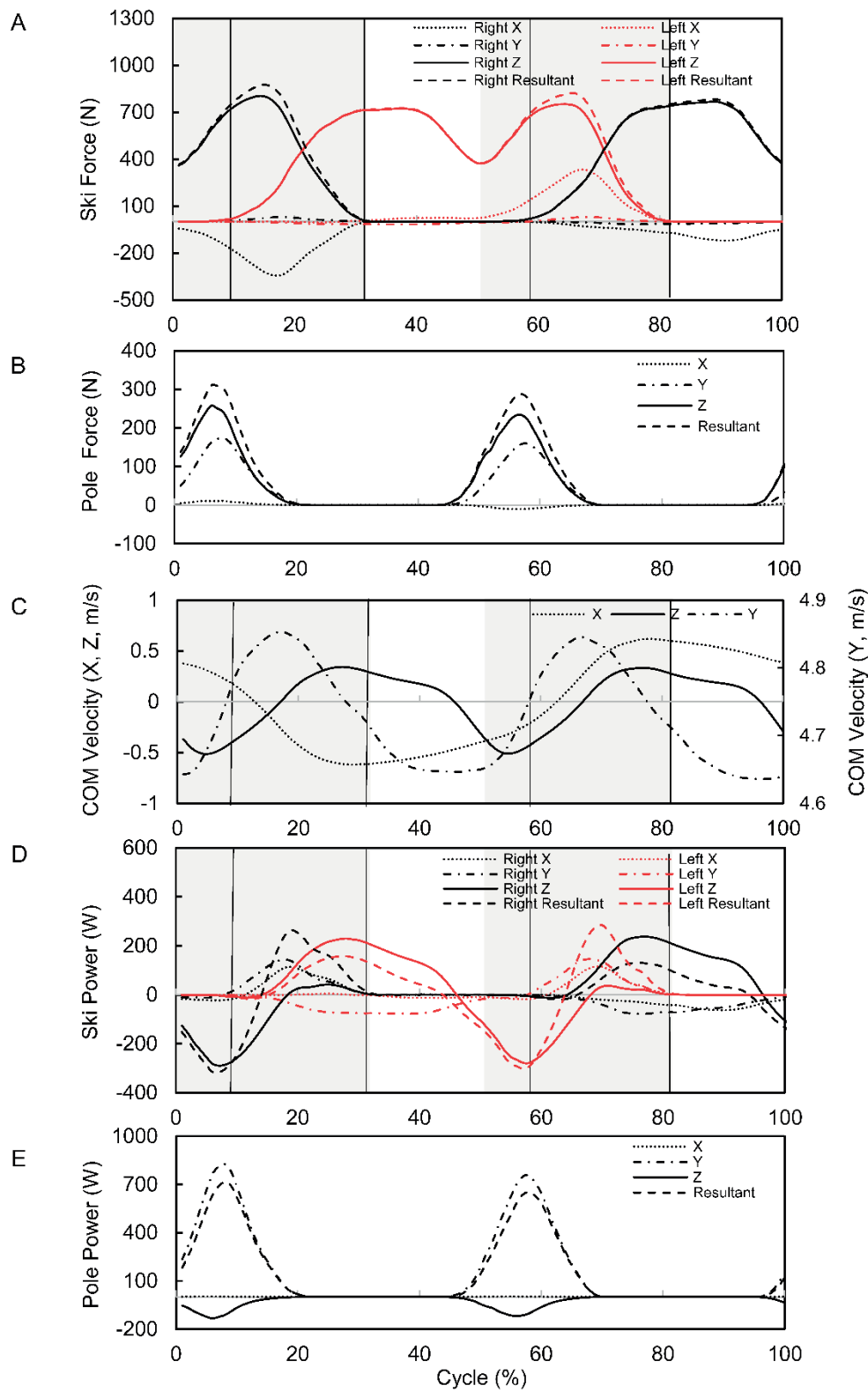
169 P_s^+ as a percentage of $(P_s^+ + |P_s^-|)$. The effectiveness index of pole power was calculated by
170 expressing the propulsive pole power P_p^+ as a percentage of $(P_p^+ + |P_p^-|)$.

171 **2.6 Statistical analyses**

172 Descriptive statistics are presented as mean \pm SD. The normal distribution of the data was confirmed
173 by the Shapiro-Wilk normality test. The difference between P_{mean} and P_{tot} at varied speeds was
174 tested by two-way analysis of variance (ANOVA) with repeated measures (2 ways to calculate the
175 power *5 speeds). In the case of significant differences were found between P_{mean} and P_{tot} , linear
176 regression was used to determine the relation between the calculated external powers (P_{mean} and
177 P_{tot}) and the treadmill speeds. For other parameters, one-way ANOVA with repeated measures and
178 Bonferroni post hoc analysis were conducted. The values obtained were evaluated further by
179 calculating the effect size ($P\eta^2$) and observed power. For all analyses, the level of statistical
180 significance was set at 0.05. All statistical analyses were carried out using SPSS 22.0 software (SPSS,
181 Inc., Chicago, IL).

182 **3 Results**

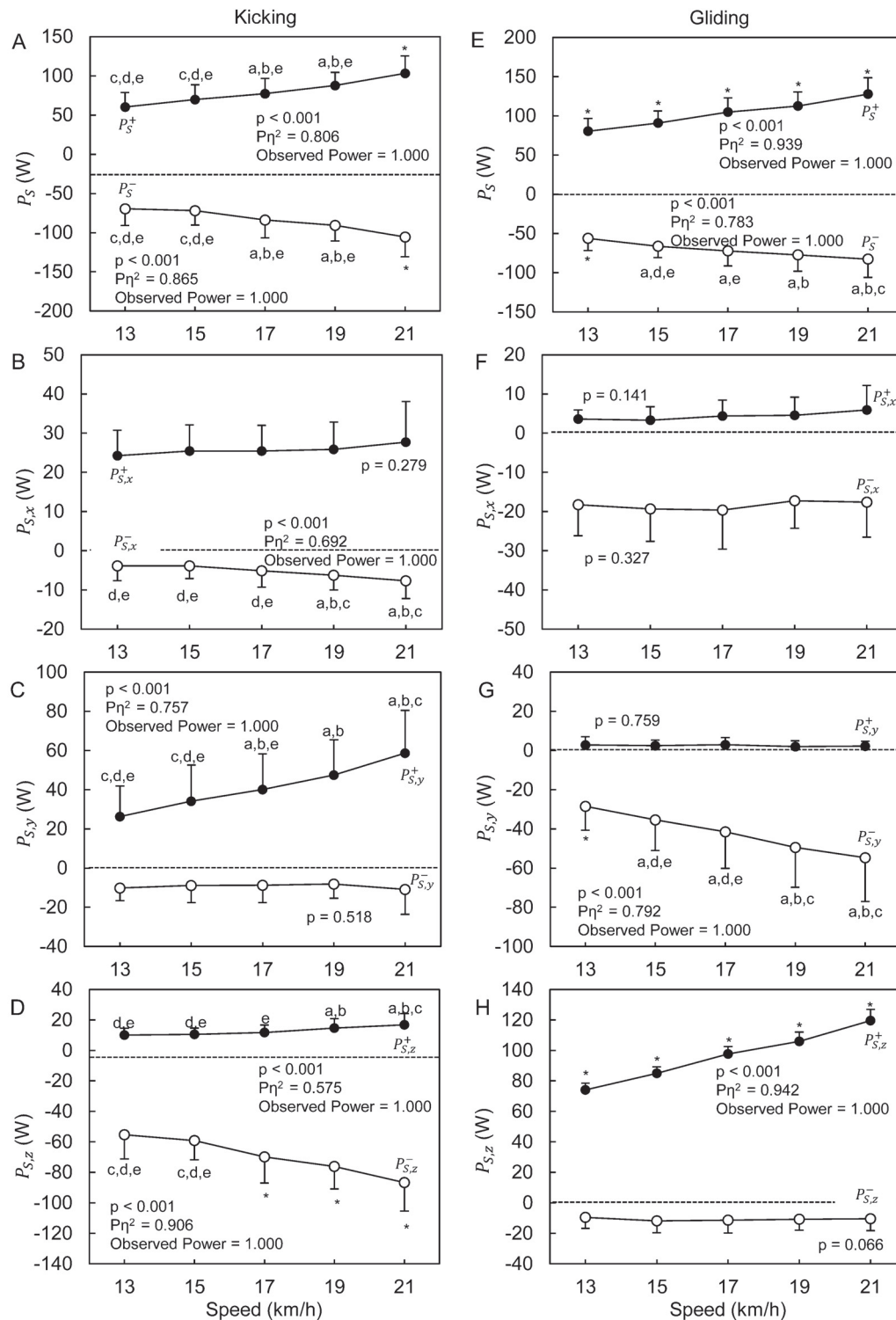
183 The patterns of ski and pole forces, COM velocity, and external powers are shown in Fig. 3. During
184 the kicking phase, the ground reaction forces produced by the push off ski accelerate the medio-lateral
185 velocity in the opposite direction (i.e., when the right ski acts as kicking ski, the COM velocity
186 accelerates to the left side). The direction change of medio-lateral, and vertical COM velocity was
187 observed during the overlap phase (Fig 3). During the kicking phase, the kicking ski performed both
188 negative and positive resultant external power. The power performed by the kicking ski changed to
189 positive mainly during the overlap phase. The gliding ski during the overlap phase mainly produced
190 positive resultant external power. Poles always produced positive resultant external power while
191 poling.



192

193 **Fig 3. The patterns of ski and pole forces, COM velocity, and ski and pole powers at 17km/h.** (A) Forces
 194 from right and left skis. (B) Forces from poles. Pole forces were the sum of left and right. (C) COM velocity. X,
 195 and Z components, left axis, Y component, right axis. (D) Power from right and left skis. (E) Power from poles.
 196 Note: Dotted, dot-dash, solid, and dash curves represent the X, Y, Z, and resultant component, respectively.
 197 Black and red curves represent the right and left ski, respectively. The light gray areas represent the kicking
 198 phase of right and left skis. The areas between the vertical solid lines represent the ski overlapping phase. The
 199 horizontal time scale for each figure is normalized to the V2 skating cycle.

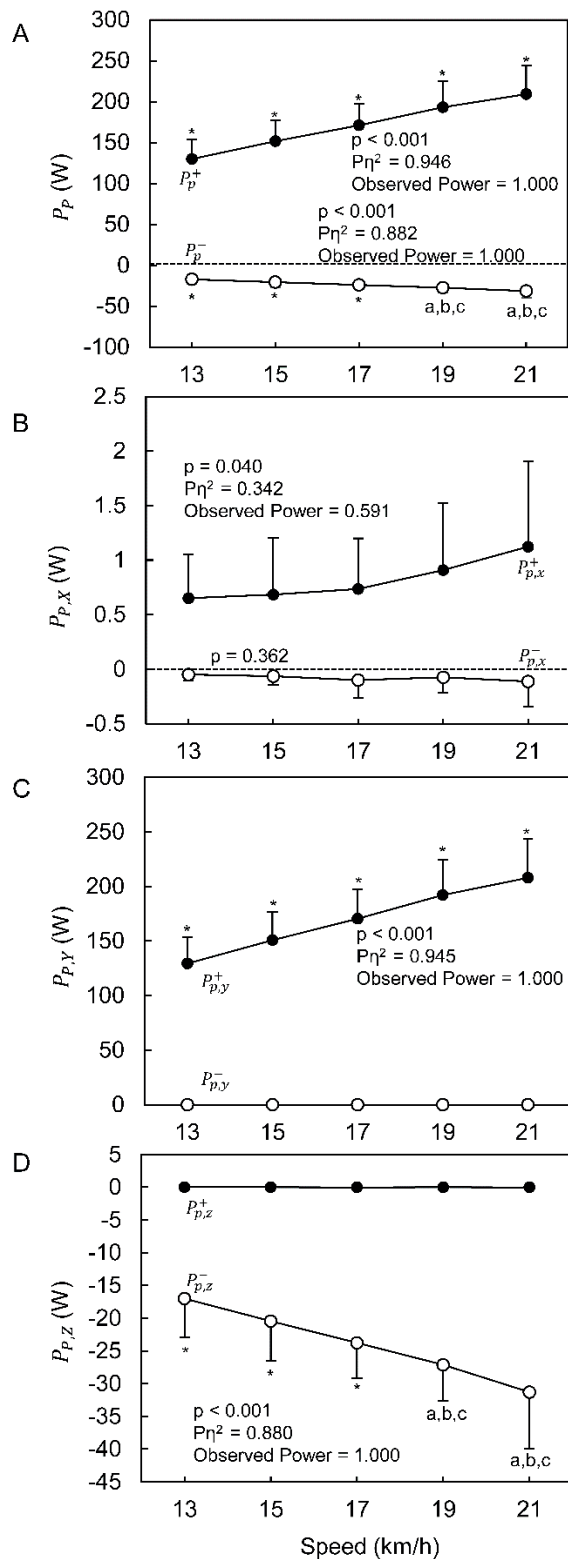
200 When acted as kicking ski, both P_s^+ and P_s^- were depended on the treadmill speed ($p < 0.001$, $p <$
201 0.001 , Fig 4.A) and the magnitude increased with the increasing speed. In the X (medio-lateral)
202 component, the $P_{s,x}^+$ was independent from the treadmill speed ($p = 0.279$, Fig 4.B). However, the
203 magnitude of $P_{s,x}^-$ increased with the increasing speed ($p < 0.001$, Fig 4.B). In the Y (fore-aft)
204 component, the $P_{s,y}^+$ increased with the increasing speed ($p < 0.001$, Fig 4.C). The $P_{s,y}^-$ was
205 independent from the treadmill speed ($p = 0.518$, Fig 4.C). In the Z (vertical) component, both $P_{s,z}^+$
206 and $P_{s,z}^-$ were depended on the treadmill speed ($p < 0.001$, $p < 0.001$, Fig 4.D). When acted as gliding
207 ski, both P_s^+ and P_s^- were depended on the treadmill speed ($p < 0.001$, $p < 0.001$, Fig 4.E). The P_s^+
208 increased by 58.6% from 13km/h to 21km/h ($p \leq 0.010$). In the X component, the $P_{s,x}^+$ and $P_{s,x}^-$
209 were all independent from the treadmill speed ($p = 0.141$, $p = 0.327$, Fig 4.F). In the Y component, the
210 $P_{s,y}^+$ was small and was not affected by the treadmill speed ($p = 0.759$, Fig 4.G). The magnitude of
211 $P_{s,y}^-$ increased with the increasing speed ($p \leq 0.001$, Fig 4.G). In the Z component, the $P_{s,z}^+$
212 increased by 61.6% from 13km/h to 21km/h ($p \leq 0.001$). No effect of speed was found on the $P_{s,z}^-$
213 ($p = 0.066$, Fig4.H). Detailed results of pairwise comparisons between speeds for each ski external
214 power parameter can be found in the Supplementary Materials.



215

216 **Fig 4. Mean positive and negative external power from skis while kicking and gliding at different speeds.**
 217 **(A)** Mean external power (P_S) while kicking. **(B)** Mean medio-lateral external power ($P_{S,x}$) while kicking.
 218 **(C)** Mean fore-aft external power ($P_{S,y}$) while kicking. **(D)** Mean vertical external power ($P_{S,z}$) while kicking.
 219 **(E)** Mean external power (P_S) while gliding. **(F)** Mean medio-lateral external power ($P_{S,x}$) while gliding. **(G)**
 220 **(H)** Mean fore-aft external power ($P_{S,y}$) while gliding. **(H)** Mean vertical external power ($P_{S,z}$) while gliding. **Note:**
 221 The data are presented as mean \pm SD. The p value, $P\eta^2$, and observed power presented in the figures are from
 222 the One-way ANOVA with repeated measurement test. * represents significantly different from all other speeds.
 223 a, b, c, d, and e represent significantly different from 13, 15, 17, 19, 21 km/h, respectively.

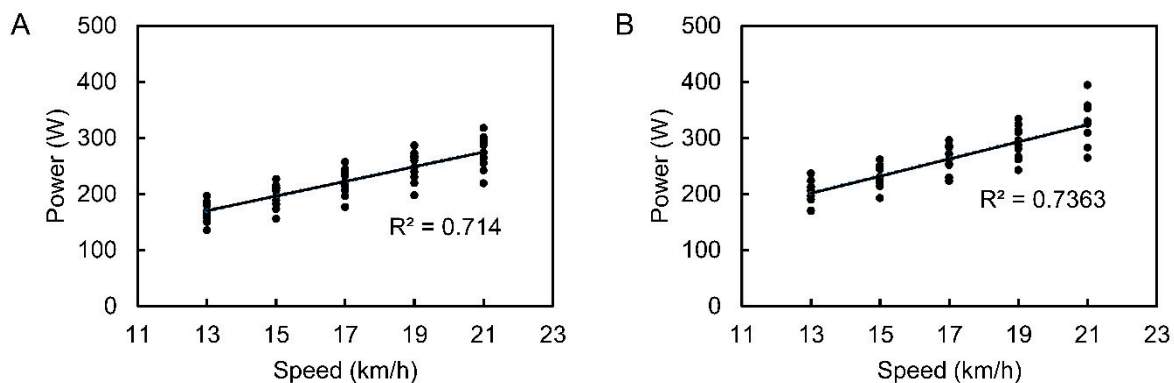
224 Both P_p^+ and P_p^- were affected by the treadmill speed ($p < 0.001$, $p < 0.001$, Fig 5.A). The P_p^+
225 increased by 60.8% from 13 to 21km/h ($p < 0.001$). The magnitude of P_p^- increased by 83.6% from
226 13 to 19km/h ($p \leq 0.002$), but no difference was found between 19 and 21km/h ($p = 0.056$). In the
227 X component, the $P_{p,x}^+$ was depended on the treadmill speed ($p = 0.040$, Fig 5.B). The $P_{p,x}^-$ was
228 independent from the treadmill speed ($p = 0.362$, Fig 5.B). In the Y component, no negative external
229 power was found (Fig 5.C), and the $P_{p,y}^+$ increased by 61.2% from 13 to 21km/h ($p < 0.001$, Fig 5.C).
230 In the Z component, no $P_{p,z}^+$ was found at any speed (Fig 5.D). The magnitude of $P_{p,z}^-$ increased by
231 59.4% from 13 to 19km/h ($p \leq 0.001$), but no significant difference was found between 19 and 21
232 km/h ($p = 0.059$). Detailed results of pairwise comparisons between speeds for each pole external
233 power parameter can be found in the Supplementary Materials.



234

235 **Fig 5. Mean positive and negative external power from poles. (A)** Mean external pole power (P_p). **(B)**
 236 Mean medio-lateral external pole power ($P_{p,x}$). **(C)** Mean medio-lateral external pole power ($P_{p,y}$). **(D)** Mean
 237 vertical external pole power ($P_{p,z}$). **Note:** The data are presented as mean \pm SD. The p value, $P\eta^2$, and
 238 observed power presented in the figures are from the One-way ANOVA with repeated measurement. *
 239 represents significantly different from all other speeds. a, b, and c represent significantly different from 13, 15,
 240 17km/h, respectively.

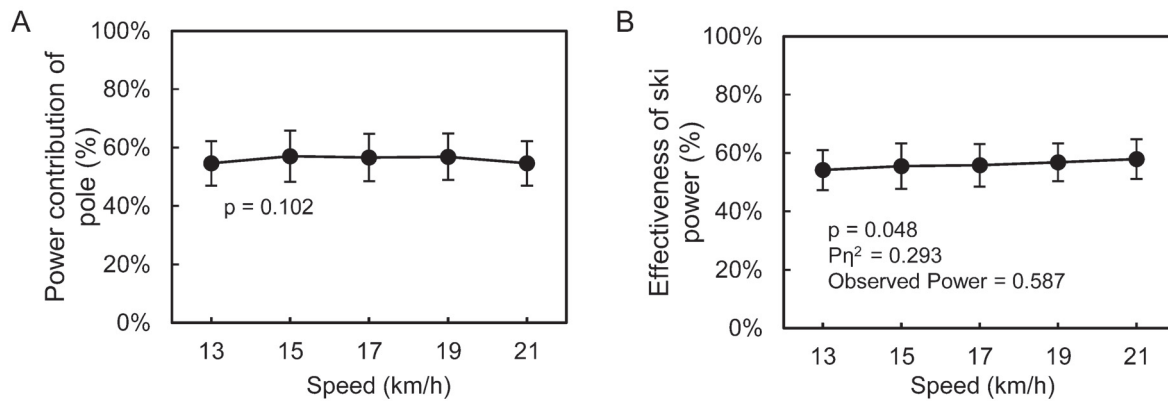
241 The interaction between speed \times power calculation method was significant from the estimated total
 242 external power ($p < 0.001$, $P\eta^2 = 0.421$, observed power = 0.982). P_{mean} and P_{tot} increased by
 243 61.6% and 60.3%, respectively, from 13 to 21km/h ($p < 0.001$, $p < 0.001$, Table 1. At any speed, P_{tot}
 244 was found about 17.3%-19.3% greater than P_{mean} ($p < 0.001$, Table 1). However, both P_{mean} and
 245 P_{tot} show high linearity with skiing speed ($r^2 = 0.714$, $r^2 = 0.736$, Fig. 6).



246

247 **Fig 6. Linearity relation between mechanical power and skiing speed.** (A) Linearity relation between P_{mean}
 248 and skiing speed. (B) Linearity relation between P_{tot} and skiing speed.
 249

250 The relative contribution from the poles toward the total external power ranged from 55%-57% and
 251 was independent from the skiing speed ($p = 0.102$, Fig.7A). As the relative contribution from poles
 252 was expressed by expressing the P_p^+ as the sum of P_p^+ and P_s^+ , the relative contribution from skis
 253 ranged from 43%-45%. The relative pole power contribution was about 0.2-0.3 times greater than the
 254 ski power contribution to the total external power. The skiing speed affected the effectiveness of the
 255 ski power ($p = 0.048$, Fig. 7B), however, no significant difference was found when compared between
 256 any two speeds ($p \geq 0.283$).



257

258 **Fig 7. Relative power contribution from the poles and the effectiveness of ski power.** (A) Relative power
 259 contribution from the poles towards the total external power. (B) The effectiveness of ski power. Note: The data
 260 are presented as mean \pm SD. The p value, $P\eta^2$, and observed power presented in the figures are from the One-
 261 way ANOVA with repeated measurement test.
 262

263 4 Discussion

264 This study aimed at understanding the roles and contributions of skis and poles during treadmill V2
 265 skating technique at different speeds. Our main findings were as follows. 1) The redirection of the
 266 COM velocity during the overlap phase was achieved by producing the braking (negative) resultant
 267 external power with the kicking ski. 2) When the speed of the treadmill increased, the amount of
 268 braking and propulsive resultant external power increased as well. 3) 43-45% of the total external
 269 power was generated by skis and the rest was generated by poles. This ratio did not change with the
 270 speed.

271 The first aim of this study was to characterize the role of skis and poles during treadmill roller skiing
 272 with V2 skating technique. The patterns of ski and pole forces, COM velocity, and external powers
 273 were shown in Fig. 3. It was observed that the X (medio-lateral) and Z (vertical) velocity of the COM
 274 start to accelerate in the opposite direction at the beginning of the kicking phase (Fig.3), and the
 275 velocities' direction changed after the other ski touched the treadmill during the overlap phase. At the
 276 beginning of the kicking phase, one ski is lifted off the treadmill. The angular moment induced by the
 277 horizontal distance between the COM and the ski force application point may produce sideward
 278 velocity [16, 27]. Therefore, the sideward velocity of the COM started to accelerate in the opposite
 279 direction at the beginning of the kicking phase. Both negative and subsequent positive resultant ski

280 external power were observed in the kicking phase for the kicking ski (Fig. 3D). The values of mean
281 positive and negative power while kicking were similar and increased with the treadmill speed (Fig.
282 4A). For resultant external power, the positive power was the propulsive power and the negative
283 power was the braking power [16]. This power producing pattern is similar to what has been found in
284 running [28]. The mechanical energy is temporally stored and recovered before the end of kicking in
285 the overlap phase, and the magnitude of the mechanical power increases with increasing speed. When
286 observing the ski mechanical power from different components separately (Fig. 4), while acting as
287 kicking ski, the negative vertical ski power was produced at the beginning of the kicking phase, and
288 the positive medio-lateral and forward ski power were then generated in the overlap phase (Fig. 3D).
289 This indicated that when the kicking action started, the potential and vertical kinetic energy started to
290 be transformed into kinetic energy in forward and medio-lateral direction. During the kicking phase,
291 the knee flexion of the kicking leg increased first and then decreased [5], which may decrease and
292 then increase the potential energy. This could help with explaining the positive vertical ski power of
293 kicking ski at the end of the kicking phase. In addition, the higher the speed that needed to be
294 maintained, the more potential and vertical kinetic energy are converted into medio-lateral and
295 forward kinetic energy (Fig. 4C and Fig. 4D).

296 During the overlap phase, the positive external ski power was generated by the gliding ski after the ski
297 contact (Fig. 3D). The gliding ski produced more vertical power (Fig. 3D) and the generated vertical
298 power increased with increasing speed (Fig. 4H). The kicking leg leans sideways, which may prevent
299 the COM from moving upwards, but more upward COM velocity should be gained by the extension
300 of the kicking leg [16]. Therefore, the positive vertical power from the gliding ski is to fill up the
301 deficiency of the vertical power by the kicking leg, and this effect becomes more pronounced as the
302 speed to be maintained increased.

303 While gliding, the ski power is decreasing (Fig. 3D). This may be due to the decrease in positive
304 vertical ski power and the negative forward power (Fig. 3D, Fig. 4G, and Fig. 4H). The negative
305 forward power is due to the resistance. The decrease in vertical ski power is mainly due to the
306 decrease in vertical kinetic energy. After the ski touched the ground, the extension of the knee joint of
307 the gliding ski increased [5], which may increase the potential energy. But the vertical speed

308 decreased (Fig. 3C) while gliding. Due to the conservation of the energy, the vertical kinetic energy
309 decreased. Therefore, when the leg acts as the kicking leg, the required negative external power was
310 produced like the leading leg did in walking to redirect the COM velocity [16, 17]. At the beginning
311 of the kicking action, body weight is “dropped” from high body position over the poles and skis to
312 achieve high force, which can be seen in external power perspective as negative external power to
313 redirect the COM velocity, especially in medio-lateral and vertical direction. And this is inconsistent
314 with our hypothesis that in V2 technique the kicking and gliding skis play similar roles as trailing and
315 leading legs in walking. The role played by the kicking ski is more like the role of leading leg in
316 walking. When the leg acts as the gliding leg, the main role is to gain more vertical power and then
317 prepare for the next kick.

318 Poles predominately produced positive resultant external power while poling (Fig.3E, Fig. 5A). This
319 positive pole power is mainly due to the positive pole forward power (Fig.3E and Fig. 5C). While
320 poling, the negative vertical pole external power was found (Fig. 3E and Fig. 5D), and the magnitude
321 increased with the increasing speed (Fig.5D). This indicated that the potential and vertical kinetic
322 energy were transformed mainly to the forward kinetic energy. Moreover, more energy or faster
323 transformation are needed while increasing the speed. Therefore, the main role for pole power is to
324 propel the body to catch up with the treadmill speed in V2 technique.

325 Our results indicated that the sum of propulsive ski and pole power (P_{tot}) was 17.3%-19.3% greater
326 than the sum of the power against the gravity and the friction (P_{mean}). These results do not support
327 our second hypothesis that P_{tot} would be equal to the P_{mean} . The generated ski and pole power is
328 used for power against gravitational losses, against roller friction, and driving changes of kinetic
329 energy [26, 29]. As the skier was roller skiing at a constant treadmill speed, we assumed that the
330 changes of the kinetic energy of the COM over one cycle could be neglected. Therefore, the generated
331 power should be equal to the power against gravitational losses and against roller friction. However,
332 the V2 skating technique also contains sideward movements. If a skier adapted to the treadmill and
333 did not drop out from the treadmill, the average forward speed should be equal to the treadmill speed.
334 But the average speed in sideward (medio-lateral) direction over one cycle did not have to be zero and
335 the medio-lateral kinetic energy may exist. This kinetic energy change rate in V2 skating technique

336 might be one reason that the P_{mean} is unequal to P_{tot} . Results from a previous study related to DP
337 technique demonstrated that the propulsive power was approximately equal to the P_{mean} [25].
338 Compared with DP technique, the V2 technique contains more angular displacements of the limbs
339 (e.g., leg swinging). This might be another reason that the P_{mean} may unequal to P_{tot} . Both P_{mean}
340 and P_{tot} are external power and are calculated to estimate the total energy use. It has been
341 demonstrated that with V2 technique the oxygen uptake as a measure of energy use increased in an
342 approximately linear manner with skiing speed [30]. Both P_{mean} ($r^2 = 0.714$) and P_{tot} ($r^2 = 0.736$)
343 in this study show high linearity (Fig.6) with the skiing speed and their enhancement with speed are
344 similar (P_{mean} increased by 61.6% and P_{tot} increased by 60.3%). This indicated that P_{mean} and
345 P_{tot} can be used for energy use estimation and further analysis.

346 The relative power contribution from the poles towards the total external power was determined by
347 expressing the averaged propulsive resultant pole power (P_p^+) as a percentage of P_{tot} . The P_{tot} in
348 this study is not exactly same with the P_{mean} . As they all have stable relation with the speed, the P_{tot}
349 was used to represent the total external power. About 55%-57% of the external propulsive power was
350 generated from poles, therefore, about 43%-45% was generated from skis (Fig. 7A). The relative
351 contribution to the total external power from poles was 22%-32% greater than from skis, which is
352 different from the result by calculating the propulsive force [11]. Previous findings showed that for
353 the V2 skating technique, about two thirds of the propulsive force is attributed to the force from poles,
354 and one third is attributed to the force from skis [9]. The relative contribution from skis to maintain
355 the speed calculated in this study is greater than what has been reported, which supports our last
356 hypothesis. Skiers who are using the V2 technique do not move forward directly, but move forward in
357 a “zig-zag” movement [14]. The leg push-off is performed perpendicular to gliding ski [6] which may
358 lead to sideward velocity of COM. As the sideward velocity can be added to the gliding velocity in a
359 more or less forward direction [15], forces and the sideward COM velocity also need to be considered
360 when calculating the relative contributions from skis. The current study mainly concentrated on power
361 analysis. The external power is the dot product of the force vector which acts on the limb and the
362 COM velocity vector. Therefore, power analysis contained the movements in all the directions. By

363 calculating the propulsive force, the contribution of ski forces to the sideward velocity was not
364 included. Thus, it would underestimate the relative contribution of ski force. Although the relative
365 contribution from poles increased from 55% to 57%, the enhancement was not statistically significant
366 (Fig. 7A). Changing the relative contribution from skis and poles might not be a strategy to cope with
367 the increase in speed. The effectiveness index has been used as a helpful tool to evaluate an athlete's
368 overall economy in terms of force production and was calculated by expressing the propulsive force
369 impulse as a percentage of the resultant force impulse [10]. In the present study, the effectiveness
370 index of ski power was calculated by expressing the mean propulsive resultant ski external power P_s^+
371 as a percentage of $(P_s^+ + |P_s^-|)$ over a cycle. Positive power indicated that the generated forces vectors
372 act in the same direction as the COM velocity vector, which is the "propulsive power". About 54%-
373 58% of the ski power acted as the "propulsive power" (Fig. 8B). The effectiveness index was
374 depended on the speed, but no significant difference was found when compared between any two
375 speeds. This may be due to the p value for the effect of speed is close to 0.05. The effectiveness index
376 of pole power was not analyzed, as almost all the pole power was positive (propulsive) power (Fig. 3).
377 It should be noted that the force measurement bindings used in the current study were higher and
378 heavier than the normal ones, which may have caused instability that decreased the use of legs and,
379 therefore, resulted in a more pronounced amount of pole contribution and affect the effectiveness of
380 the ski power.

381 **Limitations**

382 The subjects involved in this study had varying skiing levels and female participants were not
383 included, so the results could only indicate a general pattern of the V2 skating technique while roller
384 skiing on the treadmill among males. Whether a homogeneous group of elite skiers would show the
385 same pattern needs further investigation. The highest speed reached in this study was not the
386 maximum speed skiers could reach, so it does not represent the skier's top performance. The force
387 measurement bindings and pole force sensors used in this study are all heavier than normal ones,
388 which is one of the reasons why the skiers could not reach higher speeds. This may also have
389 influenced the skiing technique, including both pole and leg actions. Equipment similar to the normal
390 roller skis which can measure the ski forces [31] could be used for future study to be able to ski using

391 the normal skiing techniques. Although many parameters were affected by the speed, not all of them
392 showed significant difference between two successive speeds. 2km/h speed difference may not be big
393 enough to change the external power pattern.

394 **5 Conclusions**

395 This current study characterized the role of skis and poles during treadmill roller skiing with V2
396 skating technique from external mechanical power point of view. It was confirmed that the negative
397 external ski power was produced by the kicking ski to redirect the COM velocity, especially in medio-
398 lateral and vertical directions. When the treadmill speed increased, both positive (propulsive) and
399 negative (braking) external ski and pole powers increased considerably. About 43-45% of the total
400 external power was generated by skis. However, changing the relative contribution from skis and
401 poles may not be a strategy to cope with the increasing speed.

402 **Acknowledgements**

403 The authors would like to express their appreciation and thank to the staffs, athletes and coaches for
404 their participation, enthusiasm, and cooperation in this study.

405 **References**

- 406 1. Stöggl T, Stöggl J, Müller E. Competition analysis of the last decade (1996–2008) in crosscountry skiing.
 407 In: Erich Müller SL, Thomas Stöggl, editor. *Science and Skiing IV*; UK: Meyer & Meyer Sport; 2008. p. 657–
 408 77.
- 409 2. Losnegard T, Myklebust H, Ehrhardt A, Hallen J. Kinematical analysis of the V2 ski skating technique:
 410 A longitudinal study. *Journal of sports sciences*. 2017;35(12):1219–27. doi:
 411 10.1080/02640414.2016.1218036. PubMed PMID: 27686117.
- 412 3. Millet GY, Hoffman MD, Candau RB, Clifford PS. Poling forces during roller skiing: effects of technique
 413 and speed. *Medicine & Science in Sports & Exercise*. 1998;30(11):1645–53. doi: 10.1097/00005768-
 414 199811000-00014.
- 415 4. Nilsson J, Tveit P, Eikrehagen O. Cross-Country Skiing: Effects of speed on temporal patterns in
 416 classical style and freestyle cross - country skiing. *Sports biomechanics*. 2004;3(1):85–108. doi:
 417 10.1080/14763140408522832.
- 418 5. Ohtonen O, Linnamo V, Lindinger SJ. Speed control of the V2 skating technique in elite cross-country
 419 skiers. *International Journal of Sports Science & Coaching*. 2016;11(2):219–30. doi:
 420 10.1177/1747954116637156.
- 421 6. Sandbakk O, Ettema G, Holmberg HC. The influence of incline and speed on work rate, gross efficiency
 422 and kinematics of roller ski skating. *European journal of applied physiology*. 2012;112(8):2829–38. doi:
 423 10.1007/s00421-011-2261-0. PubMed PMID: 22127680.
- 424 7. Hebert-Losier K, Zinner C, Platt S, Stoggl T, Holmberg HC. Factors that Influence the Performance of
 425 Elite Sprint Cross-Country Skiers. *Sports medicine*. 2017;47(2):319–42. doi: 10.1007/s40279-016-0573-2.
 426 PubMed PMID: 27334280; PubMed Central PMCID: PMC5266777
- 427 8. Nilsson J, Tveit P, Eikrehagen O. Effects of speed on temporal patterns in classical style and freestyle
 428 cross-country skiing. *Sports biomechanics*. 2004;3(1):85–107. doi: 10.1080/14763140408522832. PubMed
 429 PMID: 15079990.
- 430 9. Smith G, Kvamme B, Jakobsen V. Ski skating technique choice: mechanical and physiological factors
 431 affecting performance. In: Schwameder H SG, Fastenbauer V, Lindinger S, Müller E, , editor. 24
 432 *International Symposium on Biomechanics in Sports Austria*: University of Salzburg; 2006. p. 397–400.
- 433 10. Stoggl T, Holmberg HC. Three-dimensional Force and Kinematic Interactions in V1 Skating at High
 434 Speeds. *Medicine and science in sports and exercise*. 2015;47(6):1232–42. doi:
 435 10.1249/MSS.0000000000000510. PubMed PMID: 25207933.
- 436 11. Smith GA. Biomechanics of cross country skiing. In: Rusko H, editor. *Cross Country Skiing Handbook*
 437 *of Sports Medicine*. New York: Wiley; 2003. p. 32–61.
- 438 12. Smith GA. Biomechanical analysis of cross-country skiing techniques. *Medicine and science in sports*
 439 *and exercise*. 1992;24(9):1015–22. PubMed PMID: 1406185.
- 440 13. Stoggl TL, Holmberg HC. Double-Poling Biomechanics of Elite Cross-country Skiers: Flat versus Uphill
 441 Terrain. *Medicine and science in sports and exercise*. 2016;48(8):1580–9. doi:
 442 10.1249/MSS.0000000000000943. PubMed PMID: 27031747.
- 443 14. Sandbakk O, Ettema G, Holmberg HC. The physiological and biomechanical contributions of poling
 444 to roller ski skating. *European journal of applied physiology*. 2013;113(8):1979–87. doi: 10.1007/s00421-
 445 013-2629-4. PubMed PMID: 23543069.
- 446 15. Zatsiorsky V. *Biomechanics in sport: performance enhancement and injury prevention*: John Wiley &
 447 Sons; 2008.
- 448 16. Yamashita D, Fujii K, Yoshioka S, Isaka T, Kouzaki M. Asymmetric interlimb role-sharing in mechanical
 449 power during human sideways locomotion. *Journal of biomechanics*. 2017;57:79–86.
- 450 17. Donelan JM, Kram R, Kuo AD. Simultaneous positive and negative external mechanical work in human
 451 walking. *Journal of biomechanics*. 2002;35(1):117–24.
- 452 18. van der Kruk E, Van Der Helm F, Veeger H, Schwab AL. Power in sports: a literature review on the
 453 application, assumptions, and terminology of mechanical power in sport research. *Journal of biomechanics*.
 454 2018;79:1–14.

- 455 19. Zhao S, Ohtonen O, Ruotsalainen K, Kettunen L, Lindinger S, Göpfert C, et al. Propulsion Calculated
456 by Force and Displacement of Center of Mass in Treadmill Cross-Country Skiing. *Sensors*. 2022;22(7):2777.
457 doi: 10.3390/s22072777
- 458 20. Ohtonen O, Lindinger S, Lemmettylä T, Seppälä S, Linnamo V. Validation of portable 2D force binding
459 systems for cross-country skiing. *Sports Engineering*. 2013;16(4):281-96. doi: 10.1007/s12283-013-0136-
460 9.
- 461 21. Göpfert C, Pohjola MV, Linnamo V, Ohtonen O, Rapp W, Lindinger SJ. Forward acceleration of the
462 centre of mass during ski skating calculated from force and motion capture data. *Sports Engineering*.
463 2017;20(2):141-53. doi: 10.1007/s12283-016-0223-9.
- 464 22. Selbie.W S, Hamill J, Kepple.M T. Three-Dimensional Kinetics. In: Robertson GE, Caldwell GE, Hamill J,
465 Kamen G, Whittlesey S, editors. *Research methods in biomechanics*. 2 ed. USA: Human kinetics; 2013. p.
466 159-60.
- 467 23. Ohtonen O, Ruotsalainen K, Mikkonen P, Heikkinen T, Hakkarainen A, Leppävuori A, et al. Online
468 feedback system for athletes and coaches. In: Hakkarainen A, Lindinger S, Linnamo V, editors. 3rd
469 International Congress on Science and Nordic Skiing; Finland: University of Jyväskylä; 2015. p. 35.
- 470 24. Yu B, Gabriel D, Noble L, An K-N. Estimate of the optimum cutoff frequency for the Butterworth low-
471 pass digital filter. *Journal of applied biomechanics*. 1999;15(3):318-29. doi: 10.1123/jab.15.3.318.
- 472 25. Danielsen J, Sandbakk Ø, McGhie D, Ettema G. Mechanical energetics and dynamics of uphill double-
473 poling on roller-skis at different incline-speed combinations. *PLoS one*. 2019;14(2):e0212500. doi:
474 10.1371/journal.pone.0212500.
- 475 26. Dahl C, Sandbakk O, Danielsen J, Ettema G. The Role of Power Fluctuations in the Preference of
476 Diagonal vs. Double Poling Sub-Technique at Different Incline-Speed Combinations in Elite Cross-Country
477 Skiers. *Frontiers in physiology*. 2017;8:94. doi: 10.3389/fphys.2017.00094. PubMed PMID: 28270769;
478 PubMed Central PMCID: PMC5318423.
- 479 27. Hof AL. The equations of motion for a standing human reveal three mechanisms for balance. *Journal*
480 *of biomechanics*. 2007;40(2):451-7. doi: <https://doi.org/10.1016/j.jbiomech.2005.12.016>.
- 481 28. Arampatzis A, Knicker A, Metzler V, Brüggemann G-P. Mechanical power in running: a comparison of
482 different approaches. *Journal of biomechanics*. 2000;33(4):457-63.
- 483 29. De Koning JJ, Foster C, Lampen J, Hettinga F, Bobbert MF. Experimental evaluation of the power
484 balance model of speed skating. *Journal of applied physiology*. 2005;98(1):227-33.
- 485 30. Kvamme B, Jakobsen V, Hetland S, Smith G. Ski skating technique and physiological responses across
486 slopes and speeds. *European journal of applied physiology*. 2005;95(2):205-12.
- 487 31. Zhao S, Linnamo V, Ruotsalainen K, Lindinger S, Kananen T, Koponen P, et al. Validation of 2D Force
488 Measurement Roller Ski and Practical Application. *Sensors*. 2022;22(24):9856. doi: 10.3390/s22249856.
489



IV

VALIDATION OF 2D FORCE MEASUREMENT ROLLER SKI AND PRACTICAL APPLICATION

by

Zhao, S., Linnamo, V., Ruotsalainen, K., Lindinger, S., Kananen, T.,
Koponen, P., Ohtonen, O. 2022



Sensors, 22, 9856

doi:10.3390/s22249856

© 2022 by the authors. Licensee MDPI, Basel, Switzerland. This article is an open access article distributed under the terms and conditions of [the Creative Commons Attribution \(CC BY\) license](#).

Article

Validation of 2D Force Measurement Roller Ski and Practical Application

Shuang Zhao ^{1,*}, Vesa Linnamo ¹, Keijo Ruotsalainen ¹, Stefan Lindinger ², Timo Kananen ³, Petri Koponen ³ and Olli Ohtonen ¹¹ Faculty of Sport and Health Sciences, University of Jyväskylä, 40014 Jyväskylä, Finland² Center of Health and Performance (CHP), Department of Food and Nutrition and Sport Science, University of Gothenburg, 40530 Gothenburg, Sweden³ Technical Research Centre of Finland, VTT MIKES, 87100 Kajaani, Finland

* Correspondence: zhaoshuangzs@hotmail.com

Abstract: Several methods could be used to measure the forces from skis or roller skis in cross-country skiing. Equipment that could measure medio-lateral forces may be of good help for investigating the relevant skating techniques. The aim of this study was to validate a pair of newly designed two-dimensional force measurement roller skis. The vertical and medio-lateral forces which were perpendicular to the body of the roller ski could be measured. Forces were resolved into the global coordinate system and compared with the force components measured by a force plate. A static and dynamic loading situation for the force measurement roller ski was performed to reveal the validity of the system. To demonstrate whether the force measurement roller ski would affect roller skiing performance on a treadmill, a maximum speed test with the V2 technique was performed by using both normal and force measurement roller skis. The force-time curves obtained by these two different force measurement systems were shown to have high similarity (coefficient of multiple correlations > 0.940). The absolute difference for the forces in the X and Z directions over one push-off cycle was 3.9–33.3 N. The extra weight (333 g) of the force measurement roller ski did not affect the performance of the skiers. Overall, the newly designed two-dimensional force measurement roller ski in this study is valid for use in future research during daily training for skate skiing techniques.

Keywords: cross-country skiing; force measuring device; kinetics

Citation: Zhao, S.; Linnamo, V.; Ruotsalainen, K.; Lindinger, S.; Kananen, T.; Koponen, P.; Ohtonen, O. Validation of 2D Force Measurement Roller Ski and Practical Application. *Sensors* **2022**, *22*, 9856. <https://doi.org/10.3390/s22249856>

Academic Editor: Marco Iosa

Received: 15 November 2022

Accepted: 13 December 2022

Published: 15 December 2022

Publisher's Note: MDPI stays neutral with regard to jurisdictional claims in published maps and institutional affiliations.



Copyright: © 2022 by the authors. Licensee MDPI, Basel, Switzerland. This article is an open access article distributed under the terms and conditions of the Creative Commons Attribution (CC BY) license (<https://creativecommons.org/licenses/by/4.0/>).

1. Introduction

Numerous tools are available to researchers for the measurement of ground reaction forces (GRFs). In cross-country (XC) skiing, one approach to measuring the GRFs between skis and snow in early studies was by using the force measurement systems buried under snow [1–4]. These systems allow skiers to ski freely on snow while recording the force data. However, only two or three ski contacts could be measured for one trial with classic-style XC skiing due to the length and construction of the force plate [1–3]. The system introduced by Leppävuori [4] could be used to measure the GRFs with the skating technique. This system was able to measure three-dimensional (3D) GRFs, which means the force generated by medio-lateral movement was included as well, but skiers had to position the ski directly over the force plate. Moreover, only one ski contact for one trial could be recorded. Although the force measurement systems buried under snow did not influence the skiing technique, the movements were restricted to limited space. Therefore, more flexible ski force measurement equipment has emerged.

Several studies started to implement force transducers to the ski or roller ski bindings and measure the forces between ski boots and skis (or roller skis). Small force plates were implemented in the bindings introduced by Komi [1]. The vertical and anterior–posterior forces could be measured while skiing on snow, but they could not be used

in the skate skiing technique which contains medio-lateral movements. Similarly, small force plates have also been implemented to roller ski bindings [5]. The vertical and medio-lateral forces were measured, but one equipped roller ski was about 50% heavier than a normal roller ski. In some studies, strain gauges have been installed on the bindings and measured the forces in several dimensions [6–8]. The force measurement bindings developed by Ohtonen et al. [8] have been used with both skis on snow [9–12] and roller skis on a treadmill [13]. The extra weight and height added by these bindings may, however, affect the skier's performance on the treadmill using a roller ski [13]. The pressure insoles have also been used in several studies [14–17], but only vertical forces could be obtained.

For most skiers, roller skiing is one primary form of training method during the dry land training season [5] and is a ski-specific laboratory testing model that could reveal skiing technique in more detail [18]. Therefore, instrumented roller skis have also been investigated in previous studies [19,20]. The strain gauges were installed on the roller skis directly to measure the vertical [19,20] and horizontal [19] forces. However, there is also movement in the medio-lateral direction in skate skiing techniques. Thus, instrumented force measurement roller skis which could measure medio-lateral forces may be of good help for investigating the relevant skating techniques in cross-country skiing.

Consequently, the main aim of this present study was to validate a pair of newly designed two-dimensional (2D) force measurement roller skis. This pair of roller skis were first calibrated by the Technical Research Center of Finland (VTT MIKES, Kajaani, Finland). Then, forces measured by the roller skis were resolved in the global coordinate system (GCS) [20], and the accuracy of the force measurement roller ski would be checked by comparing forces measured by the roller skis and forces measured by a 3D force plate with a static and a simulated skating push-off test. To demonstrate whether the force measurement roller ski would affect roller skiing performance on a treadmill, a maximum speed test with the V2 technique would be performed by using both normal and force measurement roller skis.

2. Materials and Methods

2.1. Construction of the Force Measurement Roller Ski

The force measurement roller skis were designed and made by the Technical Research Centre of Finland (VTT MIKES, Kajaani, Finland). A custom-made aluminum alloy frame of the roller ski has been designed using the finite element method (FEM). Finite element analysis (FEA) has been used for both dimensioning the frame and determining the location of strain gauges on the roller ski body. Both roller skis contain four full-bridge strain gauge configurations (Figures 1 and 2). There are four measurement channels for both roller skis. Two of these channels measure vertical forces (front and rear) and the other two measure medio-lateral forces (front and rear). The applied force causes a change in strain gauge resistance which causes a change in voltage, which can be measured from the Wheatstone full-bridge configuration. The amplifiers (Figure 1a) are embedded in the body of the roller skis and the voltage-level signals were acquired by the nodes (Figure 1b, Sports Technology Unit Vuokatti, University of Jyväskylä, Finland) of the Coachtech online measurement and feedback system [21], which were attached to the front part of the roller skis. The weight for one force measurement roller ski equipped with the Coachtech node was 1352 g.

2.2. Calibration and Force Calculation of the Force Measurement Roller Ski

The force measurement roller skis were calibrated in June 2022 before this validation measurement by the Technical Research Centre of Finland (VTT MIKES, Kajaani, Finland). The strain gauges were calibrated for a vertical force with forces from 0 N to 1000 N and for medio-lateral forces with forces from 0 N to 400 N. Three different types of tests (the load-up test, the signal-to-noise test, and the creep test) were performed for all force measurement roller ski sensors and for both vertical and medio-lateral directions. In the case of medio-lateral force, loading was performed from both sides. In the load-up test (the same for the vertical and medio-lateral directions), three preloads precede two increasing loads which

are followed by increasing and decreasing loads. The measurement cycle between each load was 60 s. In the signal-to-noise test, voltage levels were measured without applied load. The measurement time was 180 s and the sampling frequency was 0.5 Hz. In the creep test, a 1000 N force was applied three times for both roller skis. Forces were applied directly from 0 N to 1000 N. The measurement cycle was 180 s. The creep was determined from the last load cycle. From the calibration process, the calibration factor and measurement uncertainty for the calibration process is calculated. The following uncertainty components are used in uncertainty calculations including calibration force, repeatability, resolution of the display device, creep of the instrument, zero-point fluctuation, hysteresis, interpolation error, and crosstalk. A linear model was used to calculate the calibration factor (N/mV) for each sensor. In addition to the linear model, second-order and third-order models had been tried as well, but the errors were not significantly reduced. The calibration factor (N/mV) used in this study for each strain gauge was shown in Table 1. The force from each signal channel (F_i) was calculated with the equation $F_i = a_i * U_i$, where U_i is the voltage of signal channel i (mV) and a_i is the calibration factor (N/mV). The total force of each direction (vertical or medio-lateral) could be derived with the equation $F_{sum} = F_{front} + F_{rear}$, where F_{sum} represents the total force in one direction and F_{front} and F_{rear} are the forces in this direction from the front suspension and the rear suspension, respectively. In the measurements, only the sum of the forces was used.

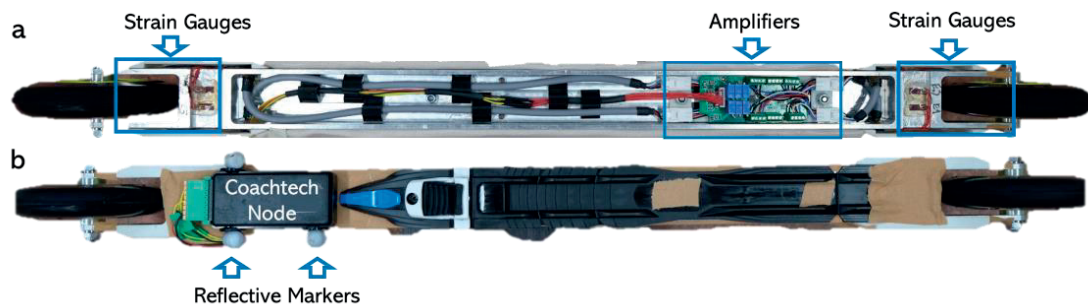


Figure 1. Construction of the force measurement roller ski. (a) Bottom view of the force measurement roller ski. (b) Top view of the force measurement roller ski.

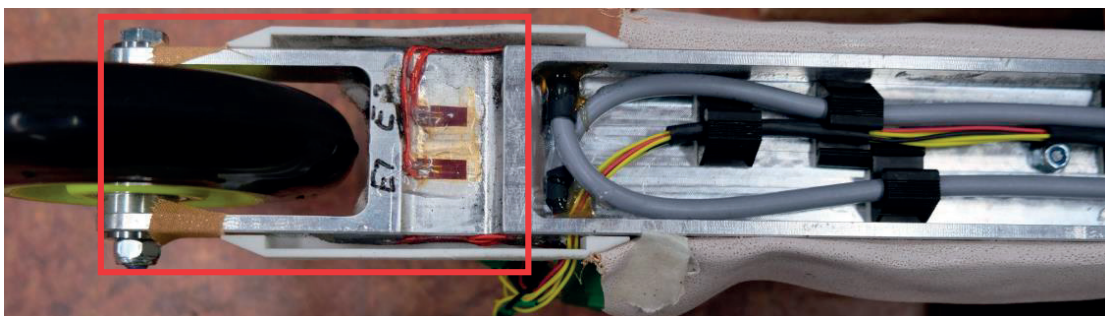


Figure 2. Diagram of strain gauge installation area.

Table 1. Calibration factors (N/mV) for each strain gauge mounted on the roller skis.

Roller Ski	Strain Gauge	Calibration Factor
Right roller ski	Front vertical	0.2444
	Front medio-lateral	0.1170
	Rear vertical	0.2418
	Rear medio-lateral	0.1154
Left roller ski	Front vertical	0.2452
	Front medio-lateral	0.1178
	Rear vertical	0.2489
	Rear medio-lateral	0.1157

2.3. Validation of the Force Measurement Roller Skis

2.3.1. Static Test

The static tests were carried out on two AMTI 3D force plates (AMTI, Watertown, MA, USA) and were conducted for each roller ski (left and right) separately. The AMTI force plates were calibrated on 7 June 2022. Each time, one roller ski was placed with one wheel on each force plate by using custom-made equipment (Figure 3a). A total of 15 (0 kg to 150 kg) loads were placed with full weight on the roller ski. The force plates measured the forces in three directions and contained the forces induced by the weight of the roller ski and the custom-made equipment (Figure 3b). Therefore, the resultant force measured by the force measurement roller ski in this study should be equal to the resultant forces measured by the force plate minus the weight of the roller ski and the equipment.

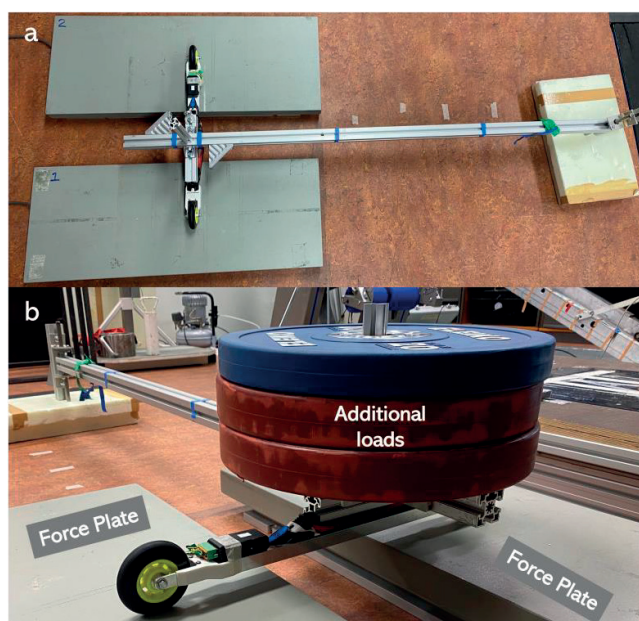


Figure 3. Diagram of the static test. (a) Custom-made equipment for placing the additional loads. (b) Static test with 70 kg additional loads.

Forces measured by the roller ski were collected by the Coachtech online measurement and feedback system [21] at a sample rate of 400 Hz. Forces measured by the AMTI force plates were collected by the AMTINetForce Version 3.5.2 (AMTI, Watertown, MA, USA) with a sample rate of 1000 Hz. All force signals for each load were collected for at least 10 s.

An average of 3 s of data was used to represent the forces under each load. The accuracy of the force measurement roller ski was quantified by using the relative difference in resultant forces between the force measurement roller ski and the AMTI force plates.

2.3.2. Simulated Skating Push-Off Jump Test

In order to test the force measurement roller ski in an applied dynamic situation, a simulated skating push-off jump test was performed over one AMTI 3D force plate (AMTI, Watertown, MA, USA). One male (age: 43 years; height: 183 cm; and weight: 83 kg) and one female (age: 27 years; height: 165 cm; and weight: 55 kg) highly skilled skier took part in this test. The maximum push-off jump distances were first found. The push-off distance was defined as the distance between the push-off foot and the landing foot (Figure 4). The maximum push-off distance for the male subject was 1.64 m with the right foot and 1.70 m with the left foot. The maximum push-off distance for the female subject was 1.49 m with the right foot and 1.45 m with the left foot. The push-off load was changed by changing the target push-off distance and the subject. The target distances were 65%, 75%, 85%, and 100% of the maximum push-off jump distance. Ten jumps at each target distance were recorded for further analysis. From a security perspective, subjects wore their normal training shoes with the landing foot. The force measurement roller ski was used by the push-off foot. The simulated skating push-off jump test was performed by both feet (left and right) separately.

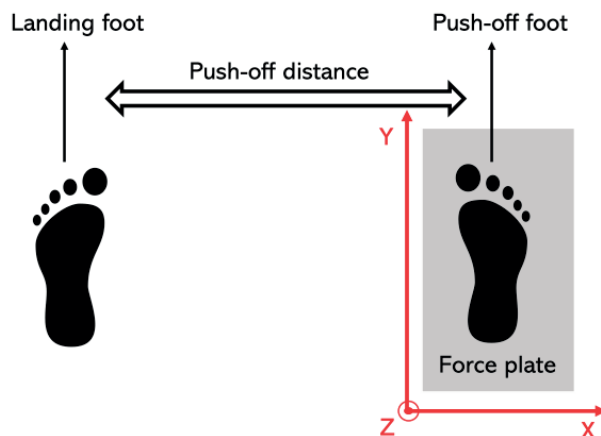


Figure 4. The definition of the push-off distance and the direction of the global coordinate system (GCS).

Forces measured by the roller ski were collected by the Coachtech system [21] at a sample rate of 1000 Hz. Forces measured by the AMTI force plates were collected by the AMTINetForce Version 3.5.2 (AMTI, Watertown, MA, USA) with a sample rate of 1000 Hz. Three passive reflective markers were attached to the force measurement roller ski (Figure 1b) to record the position of the roller ski and were used to transform forces measured by the roller ski into the GCS [13]. The markers' displacement was sampled at 250 Hz by using the Vicon motion capture system (Vicon, Oxford, UK). The weight for one force measurement roller ski with the node and the markers was 1358 g.

The force signal and the marker displacement signal were synchronized manually by using the rapid synchronization hit with the force measurement roller ski on the force plate before each push-off jump (Figure 5). The start of the push-off was defined as the vertical force minima during the unweighting phase. The end of the push-off was defined when the magnitude of the vertical force measured by the force plate was under 5 N. Forces measured directly by the force plate in the GCS (Figure 4) were treated as the reference value. As the movement in the Y direction during the simulated skating push-offs was small, forces from the force measurement roller ski and the force plate were not compared in the Y direction. The coefficient of multiple correlations (CMC, $0 < \text{CMC} < 1$) [22–24] was

calculated using MATLAB R2018a (MathWorks, Natick, MA, USA) from time-normalized curves between the force measurement roller ski and the force plate. The accuracy of the force measurement roller ski was quantified by using the absolute difference in forces between the force measurement roller ski and the force plates in the X and Z directions.

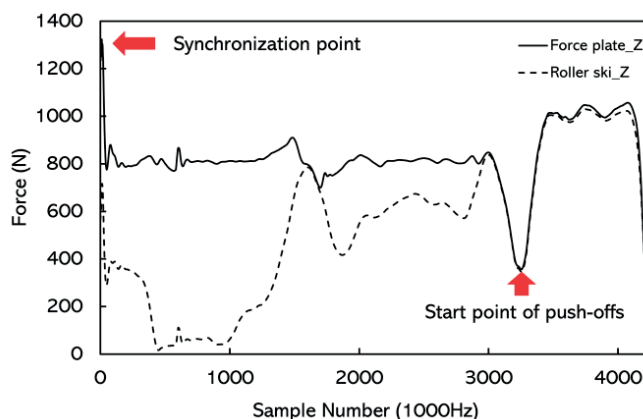


Figure 5. The synchronization of the signals and the start point of the simulated skating push-off. Force curves were from the male subject's right foot push-off and the target push-off distance was the maximum push-off distance. The difference in the force curves before the start point was due to the position of the landing leg. The subject stood on the force plate with both legs before the push-off. The whole body weight was on the force plate but half or less body weight was on the roller ski; therefore, the signals do not match.

2.3.3. Practical Application

To demonstrate the practical application of the force measurement roller skis, one male (age: 24 years; height: 179 cm; and weight: 81.5 kg) and one female (age: 26 years; height: 166.5 cm; and weight: 55.5 kg) skier were roller skiing on a treadmill using the force measurement roller skis and using the reference roller skis (Marwe, SKATING 620 XC, wheel No. 0). The force measurement and the reference roller skis had the same wheels. The main aim of this test was to find whether the extra weight of the force measurement roller ski would affect skiing performance.

For each subject, the following protocol was performed for two rounds and there was a 5 min rest in between. The incline of the treadmill for the female subject was 2° and for the male subject was 3° . The start speed of the treadmill was 18 km/h and increased by 1 km/h every 15 s. The treadmill stopped when the skier cannot keep up with the treadmill speed. The duration and the final speed were recorded as well as the cycle time, cycle rate, cycle length, and ski contact time were also obtained by using the accelerometer attached to the skis and poles with the Coachtech system [21]. The longer duration and greater final speed were used to present the performance. The protocol was performed twice within one week on different days by each subject, once with a pair of reference roller skis and another with the pair of force measurement roller skis.

The weight of the reference roller ski was 1025 g, which is 333 g lighter than the force measurement roller ski equipped with a node. As the Coachtech node is essential to the collection of the force signal, the balance point of a force measurement roller ski was measured with the Coachtech node attached to the front part of the roller ski. The balance point of the force measurement roller ski was moved 1.60 cm forward when compared to the reference roller ski. The torque around the ski boot attach point of the roller ski was calculated by using the gravitational force of the roller ski multiplied by the distance between the balance point and the ski boot attach point. The torque for the force measurement roller ski was 0.60 N·m and was 0.61 N·m for the reference roller ski.

3. Results

In the static test, the relative difference in resultant forces between the force measurement roller ski and the AMTI force plate was lower than 2.0% (0.11~1.92%). The maximum relative difference in resultant forces was 1.92% when the additional weight was 10 kg (Figure 6).

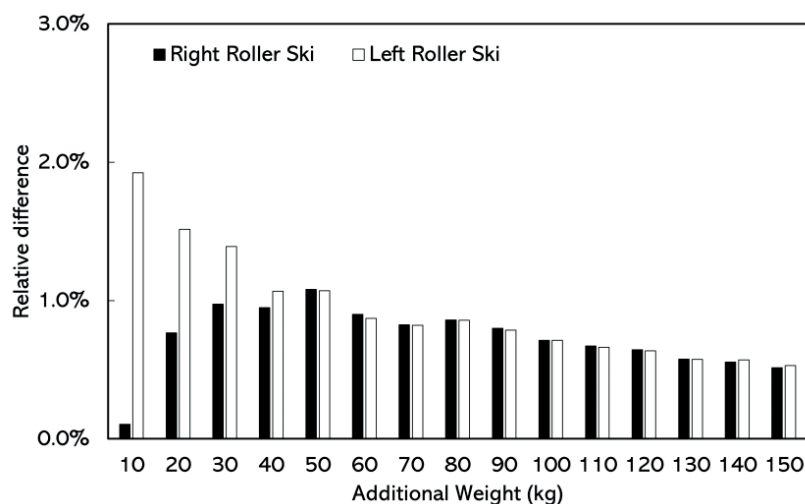


Figure 6. The absolute difference in resultant forces between force measurement roller ski and the AMTI force plates in static test at different additional loads.

In the simulated skating push-off test, the CMC values for force-time curves obtained from the force measurement roller ski and the force plate were generally above 0.940 (Figure 7). The average absolute differences for the forces in the X direction over one push-off cycle at different push-off loads were 8.5–33.3 N (Table 2). The average absolute differences for the forces in the Z direction at different push-off loads were 3.9–23.4 N (Table 3). The maximum absolute difference was 20.1–101.2 N in the X direction and was 21.0–66.6 N in the Z direction (Figures 8 and 9).

Table 2. The absolute difference (N) between force-time curves obtained by the AMTI force plate and the force measurement roller ski system in the X direction.

Loads	Right Roller Ski	Left Roller Ski
F65%	8.5 ± 5.6	18.8 ± 14.2
F75%	15.4 ± 12.3	26.1 ± 20.9
F75%	22.1 ± 17.0	28.2 ± 21.3
F100%	23.4 ± 26.5	32.5 ± 25.4
M65%	22.2 ± 10.2	18.8 ± 9.2
M75%	24.4 ± 12.6	19.4 ± 9.1
M85%	30.6 ± 19.0	21.1 ± 15.9
M100%	33.3 ± 25.0	24.4 ± 17.4

Note: The absolute differences were averaged over 10 push-off cycles. F65%, F75%, F85%, and F100% represented female subjects and the target distance was 65%, 75%, 85%, and 100% of the maximum push-off distance, respectively. M65%, M75%, M85%, and M100% represented male subjects and the target distance was 65%, 75%, 85%, and 100% of the maximum push-off distance, respectively.

Table 3. The absolute difference (N) between force-time curves obtained by the AMTI force plate and the force measurement roller ski system in the Z direction.

Loads	Right Roller Ski	Left Roller Ski
F65%	15.8 ± 2.2	9.9 ± 3.3
F75%	18.3 ± 5.0	13.5 ± 7.1
F75%	20.7 ± 8.1	14.7 ± 8.5
F100%	23.4 ± 14.9	18.8 ± 13.4
M65%	11.7 ± 5.1	3.9 ± 3.4
M75%	11.7 ± 3.2	4.1 ± 4.0
M85%	13.8 ± 6.6	5.7 ± 7.2
M100%	15.2 ± 9.7	7.3 ± 9.8

Note: The absolute differences were averaged over 10 push-off cycles. F65%, F75%, F85%, and F100% represented female subjects and the target distance was 65%, 75%, 85%, and 100% of the maximum push-off distance, respectively. M65%, M75%, M85%, and M100% represented male subjects and the target distance was 65%, 75%, 85%, and 100% of the maximum push-off distance, respectively.

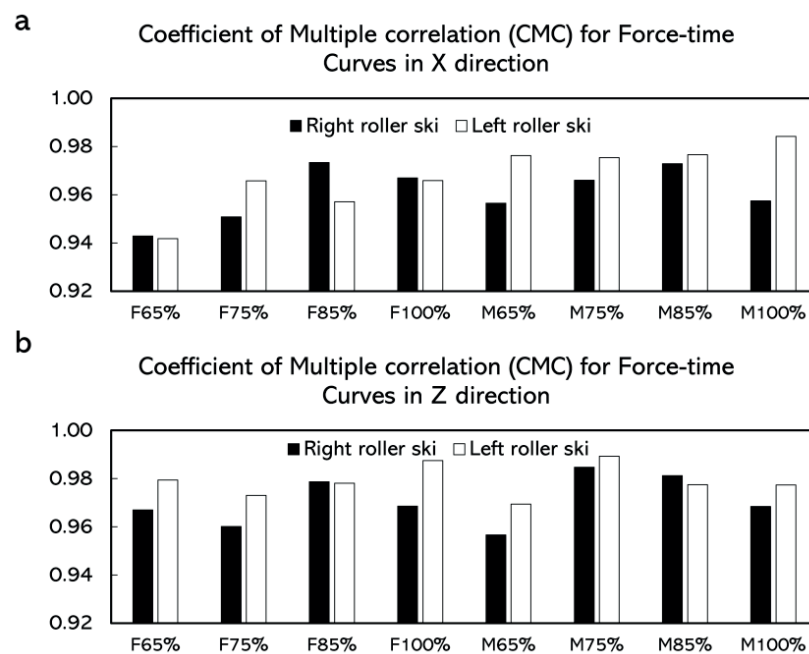
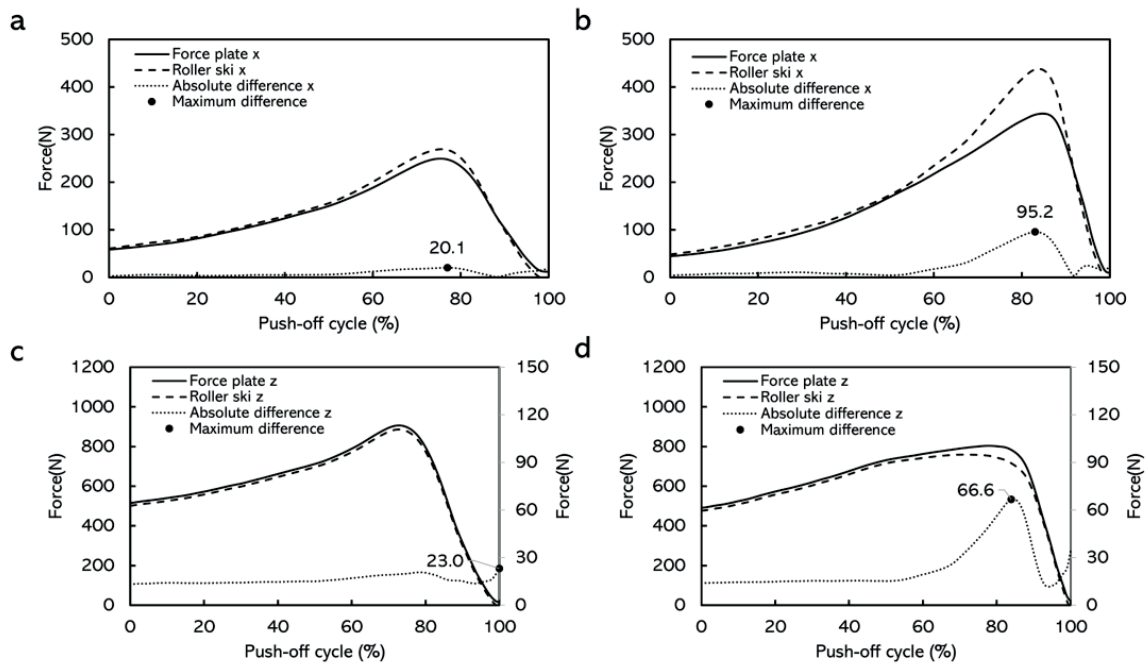


Figure 7. The coefficient of multiple correlations (CMC) for time normalized force-time curve. (a) CMC between force-time curves measured by force measurement roller ski and force plates in the X direction. (b) CMC between force-time curves measured by force measurement roller ski and force plates in the Z direction. F65%, F75%, F85%, and F100% represented female subjects and the target distance was 65%, 75%, 85%, and 100% of the maximum push-off distance, respectively. M65%, M75%, M85%, and M100% represented male subjects and the target distance was 65%, 75%, 85%, and 100% of the maximum push-off distance, respectively.

When skiing on the treadmill, the durations for the tests did not have any major differences with different roller skis. Male skiers even had longer duration and better performance by using the force measurement roller ski (Table 4). The cycle characteristics, while using both roller skis at different speeds, are shown in Figures 10 and 11. For the female skier, lower cycle rate, longer cycle length, and longer ski contact time were discovered by using the normal roller ski but for the male skier, the effects of the roller ski on cycle characteristics were not obvious (Figure 11).

Table 4. The duration (s) and the final speed by using the force measurement roller ski (FMR) and the normal roller ski (NR).

	Male		Female	
	FMR	NR	FMR	NR
Duration (s)	143	134	147	150
Final speed (km/h)	27	26	27	27

**Figure 8.** Comparison of force curves measured by force measurement roller ski versus force plate in the X direction and the Z direction with female subjects, and the absolute differences over time. (a) Force curves when the target distance was 65% of the maximum push-off distance. (b) Force curves when the target distance was 100% of the maximum push-off distance. (c) Force curves when the target distance was 65% of the maximum push-off distance. (d) Force curves when the target distance was 100% of the maximum push-off distance. Note: curves were averaged over 10 push-off cycles. The curves from these loads were chosen as examples having contained the highest and lowest maximum absolute differences.

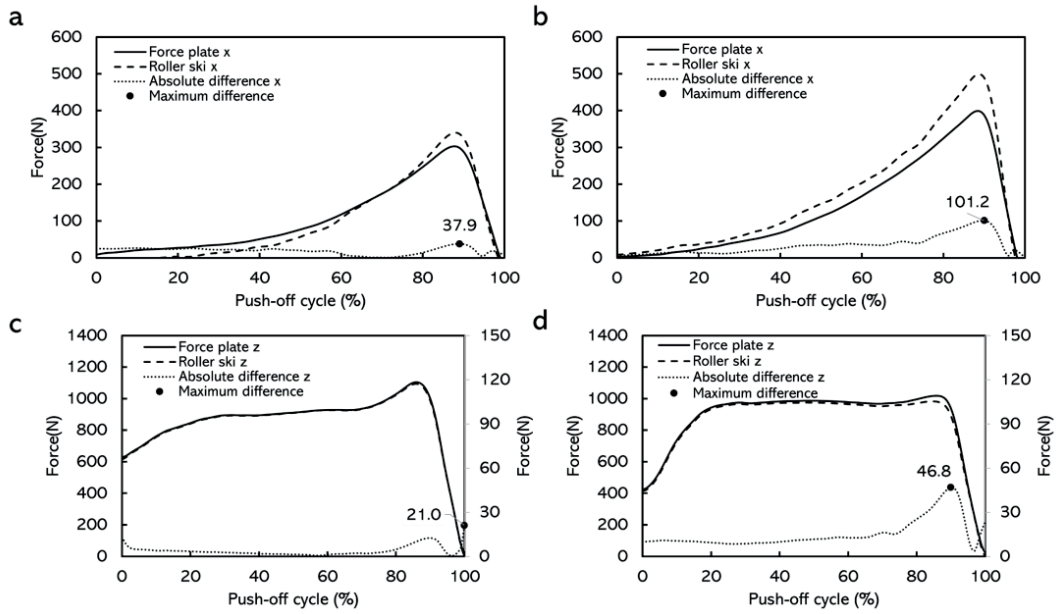


Figure 9. Comparison of force curves measured by force measurement roller ski versus force plate in the X direction and the Z direction with male subjects, and the absolute differences over time. (a) Force curves when the target distance was 65% of the maximum push-off distance. (b) Force curves when the target distance was 100% of the maximum push-off distance. (c) Force curves when the target distance was 65% of the maximum push-off distance. (d) Force curves when the target distance was 100% of the maximum push-off distance. Note: curves were averaged over 10 push-off cycles. The curves from these loads were chosen as examples having contained the highest and lowest maximum absolute differences.

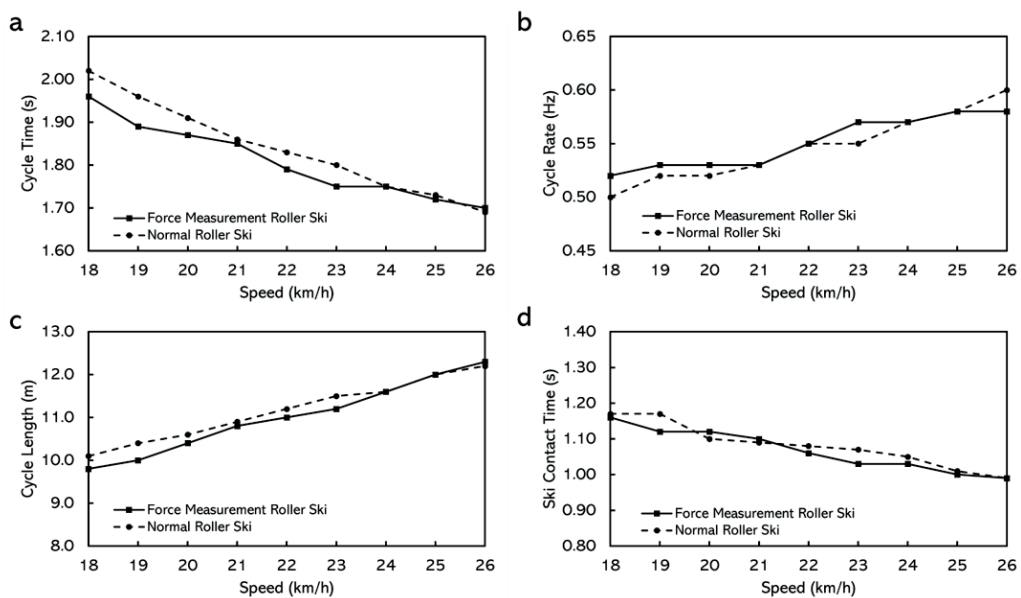


Figure 10. The cycle characteristics while using normal roller skis and force measurement roller skis for male subjects. (a) Cycle time. (b) Cycle rate. (c) Cycle length. (d) Ski contact time (from right roller ski).

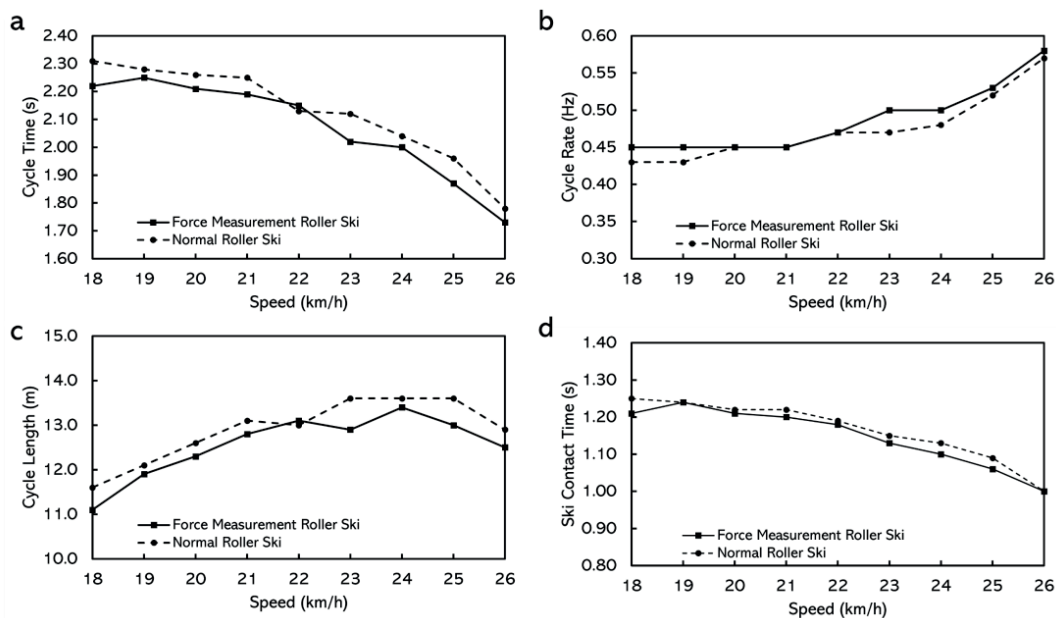


Figure 11. The cycle characteristics while using normal roller skis and force measurement roller skis for female subjects. (a) Cycle time. (b) Cycle rate. (c) Cycle length. (d) Ski contact time (from right roller ski).

4. Discussion

The force measurement roller ski used in this study was not the first one used in scientific studies. However, compared with the force measurement roller ski introduced in a previous study [20], these new roller skis can measure both vertical and medio-lateral forces which are more appropriate for the relevant skating techniques in cross-country skiing. The idea of this force measurement roller ski was from the force measurement bindings developed by Ohtonen et al. [8]. The binding was used in roller skiing on the treadmill [13] and the weight of one equipped roller ski was 1650 g, which is 27.6% heavier than the force measurement roller ski used in this current study. The Coachtech nodes placed between the binding and the front wheel of both roller skis were used for power supply and data transmission. This means that the data measured by the force measurement roller ski could be transported wirelessly via the Coachtech system. Therefore, from a construction point of view, this force measurement roller ski has the benefit of being lightweight and can wirelessly measure forces in more dimensions without any interfering cables and transmitters need to carry but subject. In addition, no extra height was added to the roller ski in the current study, which was reported as a problem in earlier studies [8]. The calibration factors used in this study were obtained in the calibration test carried out in June 2022. Another calibration test was in December 2020, and the calibration factors from this previous test can be found in the appendix (Appendix A). During these 18 months, the force measurement roller skis were used intensively by skiers to check the signal collection via the Coachtech system. The calibration factors used in this study did not change obviously when compared to the factors from the earlier calibration test, which indicated that the measurements could remain reliable and stable over several months. However, periodic calibration is recommended.

The static test was conducted to quantify the accuracy of the resultant forces obtained by the force measurement roller ski. The forces measured by the force plate also contained the weight of the roller ski and the custom-made frame; however, these weights were subtracted while doing the comparison. Although differences in relative resultant force dif-

ference were found between left and right force measurement roller skis at lower additional weights (10–30 kg), we are not focusing on the accuracy difference between left and right force measurement roller skis. In addition, the static test results are within measurement uncertainty for the vertical direction defined in the calibration process (Appendix B). The relative difference in resultant forces ranged from 0.11%~1.92% in this study. In a previous study, the difference of vertical resultant forces measured by the force plate and the instrumented one-dimensional roller ski ranged from 5.40% to 10.59% [20], which is greater than what we found in the present study. Possible reasons for improved accuracy may be due to the different construction of the force measurement roller skis.

The simulated skating push-off jump test was conducted to validate the force measurement roller ski in an applied dynamic situation. The CMC depicting the similarity between waveforms and the value of the CMC close to one implies that the curves involved were similar [13,22–24]. The CMC values in this study were generally above 0.940, which indicated that at each push-off load, the force-time curves obtained by the force plate and the force measurement roller ski after being transformed into the GCS were similar in each direction. Similar to the static test, the forces measured by the force plate contained the weight of the roller ski. However, the weight of the roller ski could not be subtracted during the dynamic test when comparing the force component in the GCS. Therefore, there must be some difference between the forces measured by the force plate and the forces measured by the roller ski. The average absolute difference for the forces in the Z direction at different push-off loads was 3.9–23.4 N (Table 3) and the maximum absolute difference was 21.0–66.6 N in the Z direction (Figures 8 and 9). The result from a previous study shows that the leg vertical force change among one skate skiing cycle from sub-maximum speed up to maximum speed was about 60–1415 N [11]. Since the differences between the forces measured by the force measurement roller ski and the reference force plate in the present study are smaller than observed during different-intensity skiing, the accuracy of the forces measured by the force measurement roller ski can be considered to be high enough to be used in practice e.g., for skiing technique observations. Although it is impossible to have the forces measured by the force measurement roller ski in full accord with forces measured by the force plate, the differences can be considered promising and acceptable. Figures 8 and 9 presented the absolute differences over time. The absolute differences were constant before the maximum push-off forces appeared. Moreover, the maximum absolute differences generally appeared around the maximum push-off force or at the end of the push-off. This may be due to the inconsistency of the force change from these two different force measurement systems. In cross-country skiing, the heel of the ski boot is not fixed on the roller ski. When the heel of the ski boot is about to go off the roller ski, the resistance of the strain gauge on the force measurement roller ski may change, thereafter leading to the change in forces. Since the full weight of the subject and the roller ski were still on the force plate, the forces measured by the force plate may not change. This inconsistency may lead to a change in the absolute difference over time. In addition, force transmission parts typically in calibrations are made from steel but, in this case, the force transmission parts are the rubber wheels which may also affect the difference in forces measured by the force measurement roller ski and the force plate. The absolute differences between these two force measurement systems in this dynamic test were greater than that in the static test. This is possibly caused by the direction of the applied force. The force measurement roller ski measured the forces between the foot and the roller ski, and the force plate measured the forces between the roller ski and the force plate. When the subject was performing the push-off jump, the roller ski was edged. The applied force on the roller ski and the force plate may not be parallel to each other. The crosstalk from the vertical force channel into the medio-lateral channel may also be an effect that may influence the amplitude of the measured force in the medio-lateral channel. These may cause some errors when comparing the force component converted to the GCS.

The extra weight of the force measurement roller ski did not affect the performance of the skiers. The duration skiers stayed on the treadmill and the final speed skiers could reach

were not affected much by the roller skis they use. Although there was a 333 g difference between the roller skis, the balance point of the roller ski changed as well. This led to the torque difference around the ski boot attach point on the roller ski being 0.01 N·m, which could be considered negligible. Therefore, the extra weight of the force measurement roller ski appears to be acceptable to the athletes. However, the extra weight may still affect the cycle characteristics while roller skiing, especially for female athletes. This may be due to the lighter body weight and relatively lower muscle strength when comparing the female athletes with the male athletes. The male athlete even seem to have a better performance by using the force measurement roller ski. This may be because the stiffness of the force measurement roller ski suited her better. The body of the force measurement roller ski is made of aluminum and the body of the reference roller ski is a honeycomb wooden structure. The stiffness of the two bodies may have some difference and, thereafter, affect the performance.

5. Conclusions

This developed instrumentation where the resistance strain gauges were mounted to the suspensions of the roller ski wheels is a practicable tool for measuring the magnitude of the forces applied on the roller skis in two dimensions in skate skiing. Markers attached to the roller skis can help transform the measured forces into the global coordinate system. Even though the transformed force component measured by the force measurement roller ski did not fully match the forces measured by the reference force plate, the possible reasons for the differences were analyzed. Despite small differences between the measurement systems, the derived forces in the X and Z directions can be considered valid and reliable. The extra weight of the force measurement roller ski has a small effect on the skier's roller skiing performance. Therefore, this instrumented force measurement roller ski can be useful for future research during daily training. One limitation of this validation study was that the validity of the force in the Y direction was not examined. In addition, skiers who participated in the practical application test were all adult skiers; whether the force measurement roller ski would have effects on roller skiing performance for junior and adolescent skiers needs further investigation.

Author Contributions: Conceptualization, S.Z., V.L., K.R., S.L., T.K., P.K. and O.O.; Data curation, S.Z.; Formal analysis, S.Z.; Funding acquisition, V.L., T.K. and P.K.; Investigation, S.Z., V.L., K.R., S.L. and O.O.; Methodology, S.Z., V.L., K.R., S.L., T.K., P.K. and O.O.; Resources, S.Z., K.R. and O.O.; Supervision, V.L., S.L. and O.O.; Validation, S.Z., T.K. and P.K.; Visualization, S.Z.; Writing—original draft, S.Z.; Writing—review and editing, S.Z., V.L., K.R., S.L., T.K., P.K. and O.O. All authors have read and agreed to the published version of the manuscript.

Funding: This research was partly funded by the Joint Authority of Kainuu Region, ERDF A77274.

Institutional Review Board Statement: Ethical review and approval were waived for this study because the Human Sciences Ethics Committee of the University of Jyväskylä concluded that an ethical review, in this case, was not required.

Informed Consent Statement: Informed consent was obtained from all subjects involved in the study.

Data Availability Statement: Pseudonymized datasets are available to external collaborators subject to agreement on the terms of data use and publication of results. To request the data, please contact Vesa Linnamo (vesa.linnamo@jyu.fi).

Acknowledgments: The authors would like to express their gratitude to the athletes who participated in the study.

Conflicts of Interest: The authors declare no conflict of interest. The funders had no role in the design of the study; in the collection, analyses, or interpretation of data; in the writing of the manuscript; or in the decision to publish the results.

Appendix A. Calibration Factors for Each Strain Gauges from the Calibration Test in December 2020

Table A1. Calibration factors (N/mV) for each strain gauges mounted on the roller skis (from the calibration test in December 2020).

Roller Ski	Strain Gauge	Calibration Factor
Right roller ski	Front vertical	0.2428
	Front medio-lateral	0.1175
	Rear vertical	0.2431
	Rear medio-lateral	0.1148
Left roller ski	Front vertical	0.2442
	Front medio-lateral	0.1174
	Rear vertical	0.2459
	Rear medio-lateral	0.1161

Appendix B. Vertical Force Combined Expanded Relative Measurement Uncertainty for Different Loading

Table A2. Vertical force combined expanded relative measurement uncertainty (%) for different loading.

	Right Roller Ski	Left Roller Ski
Force (kN)	W (k = 2)	W (k = 2)
0.2	3.5	4.5
0.4	3.4	3.6
0.6	2.7	2.9
0.7	2.5	2.7
0.8	2.3	2.2
0.9	1.0	1.4
1.0	0.4	0.8

References

- Komi, P.V. Force measurements during cross-country skiing. *J. Appl. Biomech.* **1987**, *3*, 370–381. [\[CrossRef\]](#)
- Komi, P.V.; Norman, R.W. Preloading of the thrust phase in cross-country skiing. *Int. J. Sport. Med.* **1987**, *08*, 48–54. [\[CrossRef\]](#) [\[PubMed\]](#)
- Vahasoyrinki, P.; Komi, P.V.; Seppala, S.; Ishikawa, M.; Kolehmainen, V.; Salmi, J.A.; Linnamo, V. Effect of skiing speed on ski and pole forces in cross-country skiing. *Med. Sci. Sport. Exerc.* **2008**, *40*, 1111–1116. [\[CrossRef\]](#) [\[PubMed\]](#)
- Leppävuori, A.P.; Karras, M.; Rusko, H.; Viitasaio, J.T. A new method of measuring 3-D ground reaction forces under the ski during skiing on snow. *J. Appl. Biomech.* **1993**, *9*, 315–328. [\[CrossRef\]](#) [\[PubMed\]](#)
- Street, G.M.; Frederick, E.C. Measurement of skier-generated forces during roller-ski skating. *J. Appl. Biomech.* **1995**, *11*, 245–256. [\[CrossRef\]](#)
- Pierce, J.C.; Pope, M.H.; Renstrom, P.; Johnson, R.J.; Dufek, J.; Dillman, C. Force measurement in cross-country skiing. *J. Appl. Biomech.* **1987**, *3*, 382–391. [\[CrossRef\]](#)
- Linnamo, V.; Ohtonen, O.; Stöggl, T.; Komi, P.; Müller, E.; Lindinger, S. Multi-dimensional force measurement binding used during skating in cross-country skiing. In *Science and Skiing V*; Meyer & Meyer Verlag: Oxford, UK, 2012; pp. 540–548.
- Ohtonen, O.; Lindinger, S.; Lemmettylä, T.; Seppälä, S.; Linnamo, V. Validation of portable 2D force binding systems for cross-country skiing. *Sport. Eng.* **2013**, *16*, 281–296. [\[CrossRef\]](#)
- Göpfert, C.; Pohjola, M.V.; Linnamo, V.; Ohtonen, O.; Rapp, W.; Lindinger, S.J. Forward acceleration of the centre of mass during ski skating calculated from force and motion capture data. *Sport. Eng.* **2017**, *20*, 141–153. [\[CrossRef\]](#)
- Ohtonen, O.; Lindinger, S.J.; Göpfert, C.; Rapp, W.; Linnamo, V. Changes in biomechanics of skiing at maximal velocity caused by simulated 20-km skiing race using V2 skating technique. *Scand. J. Med. Sci. Sport.* **2018**, *28*, 479–486. [\[CrossRef\]](#)
- Ohtonen, O.; Linnamo, V.; Lindinger, S.J. Speed control of the V2 skating technique in elite cross-country skiers. *Int. J. Sport. Sci. Coach.* **2016**, *11*, 219–230. [\[CrossRef\]](#)
- Ohtonen, O.L.V.; Göpfert, C.; Lindinger, S. Effect of 20km simulated race load on propulsive forces during ski skating. In *Science and Skiing VIII*; Karczewska-Lindinger, M.H.A., Linnamo, V., Lindinger, S., Eds.; University of Jyväskylä: Jyväskylä, Finland, 2019; pp. 130–137.
- Zhao, S.; Ohtonen, O.; Ruotsalainen, K.; Kettunen, L.; Lindinger, S.; Göpfert, C.; Linnamo, V. Propulsion Calculated by Force and Displacement of Center of Mass in Treadmill Cross-Country Skiing. *Sensors* **2022**, *22*, 2777. [\[CrossRef\]](#) [\[PubMed\]](#)

14. Lindinger, S.J.; Stöggl, T.; Müller, E.; Holmberg, H.C. Control of speed during the double poling technique performed by elite cross-country skiers. *Med. Sci. Sport. Exerc.* **2009**, *41*, 210–220. [[CrossRef](#)] [[PubMed](#)]
15. Stoggl, T.; Holmberg, H.C. Three-dimensional Force and Kinematic Interactions in V1 Skating at High Speeds. *Med. Sci. Sport. Exerc.* **2015**, *47*, 1232–1242. [[CrossRef](#)] [[PubMed](#)]
16. Stoggl, T.; Kappel, W.; Muller, E.; Lindinger, S. Double-push skating versus V2 and V1 skating on uphill terrain in cross-country skiing. *Med. Sci. Sport. Exerc.* **2010**, *42*, 187–196. [[CrossRef](#)]
17. Stöggl, T.; Müller, E.; Ainegren, M.; Holmberg, H.C. General strength and kinetics: Fundamental to sprinting faster in cross country skiing? *Scand. J. Med. Sci. Sport.* **2011**, *21*, 791. [[CrossRef](#)]
18. Watts, P.B.; Sulentic, J.E.; Drobish, K.M.; Gibbons, T.P.; Newbury, V.S.; Hoffman, M.D.; Mittelstadt, S.W.; O'Hagan, K.P.; Clifford, P.S. Physiological responses to specific maximal exercise tests for cross-country skiing. *Can. J. Appl. Physiol.* **1993**, *18*, 359–365. [[CrossRef](#)]
19. Bellizzi, M.J.; King, K.A.; Cushman, S.K.; Weyand, P.G. Does the application of ground force set the energetic cost of cross-country skiing? *J. Appl. Physiol.* **1998**, *85*, 1736–1743. [[CrossRef](#)]
20. Hoset, M.; Rognstad, A.; Rølvåg, T.; Ettema, G.; Sandbakk, Ø. Construction of an instrumented roller ski and validation of three-dimensional forces in the skating technique. *Sport. Eng.* **2014**, *17*, 23–32. [[CrossRef](#)]
21. Ohtonen, O.; Ruotsalainen, K.; Mikkonen, P.; Heikkinen, T.; Hakkarainen, A.; Leppävuori, A.; Linnamo, V. Online feedback system for athletes and coaches. In Proceedings of the 3rd International Congress on Science and Nordic Skiing, Vuokatti, Finland, 5–8 June 2015; p. 35.
22. Kadaba, M.; Ramakrishnan, H.; Wootten, M.; Gaine, J.; Gorton, G.; Cochran, G. Repeatability of kinematic, kinetic, and electromyographic data in normal adult gait. *J. Orthop. Res.* **1989**, *7*, 849–860. [[CrossRef](#)]
23. Yu, B. Effect of external marker sets on between-day reproducibility of knee kinematics and kinetics in stair climbing and level walking. *Res. Sport. Med.* **2003**, *11*, 209–218. [[CrossRef](#)]
24. Yu, B.; Kienbacher, T.; Growney, E.S.; Johnson, M.E.; An, K.N. Reproducibility of the kinematics and kinetics of the lower extremity during normal stair-climbing. *J. Orthop. Res.* **1997**, *15*, 348–352. [[CrossRef](#)] [[PubMed](#)]